An Ecological Study of Hunting Creek

2019

FINAL REPORT

March 10, 2020

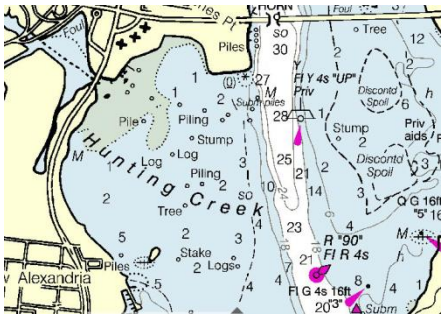

by

R. Christian Jones
Professor, Project Director

Kim de Mutsert
Assistant Professor, Co-Principal Investigator

Benoit Van Aken
Associate Professor, Co-Principal Investigator

Amy Fowler
Assistant Professor, Co-Principal Investigator

Potomac Environmental Research and Education Center
Department of Environmental Science and Policy
Department of Chemistry and Biochemistry
George Mason University

to

Alexandria Renew Enterprises
Alexandria, VA

This page intentionally blank.

Table of Contents

An Ecological Study of Hunting Creek - 2019

Executive Summary

Hunting Creek is an embayment of the tidal Potomac River located just downstream of the City of Alexandria and the I-95/I-495 Woodrow Wilson bridge. This embayment receives treated wastewater from the Alexandria Renew Enterprises wastewater treatment plant and inflow from Cameron Run which drains most of the Cities of Alexandria and Falls Church and much of eastern Fairfax County. The Hunting Creek embayment is bordered on the north by the City of Alexandria and on the west and south by the George Washington Memorial Parkway and associated park land. Due to its tidal nature and shallowness, the embayment does not seasonally stratify vertically, and its water is flushed by rainstorms and may mix readily with the adjacent tidal Potomac River mainstem. Beginning in 2013 the Potomac Environmental Research and Education (PEREC) in collaboration with Alexandria Renew Enterprises (AlexRenew) initiated a program to monitor water quality and biological communities in the Hunting Creek area including stations in the embayment itself, its tributaries, and the adjacent river mainstem. This document presents study findings from 2018 and compares them with that from the previous five years. In addition, special studies were continued on anadromous fish usage of Hunting Creek and Cameron Run and *Escherichia coli* levels in Hunting Creek and tributaries. And we completed a second year of benthic macroinvertebrate and water quality sampling on many tributaries of Cameron Run and Hunting Creek.

The Chesapeake Bay, of which the tidal Potomac River is a major subestuary, is the largest and most productive coastal system in the United States. The use of the Bay as a fisheries and recreational resource has been threatened by overenrichment with nutrients which can cause nuisance algal blooms, hypoxia in stratified areas, loss of submersed aquatic vegetation, and declining fisheries. As a major discharger of treated wastewater into Hunting Creek, AlexRenew has been proactive in decreasing nutrient loading since the late 1970's. Also of concern are E. coli and nutrients derived from combined sewer overflows (CSO's) and non point sources within the drainage basin as well as sediments derived from the watershed.

The ecological study reported here provides documentation of the current state of water quality and biological resources in Hunting Creek. In 2019 temperature was above normal for the entire study period from April through September. Precipitation was closer to normal in 2019 than in the extremely wet year 2018. However, it was again well above normal in 2019 especially in July. During mid-June, there were some noteworthy flow events related to local precipitation which occurred a few days before the June 19 sampling. And in early July there was a period of substantial rainfall which translated into significant increase in local flow which may have affected the July 17 sampling event. Potomac flows which are impacted by the much larger upstream watershed were elevated in May and July, but did not exhibit a response to the June local precipitation.

Water temperature followed a typical seasonal pattern at all stations. A steady increase was observed from April through mid-July to about 30°C followed by a gradual decline through September. Most of the embayment and river stations exhibited a gradual

increase in specific conductance over the study period which was interrupted by short declines related to flushing from storms. Dissolved oxygen was generally in the 80-100 percent saturation range indicating that photosynthesis was not robust in the absence of the SAV. There was a marked increase at AR2 in mid-July which corresponded with a peak in phytoplankton chlorophyll values. On the July water quality mapping date elevated DO was also observed in the Hunting Creek embayment. Field and lab pH was generally in the 7-8 range at all stations; in previous years with abundant SAV, pH was often higher. Total alkalinity was generally 70-120 mg/L as $CaCO_3$. Values tended to increase over the study period, but short-term declines were seen after runoff events in the same manner as those found for specific conductance.

Secchi disk transparency was generally 0.3-0.7 m. A decline was observed in early May at all stations. After that Secchi at the mainstem stations recovered to 0.6-0.8 m for the rest of the study period, but remained low (<0.5 m) at the Hunting Creek embayment stations inhibiting SAV development in 2019. Light attenuation coefficient exhibited a similar pattern with exceptionally poor transparency observed in Hunting Creek in mid-June and early July. Turbidity exhibited a similar pattern.

Ammonia nitrogen showed a general decrease from May through September and all values were quite low (<0.2 mg/L). Nitrate nitrogen also declined seasonally with additional dips in early May and late June related to flushing from the runoff events. Nitrite was very low at all stations and did not show consistent seasonal patterns except for an unexplained spike in August at all stations. Organic nitrogen was mostly in the range 0.2-1.0 mg/L and showed little seasonal pattern. Total phosphorus was generally less than 0.15 mg/L but was elevated on occasion in Hunting Creek. N/P ratio exhibited a general seasonal decline, but remained above 7.2, consistently pointing to P limitation of primary producers. Total suspended solids was typically in the 10-30 mg/L range with some higher spikes at the Hunting Creek stations related to runoff events. VSS values hovered around 5 mg/L in the river mainstem with higher values in the Hunting Creek embayment in June and early July.

In the tributaries, water temperature also generally followed air temperature with a steady rise in the spring and summer through late August. Specific conductance was generally 300-600 uS/cm with a gradual decline through July and a slight increase thereafter. Dissolved oxygen was generally near 100 percent saturation. AR11 (Lake Cook) and AR34 (Hoofs Run) were the most variable stations. pH values were consistently 6.5-7.5. Turbidity was generally low (<20 NTU). Total alkalinity was fairly uniform in all of the tributaries and did not vary much seasonally. Total phosphorus and ortho-phosphorus were variable with no clear pattern. Organic nitrogen was typically highest at AR11, AR23, and AR34. Ammonia nitrogen was uniformly low (<0.15 mg/L) at all stream stations except AR11 which was variable. Nitrate nitrogen was consistently elevated at AR33, followed by AR13. Other stations were consistently below 1 mg/L. TSS and was generally less than 20 mg/L except at AR11, AR 23, and AR34 which frequently were higher.

Phytoplankton biomass as indicated by chlorophyll *a* began the year in April and May with typical low springtime values, but increased dramatically during June and July to 20-30 µg/L with highest values in the Hunting Creek embayment. This was followed by a

dramatic decline in early August, probably in response to flushing and poor light conditions in mid- to late July. Recovery was observed in late August and September. Phytoplankton cell density were generally fairly constant and similar at AR2 and AR4 except for a strong peak in early July at AR2 at the time of high chlorophylls. There was a seasonal increase in June and July in phytoplankton biovolume at both stations. At both sites, cyanobacteria consistently dominated phytoplankton density throughout the year. *Anabaena* was dominant during the early July peak at AR2. *Oscillatoria* and an unknown cyanobacterium were dominant in cell density at AR4. Pennate 2 was the consistent diatom cell density dominant in contrast to most previous years when *Melosira* was consistently so. The green alga *Chlamydomonas* and the cryptophyte *Chroomonas* were the most important taxa in the "other" group. Phytoplankton biovolume was dominated by diatoms at both stations with "Other" algae being co-dominant at AR2 and with cryptophytes co-dominant at AR4. Diatom biovolume was a mix of smaller cells like Pennate 2 which was consistently found in all samples and larger taxa like *Surirella* which was found sporadically, but being very large made a big contribution to cell biovolume. The same was true with "other" taxa with *Peridinium* and *Euglena* (large cells) coming in and out of AR2 samples and *Cryptomonas* being consistently most important at AR4.

Rotifers maintained low levels in spring and into early summer, but exhibited a dramatic increase in mid-summer at both AR2 and AR4. Highest levels of over 3000/L were observed at AR2 in mid-August and 2500/L at AR2 in early August. These values were much higher than found in 2018 and among the highest observed to date in the study. *Brachionus* was the strong dominant on every sampling date.

All of the cladocerans displayed short early summer maxima and were generally higher in number at AR2 than at AR4. Many reached a maximum in early July before the flushing events that occurred later in that month. *Bosmina*, *Diaphanosoma*, *Daphnia*, *Sida* and Ceriodaphnia all followed this patter. *Diaphanosoma* and *Daphnia* both exceeded 1000/m^3 at this time. *Leptodora*, the large predaceous cladoceran on the other hand, had a distinct peak earlier, in early June, at both stations. Copepod nauplii peaked in early June and were already declining before the mid-July flows. *Eurytemora* was extremely abundant (>8000/m^3) at AR4 in June. *Diaptomus* and cyclopoid copepods displayed seasonal patterns similar to most of the cladocerans with a distinct maximum in the cove in early July.

As noted in last year's report many water quality and plankton variables were strongly affected by the high flows of 2018. While flows were lower on average in 2019, there were still some periods like the month of July that had highly elevated flows. Specific conductance was a variable that was markedly depressed in 2018; values in 2019 were higher and in the range of previous years. Light transparency (as measured by Secchi disk depth and light attenuation coefficient) did not show as much of a recovery especially at AR2 and AR3. At these two stations light transparency values were little changed from 2019; however, there was some improvement at AR4. TSS and VSS which impacts light transparency also continued to be elevated in 2019. Nitrate values, which were elevated in 2018, but returned to previous values in 2019 at all stations. Interestingly, chlorophyll a levels in 2019 were among the highest observed in the seven years of the study. Rotifers, particularly *Brachionus*, were also unusually high in 2019. Copepod nauplii

recovered to pre-2018 values, but were similar to recent years. Other zooplankton showed 2019 values within the range of recent years. Submersed aquatic vegetation (SAV) continued to be strongly depressed and was virtually absent for a second year in a row.

Ichthyoplankton collections were dominated by Gizzard Shad, Blueback Herring, and Alewife, all members of the family Clupeidae. Gizzard Shad accounted for over 2/3 of all collected fish larvae. Most of the non-clupeid larvae were *Morone americana*. (White Perch) which composed about 2% of total larvae. There were somewhat more larvae collected at AR4 than AR2, but not much difference in the taxa composition. A record density of fish larvae was found in 2019 owing mainly to the high number of Gizzard Shad; White Perch was also at its highest level since the study began.

White Perch made up almost 2/3 of individuals collected by trawling in 2019. Blue catfish was second (10%), followed by Spottail Shiner (8%) and Bay Anchovy (6%). Total catch at the two stations was similar, but Blue Catfish was mostly found in the river mainstem (AR4), while most other taxa were more numerous at the Hunting Creek station (AR3). White Perch were abundant at both stations. Seine sampling in 2019 was dominated by *Alosa* spp., White Perch, and Banded Killifish. The Alosids were mainly observed on one day in early May, while the other two were more evenly distributed through the summer. Collections at AR6 in Hunting Creek proper were much greater than at AR5 near Jones Point. A new gear was introduced in 2016 to overcome the drawbacks of trawling in dense SAV, the fyke net. The fyke net is a passive gear that can be deployed in shallow water. The net is static; the natural movement of the fish funnel individuals into the gear and they are generally well retained. This gear was deployed semimonthly starting in May at two locations near trawl site AR3. Catches were limited in 2018 and 2019 compared to 2016 and 2017 due to the lack of SAV in the last two years. Total collections by all gear in 2019 were at the high end of the range of abundances since the study started in 2013.

As in 2018, SAV was much reduced in 2019 as verified by surveys that were made by GMU personnel and aerial imagery from VIMS This is most certainly attributable to the very turbid water in 2018 and continued turbidity at critical periods in 2019 which obstructed light penetration.

Benthic invertebrate data from the tidal stations in 2018 indicated that the river station AR4 had the highest diversity and most samples from that station were distinctly different from the other two stations when compared by multivariate analysis. Within the embayment station samples there was distinct seasonal pattern. Annual aggregate taxa richness was 13 at AR4 and only 9 at AR2 and 7 at AR3. The low richness at AR2 and AR3 was at least partially due to the scarcity of SAV which enhances habitat. Oligochaetes, amphipods, and midges were the most abundant organisms at the tidal benthic stations. The Asiatic clam did well at AR4. Total abundance in 2019 was higher in 2019 than in 2018 and near the median over all years.

In 2016 a benthic macroinvertebrate sampling program was implemented for the flowing tributary streams starting with six stations. In 2018 two more stations were added with sampling continuing annually in November. Flatworms, chironomids, oligochaetes, baetid mayflies, and philopotamid and hydropsychid caddisflies were the dominant taxa,

all of which are taxa which are at least moderately tolerant of pollution indicating that the tributaries have been degraded by the impacts of urban development, mostly stormwater pulses and nonpoint pollution. Application of an index of biotic integrity indicated that all streams were categorized as "poor", but some were approaching "fair". However, the values of some individual metrics were "good" indicating that conditions may be improving. The values observed were typical of streams draining urban areas.

Anadromous fish sampling was conducted on a weekly basis from March 29 to May 31 in 2019 at a station just above the head of tide on Cameron Run. Hoop nets were deployed for a 24-hour period each week to collect spawning fish moving upstream and ichthyoplankton nets were deployed to collect fish larvae drifting downstream. Sixty individual fish were collected in the hoop nets in 2019, somewhat fewer than in 2018. Forty of these were adulty Alewife and 10 were adult Blueback Herring. Larvae of both Alewife and Blueback Herring were collected in Cameron Run in 2019 although levels were somewhat less than in 2018. Larvae of several other fish were also collected. Extrapolation from the sample collected to the total period of spawning yielded an estimate 389 adult river herring (Alewife + Blueback Herring) spawning in Cameron Run in 2019, similar to the values found in 2018.

E. coli sampling was expanded to a total of 16 stations in 2019, adding four additional stations as part of the semimonthly sampling program. The data continue to support a conclusion that the entire area sampled, including the mainstem of the Potomac River (AR4), is impaired for the bacteriological water quality criterion (*E. coli*) content under Section 9VAC25-260-170 of the Virginia Water Quality Standards that applies to primary contact recreational use surface waters. In 2019, highest values of *E. coli* were generally observed at Hoofs Creek stations AR13, AR33, and AR34. Lowest levels were found at A4, AR10, AR31, and AR32 which are located on the Potomac mainstem. Although our data showed an increase of the *E. coli* abundance and percent exceedance of the 235/100mL criterion from 2014 to 2016, these numbers seemed to have peaked in 2016 – 2017 and even showed a slight decrease in 2018 and 2019. It is noteworthy that the large geographical and temporal variability that we observed during the sampling events prevent to draw clear conclusion on the trend of water quality impairment. Finally, the highest counts in 2019 were observed in June and July (as in 2017), although the highest counts in 2018 were observed in April and September, revealing no clear seasonal trend in the data. High counts seem to reflect rainfall data instead of a seasonal trend.

We recommend that:

1. The basic ecosystem monitoring should continue. A range of climatic conditions is needed to effectively establish baseline conditions in Hunting Creek. Interannual, seasonal and spatial patterns are starting to appear, but need validation with future years's data. With record rainfall and runoff, 2018 provided a glimpse of the vulnerability of the system to flushing and sediment related effects. Continued monitoring will allow us to assess the resiliency of the ecosystem; i.e., how quickly will it recovery from a very wet year. The system did not recover completely in 2019.

2. Water quality mapping should be continued. This provides much needed spatial resolution of water quality patterns as well as allowing mapping of SAV distributions.
3. Fyke nets have proven to be a useful new gear to enhance fish collections and should be continued.
4. Anadromous fish sampling is an important part of this monitoring program and has gained interest now that the stock of river herring has collapsed generally, and a moratorium on these taxa has been established in 2012. The discovery and continue presence of river herring spawning in Cameron Run increases the importance of continuing studies of anadromous fish in the study area.
5. We recommend continuing the more intensive *E. coli* sampling plan which seems to be giving better insight into the dynamics of *E. coli* in the study area.
6. We recommend continuing macroinvertebrate studies the tributaries of Hunting Creek to further ascertain overall aquatic biota health and that tidal benthos sampling should continue and the data should be more thoroughly examined.

List of Abbreviations

BOD	Biochemical oxygen demand
cfs	cubic feet per second
DO	Dissolved oxygen
ha	hectare
l	liter
LOWESS	locally weighted sum of squares trend line
m	meter
mg	milligram
MGD	Million gallons per day
NS	not statistically significant
NTU	Nephelometric turbidity units
SAV	Submersed aquatic vegetation
SRP	Soluble reactive phosphorus
TP	Total phosphorus
TSS	Total suspended solids
um	micrometer
VSS	Volatile suspended solids
#	number

This page intentionally left blank.

The Aquatic Monitoring Program for the Hunting Creek Area of the Tidal Freshwater Potomac River 2019

FINAL REPORT
March 10, 2020

by

R. Christian Jones
Professor, Department of Environmental Science and Policy
Director, Potomac Environmental Research and Education Center
George Mason University
Project Director

Kim de Mutsert
Assistant Professor, Department of Environmental Science and Policy
George Mason University
Co-Principal Investigator

Amy Fowler
Assistant Professor, Department of Environmental Science and Policy
George Mason University
Co-Principal Investigator

to

Alexandria Renew Enterprises
Alexandria, VA

ACKNOWLEDGEMENTS

The authors wish to thank the numerous individuals and organizations whose cooperation, hard work, and encouragement have made this project successful. We wish to thank the Alexandria Renew Enterprises especially CEO Karen Pallansch for her vision in initiating the study and to Aster Tekle for her advice and assistance during the study.

Without a dedicated group of field and laboratory workers this project would not have been possible. Thanks go to Laura Birsa for managing water quality/plankton/benthos field trips and to field/lab workers Kristen Reck, Chelsea Gray, Tabitha King, Julia Czarnecki, Alex Mott, David Tolentino, Sam Mohney, and Steven Chan. Benthic samples were analyzed with the help of Bryce Bossuot, James Burmeister, Haley Haasch, Keith Keel and Eran O'Keefe.

Special thanks go to C.J. Schlick for her help with the report, and to Joris van der Ham, who has operated as the field manager of the fish collections. Others that have helped in the field and in the laboratory to collect and process fish samples include CJ Schlick, Beverly Bachman, Rachel Kelmartin, Christopher Bodner, Tabitha King, Sara Marriott, Philip Latasa, Alec Green, Diana Belman, Sammie Alexander, and Jeremy Williams.

Claire Buchanan served as a voluntary consultant on plankton identification.

INTRODUCTION

This section reports the results of the sixth year of an aquatic monitoring program conducted for Alexandria Renew Enterprises by the Potomac Environmental Research and Education Center (PEREC) in the College of Science at George Mason University. Two other sections of the report include an anadromous fish study of Cameron Run and a survey of *Escherichia coli* levels in the Hunting Creek area of the tidal Potomac River.

This work was in response to a request from Karen Pallansch, Chief Executive Officer of Alexandria Renew Enterprises (Alex Renew), operator of the wastewater reclamation and reuse facility (WRRF) which serves about 350,000 people in the City of Alexandria and the County of Fairfax in northern Virginia. The study is patterned on the long-running Gunston Cove Study which PEREC has been conducting in partnership with the Fairfax County Department of Public Works and Environmental Services since 1984. The goal of these projects is to provide baseline data and on-going trend analysis of the ecosystems receiving reclaimed water from wastewater treatment facilities with the objective of adaptive management of these valuable freshwater resources. This will facilitate the formulation of well-grounded management strategies for maintenance and improvement of water quality and biotic resources in the tidal Potomac. A secondary but important educational goal is to provide training for Mason graduate and undergraduate students in water quality and biological monitoring and assessment.

Setting of Hunting Creek

Hunting Creek is an embayment of the tidal Potomac River located just downstream of the City of Alexandria and the Woodrow Wilson Bridge. Waters are shallow with the entire embayment having a depth of 2 m or less at mean tide. According to the "Environmental Atlas of the Potomac Estuary" (Lippson et al. 1981), the mean depth of Hunting Creek is 1.0 m, the surface area is 2.26 km^2, and the volume of 2.1 x 10^6 m^3.

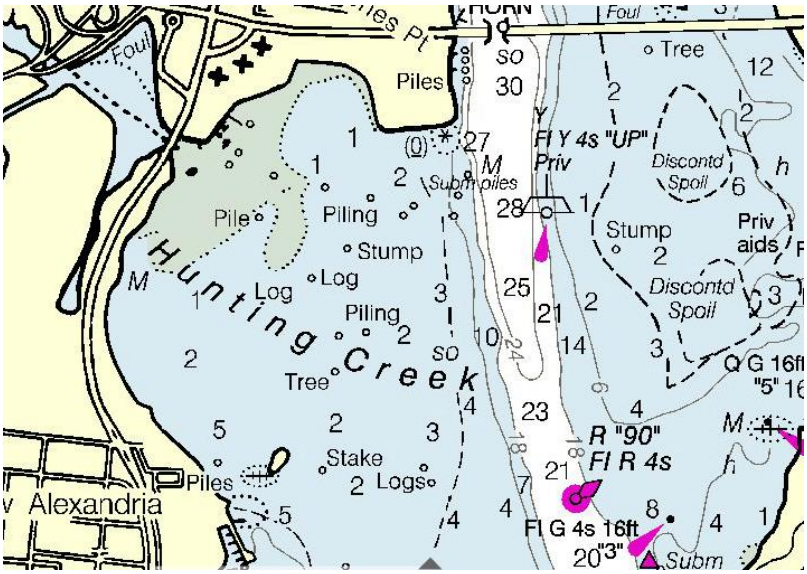

On the left is the Hunting Creek embayment. The Woodrow Wilson Bridge spans the tidal Potomac River at the top of the map. The Potomac River main channel is the whitish area running from north to south through the middle of the map. Soundings (numbers on the map) are in feet at mean low water. For the purposes of this report "Hunting Creek" will extend to the head of tide, roughly to Telegraph Rd.

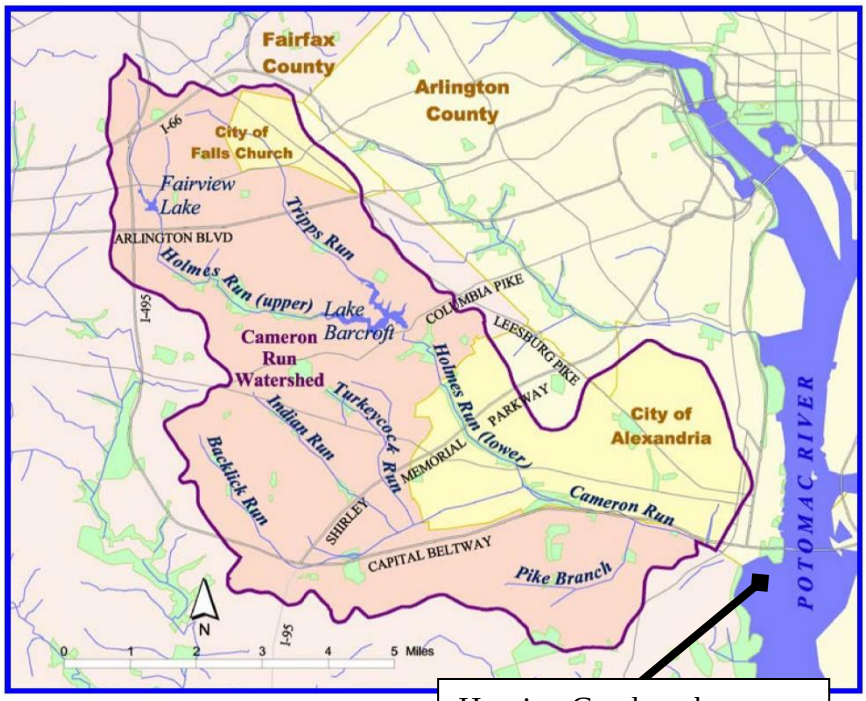

On the left is a map of the Hunting Creek watershed. Cameron Run is the freshwater stream which drains the vast majority of the watershed of Hunting Creek. The watershed is predominantly suburban in nature with areas of higher density commercial and residential development. The watershed has an area of 44 square miles and drains most of the Cities of Alexandria and Falls Church and much of east central Fairfax County. A major aquatic feature of the watershed is Lake Barcroft. The suburban land uses in the watershed are a source of nonpoint pollution to Hunting Creek.

Hunting Creek embayment

The Alex Renew WRRF serves an area similar in extent to the Cameron Run watershed with the addition of some areas along the Potomac shoreline from Four Mile Run to Dyke Marsh. The effluent of the Alexandria Renew Enterprises plant enters the upper tidal reach of Hunting Creek under the Rt 1/I-95 interchange.

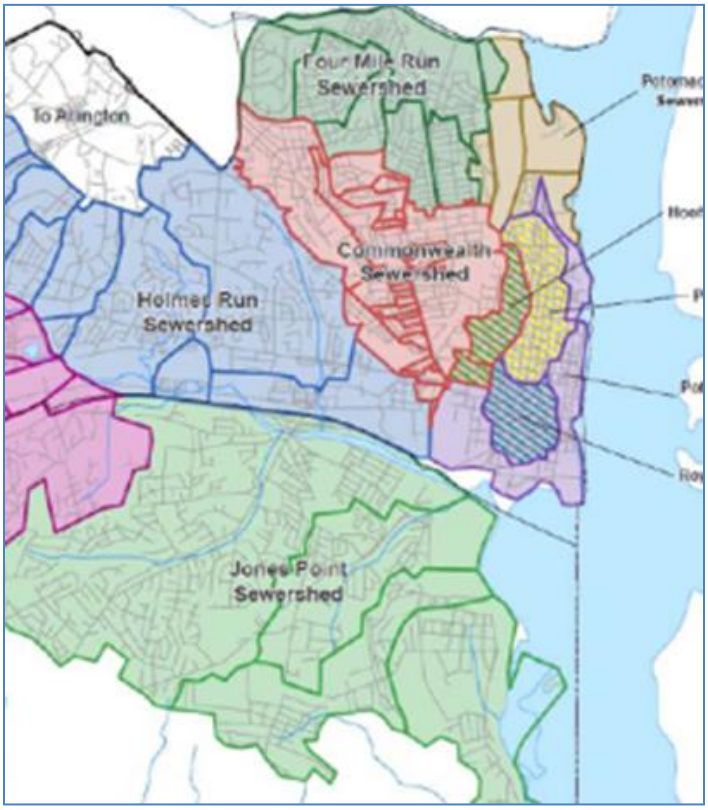

The map at the left shows the sewersheds which contribute to the AlexRenew WRRF. Of particular note are the shaded areas within the City of Alexandria. These sewersheds (Hooffs Run, Pendleton, and Royal St.) all contain combined sewers meaning that domestic wastewater is co-mingled with street runoff. Under most conditions, all of this water is directed to the AlexRenew WRRF for treatment. But in extreme runoff conditions (like torrential rains), some may be diverted directly into the tidal Potomac via a Combined Sewer outfall (CSO).

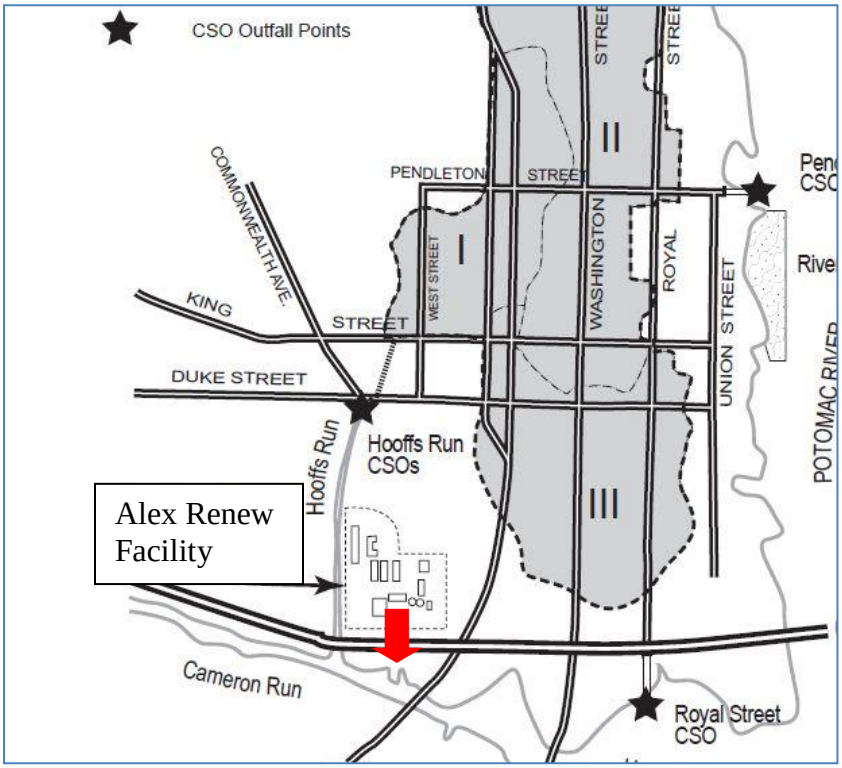

The map at the left is an enlargement of the area where the Alex Renew WRRF is found and where the discharge sites of the CSO's are located. Note the close proximity of two of the CSO's to the Alex Renew WRRF discharge (shown as red arrow).

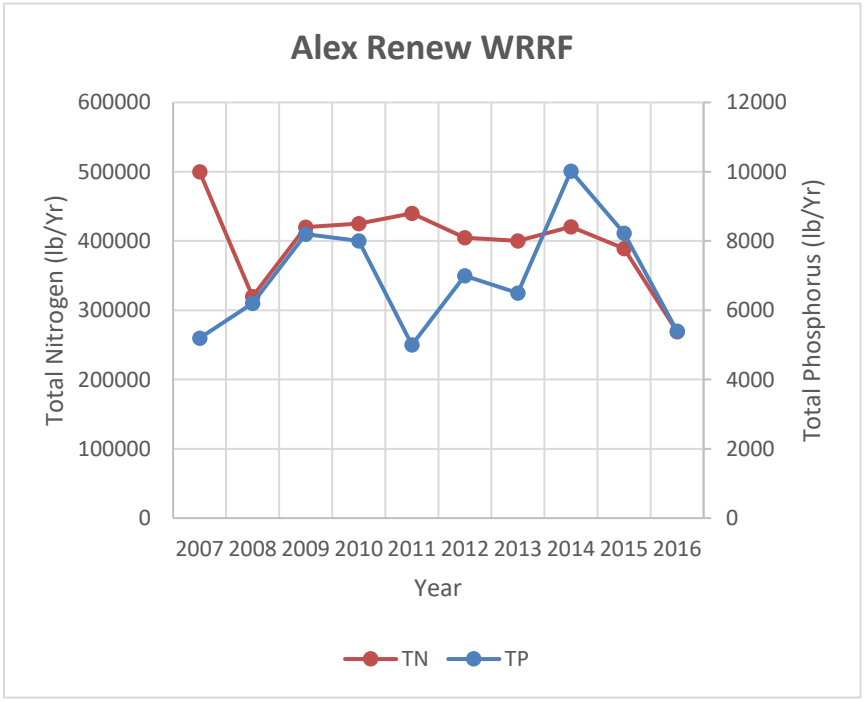

The graph at the left shows the loading of nitrogen and phosphorus from the Alexandria Renew WRRF for the last seven years. Loadings of both nutrient elements were among the lowest in the last decade in 2016: 269,000 lb/yr for nitrogen and 5,400 lb/yr for phosphorus.

Ecology of the Freshwater Tidal Potomac

The tidal Potomac River is an integral part of the Chesapeake Bay tidal system and at its mouth the Potomac is contiguous to the bay proper. The tidal Potomac is often called a subestuary of the Chesapeake Bay and as such it is the largest subestuary of the bay in terms of size and amount of freshwater input. The mixing of freshwater with saltwater is the hallmark of an estuary. While the water elevation in an estuary is "sea level", the water contained in an estuary is not pure sea water such as found in the open ocean. Pure ocean sea water has a salt concentration of about 35 parts per thousand by weight (ppt). Water in Chesapeake Bay ranges from about 30 ppt near its mouth to 0 ppt in the upper reaches where there is substantial freshwater inflow such as in the upper tidal Potomac River. Salinity at a given location is determined by the balance between freshwater input and salt water mixing in from the ocean. It generally varies with season being lower in spring when freshwater inflows are greater and higher in summer when there is less freshwater inflow. In the Hunting Creek study area, the salinity is essentially 0 yearround.

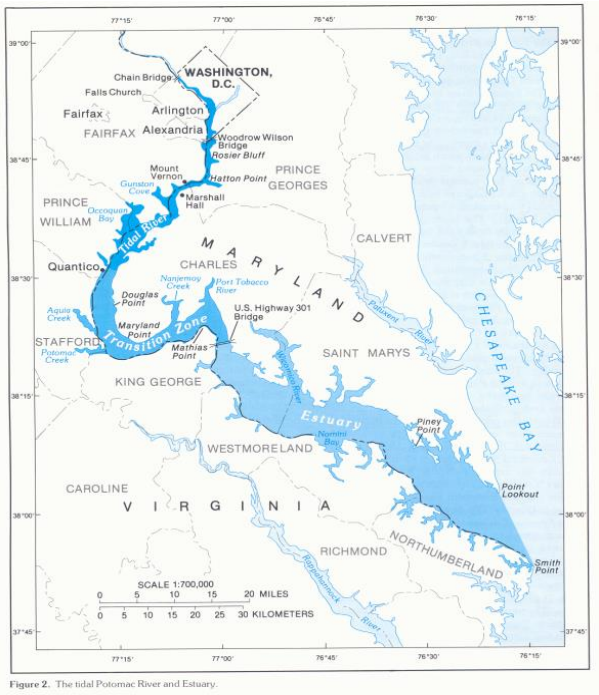

Figure 2. The tidal Potomac River and Estuary.

(map courtesy USGS)

The tidal Potomac is generally divided into three salinity zones as indicated by the map to the left:
-Estuarine or Mesohaline zone (6-14 ppt)
-Transition or Oligohaline zone (0.5-6 ppt)
-Tidal River or Tidal Fresh zone (<0.5 ppt)
Hunting Creek is in the upper part of the Tidal River/Tidal Fresh zone and as such it never experiences detectable salinity

Within the tidal freshwater zone, the flora and fauna are generally characterized by the same species that would occur in a freshwater lake in this area and the food web is similar. Primary producers are freshwater species of submersed aquatic vegetation (SAV) such as native taxa *Vallisneria americana* (water celery), *Potomogeton* spp, (pondweeds), and *Ceratophyllum* (coontail) as well as introduced species such as *Hydrilla verticallata* (hydrilla) and *Myriophyllum spicatum* (water milfoil). Historical accounts indicate that most of the shallow areas of the tidal freshwater Potomac were colonized by SAV when observations were made around 1900 (Carter et al. 1985).

The other group of important primary producers are phytoplankton, a mixed assemblage

of algae and cyanobacteria which may turn over rapidly on a seasonal basis. The dominant groups of phytoplankton in the tidal freshwater Potomac are diatoms (considered a good food source for aquatic consumers) and cyanobacteria (considered a less desirable food source for aquatic consumers). For the latter part of the 20th century, the high nutrient loadings into the river favored cyanobacteria over both diatoms and SAV resulting in large production of undesirable food for consumers. In the last decade or so, as nutrient reductions have become manifest, cyanobacteria have decreased and diatoms and SAV have increased.

The biomass contained in the cells of phytoplankton nourishes the growth of zooplankton and benthic macroinvertebrates which provide an essential food supply for the juvenile and smaller fish. These in turn provide food for the larger fish like striped bass and largemouth bass. The species of zooplankton and benthos found in the tidal fresh zone are similar to those found in lakes in the area, but the fish fauna is augmented by species that migrate in and out from the open interface with the estuary.

Resident fish species include typical lake species such as sunfish (*Lepomis* spp.), bass (*Micropterus* spp.), and crappie (*Pomoxis* spp.) as well as estuarine species such as white perch (*Morone americana*) and killifish (*Fundulus* spp.). Species which spend part of their year in the area include striped bass (*Morone saxitilis*) and river herrings and shad (*Alosa* spp.). Non-native fish species have also become established in the tidal freshwater Potomac such as northern snakehead (*Channa argus*) and blue catfish (*Ictalurus furcatus*).

Larval fishes are transitional stages in the development of juvenile fishes. They range in development from newly hatched, embryonic fish to juvenile fish with morphological features similar to those of an adult. Many fishes such as clupeids (herring family), white perch, striped bass, and yellow perch disperse their eggs and sperm into the open water. The larvae of these species are carried with the current and termed “ichthyoplankton”. Other fish species such as sunfish and bass lay their eggs in “nests” on the bottom and their larvae are rare in the plankton.

After hatching from the egg, the larva draws nutrition from a yolk sack for a few days. When the yolk sack diminishes to nothing, the fish begins a life of feeding on other organisms. This post yolk sack larva feeds on small planktonic organisms (mostly small zooplankton) for a period of several days. It continues to be a fragile, almost transparent larva and suffers high mortality to predatory zooplankton and juvenile and adult fishes of many species, including its own. When it has fed enough, it changes into an opaque juvenile, with greatly enhanced swimming ability. It can no longer be caught with a slow-moving plankton net, but is soon susceptible to capture with the seine or trawl net.

METHODS

A. Profiles and Plankton: Sampling Day

Sampling was conducted on a semimonthly basis at stations representing both Hunting Creek and the Potomac mainstem (Figure 1a). One station (AR 1) was located near the mouth of Cameron Run at the George Washington Parkway bridge. Two stations (AR 2 & 3) were located in the Hunting Creek embayment proper. A fourth station was located in the river channel about 100 m upstream from Buoy 90. Dates for sampling as well as weather conditions on sampling dates and immediately preceding days are shown in Table 1. Note that certain dates had significant rainfall in days preceding sampling which may have impacted conditions in Hunting Creek due to it shallow nature and relatively large watershed contributing runoff.

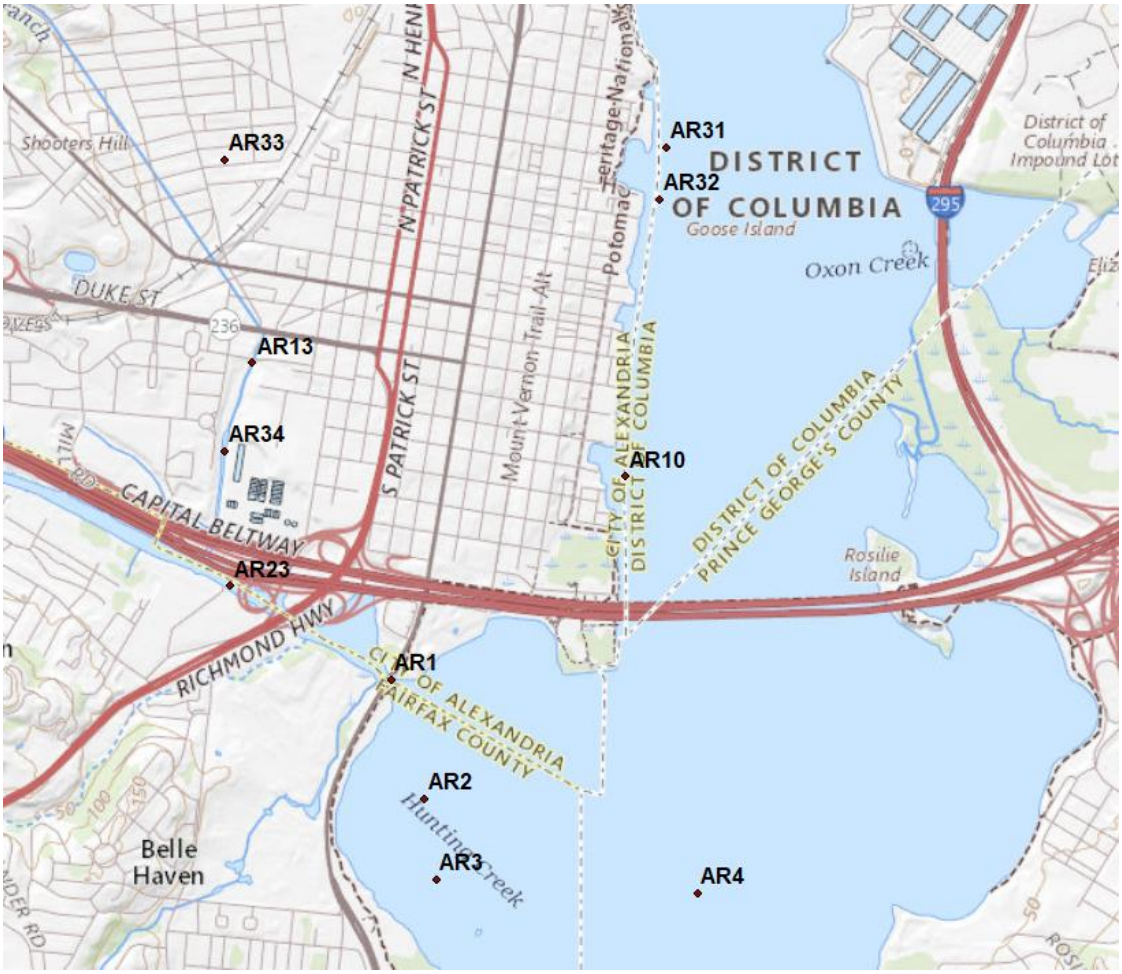

Figure 1a. Hunting Creek area of the Tidal Potomac River showing water quality, plankton, and benthos sampling stations. AR1, AR2, AR3, AR4, AR10, AR23, AR31, AR32, AR33, and AR34 represent water quality stations, AR2 and AR4 are the phytoplankton and zooplankton stations and AR2, AR3, and AR4 are tidal benthos stations.

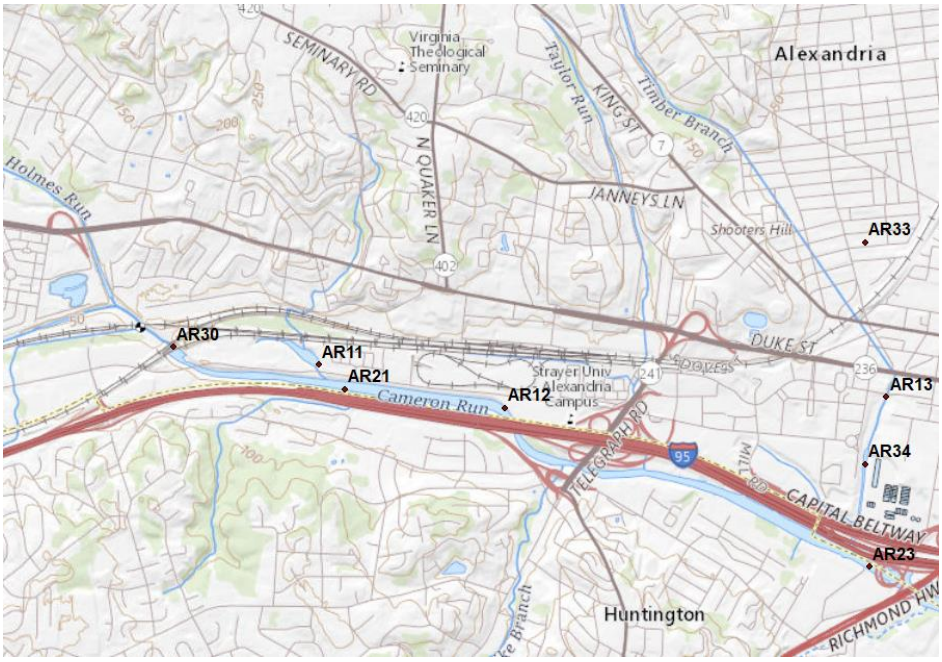

Figure 1b. Cameron Run portion of the study area showing water quality stations.

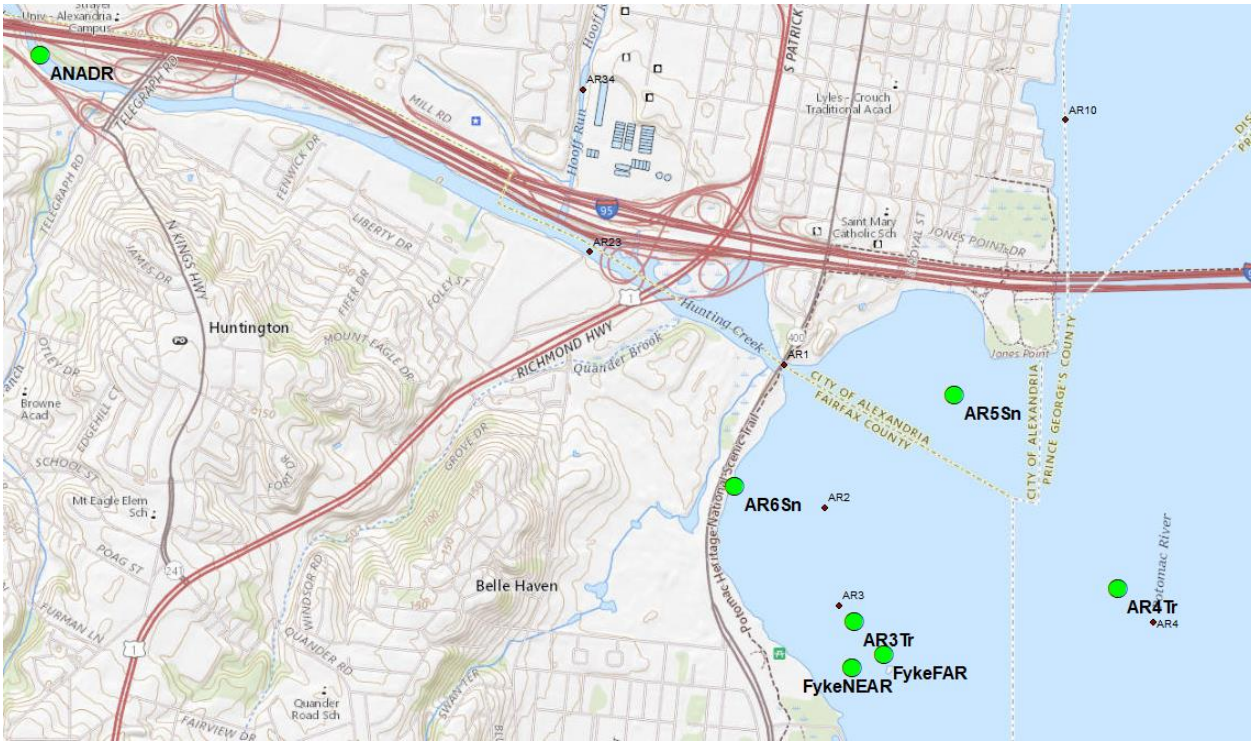

Figure 1c. Hunting Creek area of the Tidal Potomac River showing fish monitoring stations – Large Green circles. Stations with Tr in name are trawl stations; those with Sn in name are seine stations and those with Fyke in name are fyke stations. ANADR is the anadromous station. Water quality stations shown as small symbols and lettering for comparison.

Table 1
Hunting Creek Study: Sampling Dates and Weather Data for 2019

	Type of Sampling						Avg Daily Temp (°C)		Precipitation (cm)	
Date	WP	B	D	T	S	F	1-Day	3-Day	1-Day	3-Day
April 18	X						20.0	17.2	0	0
May 3				X	X	X	22.2	21.3	T	1.23
May 8	X	B					20.6	20.9	0	0
May 13				X	X	X	12.8	15.0	1.50	3.78
May 22	X						18.3	22.0	0	T
May 29				X	X	X	28.9	27.2	0	0.48
June 5	X	B					23.3	20.6	0.03	0.03
June 11				X	X	X	22.8	21.9	0.36	1.63
June 19	X						26.7	27.2	0.20	3.16
June 25				X	X	X	27.8	25.7	0.48	0.53
July 3	X	B					28.3	25.7	T	1.08
July 9				X	X	X	25.0	25.7	0	8.74
July 17	X						29.4	28.5	0.74	0.75
July 18			D				30.0	29.4	0	0.75
July 23				X	X	X	23.3	28.5	0.20	0.29
August 1	X	B					27.2	28.3	0	0.03
August 13				X	X		27.2	26.5	0.30	0.30
August 14	X						28.3	27.6	0.01	0.32
August 21			D				28.3	29.6	0.03	0.95
August 28				X	X	X	24.4	22.8	0.05	0.06
Sept 4	X	B					28.9	27.6	0.05	0.18
Sept 17	X						23.9	25.9	0	0
Sept 18				X	X	X	22.2	24.3	0	0

Type of Sampling: WP: Water quality (samples to AlexRenew Lab), profiles and plankton, B: benthos (station numbers indicated), D: dataflow (water quality mapping), T: fish collected by trawling, S: fish collected by seining. F: fish collected by fyke net. T under Precipitation equals "trace". X indicates full station suite on that date.

Sampling was initiated about 10:00 am. Four types of measurements or samples were obtained at each station: (1) depth profiles of temperature, conductivity, dissolved oxygen, pH, and irradiance (photosynthetically active radiation, PAR) measured directly in the field; (2) water samples for GMU lab determination of chlorophyll *a* and phytoplankton species composition and abundance; (3) water samples for determination of N and P forms, BOD, COD, alkalinity, hardness, suspended solids, chloride, and pH by the Alexandria Renew Enterprises lab; (4) net sampling of zooplankton and ichthyoplankton.

Profiles of temperature, conductivity, and dissolved oxygen were conducted at each station using a YSI 6600 datasonde with temperature, conductivity, dissolved oxygen and pH probes. Measurements were taken at 0.3 m increments from surface to bottom at the embayment stations. In the river measurements were made with the sonde at depths of 0.3 m and 2.0 m increments to the bottom. Meters were checked for calibration before and after sampling. Profiles of irradiance (photosynthetically active radiation, PAR) were collected with a LI-COR underwater flat scalar PAR probe. PAR measurements were taken at 10 cm intervals to a depth of 1.0 m. Simultaneous measurements were made with a terrestrial probe in air during each profile to correct for changes in ambient light if needed. Secchi depth was also determined. The readings of at least two crew members were averaged due to variability in eye sensitivity among individuals. If the Secchi disk was still visible at the bottom or if its path was block by SAV while still visible, a proper reading could not be obtained.

A 1-liter depth-composited sample for GMU lab work was constructed from equal volumes of water collected at each of three depths (0.3 m below the surface, middepth, and 0.3 m off of the bottom) using a submersible bilge pump. A 100-mL aliquot of this sample was preserved immediately with acid Lugol's iodine for later identification and enumeration of phytoplankton at stations AR2 and AR4. The remainder of the sample was placed in an insulated cooler with ice. A separate 1-liter surface sample was collected from 0.3 m using the submersible bilge pump and placed in the insulated cooler with ice for lab analysis of surface chlorophyll *a*.

At embayment and river mainstream sampling stations (AR2, AR3, and AR4), 2-liter samples were collected monthly at each station from just below the surface (0.3 m) and near the bottom (0.3 m off bottom) at each station using the submersible pump. At tributary stations (AR1, AR 10, AR11, AR12, AR13, AR21, AR22, AR23, and AR30), 2-liter samples were collected by hand from just below the surface. This water was promptly delivered to the nearby Alexandria Renew Laboratory for determination of nitrogen, phosphorus, BOD, TSS, VSS, pH, total alkalinity, and chloride.

At stations AR2 and AR4, microzooplankton was collected by pumping 32 liters from each of three depths (0.3 m, middepth, and 0.3 m off the bottom) through a 44 μm mesh sieve. The sieve consisted of a 12-inch long cylinder of 6-inch diameter PVC pipe with a piece of 44 μm nitex net glued to one end. The 44 μm cloth was backed by a larger mesh cloth to protect it. The pumped water was passed through this sieve from each depth and then the collected microzooplankton was backflushed into the sample bottle. The resulting sample was treated with about 50 mL of club soda and then preserved with formalin containing a small amount of rose bengal to a concentration of 5-10%.

At stations AR2 and AR4, macrozooplankton was collected by towing a 202 µm net (0.3 m opening, 2 m long) for 1 minute at each of three depths (near surface, middepth, and near bottom). Ichthyoplankton (larval fish) was sampled by towing a 333 µm net (0.5 m opening, 2 m long) for 2 minutes at each of the same depths at Stations AR2 and AR4. In the embayment, the boat traveled from AR2 toward AR3 during the tow while in the river the net was towed in a linear fashion along the channel. Macrozooplankton tows were about 300 m and ichthyoplankton tows about 600 m. Actual distance depended on specific wind conditions and tidal current intensity and direction, but an attempt was made to maintain a constant slow forward speed (approximately 2 miles per hour) through the water during the tow. The net was not towed directly in the wake of the engine. A General Oceanics flowmeter, fitted into the mouth of each net, was used to establish the exact towing distance. During towing the three depths were attained by playing out rope equivalent to about 1.5-2 times the desired depth. Samples which had obviously scraped bottom were discarded and the tow was repeated. Flowmeter readings taken before and after towing allowed precise determination of the distance towed and when multiplied by the area of the opening produced the total volume of water filtered.

Macrozooplankton were preserved immediately with rose bengal formalin with club soda pretreatment. Ichthyoplankton was preserved in 70% ethanol. Macrozooplankton was collected on each sampling trip; ichthyoplankton collections ended after July because larval fish were normally not found after this time.

Benthic macroinvertebrate samples were collected monthly at stations AR2, AR3, and AR4. Three samples were collected at each station using a petite ponar grab. The bottom material was sieved through a 0.5 mm stainless steel sieve and resulting organisms were preserved in rose bengal formalin for lab analysis.

Samples for water quality determination were maintained on ice and delivered to the Alexandria Renew Enterprises (AlexRenew) Laboratory by 2 pm on sampling day and returned to GMU by 3 pm. At GMU 10-15 mL aliquots of both depth-integrated and surface samples were filtered through 0.45 µm membrane filters (Gelman GN-6 and Millipore MF HAWP) at a vacuum of less than 10 lbs/in^2 for chlorophyll a and pheopigment determination. During the final phases of filtration, 0.1 mL of $MgCO_3$ suspension (1 g/100 mL water) was added to the filter to prevent premature acidification. Filters were stored in 20 mL plastic scintillation vials in the lab freezer for later analysis. Seston dry weight and seston organic weight were measured by filtering 200-400 mL of depth-integrated sample through a pretared glass fiber filter (Whatman 984AH).

Sampling day activities were normally completed by 5:30 pm.

B. Profiles and Plankton: Follow-up Analyses

Chlorophyll *a* samples were extracted in a ground glass tissue grinder to which 4 mL of dimethyl sulfoxide (DMSO) was added. The filter disintegrated in the DMSO and was ground for about 1 minute by rotating the grinder under moderate hand pressure. The ground suspension was transferred back to its scintillation vial by rinsing with 90% acetone. Ground samples were

stored in the refrigerator overnight. Samples were removed from the refrigerator and centrifuged for 5 minutes to remove residual particulates.

Chlorophyll *a* concentration in the extracts was determined fluorometrically using a Turner Designs Model 10 field fluorometer configured for chlorophyll analysis as specified by the manufacturer. The instrument was calibrated using standards obtained from Turner Designs. Fluorescence was determined before and after acidification with 2 drops of 10% HCl. Chlorophyll *a* was calculated from the following equation which corrects for pheophytin interference:

$$\text{Chlorophyll } a\ (\mu g/L) = F_s R_s (R_b - R_a)/(R_s - 1)$$

where F_s=concentration per unit fluorescence for pure chlorophyll *a*
R_s=fluorescence before acid/fluorescence after acid for pure chlorophyll *a*
R_b=fluorescence of sample before acid
R_a=fluorescence of sample after acid

All chlorophyll analyses were completed within one month of sample collection.

Phytoplankton species composition and abundance was determined using the inverted microscope-settling chamber technique (Lund et al. 1958). Ten milliliters of well-mixed algal sample were added to a settling chamber and allowed to stand for several hours. The chamber was then placed on an inverted microscope and random fields were enumerated. At least two hundred cells were identified to species and enumerated on each slide. Counts were converted to number per mL by dividing number counted by the volume counted. Biovolume of individual cells of each species was determined by measuring dimensions microscopically and applying volume formulae for appropriate solid shapes.

Microzooplankton and macrozooplankton samples were rinsed by sieving a well-mixed subsample of known volume and resuspending it in tap water. This allowed subsample volume to be adjusted to obtain an appropriate number of organisms for counting and for formalin preservative to be purged to avoid fume inhalation during counting. One mL subsamples were placed in a Sedgewick-Rafter counting cell and whole slides were analyzed until at least 200 animals had been identified and enumerated. A minimum of two slides was examined for each sample. References for identification were: Ward and Whipple (1959), Pennak (1978), and Rutner-Kolisko (1974). Zooplankton counts were converted to number per liter (microzooplankton) or per cubic meter (macrozooplankton) with the following formula:

$$\text{Zooplankton } (\#/L \text{ or } \#/m^3) = NV_s/(V_c V_f)$$

where N = number of individuals counted
V_s = volume of reconstituted sample, (mL)
V_c = volume of reconstituted sample counted, (mL)
V_f = volume of water sieved, (L or m^3)

Larval fish were picked from the ethanol-preserved ichthyoplankton samples with the aid of a stereo dissecting microscope. Identification of ichthyoplankton was made to family and

further to genus and species where possible. If the number of animals in the sample exceeded several hundred, then the sample was split with a plankton splitter and the resulting counts were multiplied by the subsampling factor. The works Hogue et al. (1976), Jones et al. (1978), Lippson and Moran (1974), and Mansueti and Hardy (1967) were used for identification. The number of ichthyoplankton in each sample was expressed as number per 10 m^3 using the following formula:

Ichthyoplankton (#/10m^3) = 10N/V
where N = number ichthyoplankton in the sample
V = volume of water filtered, (m^3)

C. Adult and Juvenile Fish

Fishes were sampled by trawling at stations AR3 and AR4, and seining at stations AR5 and AR6 (Figure 1). For trawling, a try-net bottom trawl with a 15-foot horizontal opening, a ¾ inch square body mesh and a ¼ inch square cod end mesh was used. The otter boards were 12 inches by 24 inches. Towing speed was 2-3 miles per hour and tow length was 5 minutes. The trawls were towed upriver parallel to the channel at AR4, and following the curve away from the channel at AR3. The direction of tow should not be crucial. Dates of sampling and weather conditions are found in Table 1.

Seining was performed with a bag seine that was 50 feet long, 3 feet high, and made of knotted nylon with a ¼ inch square mesh. The bag is located in the middle of the net and measures 3 ft^3. The seining procedure was standardized as much as possible. The net was stretched out perpendicular to the shore with the shore end right at the water line. The net was then pulled parallel to the shore for a distance of 100 feet by a worker at each end moving at a slow walk. Actual distance was recorded if in any circumstance it was lower than 100 feet. At the end of the prescribed distance, the offshore end of the net was swung in an arc to the shore and the net pulled up on the beach to trap the fish. Dates for seine sampling were the same as those for trawl sampling (Table 1). An additional seine sample was collected on June 25.

Due to extensive submerged aquatic vegetation (SAV) cover in Hunting Creek, we adjusted our sampling regime in 2016. The trawl at AR3 has been impeded more frequently each year due to this vegetation, and two fyke nets were set in the area close to AR3 (Figure 1). The fyke net sampling stations are called ‘fyke near’ and ‘fyke far’ in reference to their distance from shore. These fyke nets were set within the SAV to sample the fish community that uses the SAV cover as habitat. Fyke nets were set for 4 hours to passively collect fish. The fyke nets have 5 hoops, a 1/4 inch mesh size, 16 feet wings and a 32 feet lead. Fish enter the net by actively swimming and/or due to tidal motion of the water. The lead increases catch by capturing the fish swimming parallel to the wings. Fyke nets were set each sampling date; due to lower densities of SAV in 2019, trawling in this location (AR3) continued throughout the year (Table 1).

After the catch from each of these three gear types was hauled in, the fishes were measured for standard length and total length to the nearest mm. Standard length is the distance from the front tip of the snout to the end of the vertebral column and base of the caudal fin. This is evident in a crease perpendicular to the axis of the body when the caudal fin is pulled to the

side. Total length is the distance from the tip of the snout to the tip of the longer lobe of the caudal fin, measured by straightening the longer lobe toward the midline.

If the identification of the fish was not certain in the field, a specimen was preserved in 70% ethanol and identified later in the lab. Fishes kept for chemical analysis were kept on ice wrapped in aluminum foil until frozen in the lab. All fishes retained for laboratory analysis or identification were first euthanized by submerging them in an ice sludge conforming to the AICUC protocol. Identification was based on characteristics in dichotomous keys found in several books and articles, including Jenkins and Burkhead (1983), Hildebrand and Schroeder (1928), Loos et al (1972), Dahlberg (1975), Scott and Crossman (1973), Bigelow and Schroeder (1953), Eddy and Underhill (1978), Page and Burr (1998), and Douglass (1999).

D. Submersed Aquatic Vegetation

Data on coverage and composition of submersed aquatic vegetation (SAV) are generally obtained from the SAV webpage of the Virginia Institute of Marine Science (http://www.vims.edu/bio/sav). Information on this web site is obtained from aerial photographs near the time of peak SAV abundance as well as ground surveys which are used to determine species composition. We also recorded SAV relative abundance on a 0-3 scale at 4 minute intervals using visual observations and rake tow during data mapping cruises.

E. Benthic Macroinvertebrates

Benthic macroinvertebrates were sampled monthly using a petite ponar sampler at embayment stations AR2, AR3, and AR4. Triplicate samples were collected at each station monthly. Bottom samples were sieved on-site through a 0.5 mm stainless steel sieve and preserved with rose bengal formalin. In the laboratory benthic samples were rinsed with tap water through a 0.5 mm sieve to remove formalin preservative and resuspended in tap water. All organisms were picked, sorted, identified and enumerated.

In 2019 for the third year, benthic invertebrates were also sampled at selected flowing tributary stations which possessed natural riffle-run areas. At each site one-minute kick samples were collected at one riffle and one run and composited in a single bottle. The sample was preserved with formalin to a concentration of 5%. In the lab the sample was sieved through a 0.5 mm mesh (same as the kick net) and thoroughly washed with tap water before picking and sorting. Following sorting animals were enumerated by taxon and held in ethanol-glycerin. Sampling sites for tributary macroinvertebrate sampling are shown in Figure 1d. Two additional sites, not shown in Figure 1d, were added in 2018: Taylor Run and Timber Branch.

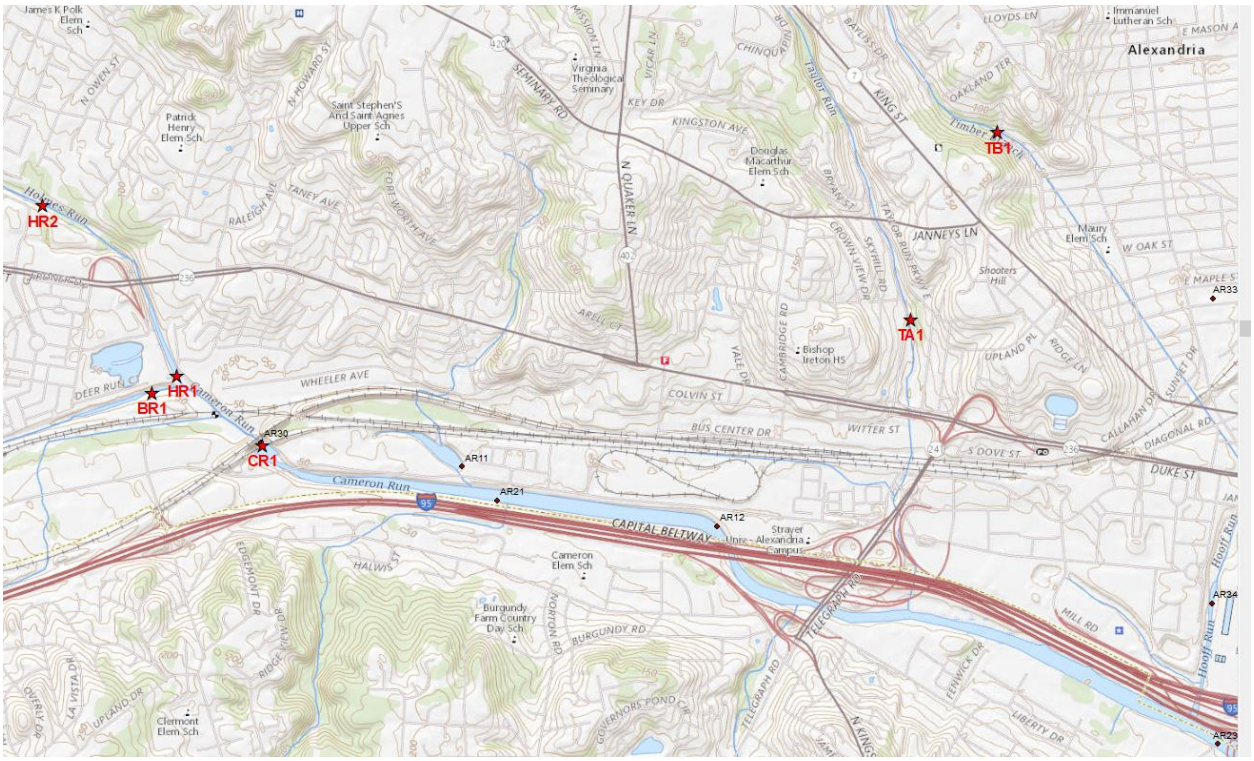

Figure 1d. Benthic sampling stations on flowing tributaries of Cameron Run. CR1: Cameron Run: HR1, HR2: Holmes Run; BR: Backlick Run; IR: Indian Run; TR: Turkeycock Run.

F. Water Quality Mapping (Dataflow)

On two additional dates in 2019 (July 18 and August 18) *in situ* water quality mapping was conducted by slowly transiting through much of the Hunting Creek study area as water was pumped through a chamber containing a YSI 6600 sonde equipped with temperature, specific conductance, dissolved oxygen, pH, turbidity, and chlorophyll probes. Readings were recorded at 15 second intervals along with simultaneous GPS position readings. Every 2 minutes SAV relative abundance by species was recorded and every 4 minutes water samples were collected for extracted chlorophyll and TSS determination. Some areas of the Hunting Creek embayment could not be surveyed due to shallow water or heavy SAV growth. These surveys allowed a much better understanding of spatial patterns in water quality within the Hunting Creek area which facilitated interpretation of data from the fixed stations. This approach is in wide use in the Chesapeake Bay region by both Virginia and Maryland under the name “dataflow”.

G. Data Analysis

Data for each parameter were entered into spreadsheets (Excel or SigmaPlot) for graphing of temporal and spatial patterns. SYSTAT was used for statistical calculations and to create illustrations of the water quality mapping cruises. JMP v8.0.1was used for fish graphs. Other data analysis approaches are explained in the text.

RESULTS

A. Climatic and Hydrologic Factors - 2019

In 2019 temperature was above normal for the entire study period from April through September (Table 3). There were 41 days with maximum temperature above 32.2°C (90°F) in 2019 which is well above the median number over the past decade. Precipitation closer to normal in 2019 than in the extremely wet year 2018. However, was again well above normal in 2019. The largest daily rainfall total was 10.2 cm on July 21 which followed a 7.1 cm day on July 17.

Table 2. Meteorological Data for 2019. National Airport. Monthly Summary.

	Air Temp (°C)		Precipitation (cm)	
MONTH				
March	8.2	(8.1)	10.2	(9.1)
April	16.9	(13.4)	5.7	(7.0)
May	21.7	(18.7)	12.6	(9.7)
June	24.7	(23.6)	10.8	(8.0)
July	27.8	(26.2)	16.5	(9.3)
August	26.7	(25.2)	5.0	(8.7)
September	24.7	(21.4)	0.6	(9.6)
October	17.8	(14.9)	16.9	(8.2)
November	7.8	(9.3)	1.4	(7.7)
December	5.7	(4.2)	3.3	(7.8)

Note: 2019 monthly averages or totals are shown accompanied by long-term monthly averages (1971-2000). Source: Local Climatological Data. National Climatic Data Center, National Oceanic and Atmospheric Administration.

River and stream flow in 2019 was above average for most months in both the Potomac mainstem and in Cameron Run and well average at both stations in July (Table 3).

Table 3. Monthly mean discharge at USGS Stations representing freshwater flow into the study area. (+) 2019 month > 2x Long Term Avg. (-) 2019 month < ½ Long Term Avg.

	Potomac River at Little Falls (cfs)		**Cameron Run at Wheeler Ave (cfs)**	
	2019	**Long Term Average**	**2019**	**Long Term Average**
March	30848	23600	93.9	55
April	22170	20400	2.6	42
May	26419	15000	66.5	41
June	7539	9030	42.9	38
July	8902 (+)	4820	71.6 (+)	31
August	3784	4550	16.5	28
September	2044 (-)	5040	4.5 (-)	38
October	2560 (-)	5930	44.2	33

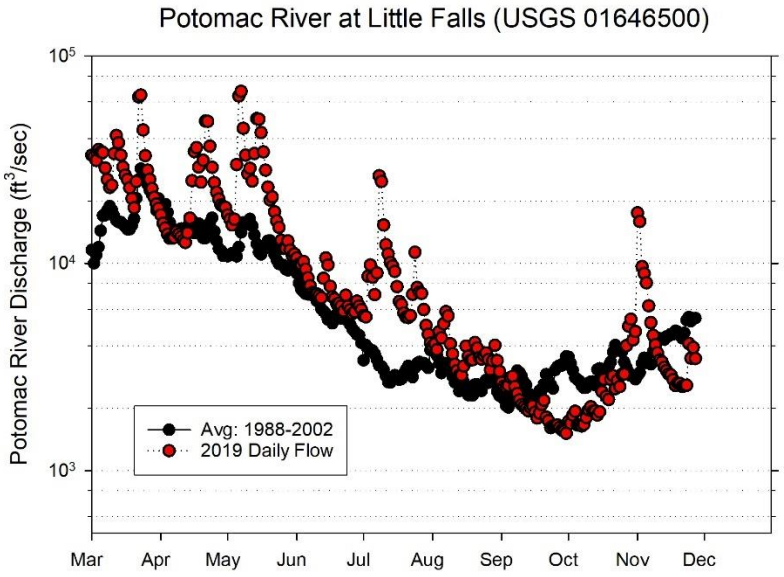

In a tidal freshwater system like the Potomac River, river flow entering from upstream is important in maintaining freshwater conditions and also serves to bring in dissolved and particulate substances from the watershed. High freshwater flows may also flush planktonic organisms downstream and bring in suspended sediments that decrease water clarity. The volume of river flow per unit time is referred to as "river discharge" by hydrologists. Note the general long term seasonal pattern of higher discharges in winter and spring and lower discharges in summer and fall.

Figure 2. Mean Daily Discharge: Potomac River at Little Falls (USGS Data). Month tick is at the beginning of the month.

These same patterns were seen in the graphs of daily river flow when compared to long-term averages. The long term average shows a steadily decreasing trend from April through September. In 2019 this general seasonal pattern was observed except for the notable surge in July which has the potential to strongly impact the ongoing growth of SAV and plankton in the river. Discharge in Cameron Run showed a stronger summer decline in 2019 than in previous years.

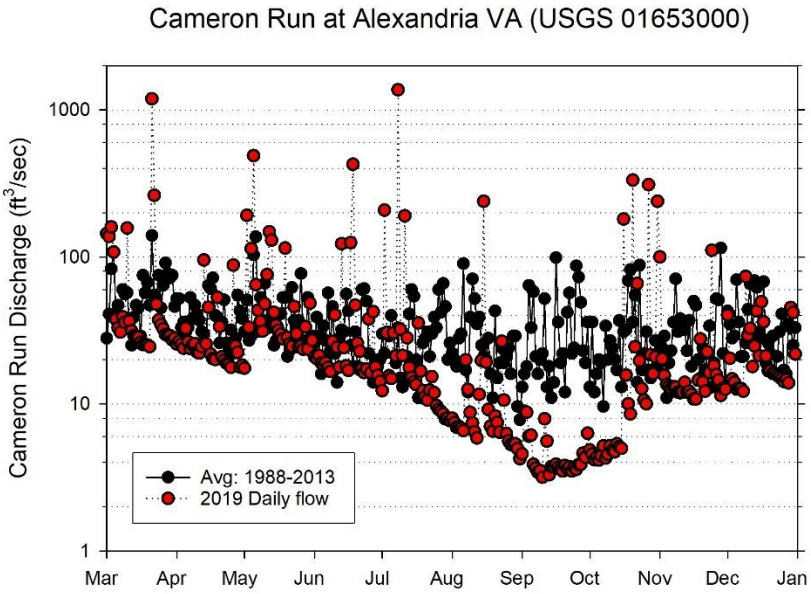

In the Hunting Creek region of the tidal Potomac, freshwater discharge is occurring from both the major Potomac River watershed upstream (measured at Little Falls) and from immediate tributaries, principally Cameron Run which empties directly into Hunting Creek. The gauge on Cameron Run at Wheeler Avenue is located just above the head of tide and covers most area which contributes runoff directly to the Hunting Creek embayment from the watershed. The contributing area to the Wheeler Ave gauge is 33.9 sq mi. (USGS)

.

Figure 3. Mean Daily Discharge: Cameron Run at Alexandria (Wheeler Ave) (USGS Data).

B. Physico-chemical Parameters: Embayment and River Stations – 2019

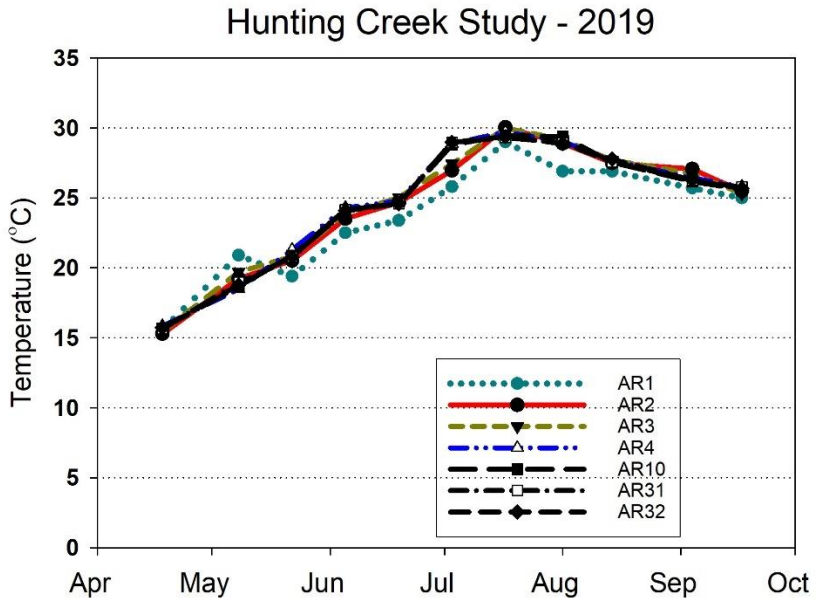

Water temperature is an important factor affecting both water quality and aquatic life. In a well-mixed system like the tidal Potomac, water temperatures are generally fairly uniform with depth. In a shallow mixed system such as the tidal Potomac, water temperature often closely tracks daily changes in air temperature.

Figure 4. Water Temperature (ºC). GMU Field Data. Month tick is at first day of month.

In 2019 water temperature followed the typical seasonal pattern at all stations (Figure 4). Temperatures increased steadily from April to mid-July approaching 30°C. A fairly steady decline was observed through August and September. These patterns were similar to the general trends in mean air temperature (Figure 5).

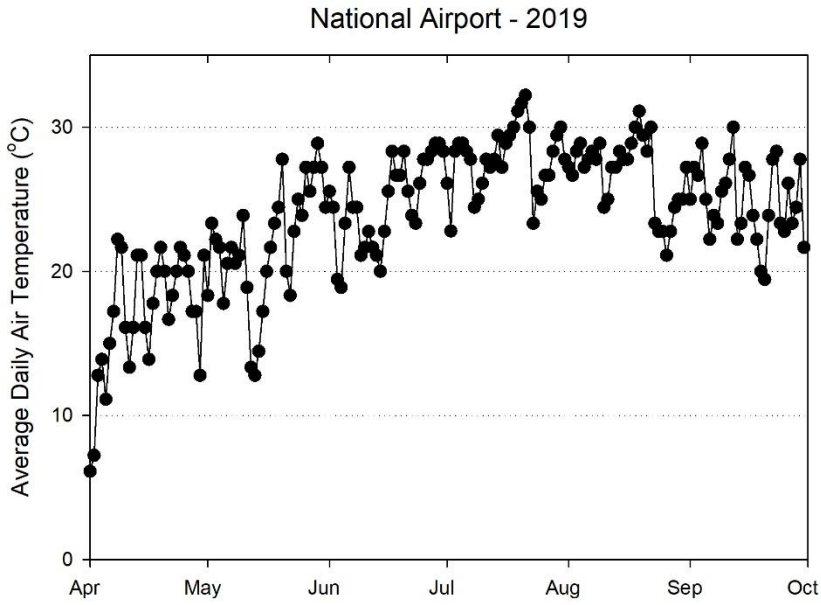

Mean daily air temperature (Figure 5) was a good predictor of water temperature (Figure 4).

Figure 5. Average Daily Air Temperature (ºC) at Reagan National Airport.

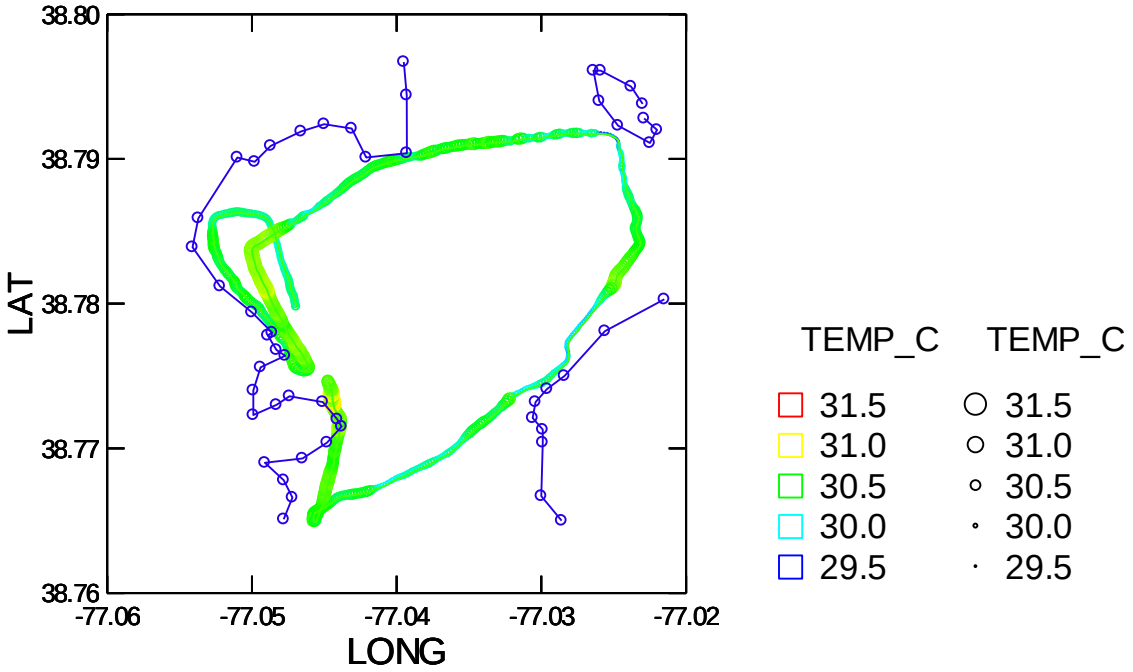

Figure 6a. Water Quality Mapping. July 18, 2019. Temperature (°C).

Mapping of water temperature was conducted on two dates in 2019: July 18 and August 19. In July water temperature through the study area was about 30°C (Figure 6a). In August the range of temperatures was similar. A zone of slightly higher temperatures was observed at the southern end of the study area (Figure 6b).

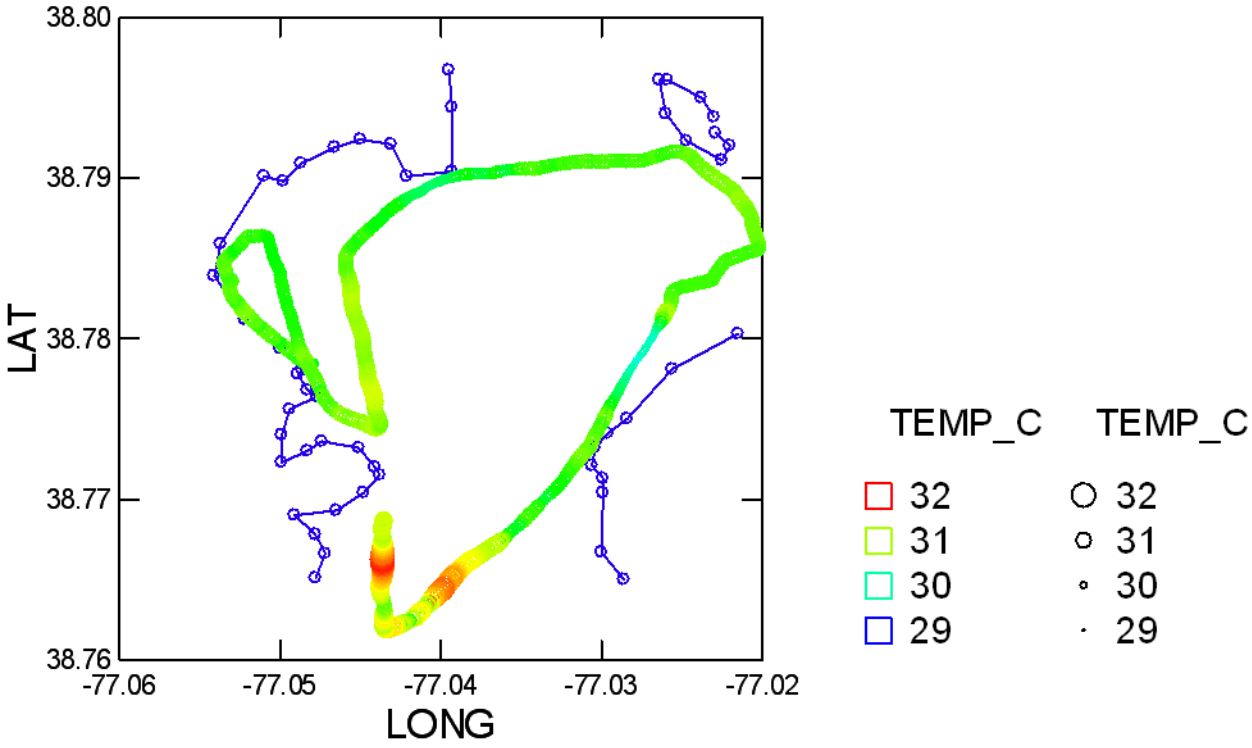

Figure 6b. Water Quality Mapping. August 19, 2019. Temperature (°C).

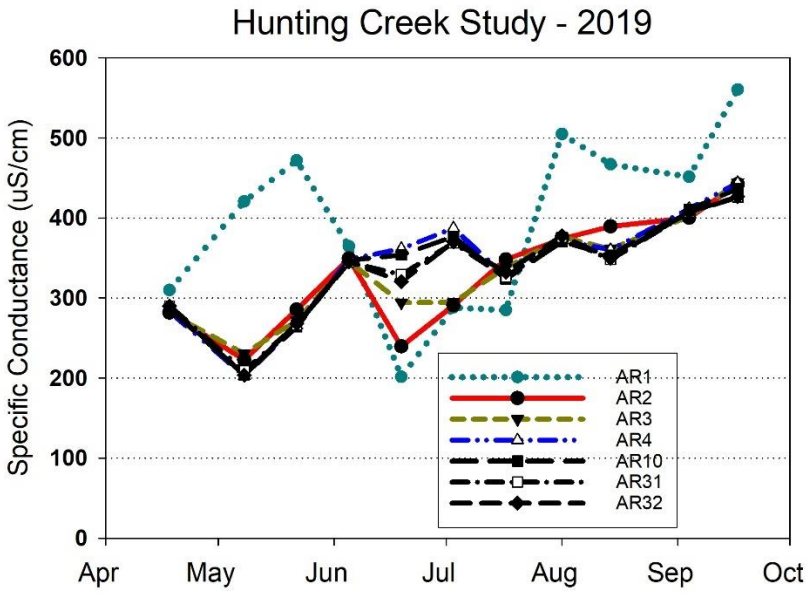

Specific conductance measures the capacity of the water to conduct electricity standardized to 25°C. This is a measure of the concentration of dissolved ions in the water. In freshwater, conductivity is relatively low. Ion concentration generally increases slowly during periods of low freshwater inflow and decreases during periods of high freshwater inflow. Sewage treatment facilities can be a source of elevated conductivity. In winter road salts can be a major source of conductivity in urban streams.

Figure 7. Specific Conductance (µS/cm). GMU Field Data. Month tick is at first day of month.

Specific conductance was often substantially higher at AR1 than at the other stations reflecting its location just downstream of the Alex Renew outfall (Figure 7). AR1 was lower in late June and July, perhaps due to higher flow in Cameron Run. There was a general seasonal increase at most stations. As one of the major ions contributing to specific conductance, chloride exhibited much higher values at AR1 than at the other sites (Figure 8). The same seasonal patterns were found for chloride as for specific conductance.

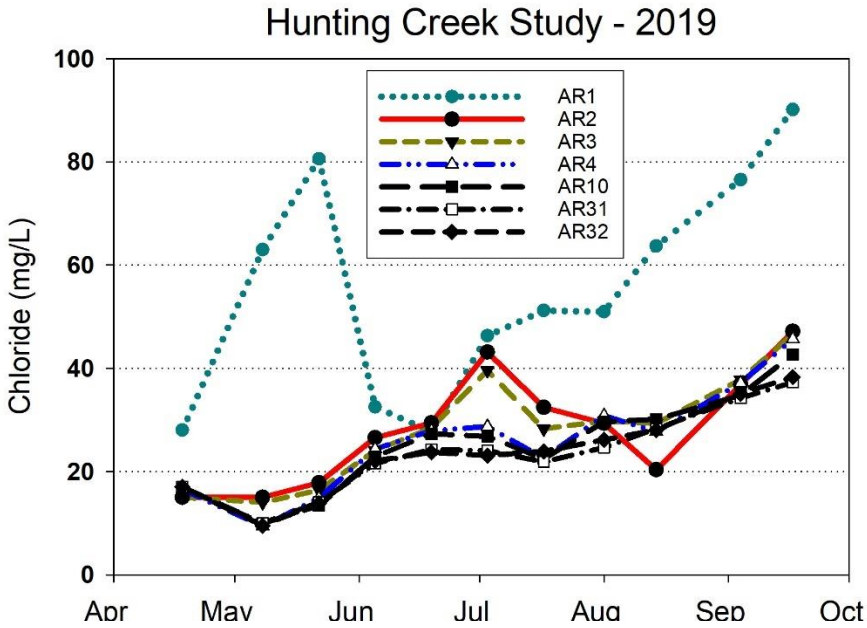

Chloride ion (Cl-) is a principal contributor to conductance. Major sources of chloride in the study area are sewage treatment plant discharges, road salt, and brackish water from the downriver portion of the tidal Potomac. Chloride concentrations observed in the Hunting Creek area are very low relative to those observed in brackish, estuarine, and coastal areas of the Mid-Atlantic region. Chloride may increased slightly in late summer or fall when brackish water from down estuary may reach the area as freshwater discharge declines.

Figure 8. Chloride (mg/L). Alexandria Renew Lab Data. Month tick is at first day of month.

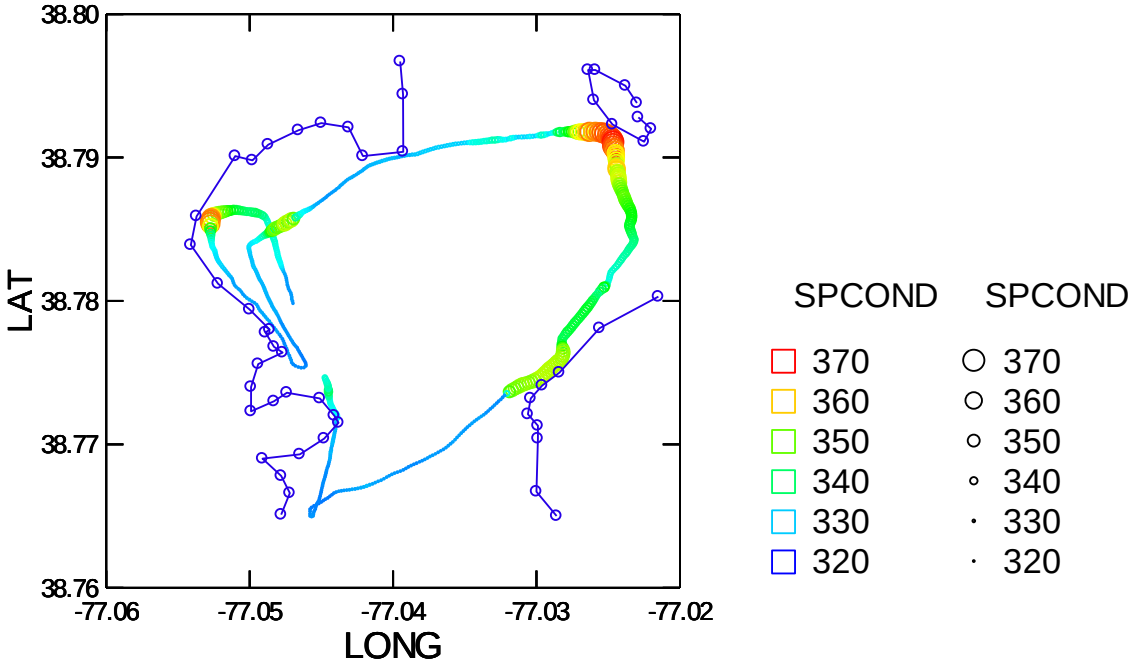

Figure 9a. Water Quality Mapping. July 18, 2019. Specific conductance (µS).

Mapping of specific conductance on July 18 showed that values were generally the lowest in the outer part of Hunting Creek and in the western side of the mainstem (Figure 9a). The somewhat elevated values found in the shoreward part of Hunting Creek and the Maryland side of the channel can be explained by proximity to the Alex Renew and Blue Plains discharge sites, respectively. On August 19 specific conductance was slightly lower throughout the Hunding Creek embayment and somwhat higher in the river channel (Figure 9b).

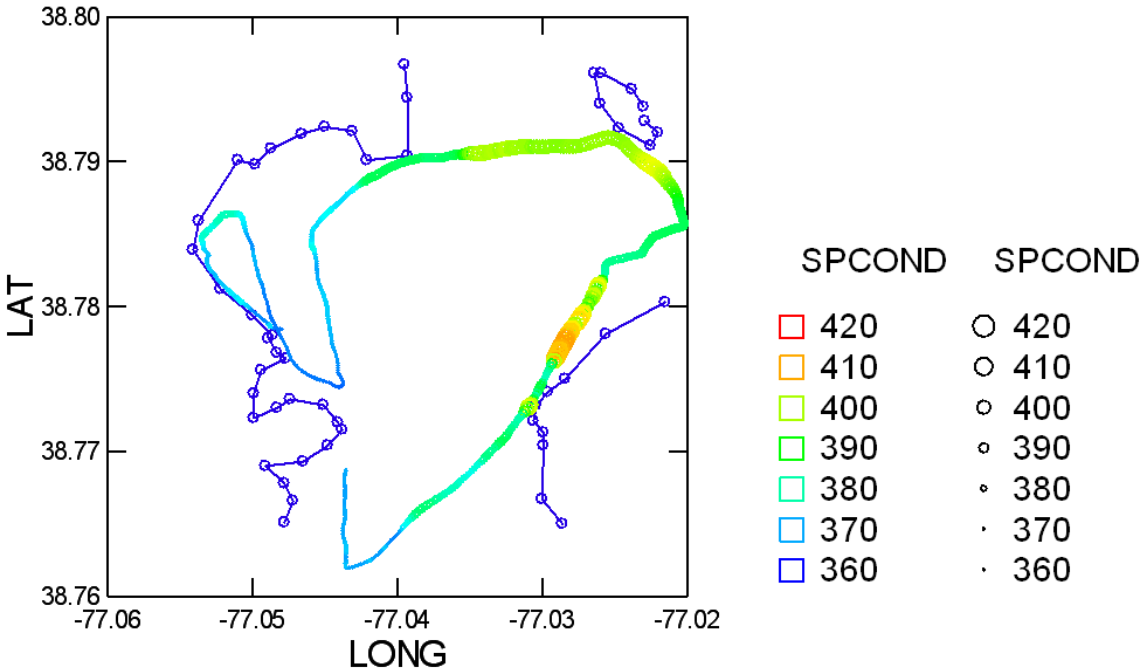

Figure 9b. Water Quality Mapping. August 19, 2019. Specific conductance (µS).

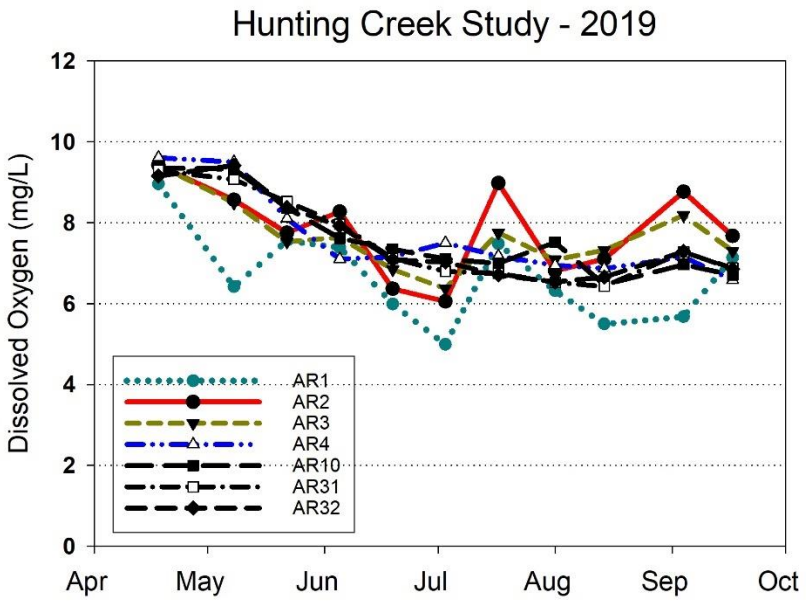

Oxygen dissolved in the water is required by freshwater animals for survival. The standard for dissolved oxygen (DO) in most surface waters is 5 mg/L. Oxygen concentrations in freshwater are in balance with oxygen in the atmosphere, but oxygen is only weakly soluble in water so water contains much less oxygen than air. This solubility is determined by temperature with oxygen more soluble at low temperatures.

Figure 10. Dissolved Oxygen (mg/L). GMU Field Data. Month tick is at first day of month.

The general pattern for dissolved oxygen (mg/L) was a seasonal decline from May through early July and steady values through September (Figure 10). Looking at DO as percent saturation (Figure 11), the basic seasonal pattern was less pronounced indicating that temperature was the main variable driving the seasonal pattern in DO as mg/L. DO rarely exceeded 100% and was below 80% only rarely indicating that photosynthesis and respiration were not major factors.

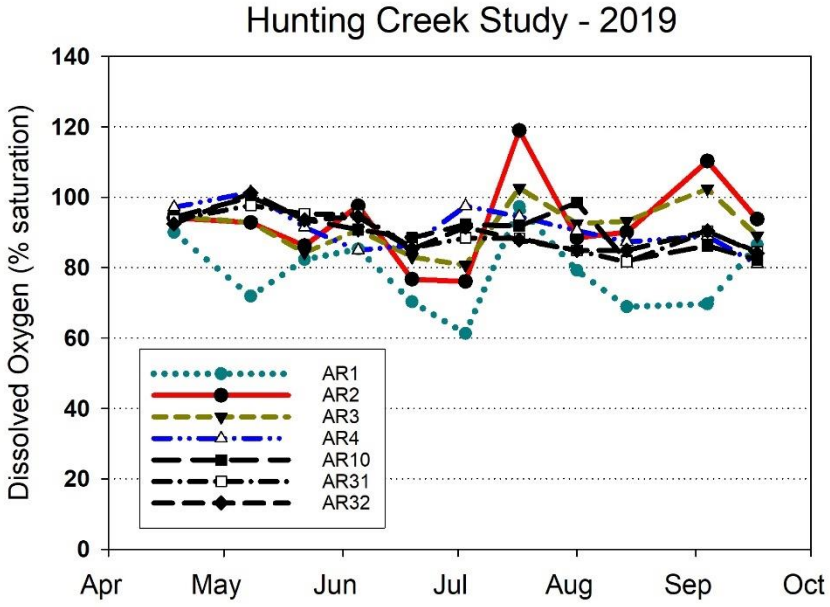

The temperature effect on oxygen concentration can be removed by calculating DO as percent saturation. This allows examination of the balance between photosynthesis and respiration both of which also impact DO. Photosynthesis adds oxygen to the water while respiration removes it. Values above 120% saturation are indicative of intense photosynthesis while values below 80% reflect a preponderance of respiration or decomposition.

Figure 11. Dissolved Oxygen (% saturation). GMU Field Data. Month tick is at first day.

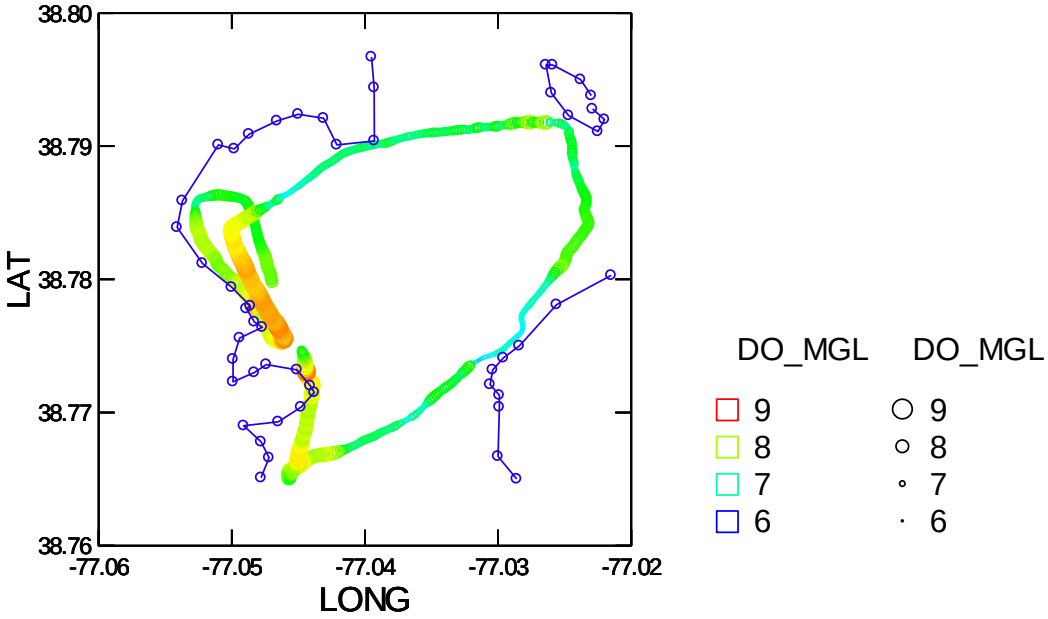

Figure 12a. Water Quality Mapping. July 18, 2019. Dissolved oxygen (mg/L).

On July 18 dissolved oxygen (both mg/L and percent saturation) exhibited clear spatial patterns (Figures 12a&b). Levels were lowest in the river running about 90% saturation and 7-8 mg/L. Higher levels were found in the most westerly part of Hunting Creek attaining 9 mg/L and nearly 120% saturation. While SAV was limited in Hunting Creek and the adjacent mainstem in 2019, there were some growths in the shallows which might expain the spatial pattern observed.

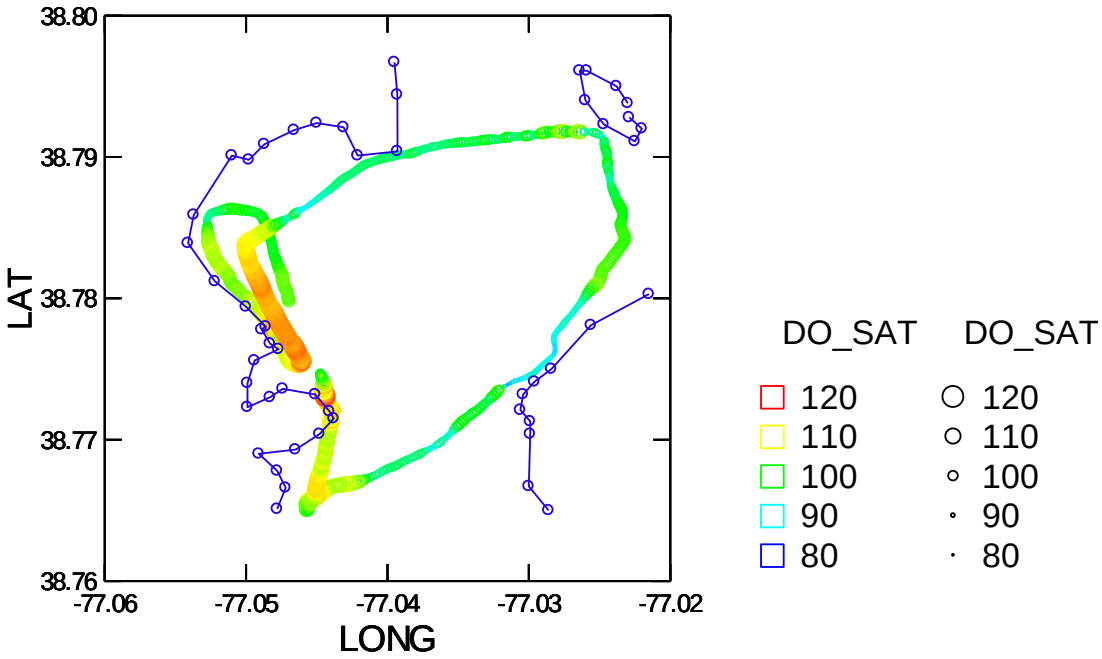

Figure 12b. Water Quality Mapping. July 18, 2019. Dissolved oxygen (percent saturation).

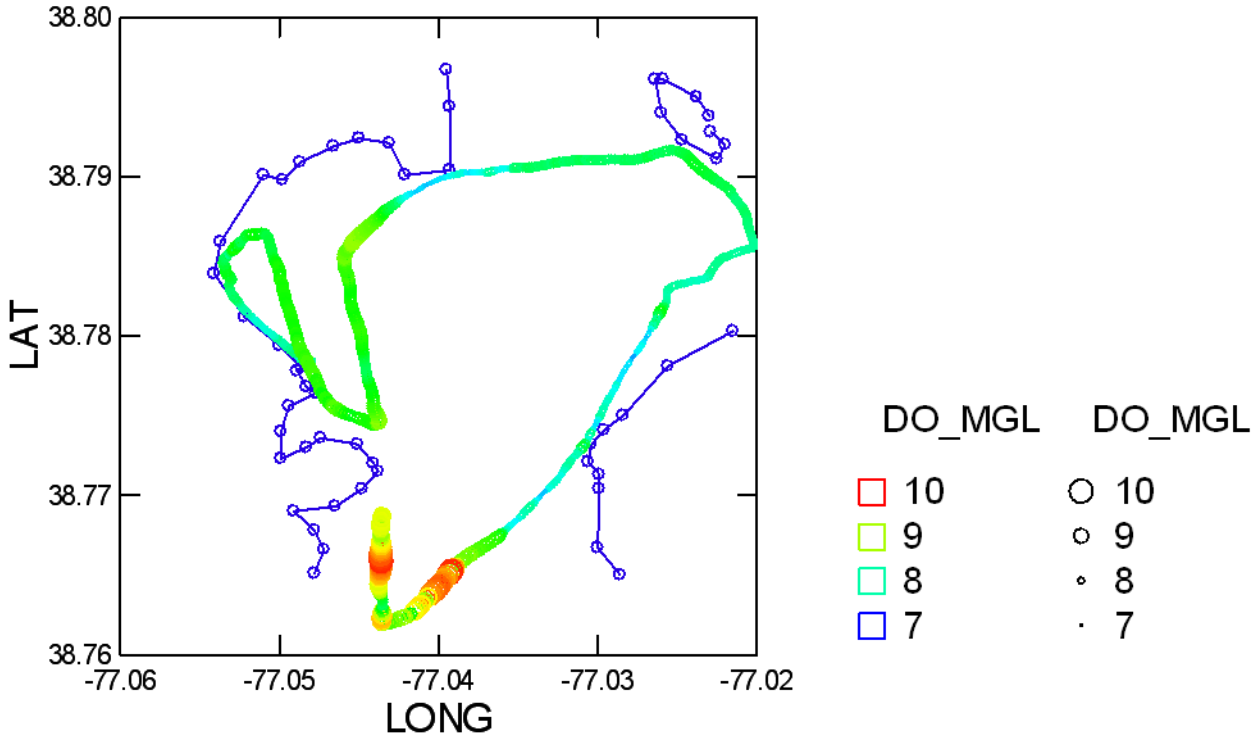

Figure 13a. Water Quality Mapping. August 19, 2019. Dissolved oxygen (mg/L).

On August 18. DO concentrations showed a marked increase on the Virginia side of the river at the southern end of the study area with values approaching 140% saturation and 10 mg/L (Figures 13a,b). This area corresponded to the zone of slightly higher temperatures shown above.

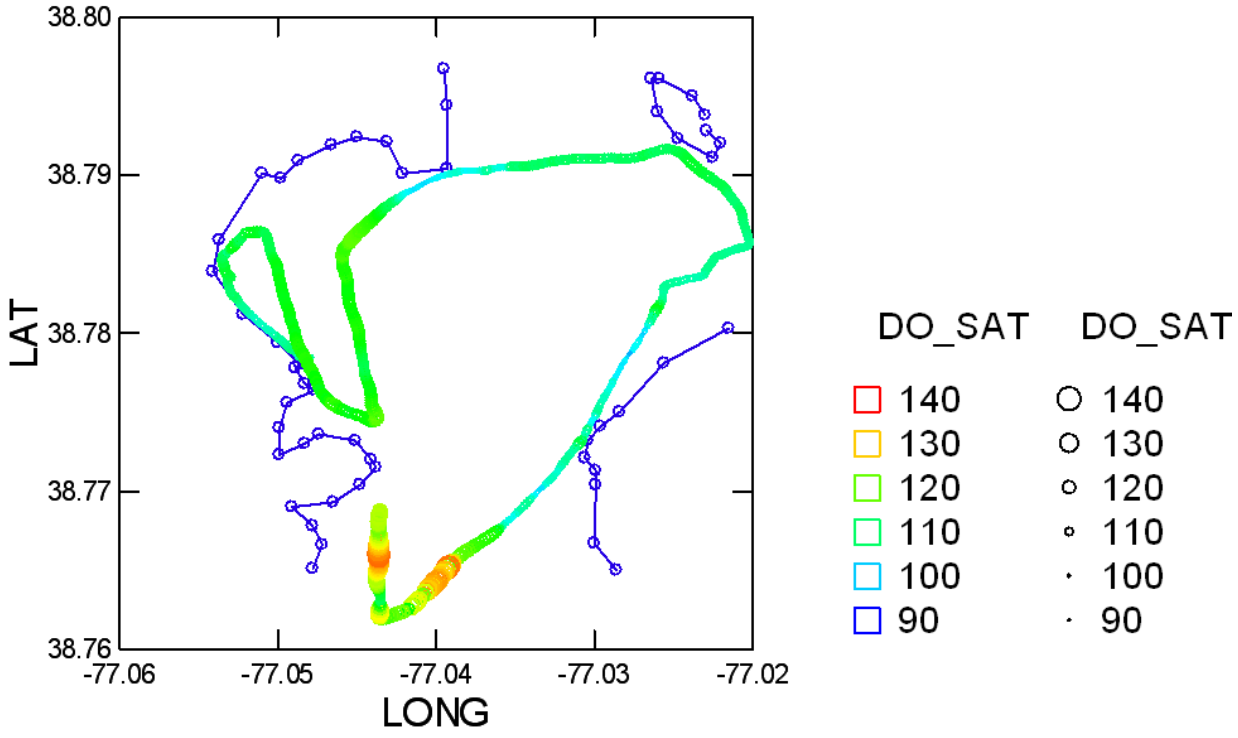

Figure 13b. Water Quality Mapping. August 19, 2019. Dissolved oxygen (percent saturation).

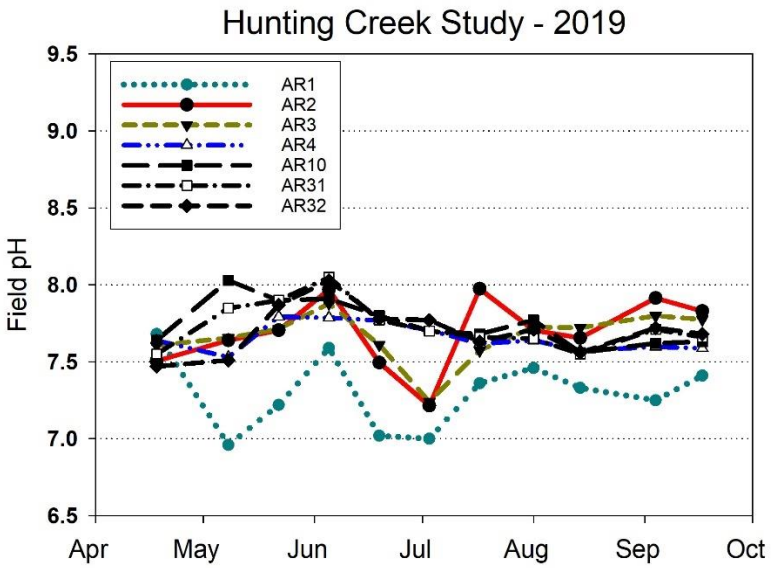

pH is a measure of the concentration of hydrogen ions (H+) in the water. Neutral pH in water is 7. Values between 6 and 8 are often called circumneutral, values below 6 are acidic and values above 8 are termed alkaline. Like DO, pH is affected by photosynthesis and respiration. In the tidal Potomac, pH above 8 indicates active photosynthesis and values above 9 indicate intense photosynthesis. A decrease in pH following a rainfall event may be due to acids in the rain or in the watershed.

Figure 14. pH. GMU Field Data. Month tick is at first day of month.

In 2019 pH values remained in a fairly narrow range (7.2-8.0) with little seasonal pattern at most sample stations (Figure 14, 15). pH was consistently lower at AR1, but the values at the other stations were very similar.

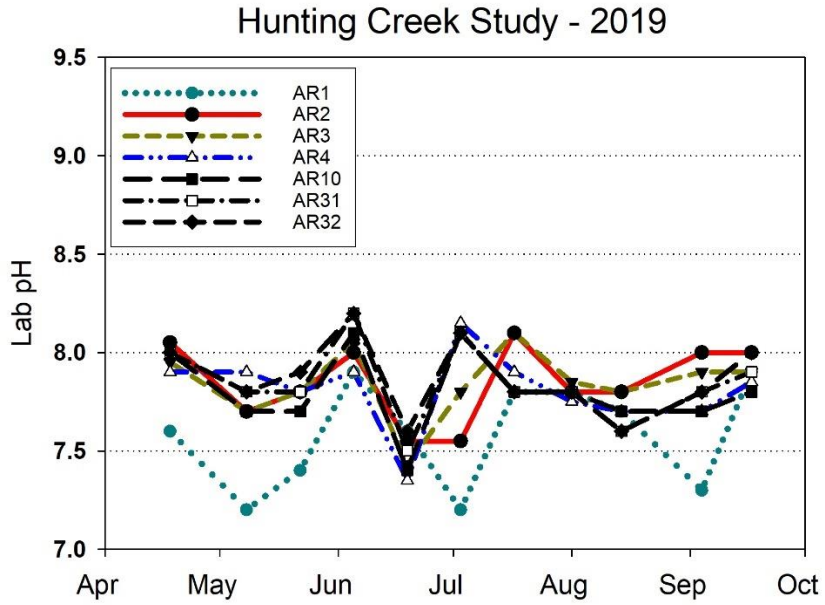

pH may be measured in the field or in the lab. Field pH is more reflective of in situ conditions while lab pH is done under more stable and controlled laboratory conditions and is less subject to error. Newer technologies such as the Hydrolab and YSI sondes used in GMU field data collection are more reliable than previous field pH meters and should give results that are most representative of values actually observed in the river.

Figure 15. pH. AlexRenew Lab Data. Month tick is at first day of month.

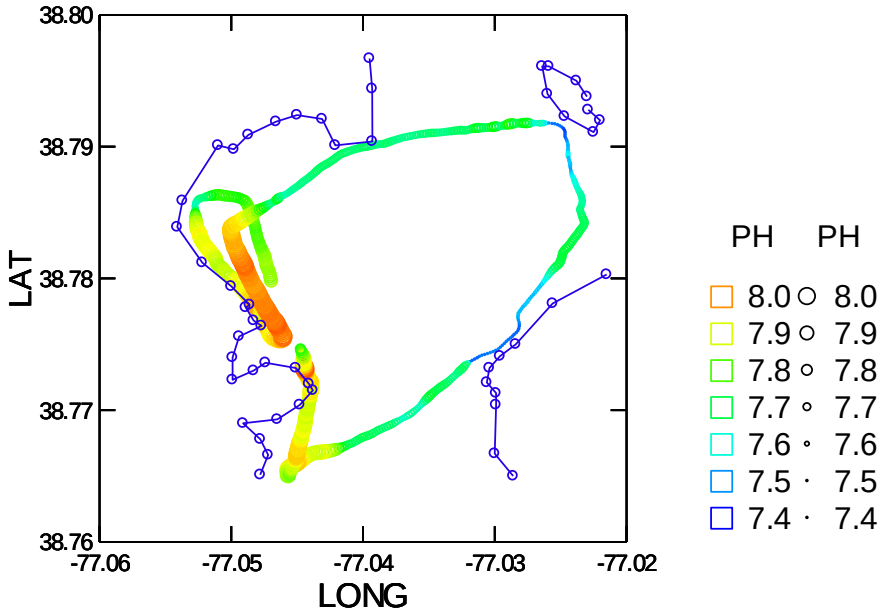

Figure 16a. Water Quality Mapping. July 18, 2019. pH.

Water quality mapping of pH on July 18 (Figure 16a) showed showed a pattern similar to that of DO. Values were substantially higher in inner Hunting Creek than elsewhere attaining 8.0 indicating substantial photosynthesis. In August (Figure 16b) overall spatial patterns were similar, but peak values were observed down river on the Virginia side at the same place as elevated DO's indicating increased photosynthesis as a cause.

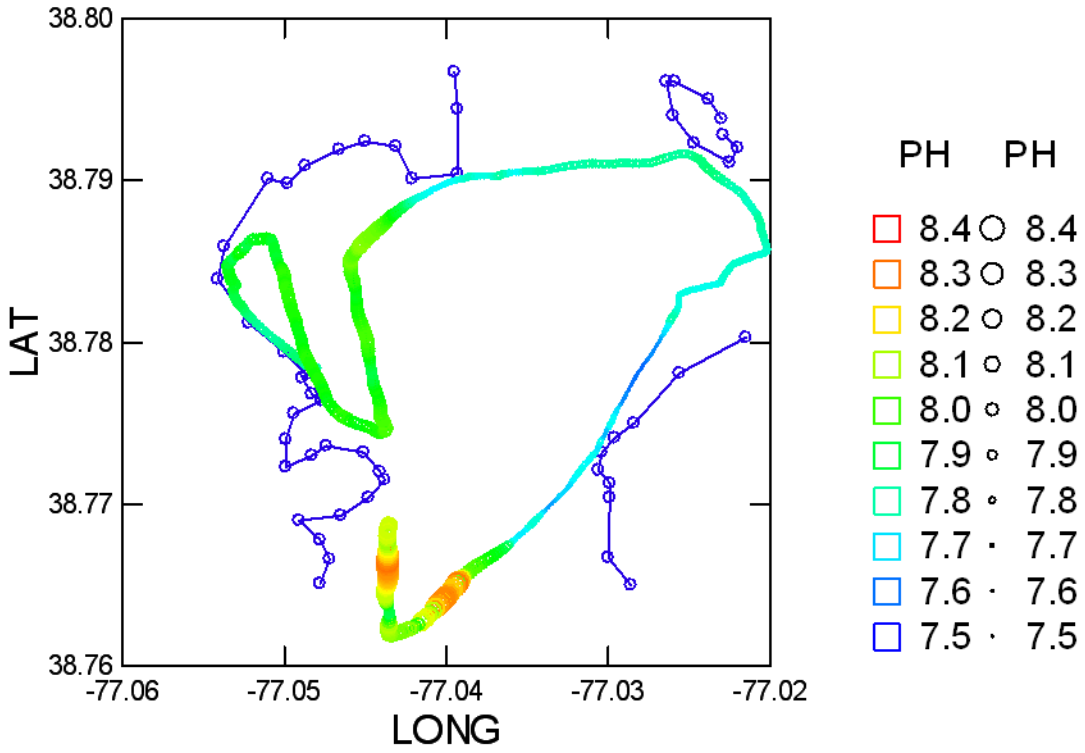

Figure 16b. Water Quality Mapping. August 19, 2019. pH.

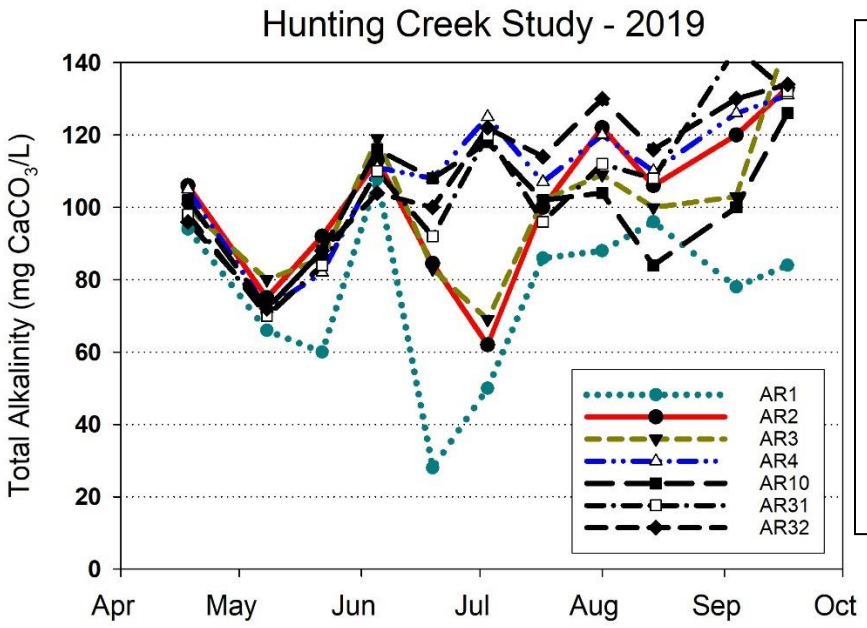

Total alkalinity measures the amount of bicarbonate and carbonate dissolved in the water. In freshwater this corresponds to the ability of the water to absorb hydrogen ions (acid) and still maintain a near neutral pH. Alkalinity in the tidal freshwater Potomac generally falls into the moderate range allowing adequate buffering without carbonate precipitation.

Figure 17. Total Alkalinity (mg/L as $CaCO_3$). AlexRenew Lab data. Month tick is at first day.

Total alkalinity exhibited an overall pattern of seasonal increase at most stations (Figure 17). The river stations (AR4, AR10, AR31, and AR32) were more consistent in their seasonal increase while a marked decline was observed at embayment stations AR2, AR3, and, particularly AR1 in late July and early July. Water clarity as reflected by Secchi disk did not show strong seasonal patterns, but was consistently higher at the river stations than in the Hunting Creek embayment (Figure 18). Water clarity in Hunting Creek (AR2 and AR3) dipped strongly early May and never recovered which had a negative impact on SAV development.

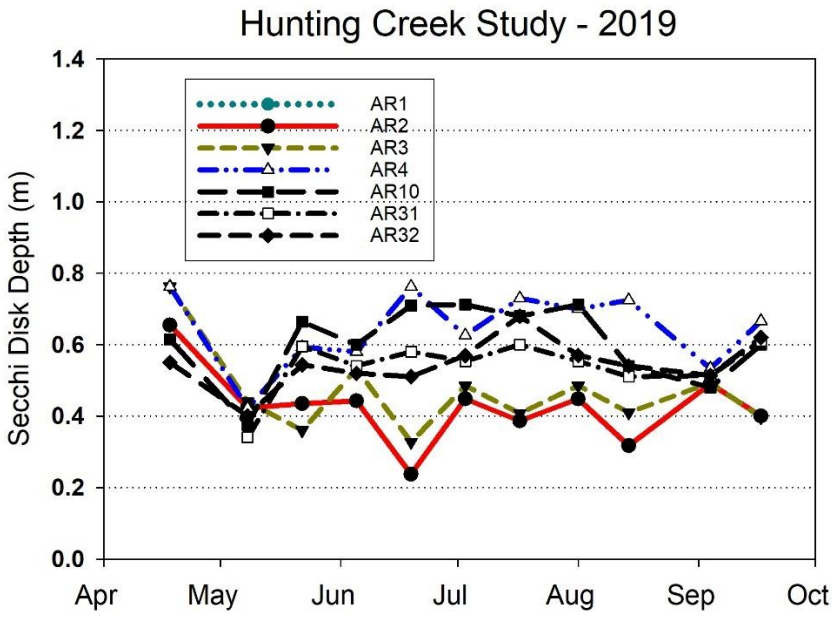

Secchi Depth is a measure of the transparency of the water. The Secchi disk is a flat circle of thick sheet metal or plywood about 6 inches in diameter which is painted into alternate black and white quadrants. It is lowered on a calibrated rope or rod to a depth at which the disk disappears. This depth is termed the Secchi Depth. This is a quick method for determining how far light is penetrating into the water column. Light is necessary for photosynthesis and thereby for growth of aquatic plants and algae.

Figure 18. Secchi Disk Depth (m). GMU Field Data. Month tick is at first day of month.

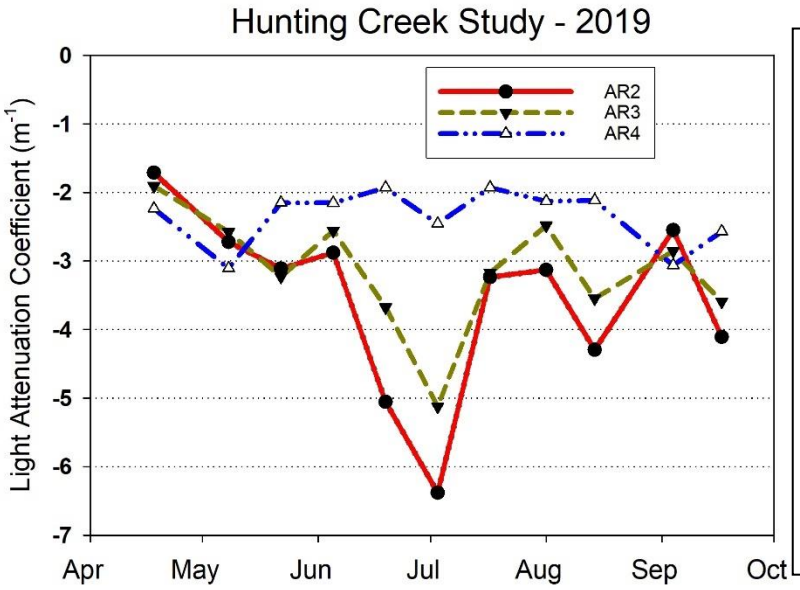

Light Attenuation is another approach to measuring light penetration. This is determined by measuring light levels at a series of depths starting near the surface. The resulting relationship between depth and light is fit to a semi-logarithmic curve and the resulting slope is called the light attenuation coefficient. This relationship is called Beer's Law. It is analogous to absorbance on a spectrophotometer. The greater the light attenuation, the faster light is absorbed with depth. More negative values indicate greater attenuation. Greater attenuation is due to particulate and dissolved material which absorbs and deflects light.

Figure 19. Light Attenuation Coefficient (m^{-1}). GMU Field Data. Month tick is at first day of month.

Light attenuation coefficient data reflected a very similar pattern with an even more marked response to the runoff events and elevated flows in late June and early July (Figure 19). As in 2018, light attenuation (due primarily to suspended sediment from runoff events) was greater than normal at the Hunting Creek embayment stations. Turbidity also showed this effect with values increasing markedly in late June and early July (Figure 20).

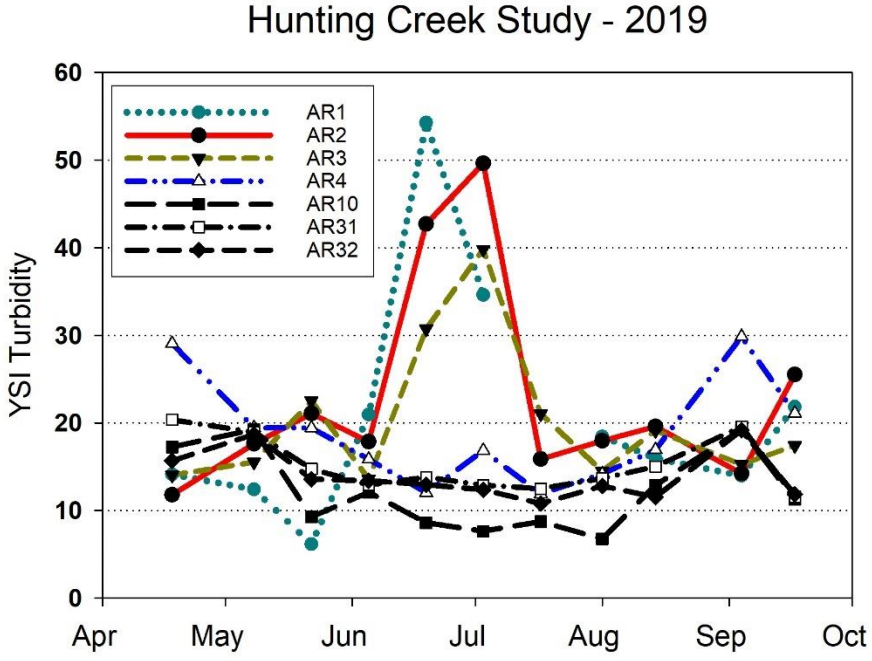

Turbidity is yet a third way of measuring light penetration. Turbidity is a measure of the amount of light scattering by the water column. Light scattering is a function of the concentration and size of particles in the water. Small particles scatter more light than large ones (per unit mass) and more particles result in more light scattering than fewer particles.

Figure 20. Turbidity (NTU). GMU Lab Data. Month tick is at first day of month.

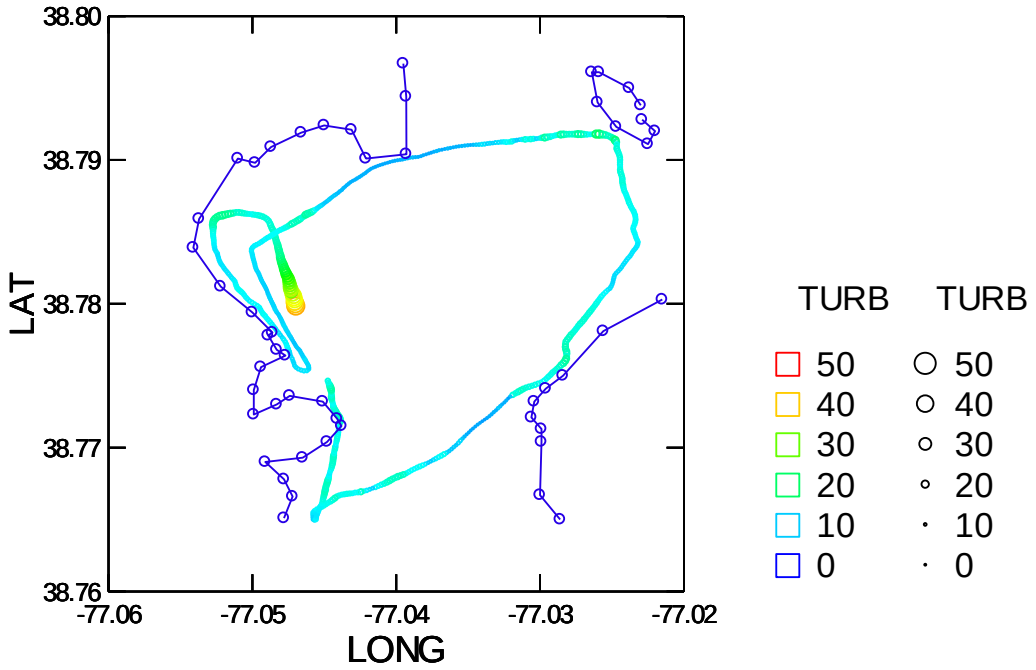

Figure 21a. Water Quality Mapping. July 18, 2019. Turbidity YSI.

By the time of the July 18 mapping, turbidity had declined greatly and was below 20 NTU through out the study area (Figure 21a). On August 19, turbidity was agin low over most of the study area except for increased values observed at the southern end on the Virginia side at the same spot as higher DO and pH levels Figure 21b).

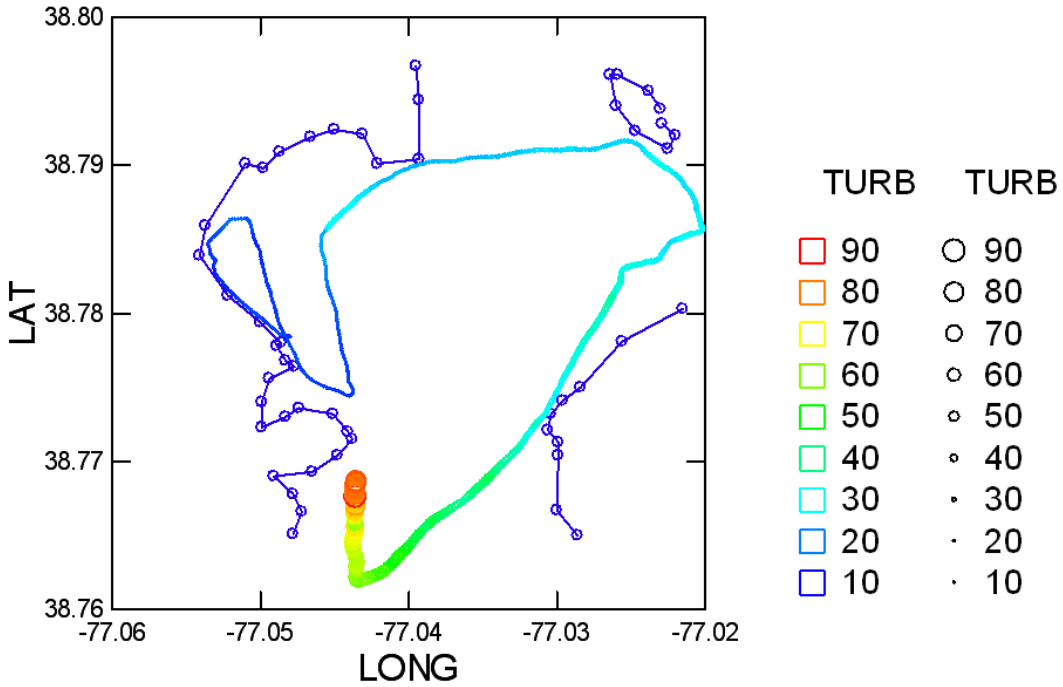

Figure 21b. Water Quality Mapping. August 19, 2019. Turbidity YSI.

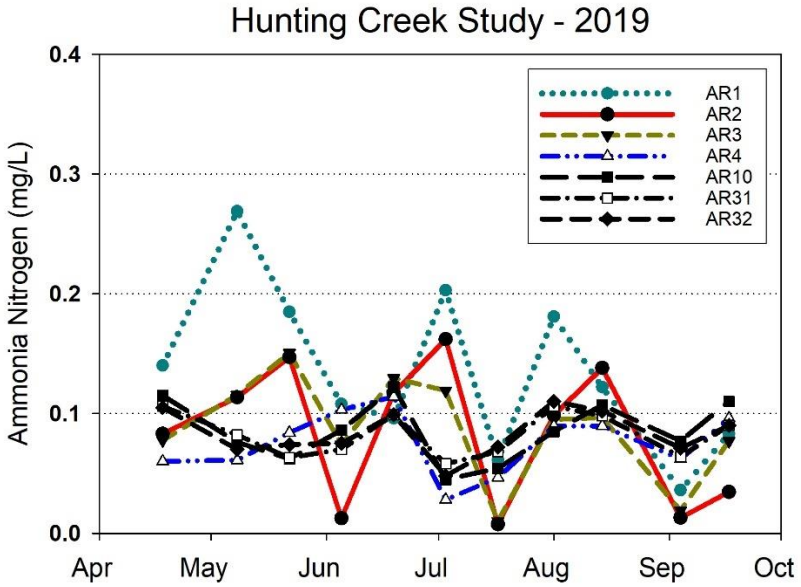

Ammonia nitrogen measures the amount of ammonium ion (NH_4^+) and ammonia gas (NH_3) dissolved in the water. Ammonia nitrogen is readily available to algae and aquatic plants and acts to stimulate their growth. While phosphorus is normally the most limiting nutrient in freshwater, nitrogen is a close second. Ammonia nitrogen is rapidly oxidized to nitrate nitrogen when oxygen is present in the water so high ammonia levels suggest proximity to a source.

Figure 22. Ammonia Nitrogen (mg/L). AlexRenew Lab Data. Month tick is at first day of month.

Ammonia nitrogen was consistently low (<0.2 mg/L) for the entire study period (Figure 22). A slight seasonal pattern was seen at all stations with a general decline. Nitrate nitrogen levels also showed a general pattern of decrease through the year starting near 1.5 mg/L and ending below 1.0 mg/L (Figure 23).

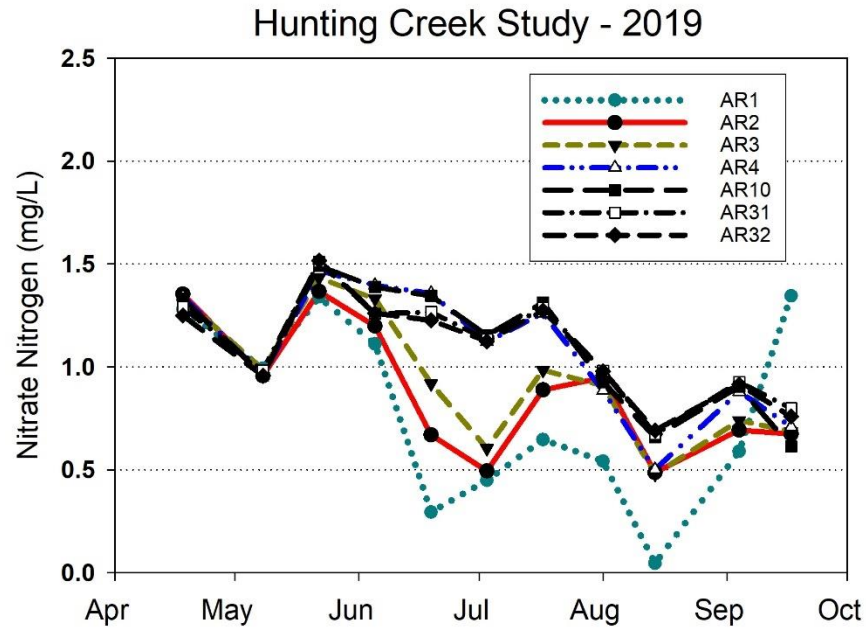

Nitrate Nitrogen refers to the amount of N that is in the form of nitrate ion (NO_3^-). Nitrate ion is the most common form of nitrogen in most well oxidized freshwater systems. Nitrate concentrations are increased by input of wastewater, nonpoint sources, and oxidation of ammonia in the water. Nitrate concentrations decrease when algae and plants are actively growing and removing nitrogen as part of their growth.

Figure 23. Nitrate Nitrogen (mg/L). AlexRenew Lab Data. Month tick is at first day of month.

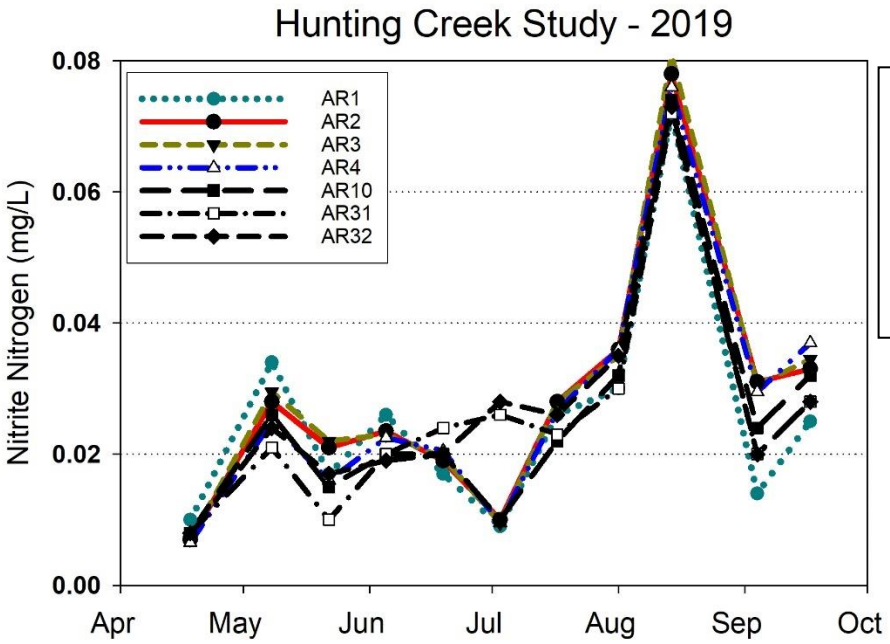

Nitrite nitrogen consists of nitrogen in the form of nitrite ion (NO_2^-). Nitrite is an intermediate in the oxidation of ammonia to nitrate, a process called nitrification. Nitrite is usually in very low concentrations unless there is active nitrification.

Figure 24. Nitrite Nitrogen (mg/L). AlexRenew Lab Data. Month tick is at first day of month.

Nitrite nitrogen was generally low (<0.03 mg/L) throughout the year (Figure 24). A clear spike was observed in mid-August. Organic nitrogen values were generally in the range of 0.2-1.0 mg/L with a gradual increase from May through September (Figure 25). AR1 was generally higher than the other stations. And this was especially true in early September.

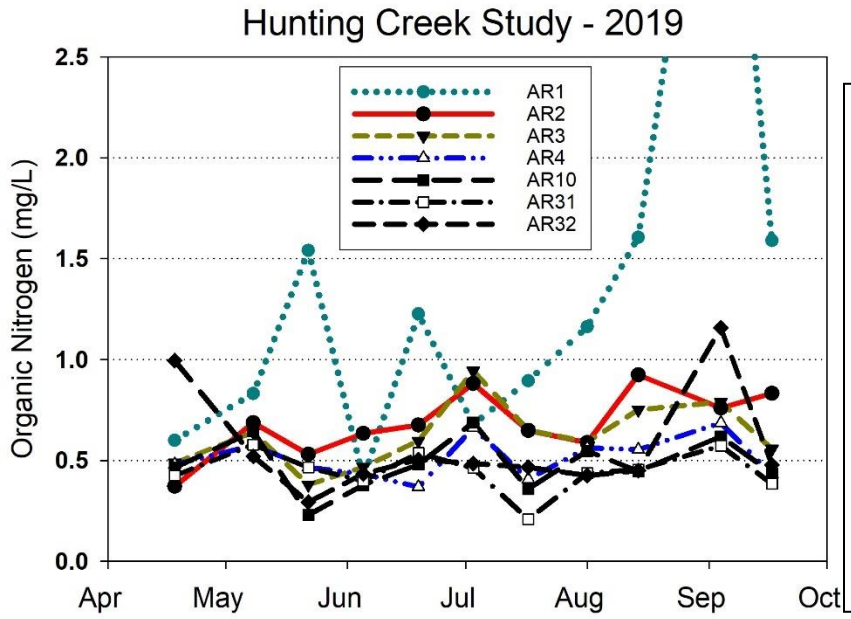

Organic nitrogen measures the nitrogen in dissolved and particulate organic compounds in the water. Organic nitrogen comprises algal and bacterial cells, detritus (particles of decaying plant, microbial, and animal matter), amino acids, urea, and small proteins. When broken down in the environment, organic nitrogen results in ammonia nitrogen. Organic nitrogen is determined as the difference between total Kjeldahl nitrogen and ammonia nitrogen.

Figure 25. Organic Nitrogen (mg/L). AlexRenew Lab Data. Month tick is at first day of month.

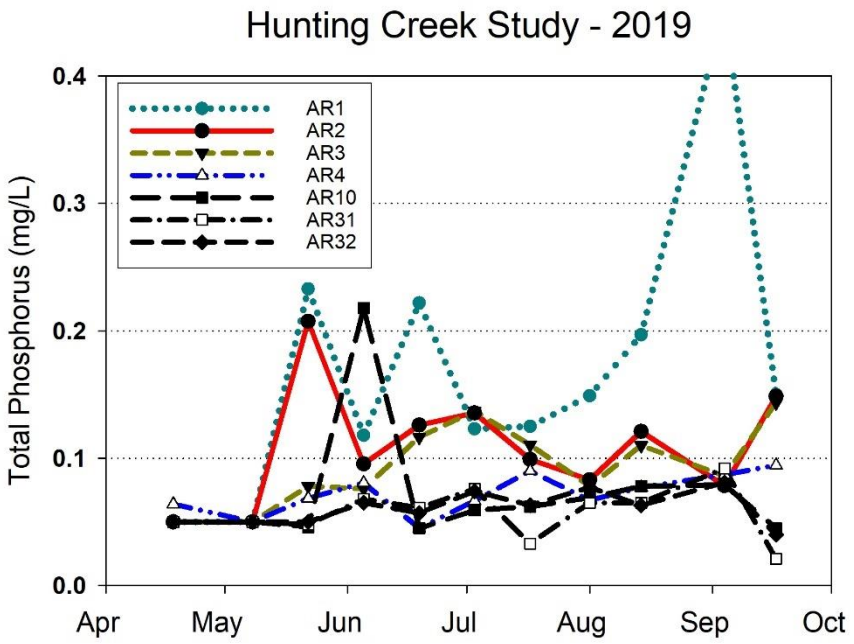

Phosphorus (P) is often the limiting nutrient in freshwater ecosystems. As such the concentration of P can set the upper limit for algal growth. Total phosphorus is the best measure of P availability in freshwater since much of the P is tied up in biological tissue such as algal cells. Total P includes phosphate ion (PO_4^{-3}) as well as phosphate inside cells and phosphate bound to inorganic particles such as clays.

Figure 26. Total Phosphorus (mg/L). AlexRenew Lab Data. Month tick is at first day of month.

Total phosphorus did not exhibit a clear seasonal pattern in 2019, but rose and fell over the year, probably in response to storm flows especially at AR2 and AR3 (Figure 26). AR1 total P spiked in early September just as organic N had. Ortho-phosphorus was generally quite low (<0.04 mg/L) followed similar patterns at all stations (Figure 27). Values at AR1 were uniformly lower. SRP (ortho-phosphorus) values generally declined over the year being near 0.02 mg/L in spring and generally 0.01-0.015 mg/L for the rest of the year.

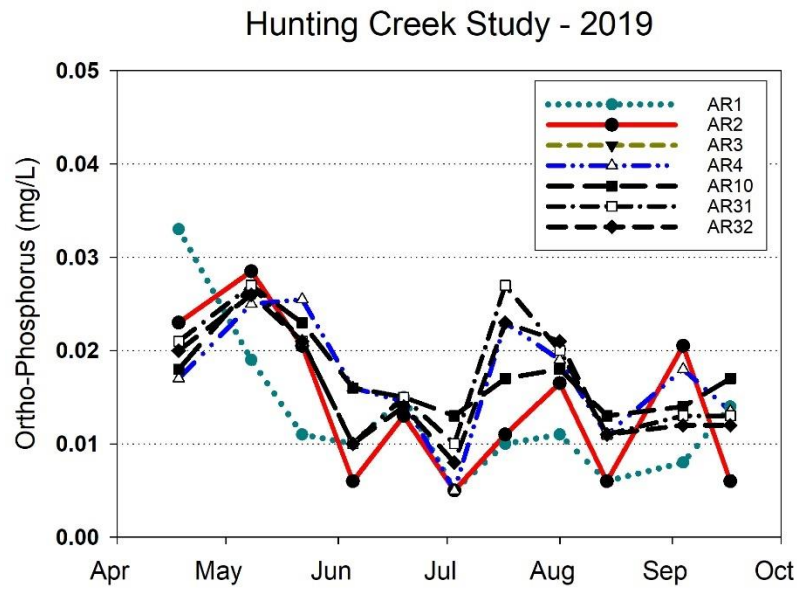

Soluble reactive phosphorus (SRP) is a measure of phosphate ion (PO_4^{-3}). Phosphate ion is the form in which P is most available to primary producers such as algae and aquatic plants in freshwater. However, SRP is often inversely related to the activity of primary producers because they tend to take it up so rapidly. So, higher levels of SRP indicate either a local source of SRP to the waterbody or limitation by a factor other than P.

Figure 27. Soluble Reactive Phosphorus (mg/L). AlexRenew Lab Data. Month tick is at first day of month.

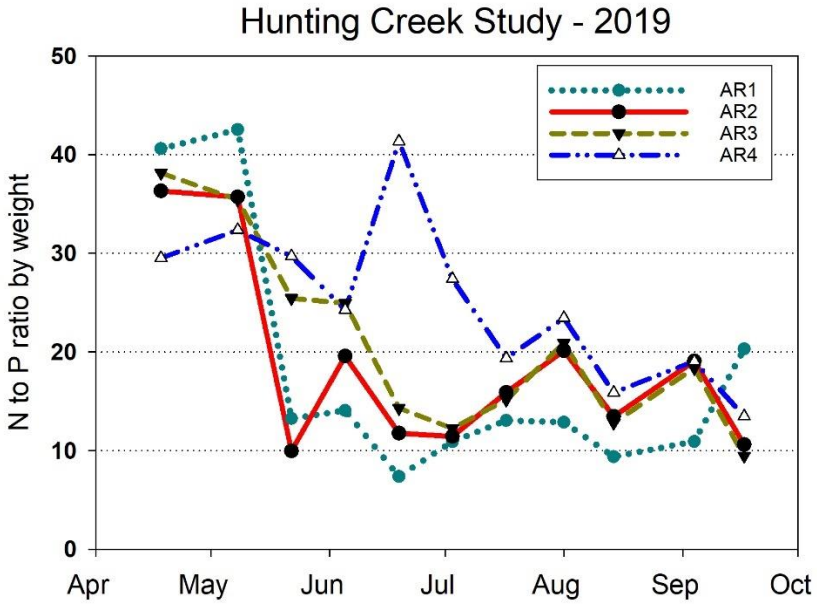

N:P ratio is determined by summing all of the components of N (ammonia, nitrate, nitrite, and organic nitrogen) and dividing by total P. This ratio gives an indication of whether N or P is more likely to be limiting primary production in a given freshwater system. Generally, values above 7.2 are considered indicative of P limitation while values below 7.2 suggest N limitation. N limitation could lead to dominance by cyanobacteria who can fix their own N from the atmosphere.

Figure 28. N/P Ratio (by mass). AlexRenew Lab Data. Month tick is at first day of month.

N/P ratio consistently pointed to P limitation, being greater than 7.2 in all samples (Figure 28). Values were generally in the 10 to 30 range. Biochemical oxygen demand (BOD) was often below the detection limit of 2 mg/L, but was somewhat higher on several dates (Figure 29).

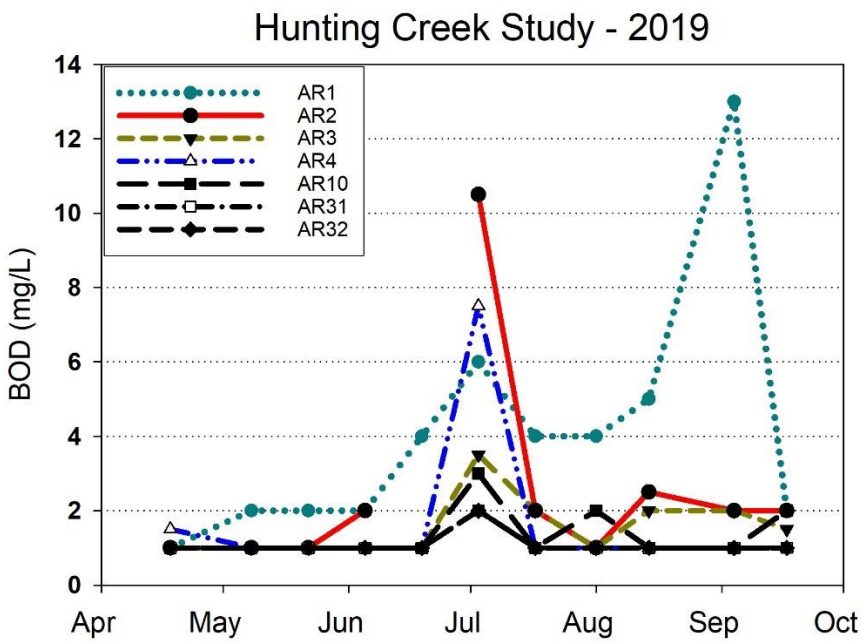

Biochemical oxygen demand (BOD) measures the amount of decomposable organic matter in the water as a function of how much oxygen it consumes as it breaks down over a given number of days. Most commonly the number of days used is 5. BOD is a good indicator of the potential for oxygen depletion in water. BOD is composed both dissolved organic compounds in the water as well as microbes such as bacteria and algae which will respire and consume oxygen during the period of measurement.

Figure 29. Biochemical Oxygen Demand (mg/L). AlexRenew Lab Data. Month tick is at first day of month.

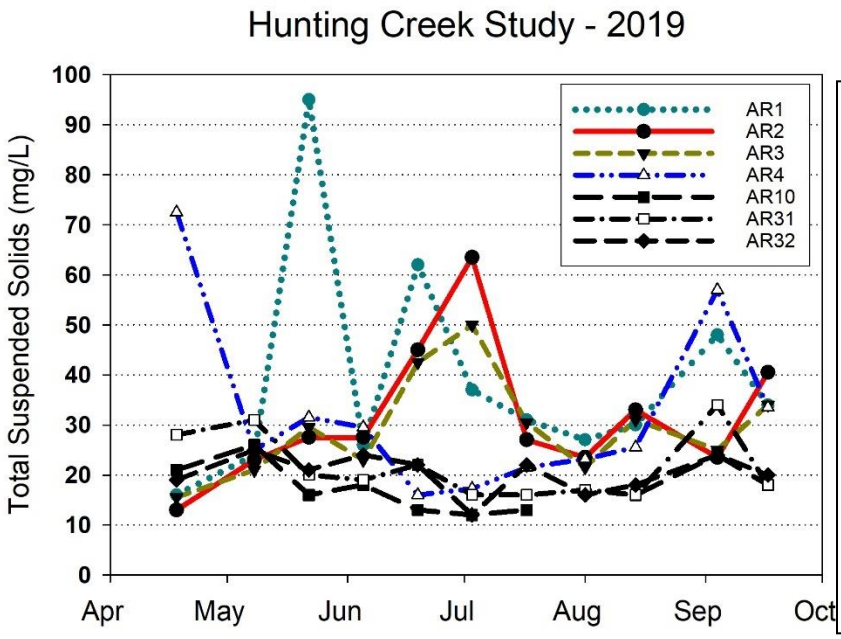

Total suspended solids (TSS) is measured by filtering a known amount of water through a fine filter which retains all or virtually all particles in the water. This filter is then dried and the weight of particles on the filter determined by difference. TSS consists of both organic and inorganic particles. During periods of low river and tributary inflow, organic particles such as algae may dominate. During storm flow periods or heavy winds causing resuspension, inorganic particles may dominate.

Figure 30. Total Suspended Solids (mg/L). AlexRenew Lab Data. Month tick is at first day of month.

Total suspended solids was generally in the range 15-30 mg/L at the river mainstem stations (AR4, AR10, AR31, and AR32) (Figure 30). At the Hunting Creek embayment stations TSS showed a more variable pattern with elevated values in late June/early July and early September. VSS values mirrored TSS, but at lower levels (Figure 31).

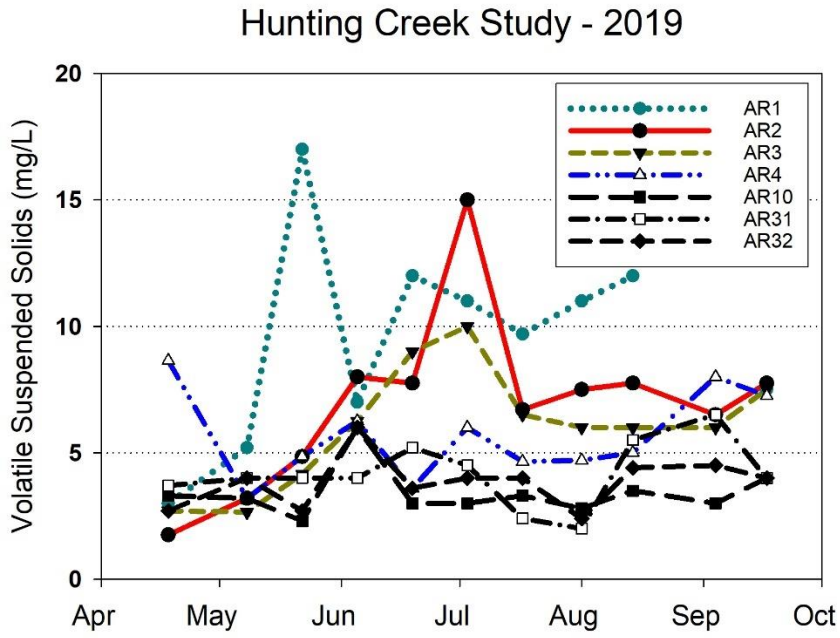

Volatile suspended solids (VSS) is determined by taking the filters used for TSS and then ashing them to combust (volatilize) the organic matter. The organic component is then determined by difference. VSS is a measure of organic solids in a water sample. These organic solids could be bacteria, algae, or detritus. Origins include sewage effluent, algae growth in the water column, or detritus produced within the waterbody or from tributaries. In summer in Gunston Cove a chief source is algal (phytoplankton) growth.

Figure 31. Volatile Suspended Solids (mg/L). AlexRenew Lab Data. Month tick is at first day of month.

C. Physico-chemical Parameters: Tributary Stations – 2019

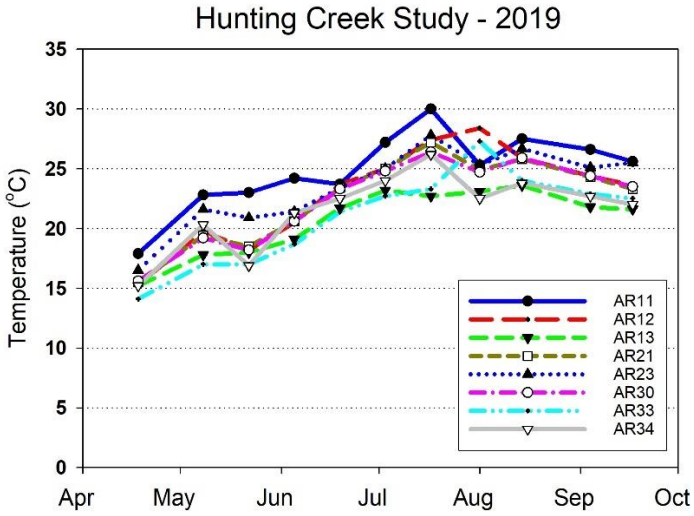

Figure 32. Water Temperature (ºC). GMU Field Data. Month tick is at first day of month.

Water quality data for the tributary stations was combined into a series of graphs by parameter. Temperatures at almost all stations closely followed air temperatures (Figure 32). The most obvious exception was AR13 which exhibited lower temperatures during most of the year. The water at AR13 is just emerging from underground storm sewers and is buffered from the higher air temperatures. Specific conductance was generally in the 200-600 uS/cm range (Figure 33). Values were generally lower than in previous years due to the wet conditions. There was little seasonal pattern at most stations.

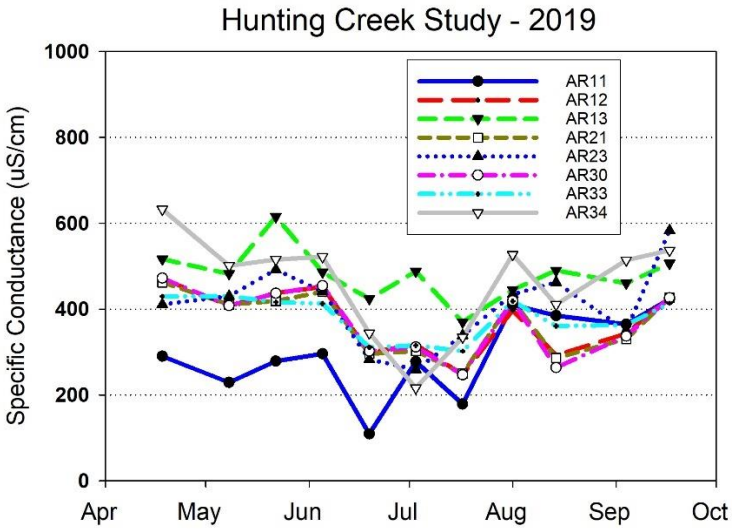

Figure 33. Specific Conductance (uS/cm). GMU Field Data. Month tick is at first day of month.

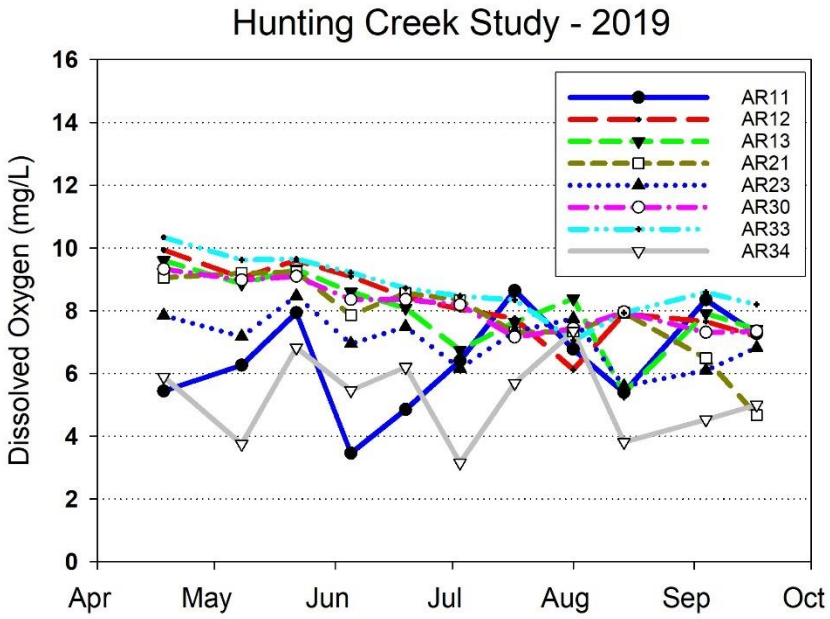

Figure 34. Dissolved Oxygen (mg/L) GMU Field Data. Month tick is at first day of month.

Dissolved oxygen (mg/L) in the tributaries exhibited a clear seasonal pattern that was mainly reflective of changes in DO saturation with temperature (Figure 34). The only stations that exhibited concentrations that were substantially below saturation were AR11 and AR34 which dropped below 6 mg/L and 50% saturation on several occasions. AR11 is the outflow from Lake Cook and SR34 is in the tidal part of Hoff's Run. When expressed in percent saturation, most of the seasonal pattern disappeared (Figure 35).

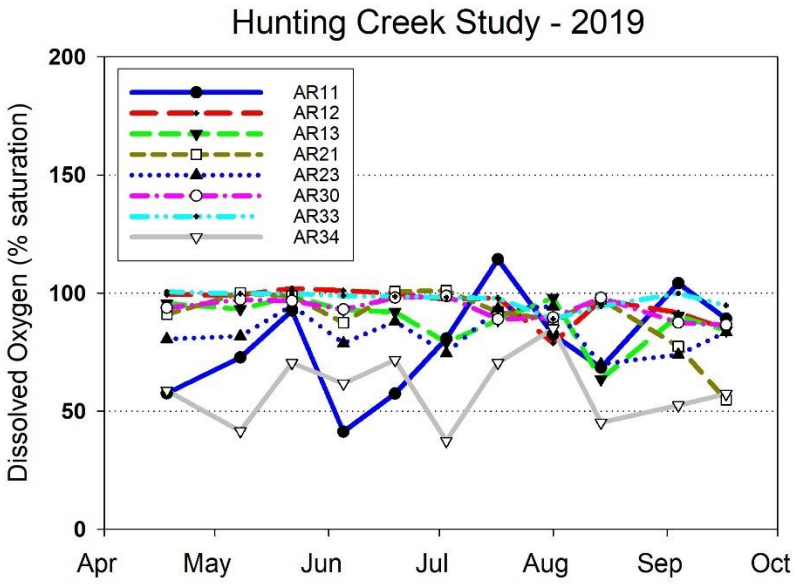

Figure 35. Dissolved Oxygen (% saturation) GMU Field Data. Month tick is at first day of month.

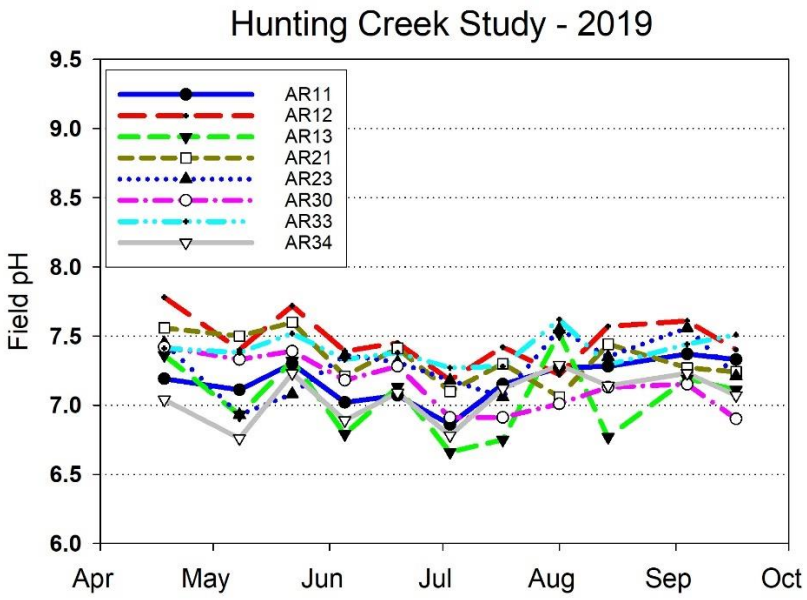

Figure 36. Field pH. GMU Field Data. Month tick is at first day of month.

Field pH was consistently in the 6.7-7.7 range at tributary stations (Figures 36 and 37). Lab pH displayed similar patterns with fewer values below 7.

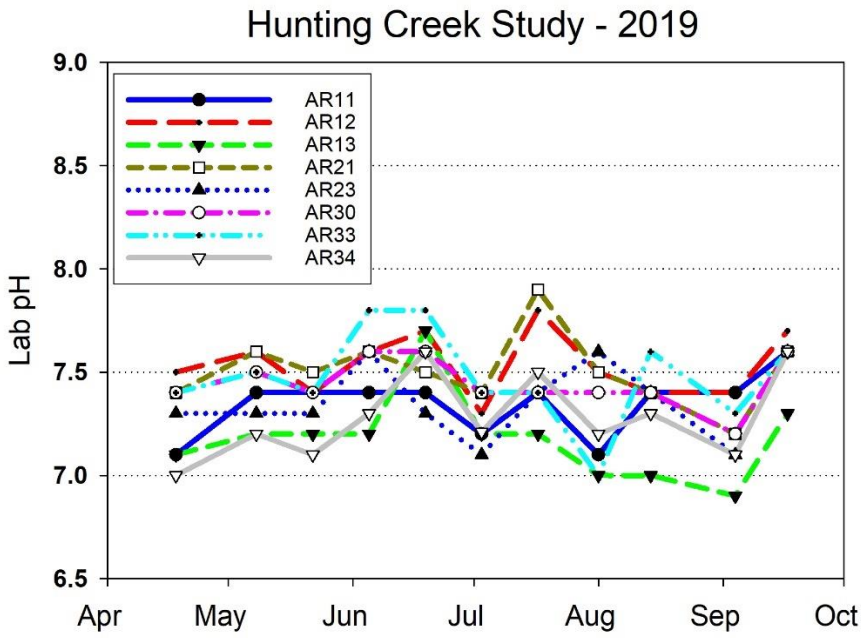

Figure 37. Lab pH. Alex Renew Lab Data. Month tick is at first day of month.

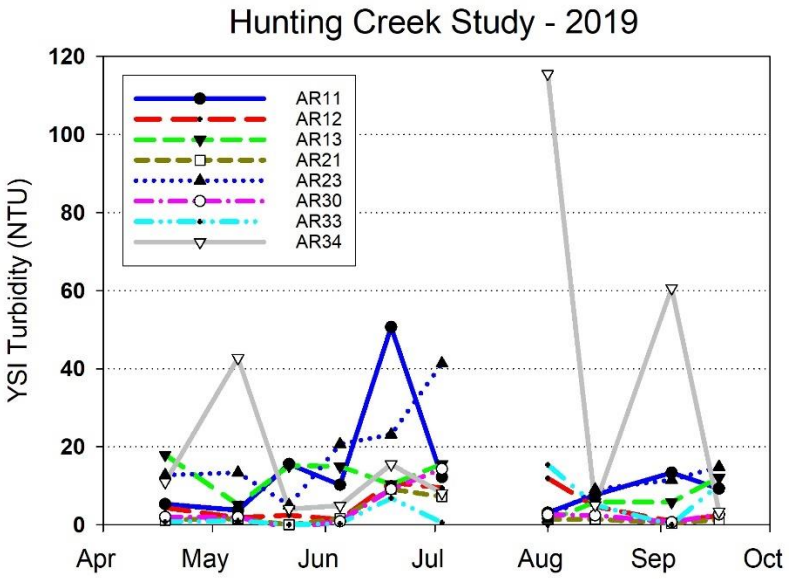

Figure 38. YSI Turbidity. GMU Field Data. Month tick is at first day of month.

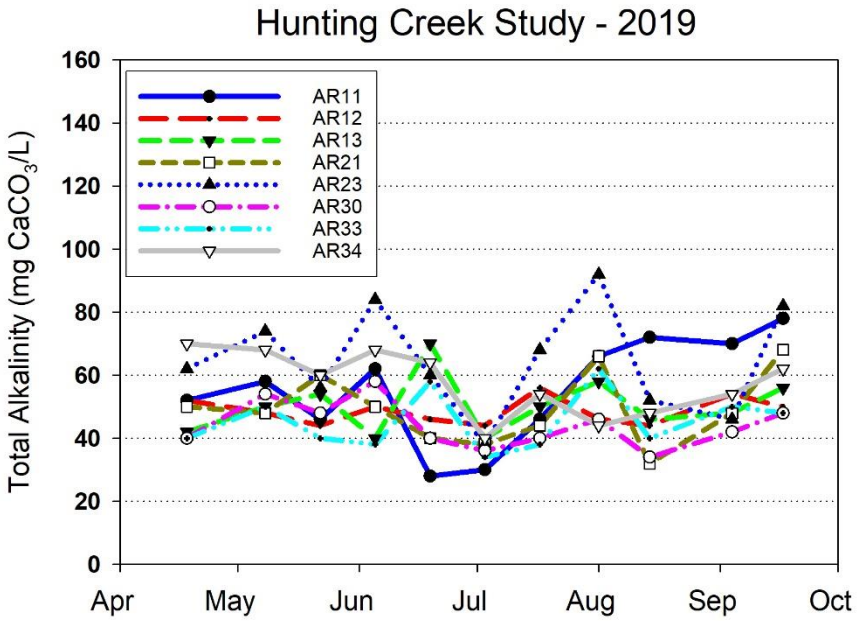

Figure 40. Total Alkalinity (mg/L as $CaCO_3$) AlexRenew Lab Data. Month tick is at first day of month.

Total alkalinity was generally in the 40-60 mg/L range with little seasonal pattern apparent (Figure 40). Chloride levels showed some broad seasonal patterns being lowest in June and highest in spring and mid-July (Figure 41).

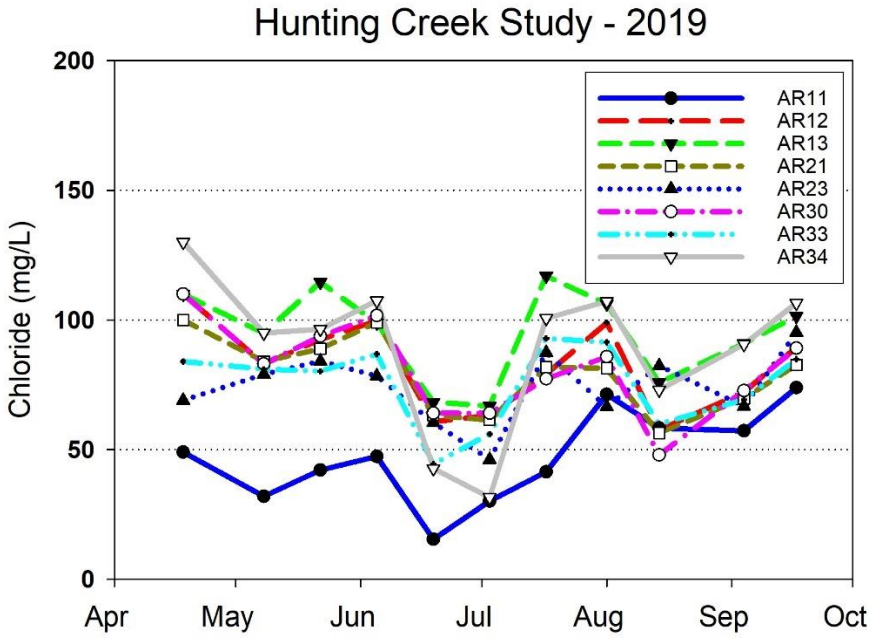

Figure 41. Chloride (mg/L) AlexRenew Lab Data. Month tick is at first day of month.

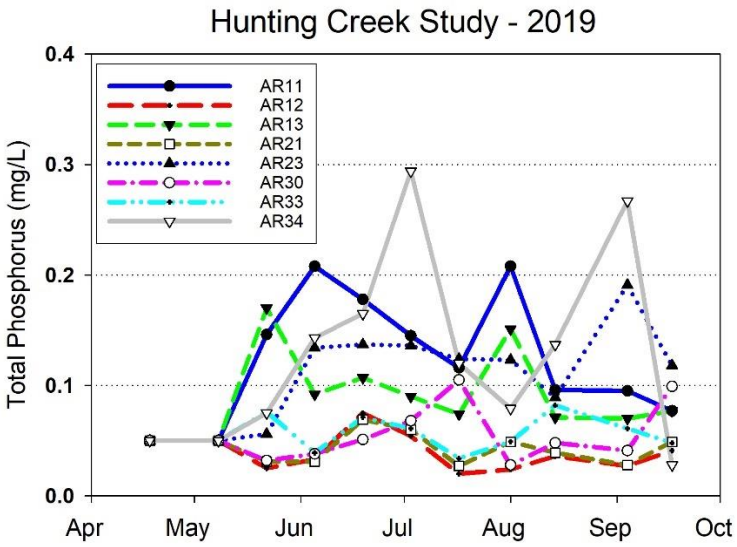

Figure 42. Total Phosphorus (mg/L) AlexRenew Lab Data. Month tick is at first day of month.

Total phosphorus levels were generally relatively low at most tributary stations (<0.2 mg/L) and did not vary much seasonally (Figure 42). Highest values were observed sporadically at AR34 and AR11. Ortho phosphorus levels hovered around 0.02 mg/L (Figure 43). Some higher readings were observed on two occasions at AR13, AR33, and AR34, all Hooffs Run.

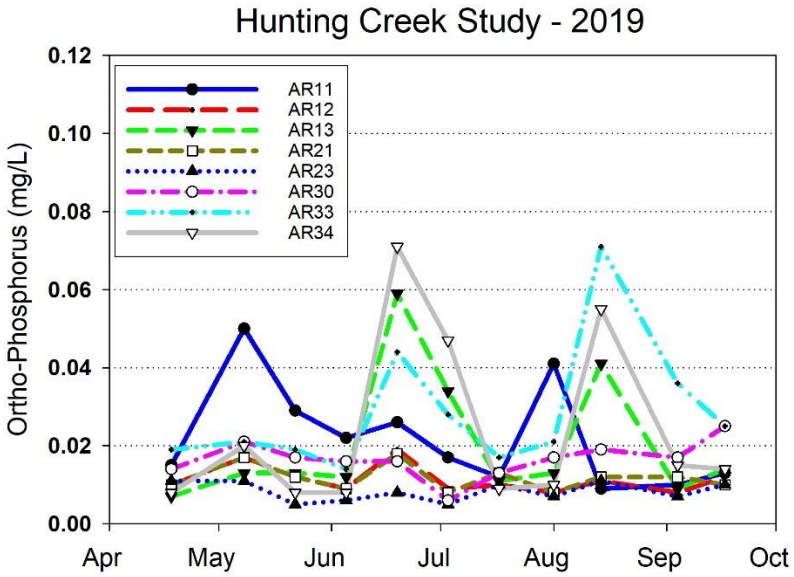

Figure 43. Ortho-Phosphorus (mg/L) AlexRenew Lab Data. Month tick is at first day of month.

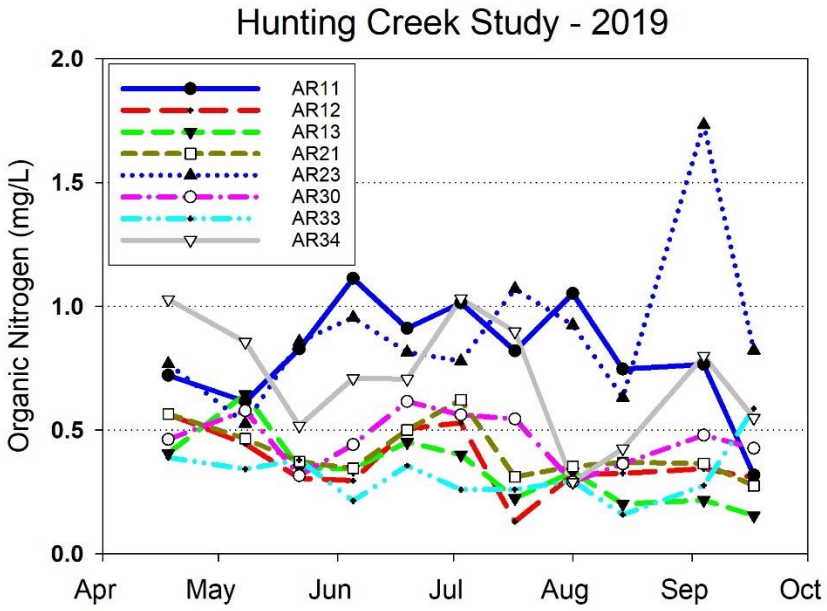

Figure 44. Organic Nitrogen (mg/L) AlexRenew Lab Data. Month tick is at first day of month.

Tributary levels of organic nitrogen are depicted in Figure 44. Values were generally below 0.5 mg/L except at AR23, AR11, and AR34. Ammonia nitrogen values were below 0.1 mg/L at most sites. However, AR11 was consistently above 0.1 mg/L (Figure 45).

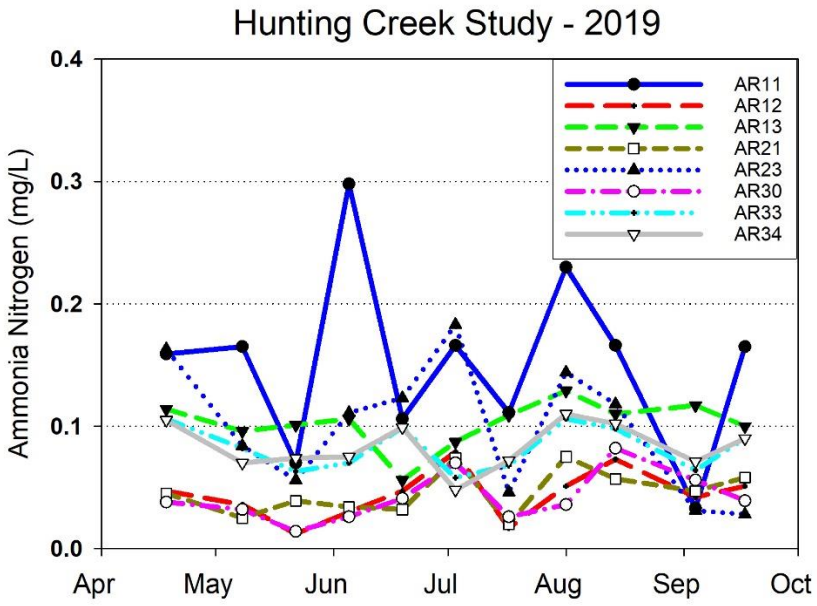

Figure 45. Ammonia Nitrogen (mg/L) AlexRenew Lab Data. Month tick is at first day of month.

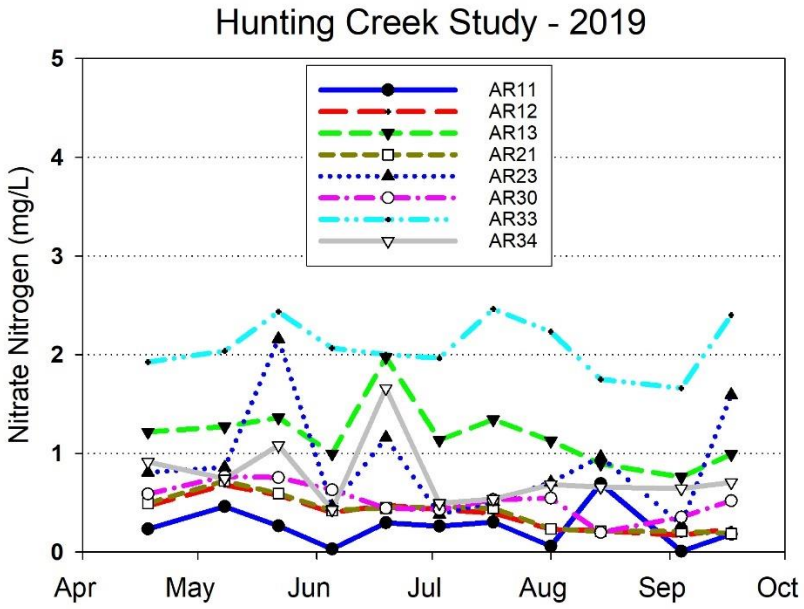

Figure 46. Nitrate Nitrogen (mg/L) AlexRenew Lab Data. Month tick is at first day of month.

Nitrate nitrogen values was generally below 1.0 mg/L. AR33 had values near 2.0 mg/L and AR13 was consistently above 1.0 mg/L. Nitrite nitrogen was generally quite low at all stations (Figure 47). The exception was exceptionally high values at all stations in August.

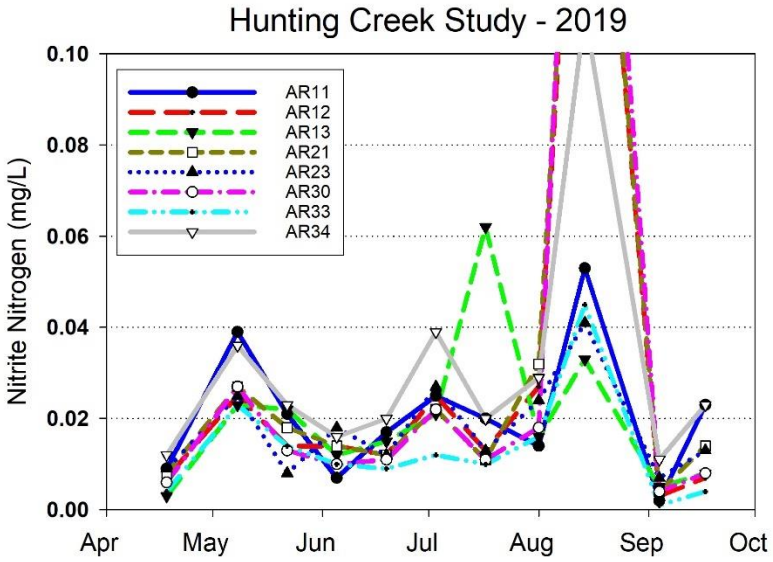

Figure 47. Nitrite Nitrogen (mg/L) AlexRenew Lab Data. Month tick is at first day of month.

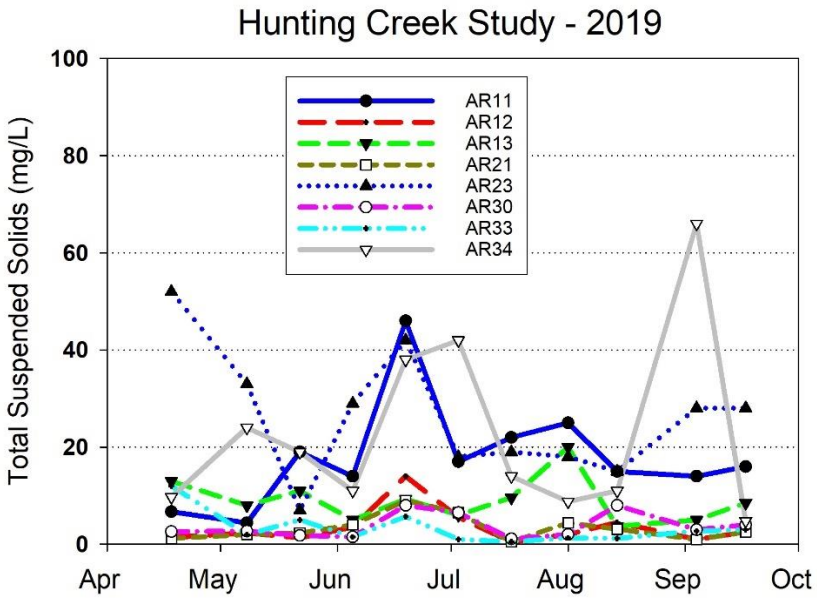

Figure 48. Total Suspended Solids (mg/L) AlexRenew Lab Data. Month tick is at first day of month.

Total suspended solids concentrations at tributary stations are shown in Figure 48. TSS was quite low (<20 mg/L) at most stations for most of the year. The exceptions were AR11, AR23, and AR34 which had frequently higher values. Similar trends were observed volatile suspended solids (Figure 49).

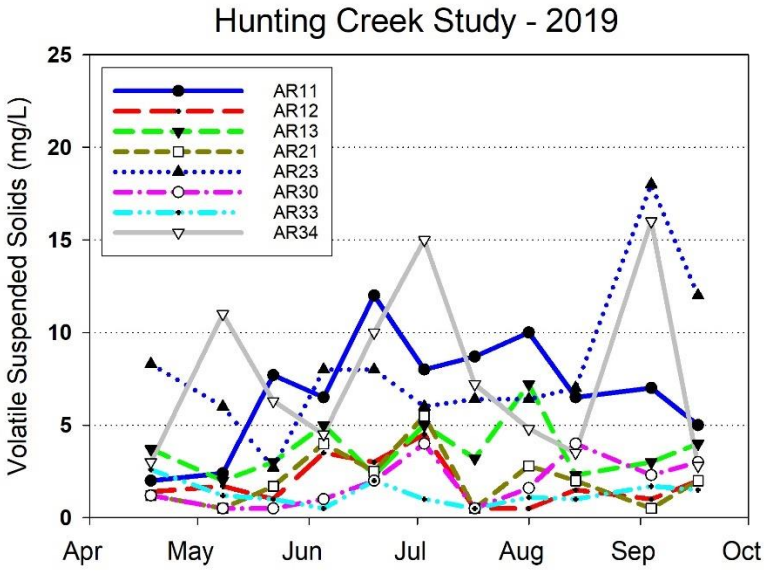

Figure 49. Volatile Suspended Solids (mg/L) AlexRenew Lab Data. Month tick is at first day of month.

D. Phytoplankton - 2019

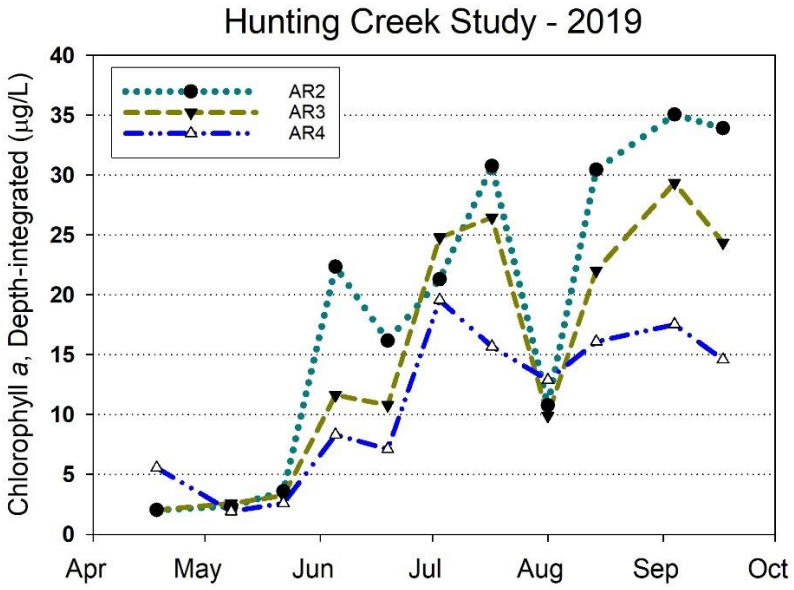

Chlorophyll *a* is a measure of the amount of algae growing in the water column. These suspended algae are called phytoplankton, meaning "plant wanderers". In addition to the true algae (greens, diatoms, cryptophytes, etc.) the term phytoplankton includes cyanobacteria (sometimes known as "blue-green" algae). Both depth-integrated and surface chlorophyll values are measured due to the capacity of phytoplankton to aggregate near the surface under certain conditions.

Figure 50. Chlorophyll *a* (µg/L). Depth-integrated. GMU Lab Data. Month tick is at the first day of month.

Chlorophyll *a* began the year at low levels (5-10 µg/L) at all stations in April (Figure 50). Levels remained low through May, but rapidly increased in early June and then again in July attaining levels of 20-30 µg/L before declining strongly in early August. The levels rebounded in late August and early September. Surface levels (Figure 51) were similar at AR2, AR3, and AR4, but exhibited sporadically much higher at AR1.

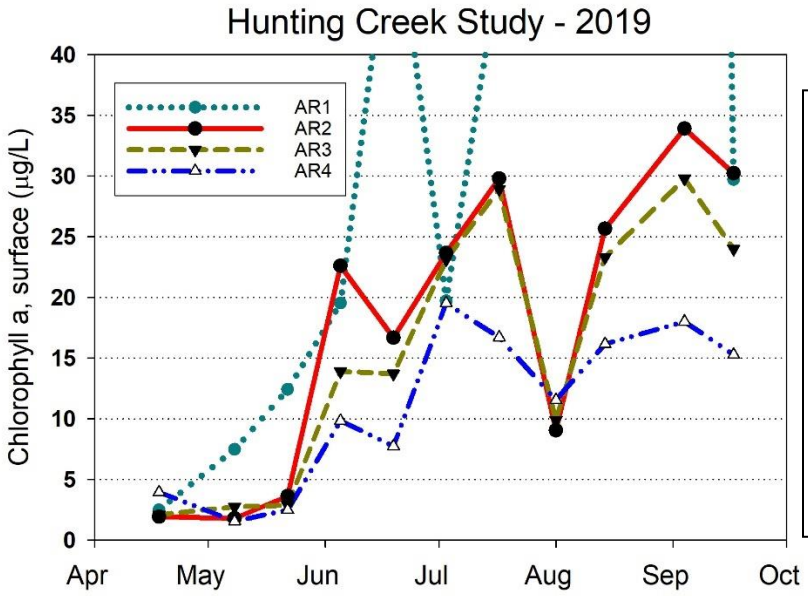

In the tidal freshwater Potomac generally, there is very little difference in surface and depth-integrated chlorophyll levels because tidal action keeps the water well-mixed which overcomes any potential surface aggregation by the phytoplankton. Summer chlorophyll concentrations above 30 ug/L are generally considered characteristic or eutrophic conditions.

Figure 51. Chlorophyll *a* (µg/L). Surface. GMU Lab Data. Month tick is at first day of month.

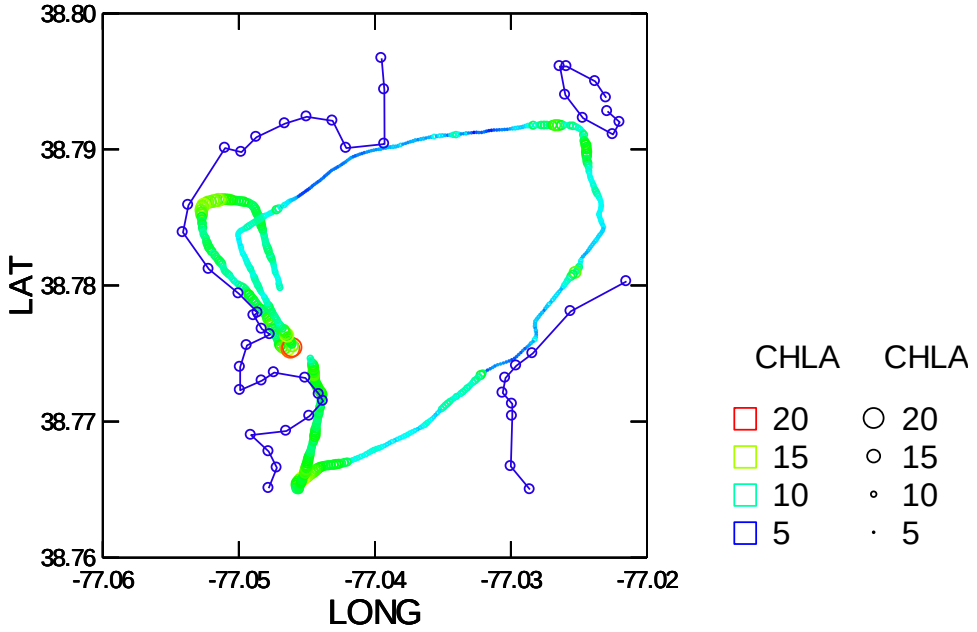

Figure 52a. Water Quality Mapping. July 18, 2019. Chlorophyll YSI (mg/L).

On the July 16 a spatial pattern was observed in chlorophyll with very low values in the river mainstem and somewhat higher values in the Hunting Creek embayment, but not on the Maryland side of the river (Figure 52a). On August 19 values were highest in the southern part of the study area and in some parts of nearshore Hunting Creek (Figure 52b).

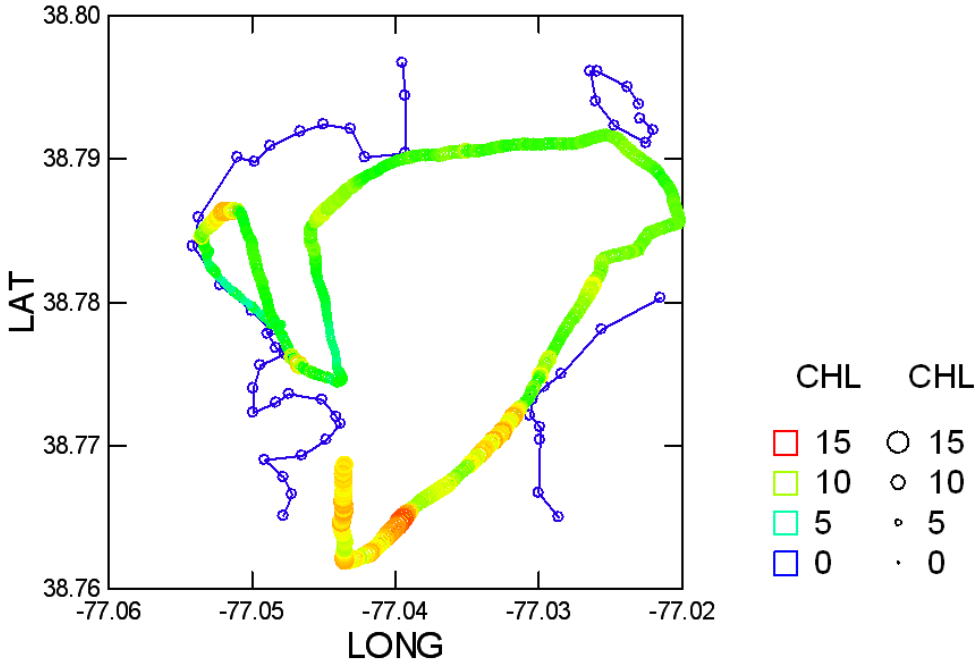

Figure 52b. Water Quality Mapping. August 19, 2019. Chlorophyll YSI (mg/L).

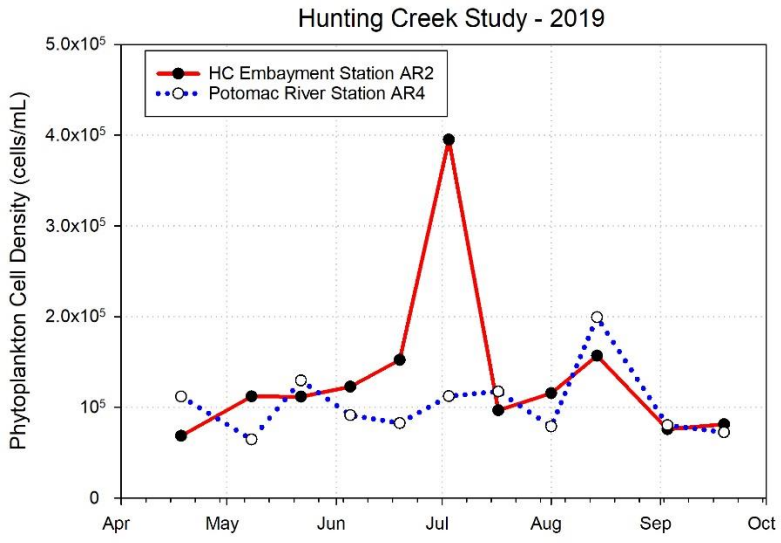

Phytoplankton cell density provides a measure of the number of algal cells per unit volume. This is a rough measure of the abundance of phytoplankton, but does not discriminate between large and small cells. Therefore, a large number of small cells may actually represent less biomass (weight of living tissue) than a smaller number of large cells. However, small cells are typically more active than larger ones so cell density is probably a better indicator of activity than of biomass. The smaller cells are mostly cyanobacteria.

Figure 53. Phytoplankton Cell Density (cells/mL).

Phytoplankton cell density was similar and constant through June at both stations (Figure 53). A distinct peak was observed at AR2 in early July, but values declined in late July. There was a slight peak at both stations in August. Total biovolume exhibited a clearly seasonal pattern increasing through July at both stations (Figure 54). In late July values declined through the rest of the summer.

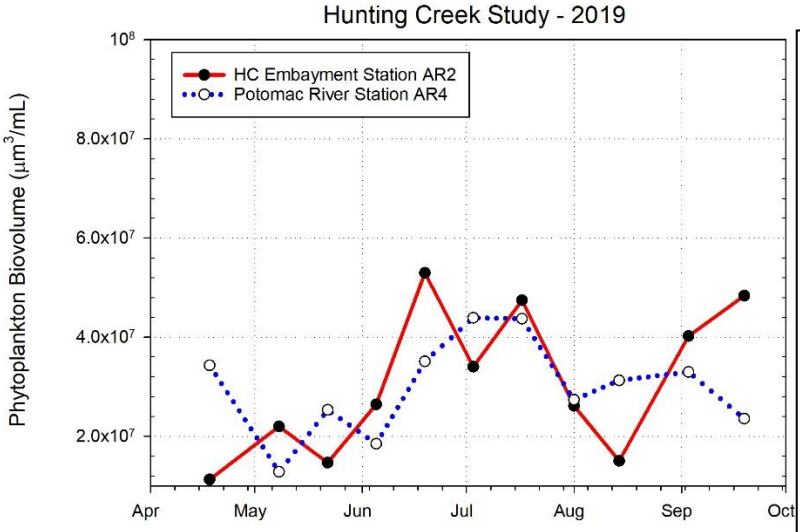

The volume of individual cells of each species is determined by approximating the cells of each species to an appropriate geometric shape (e.g. sphere, cylinder, cone, cube, etc.) and then making the measurements of the appropriate dimensions under the microscope. Total phytoplankton biovolume (shown here) is determined by multiplying the cell density of each species by the biovolume of each cell of that species. Biovolume accounts for the differing size of various phytoplankton cells and is probably a better measure of biomass. However, it does not account for the varying amount of water and other nonliving constituents in cells.

Figure 54. Phytoplankton Biovolume (um^3/mL).

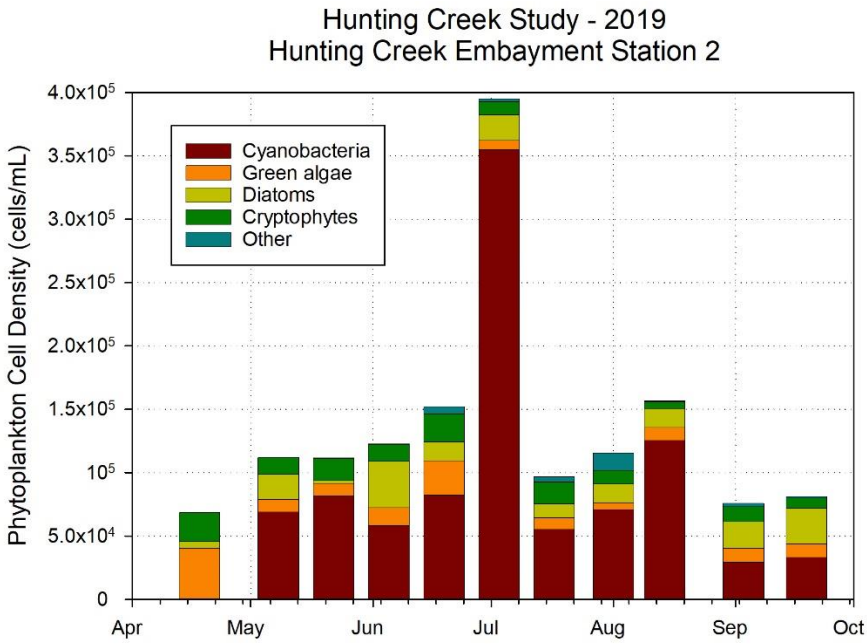

Total phytoplankton cell density can be broken down by major group. **Cyanobacteria** are sometimes called "blue-green algae". **Other** includes euglenoids and dinoflagellates. Due to their small size cyanobacteria typically dominate cell density numbers. Their numbers are typically highest in the late summer reflecting an accumulation of cells during favorable summer growing conditions.

Figure 55. Phytoplankton Density by Major Group (cells/mL). Hunting Creek.

Phytoplankton cell density at AR2 was strongly dominated by cyanobacteria including the very large peak in early July (Figure 55). In the river mainstem (AR4), cyanobacteria were again dominant, but not quite as overwhelmingly so.

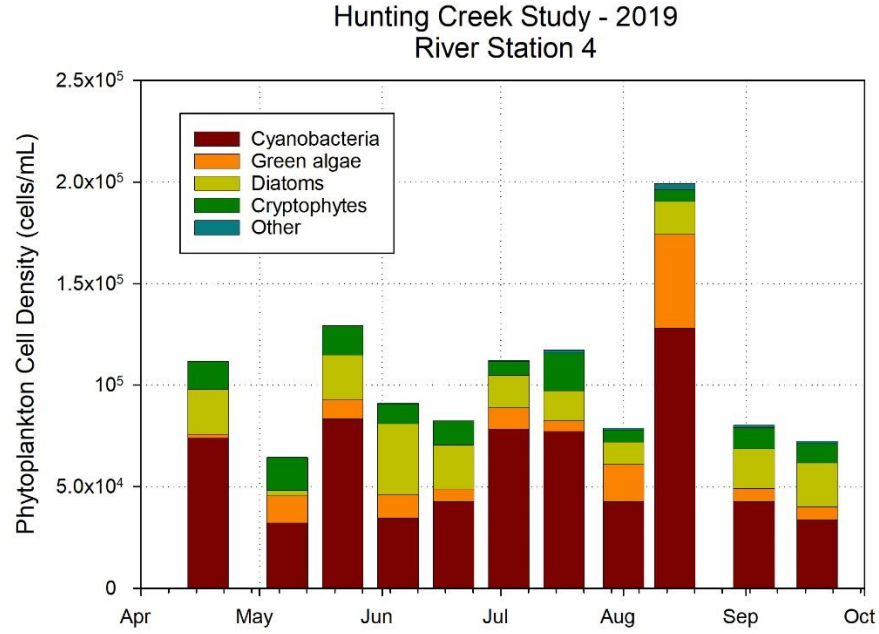

In the river cyanobacteria normally follow similar patterns as in the embayments, but may attain lower abundances. This is probably due to the deeper water column which leads to lower effective light levels and greater mixing. Other groups such as diatoms and green algae tend to be more important on a relative basis than in the embayments.

Figure 56. Phytoplankton Density by Major Group (cells/mL). River.

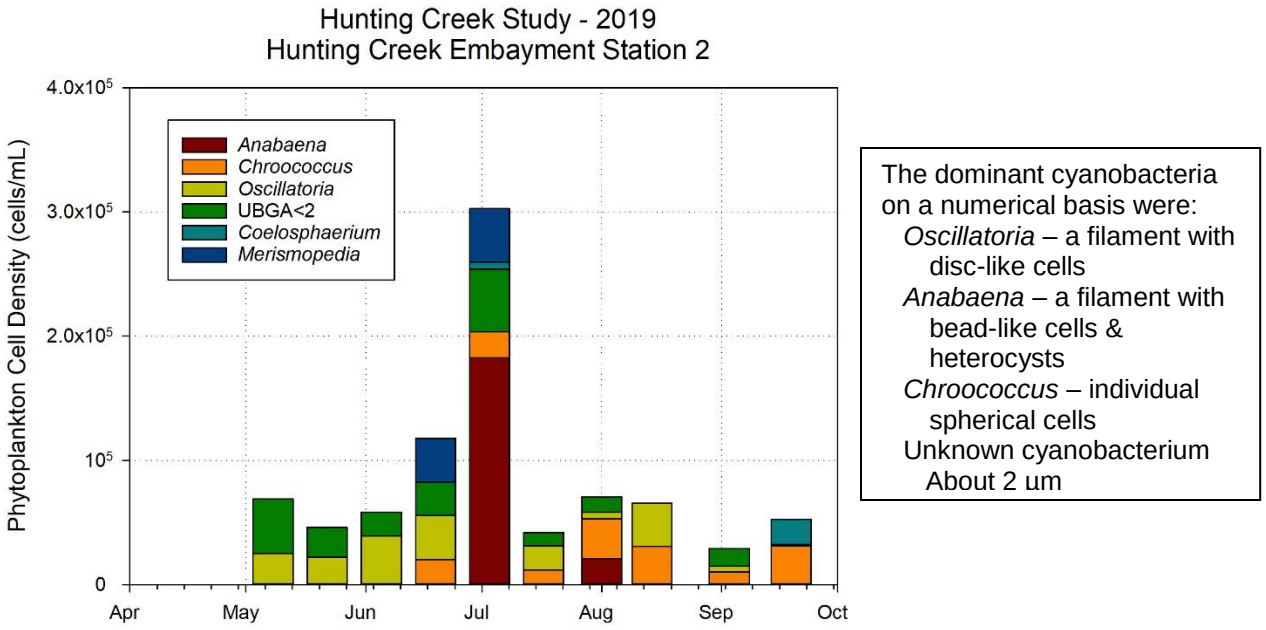

Figure 57. Phytoplankton Density by Dominant Cyanobacteria (cells/mL). Hunting Creek.

Oscillatoria, Chroococcus, and an unknown cyanobacterium were the most important at the embayment station (AR2) (Figure 57). The major peak in early July was due to *Anabaena*. In the river mainstem *Oscillatoria* and the unknown cyanobacterium were important for the entire year. *Chroococcus* was mainly a summer and fall genus (Figure 58). *Anabaena* was particularly abundant in mid-August.

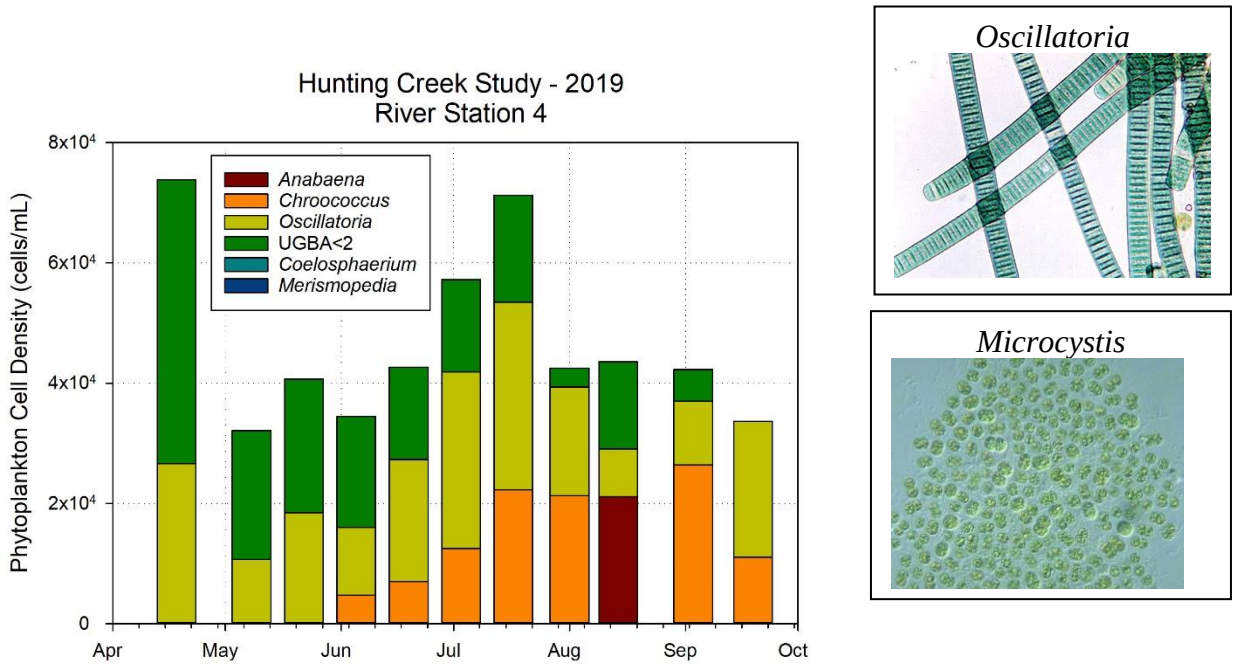

Figure 58. Phytoplankton Density by Dominant Cyanobacteria (cells/mL). River.

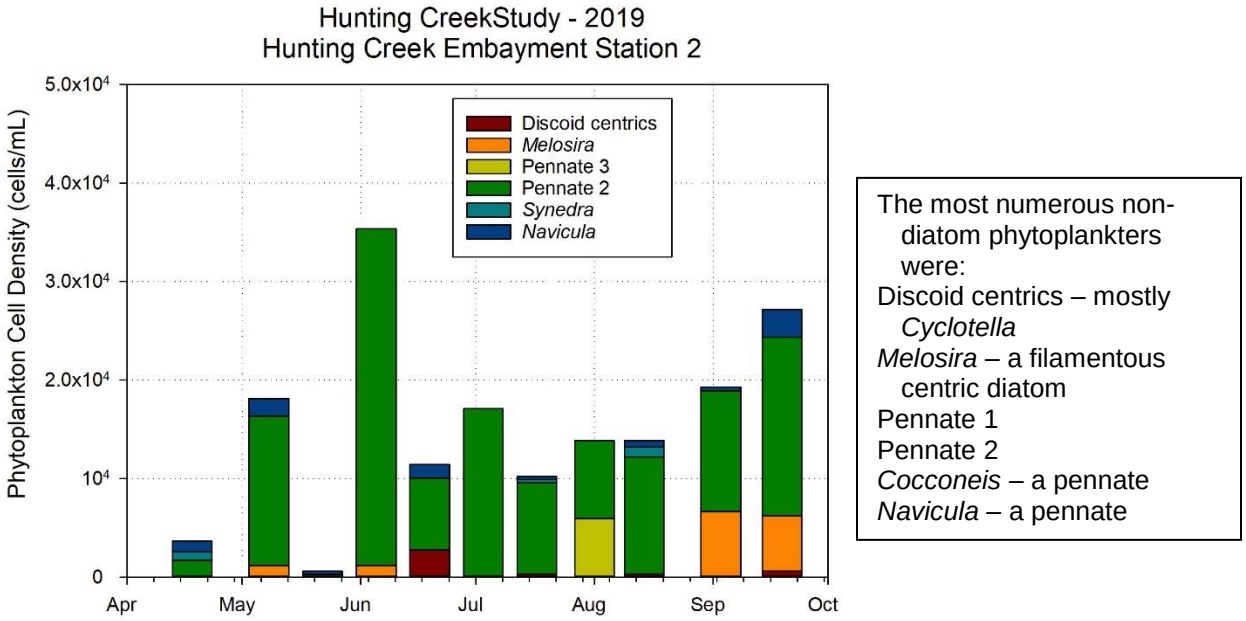

Figure 59. Phytoplankton Density (#/mL) by Dominant Diatom Taxa. Hunting Creek.

Pennate 2 was the dominant diatom in almost every sample at both stations in 2019 (Figures 59&60). *Melosira* was important in only some samples in 2019 which was a change from earlier years when it was typically the dominant all year.

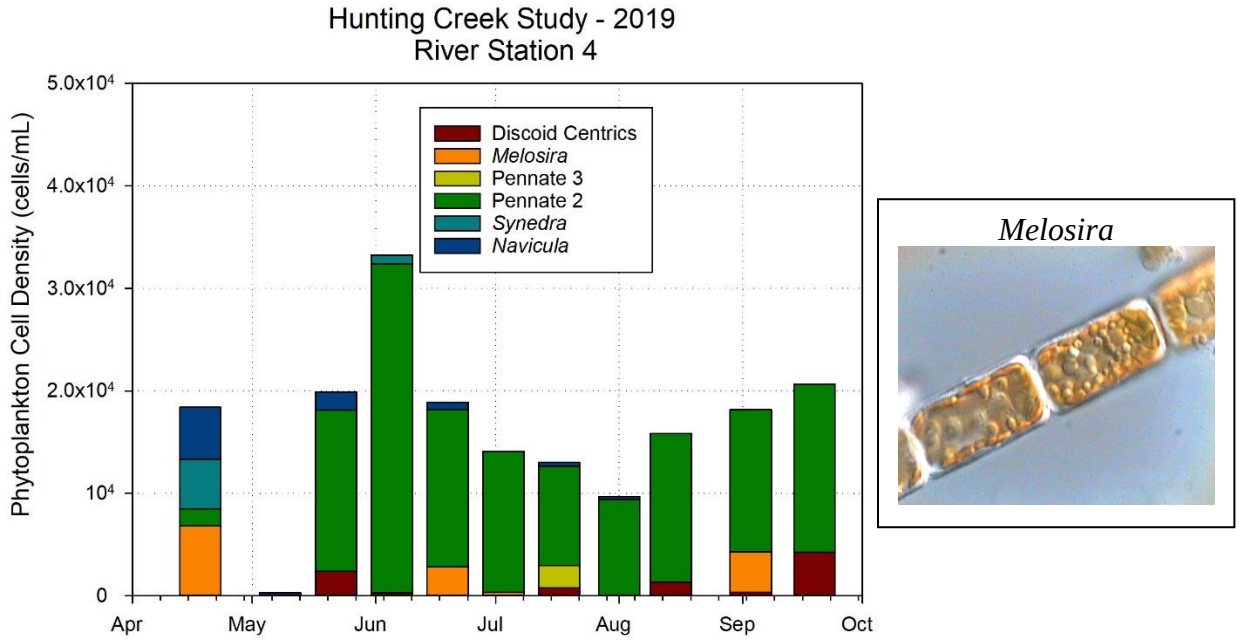

Figure 60. Phytoplankton Density (#/mL) by Dominant Diatom Taxa. River.

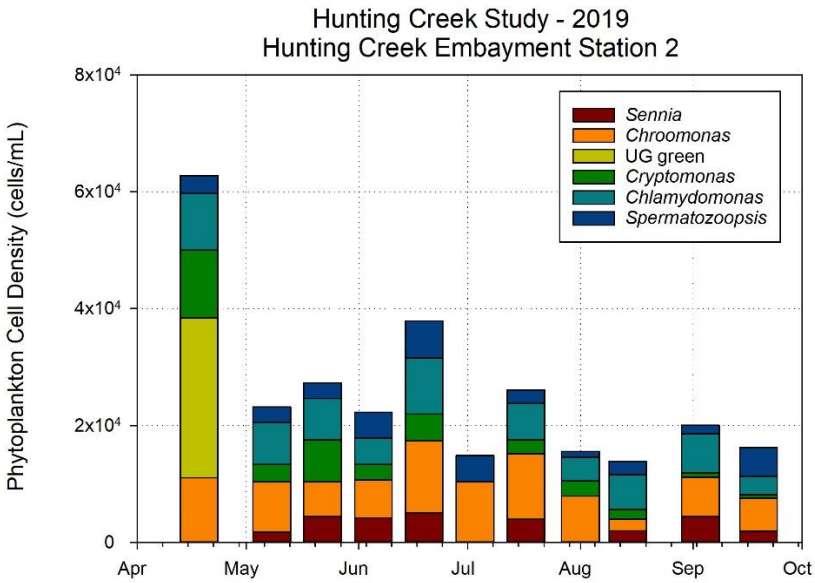

The most numerous other phytoplankton were:
- *Chromulina* – a flagellated chrysophyte
- *Chroomonas* – a flagellated cryptomonad unicell
- Kirchneriella – a colonial green alga
- *Cryptomonas* – a flagellated cryptomonad unicell
- Chlamydomonas – a biflagellate green unicell
- *Spermatozoopsis* – flagellated green unicell

Figure 61. Phytoplankton Density (#/mL) by Dominant Other Taxa. Hunting Creek.

Phytoplankton species that were neither cyanobacteria nor diatoms were grouped together as "other" for these graphs; these included most numerous taxa of green algae, cryptophytes, euglenoids, and dinoflagellates. At both stations the green alga *Chlamydomonas* and the cryptophytes *Cryptomonas* and *Chroomonas* were consistently the most numerous at both stations (Figure 61&62).

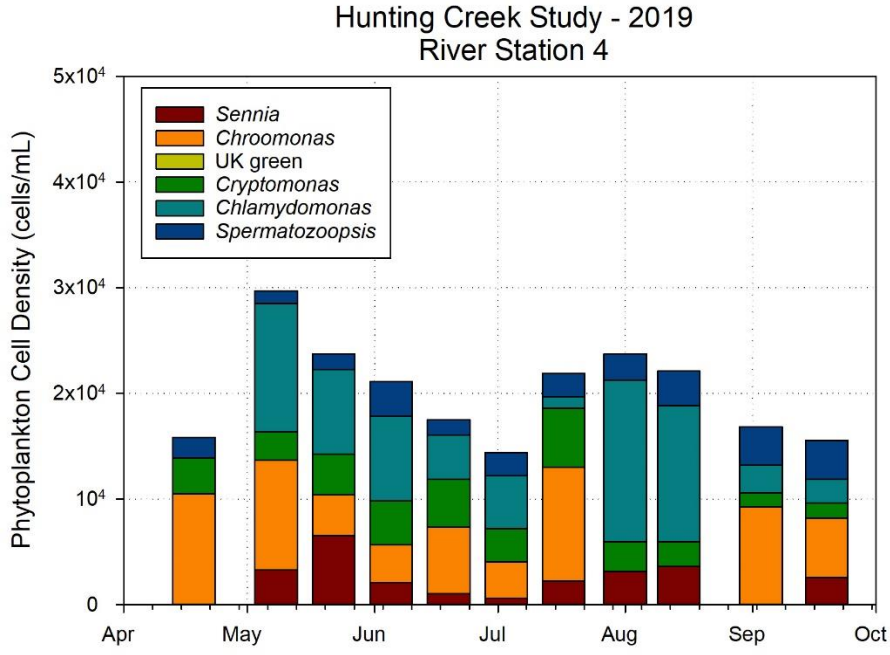

Figure 62. Phytoplankton Density (#/mL) by Dominant Other Taxa. River.

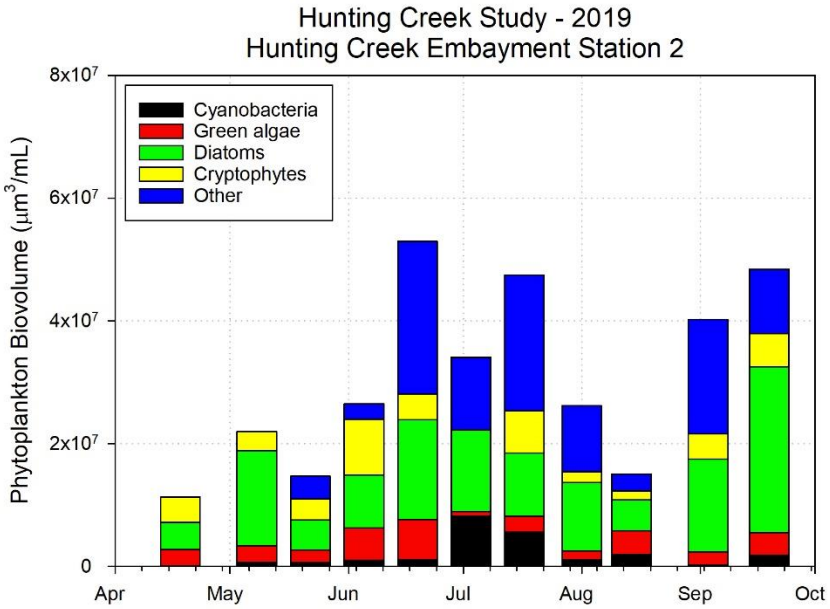

Total phytoplankton biovolume can be broken down into groups:

- **Cyano** – cyanobacteria ("blue-green" algae)
- **Greens** – green algae
- **Diatoms** – includes both centric and pinnate
- **Cryptos** – cryptophytes
- **Other** – includes euglenoids, chrysophytes, and dinoflagellates

Figure 63. Phytoplankton Biovolume (um³/mL) by Major Groups. Hunting Creek.

At AR2 in Hunting Creek diatoms were dominant in biovolume in most samples although there was a strong contribution from other algae in mid-summer and fall (Figure 63). Peak biovolumes were observed in June, July, and September. In the river, diatoms were again dominant on most dates with cryptophytes making a strong contribution on some dates (Figure 64).

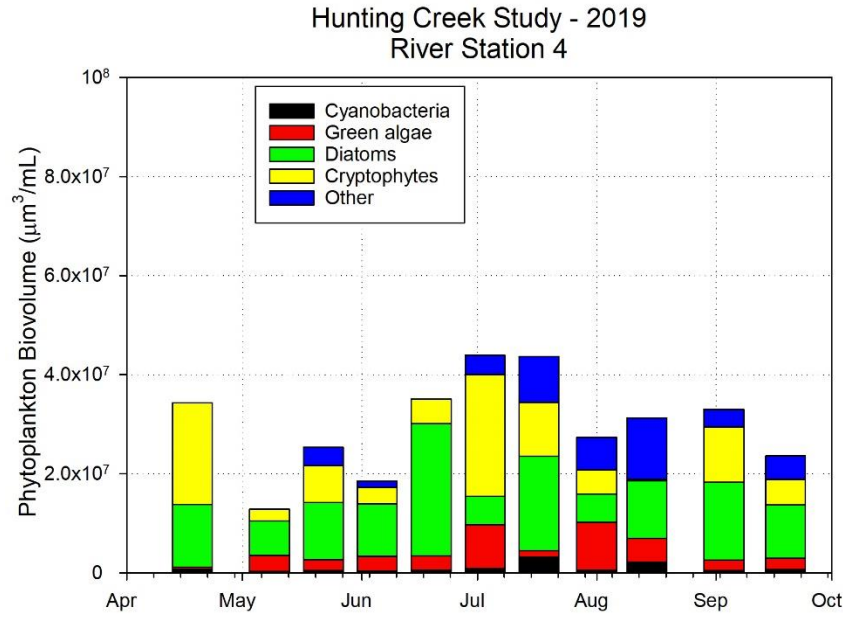

While dominating cell density, cyanobacteria typically make up a much smaller portion of phytoplankton biovolume. Diatoms generally are dominant.

Figure 64. Phytoplankton Biovolume (um³/mL) by Major Groups. River.

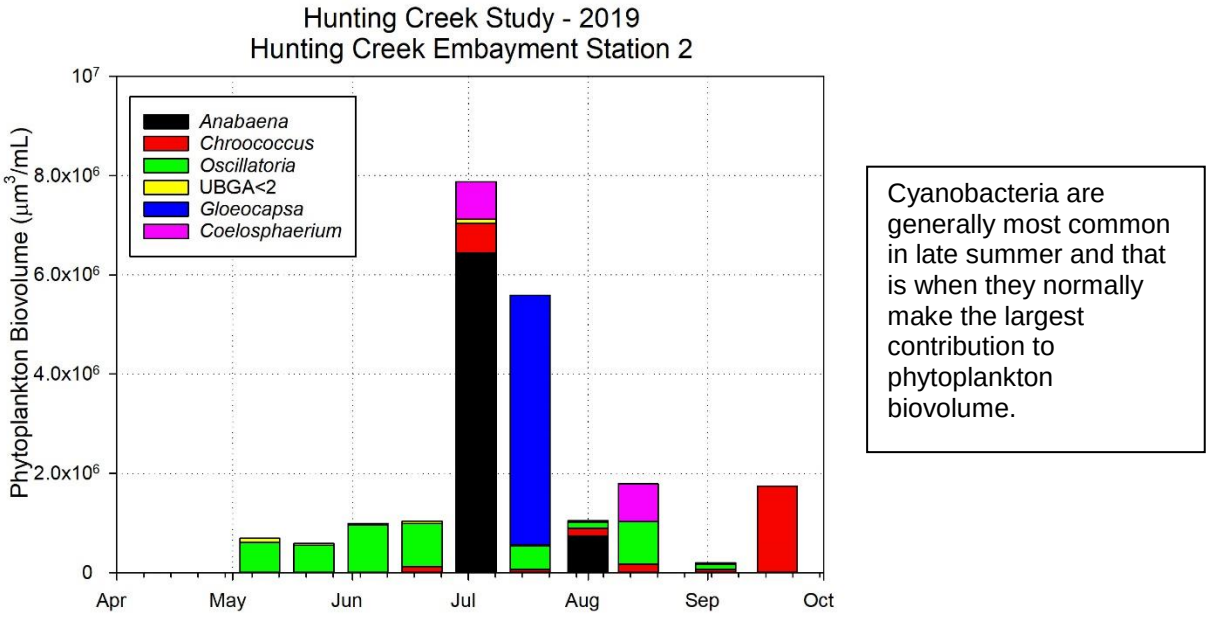

Figure 65. Phytoplankton Biovolume (um³/mL) by Cyanobacteria Taxa. Hunting Creek.

At both stations *Oscillatoria* substantial in almost all samples and dominant in many (Figures 65&66). However, in certain samples *Anabaena* and/or *Gloeocapsa* had high levels that exceeded *Oscillatoria*.

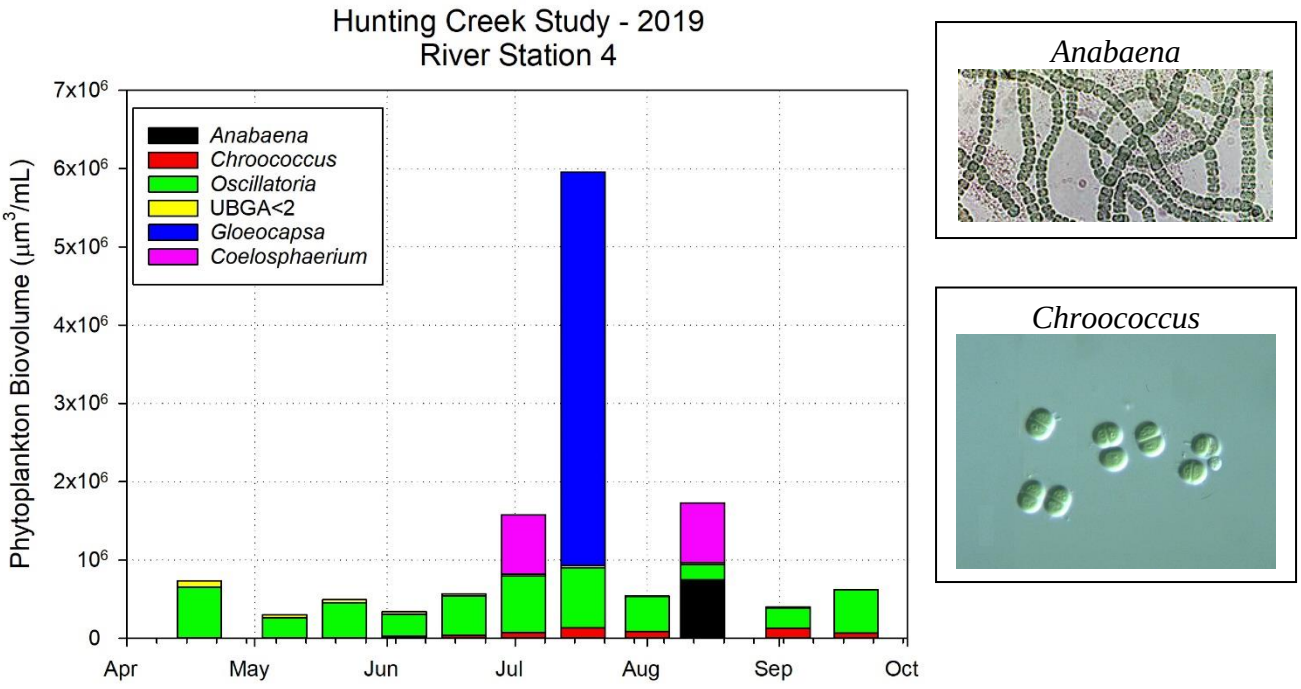

Figure 66. Phytoplankton Biovolume (um³/mL) by Cyanobacterial Taxa. River.

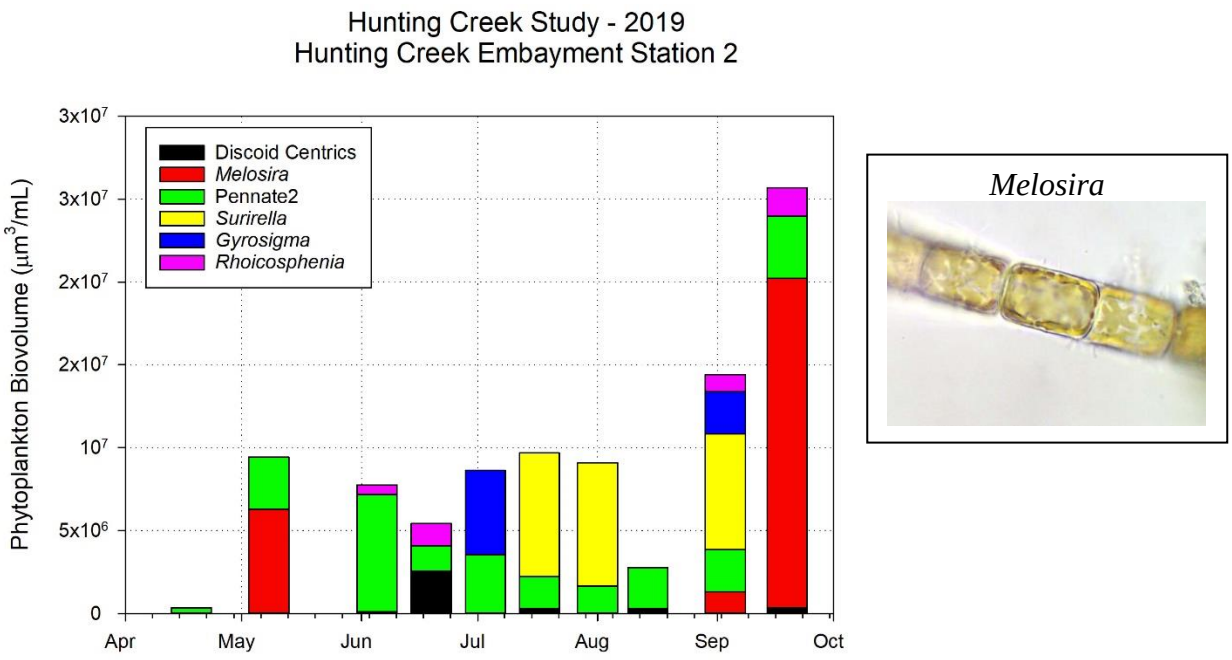

Figure 67. Phytoplankton Biovolume (um³/mL) by Dominant Diatom Taxa. Hunting Creek.

At both stations, the dominant diatom taxa varied from date to date (Figures 67&68). Pennate2 was generally part of the assemblage. The pennate *Surirella* was often present at high levels as was *Melosira*, but neither was consistently found.

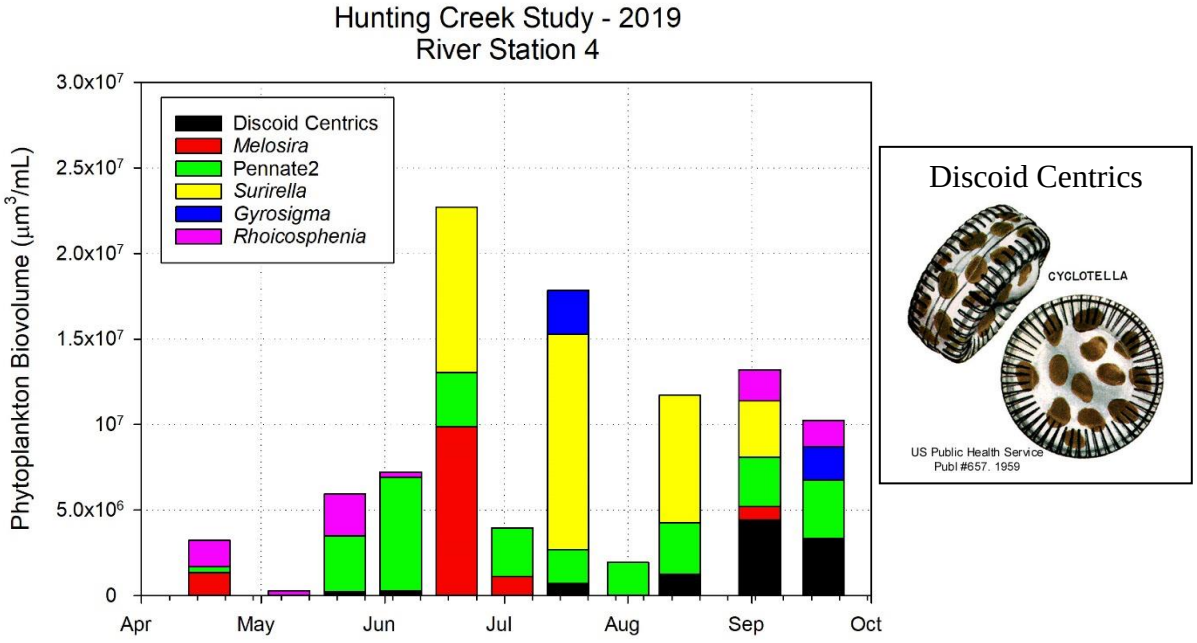

Figure 68. Phytoplankton Biovolume (um³/mL) by Dominant Diatom Taxon. River.

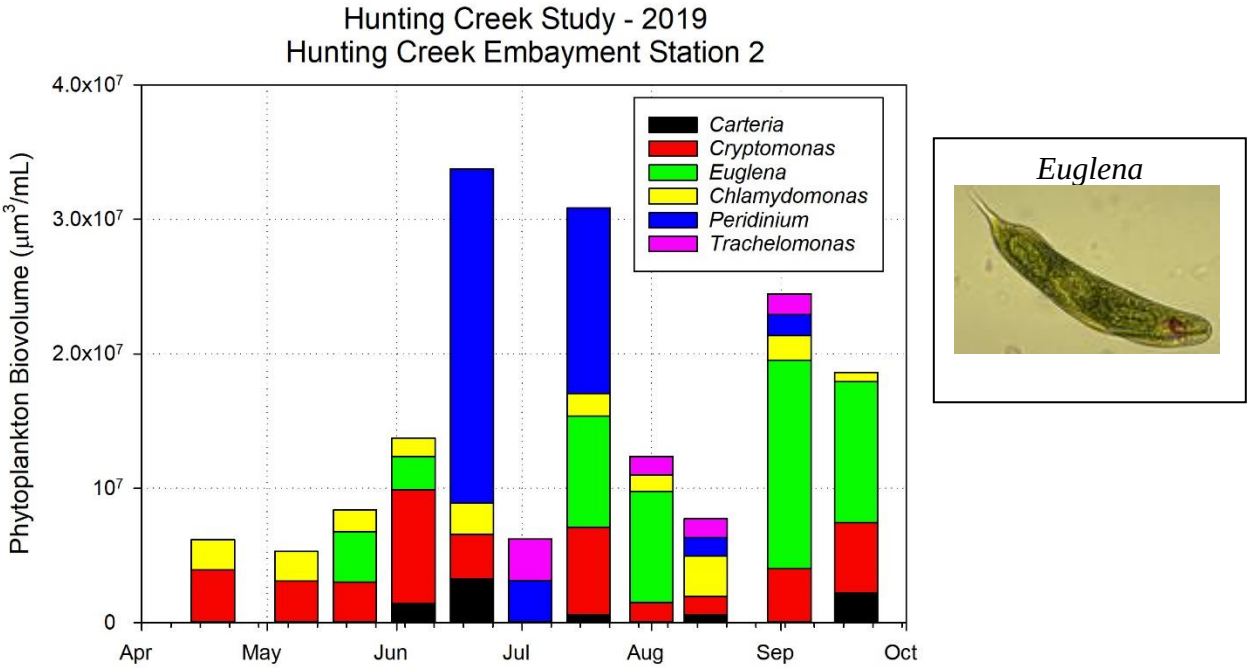

Figure 69. Phytoplankton Biovolume (um³/mL) by Dominant Other Taxa. Hunting Creek.

The large dinoflagellate *Peridinium* was a strong contributor to biovolume in Hunting Creek in late June and July (Figure 69). *Euglena* was important in August and September. *Cryptomonas* was present in most samples at both stations and was frequently dominant in the river (Figure 70).

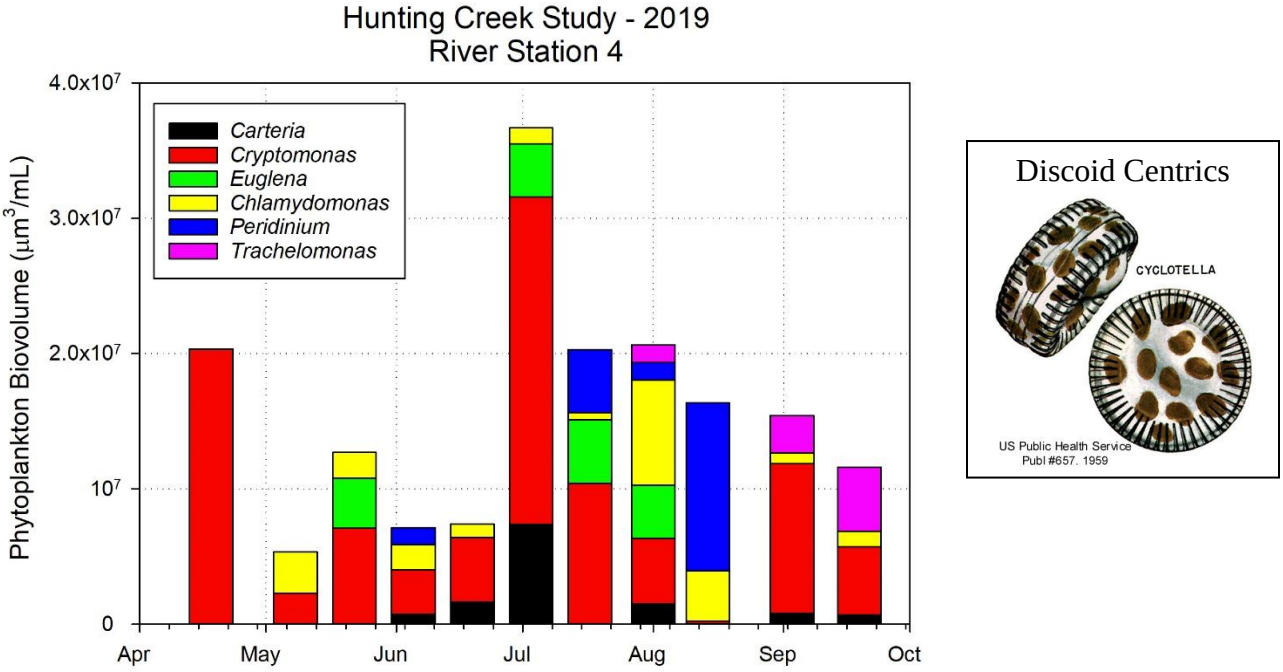

Figure 70. Phytoplankton Biovolume (um³/mL) by Dominant Other Taxon. River.

E. Zooplankton – 2019

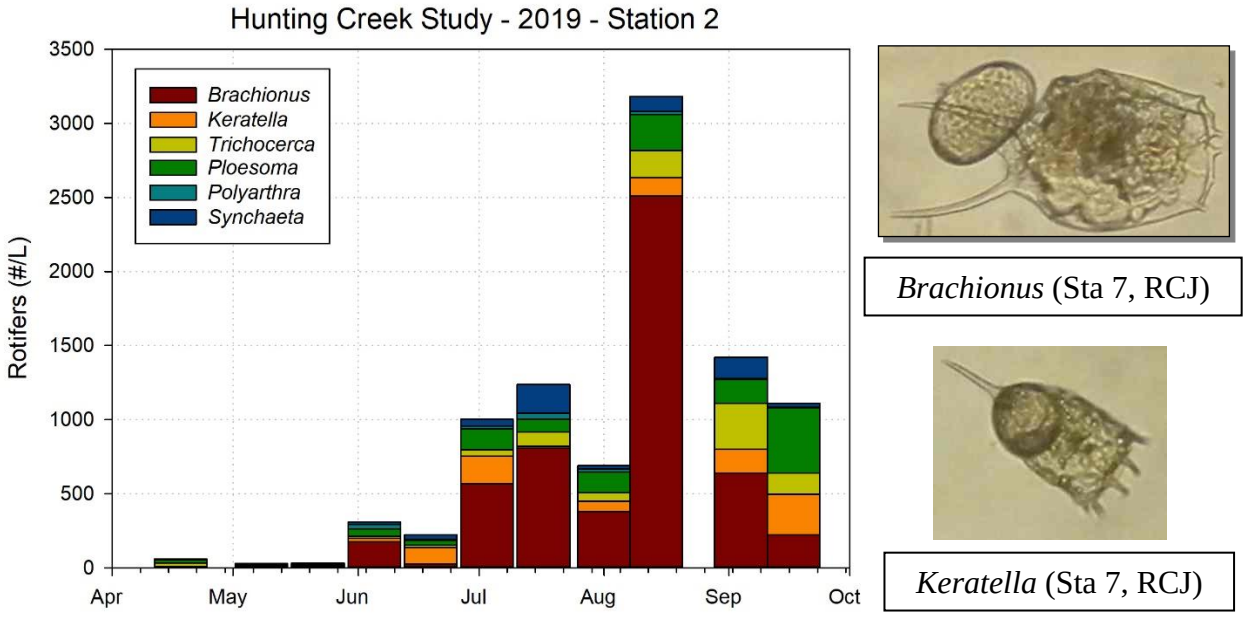

Figure 71. Rotifer Density by Dominant Taxa (#/L). Hunting Creek.

At the embayment station AR2, rotifer populations were very low in April and May. Densities increased in June and July reaching a strong peak in mid-August at over 3000/L (Figure 71). In the river at AR4, rotifer populations did not start to grow until July, but still had a strong peak in early August, slightly below the AR2 peak. *Brachionus* was dominant in almost all samples with *Keratella* and *Ploesoma* being important at some times.

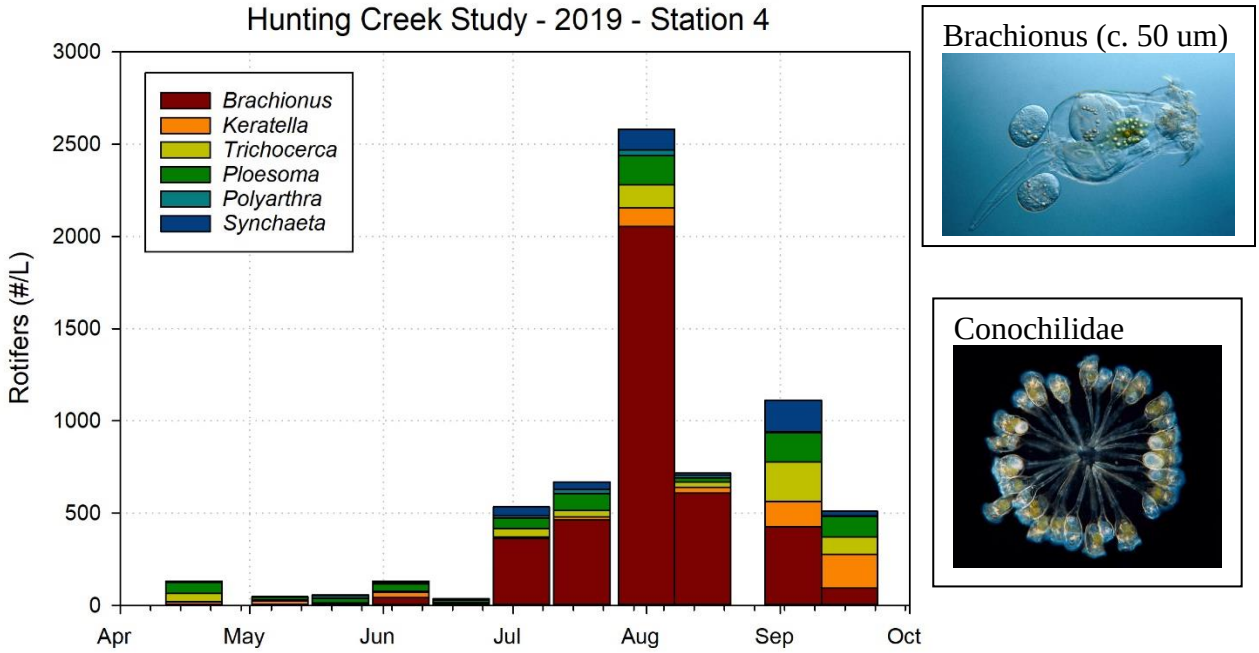

Figure 72. Rotifer Density by Dominant Taxa (#/L). River.

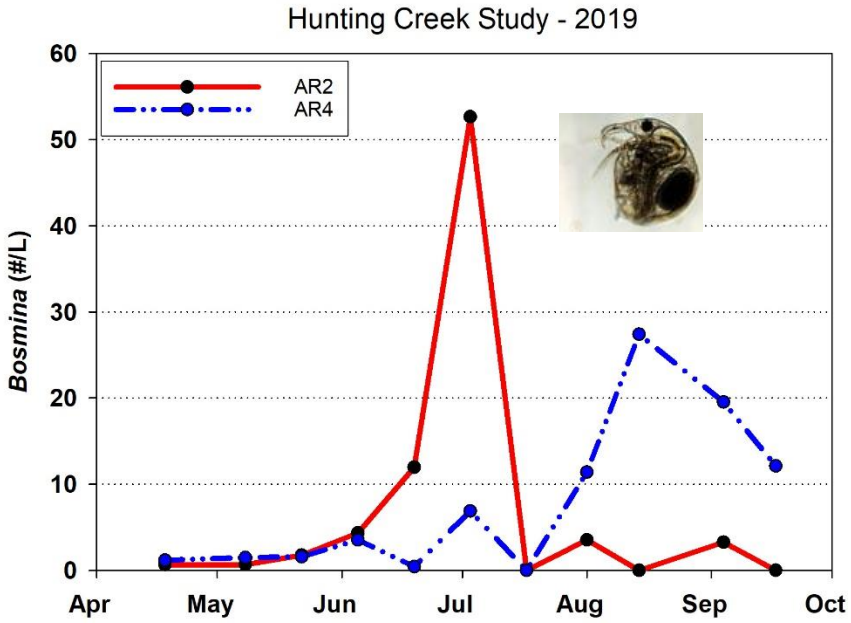

Bosmina is a small-bodied cladoceran, or "waterflea", which is common in lakes and freshwater tidal areas. It is typically the most abundant cladoceran with maximum numbers generally about 100-1000 animals per liter. Due to its small size and relatively high abundances, it is enumerated in the micro-zooplankton samples. *Bosmina* can graze on smaller phytoplankton cells, but can also utilize some cells from colonies by knocking them loose.

Figure 73. *Bosmina* Density by Station (#/L).

At the embayment station AR2 the small cladoceran *Bosmina* reached a peak at about 50/L in early July and then dropped off rapidly (Figure 73). In the river the Bosmina increase was delayed until August and approached 30/L before dropping off. *Diaphanosoma*, typically the most abundant larger cladoceran in the tidal Potomac, was moderately abundant in June and early July at AR2 and was similarly abundant at AR4, but for a shorter period (Figure 74).

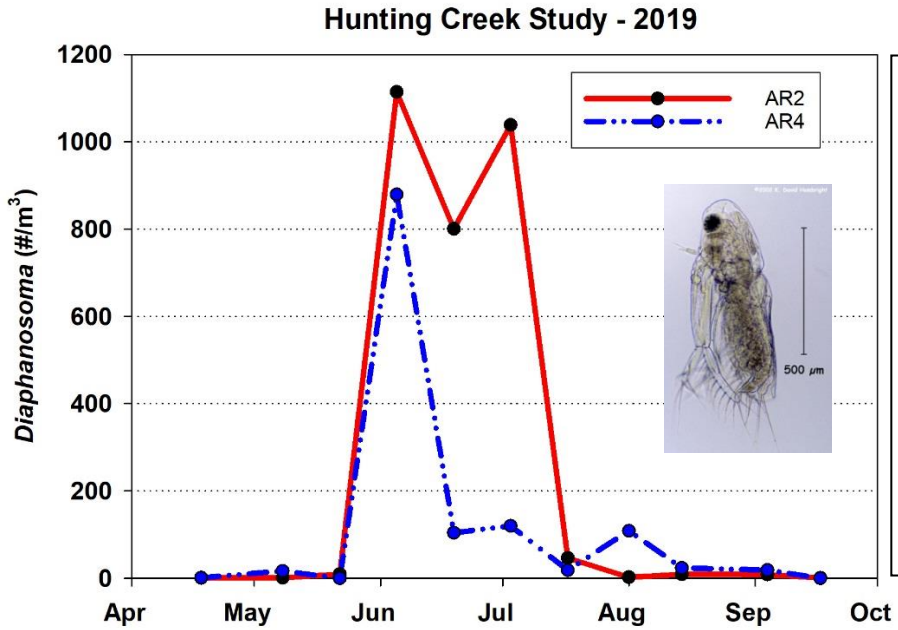

Diaphanosoma is the most abundant larger cladoceran found in the tidal Potomac River. It generally reaches numbers of 1,000-10,000 per m^3 (which would be 1-10 per liter). Due to their larger size and lower abundances, *Diaphanosoma* and the other cladocera are enumerated in the macrozooplankton samples. *Diaphanosoma* prefers warmer temperatures than some cladocera and is often common in the summer.

Figure 74. *Diaphanosoma* Density by Station (#/m^3).

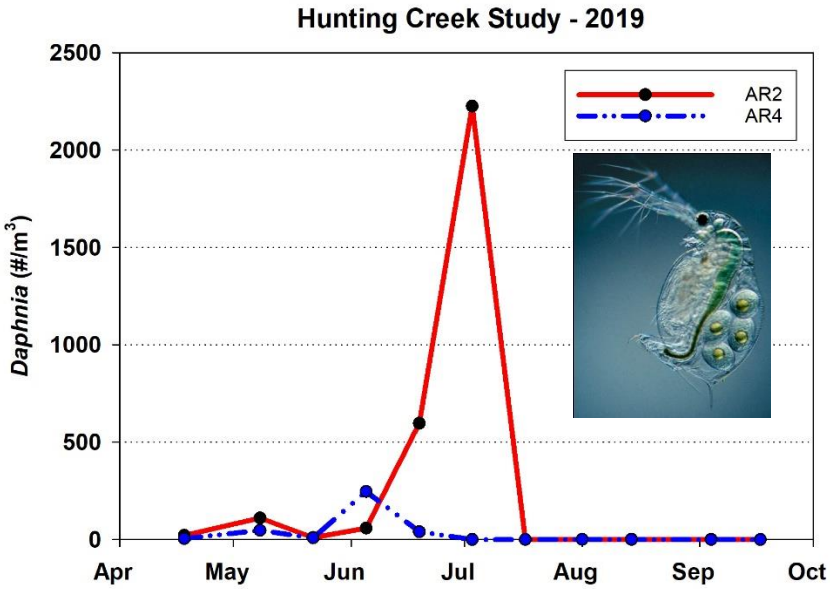

Daphnia, the common waterflea, is one of the most efficient grazers of phytoplankton in freshwater ecosystems. In the tidal Potomac River it is present, but has not generally been as abundant as *Diaphanosoma*. It is typically most common in spring.

Figure 75. *Daphnia* Density by Station (#/m^3).

Daphnia was one of the few plankters that reached higher levels in 2019 than in most previous years (Figure 75). Peak values of over 2000/m^3 were observed at AR2 in early July. At AR4 *Daphnia* was much lower. *Ceriodaphnia* showed a similar temporal pattern reaching a maximum of 650/m^3 in early July (Figure 76).

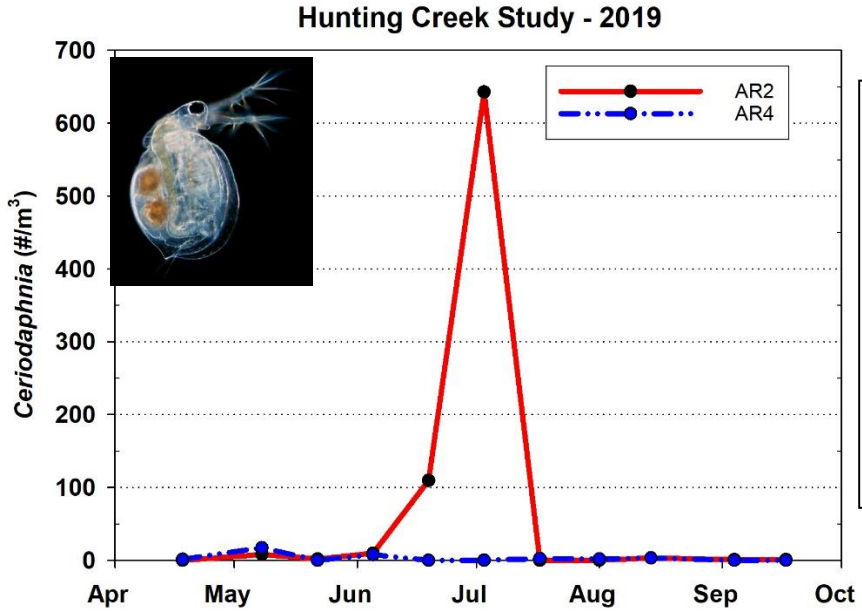

Ceriodaphnia, another common large-bodied cladoceran, is usually present in numbers similar to *Daphnia*. Like all waterfleas, the juveniles look like miniature adults and grow through a series of molts to a larger size and finally reach reproductive maturity. Most reproduction is asexual except during stressful environmental conditions.

Figure 76. *Ceriodaphnia* Density by Station (#/m^3).

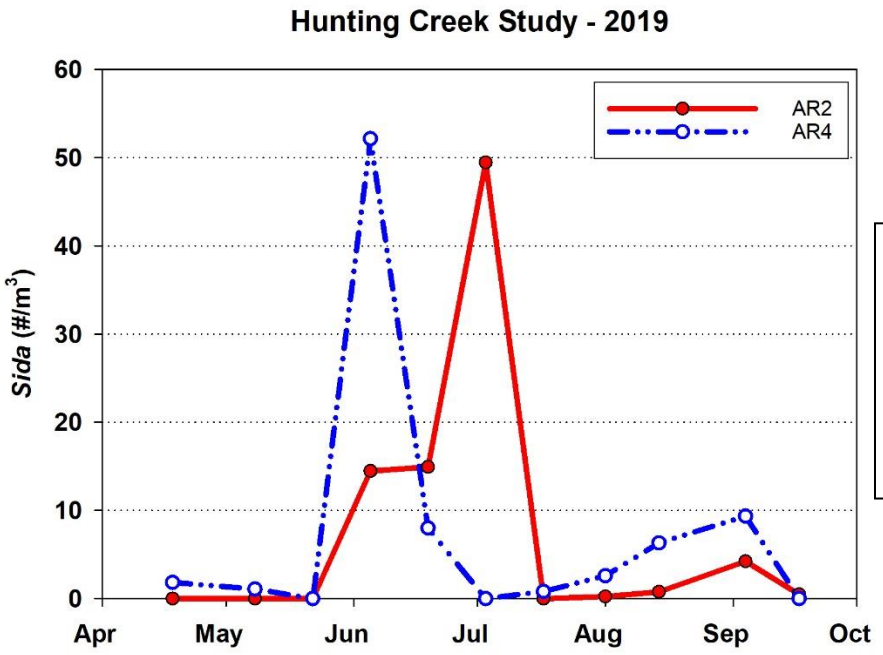

Sida is another waterflea that is often observed in the tidal Potomac River. Like the other cladocera mentioned so far, *Sida* grazes on phytoplankton to obtain its food supply.

Figure 77. *Sida* Density by Station (#/m^3).

Sida was found at moderate levels in early June in the river and at similar levels in early July in the embayment (Figure 77). *Leptodora*, the large cladoceran predator, was found at relatively high levels in early June at both stations and again at moderate levels in early July at the river station (Figure 78).

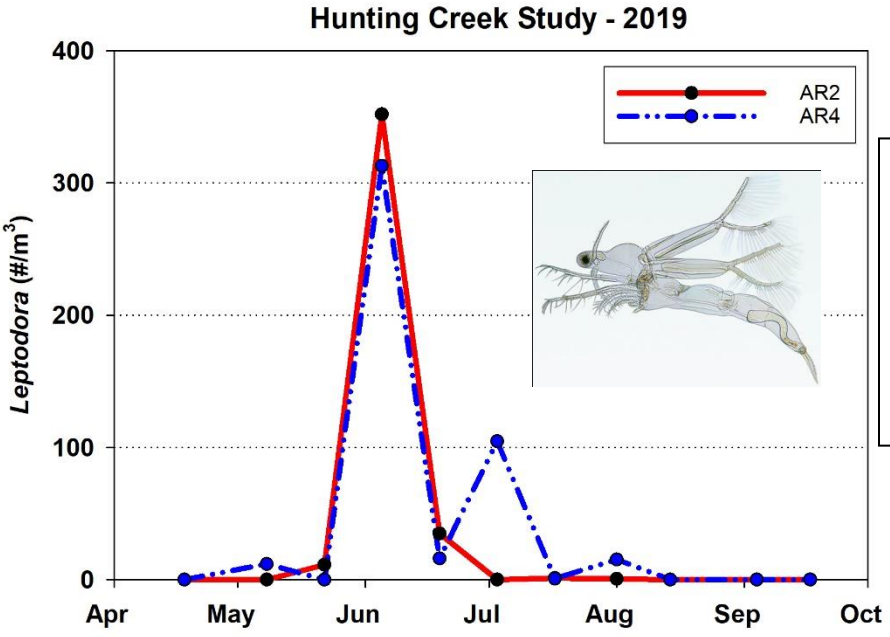

Leptodora is substantially larger than the other cladocera mentioned. Also different is its mode of feeding – it is a predator on other zooplankton. It normally occurs for brief periods in the late spring or early summer.

Figure 78. *Leptodora* Density by Station (#/m^3).

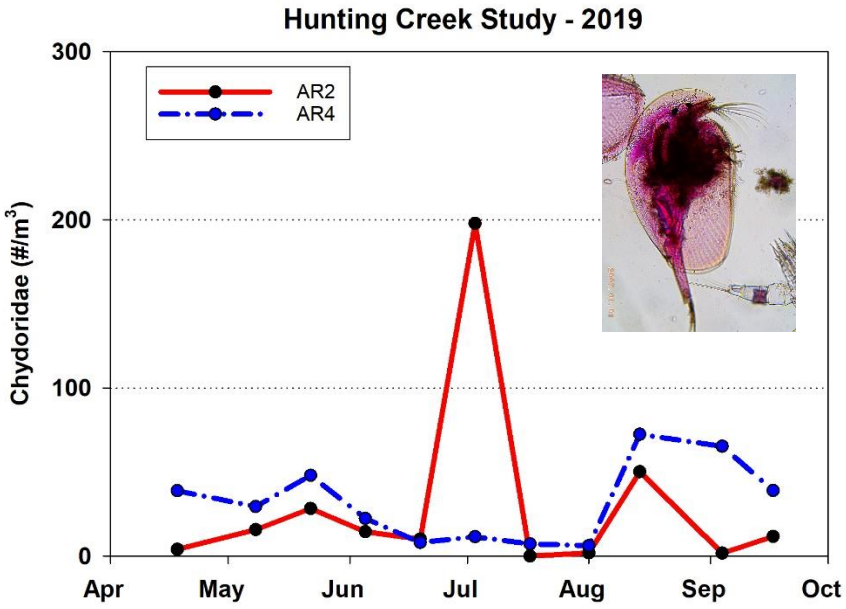

Figure 79. Chydoridae Density by Station (#/m^3). (photo: L. Birsa from HC samples)

Chydoridae is a cladoceran family whose members are associated with SAV (Figure 79). In 2019, levels wre quite low except at AR2 in early July. Macrothricids, another group associated with SAV, were of very minor importance in 2019 (Figure 80).

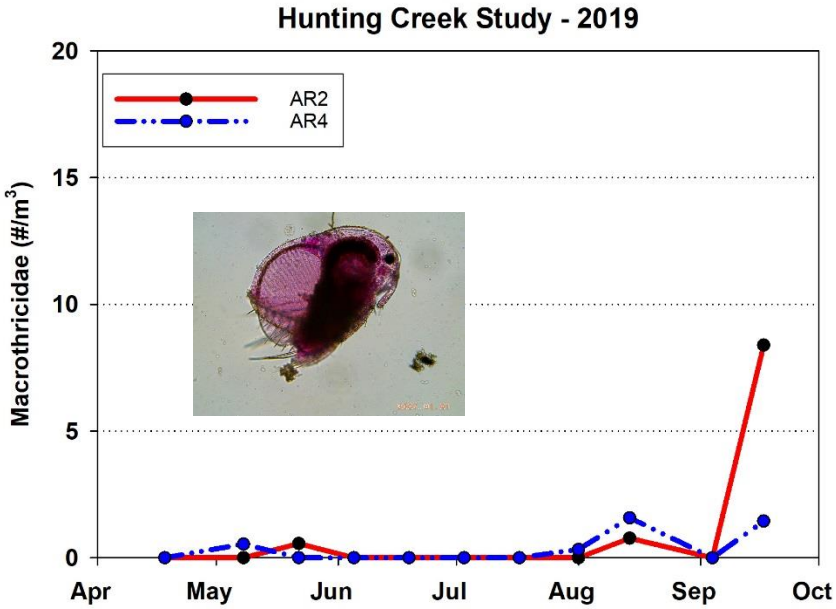

Figure 80. Macrothricid Density by Station (#/m^3). (photo: L. Birsa from HC samples)

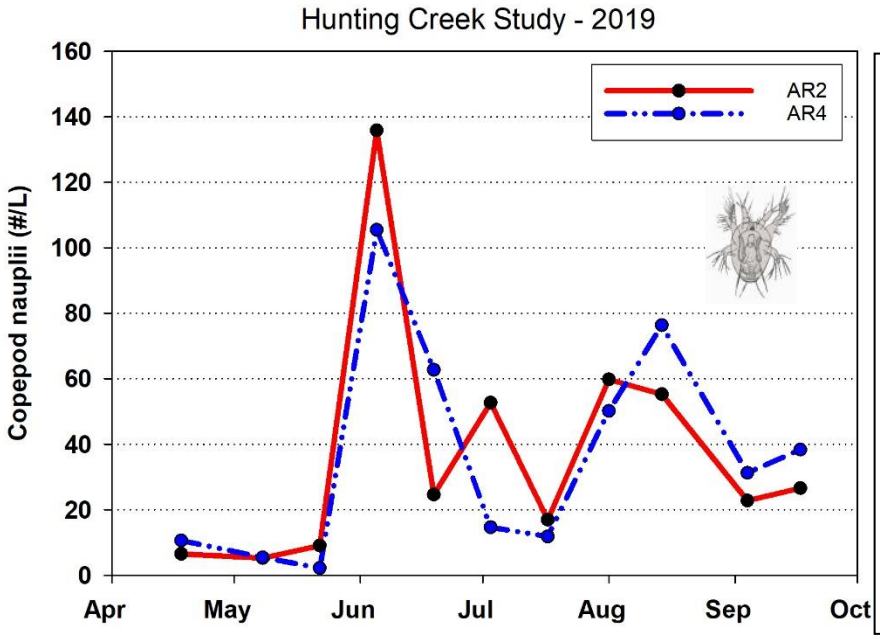

Copepod eggs hatch to form an immature stage called a nauplius. The nauplius is a larval stage that does not closely resemble the adult and the nauplii of different species of copepods are not easily distinguished so they are lumped in this study. Copepods go through 5 naupliar molts before reaching the copepodid stage which is morphologically very similar to the adult. Because of their small size and high abundance, copepod nauplii are enumerated in the micro-zooplankton samples.

Figure 81. Copepod Nauplii Density by Station (#/L).

Copepod nauplii were the most numerous group of crustacean zooplankton. They were present at both stations at similar levels in 2019 (Figure 81). Densities were low in spring, but increased sharply in early June. They decreased somewhat in July and then increased again in August. In the river *Eurytemora*, a large calanoid copepod, increased in May and June reaching a strong peak of over 8000/m^3 in mid-June declining strongly in early July and remaining low for the rest of the year. A lower peak was found at AR2 and it only was present in early June (Figure 82).

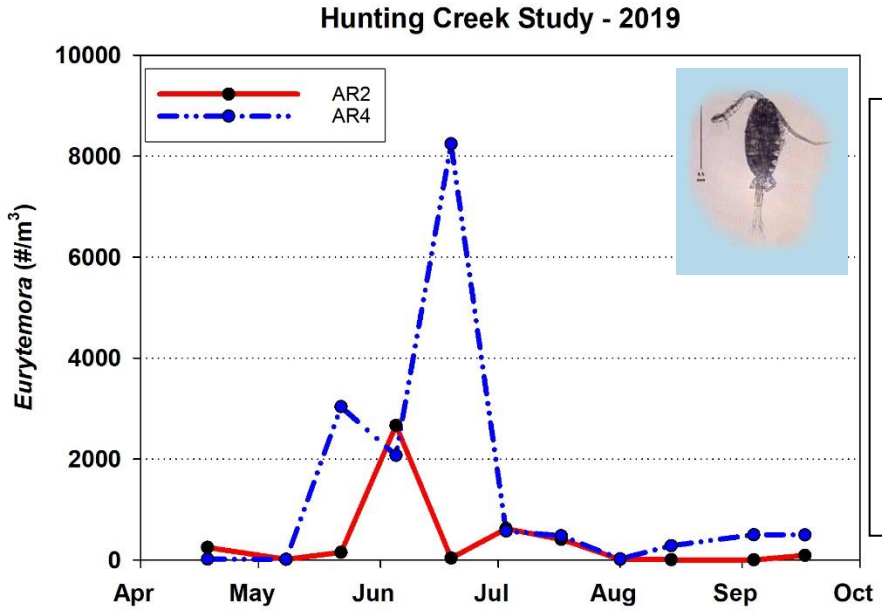

Eurytemora affinis is a large calanoid copepod characteristic of the freshwater and brackish areas of the Chesapeake Bay. *Eurytemora* is a cool water copepod which often reaches maximum abundance in the late winter or early spring. Included in this graph are adults and those copepodids that are recognizable as *Eurytemora*.

Figure 82. *Eurytemora* Density by Station (#/m^3).

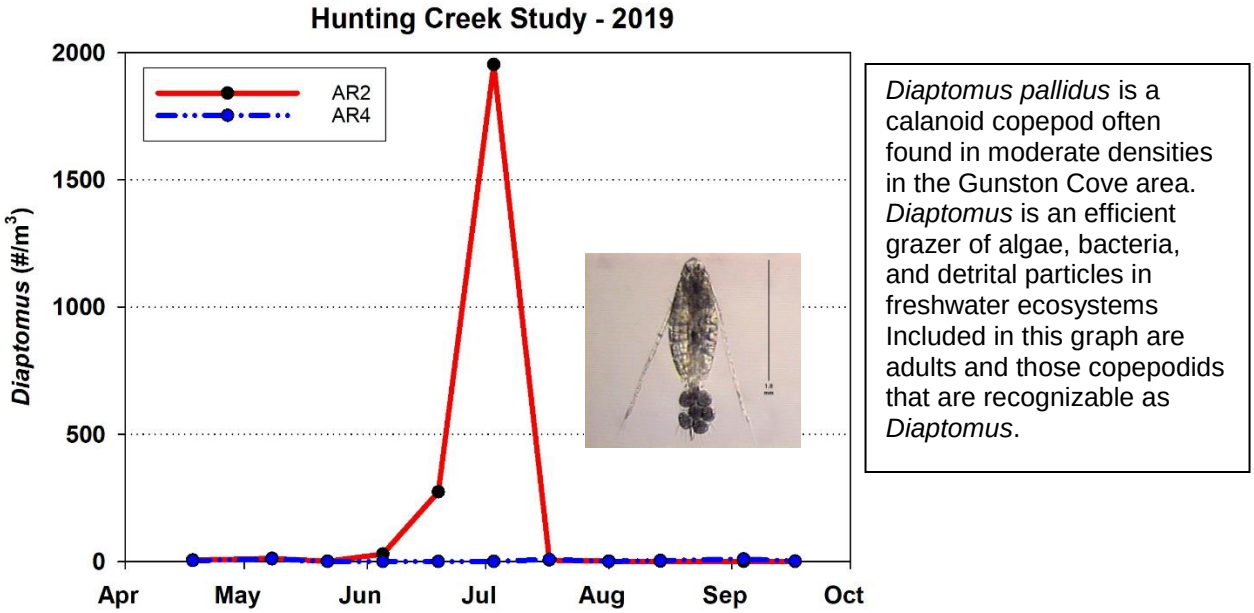

Figure 83. *Diaptomus* Density by Station (#/m^3).

Diaptomus was almost exclusively found in Hunting Creek where it reached a substantial peak of about 2000/m^3 in early July (Figure 83). As in most years *Diaptomus* was very rare in the river mainstem. Cyclopoid copepods were present at moderately high levels at AR2 in early July and at lower levels in early September at AR4 (Figure 84).

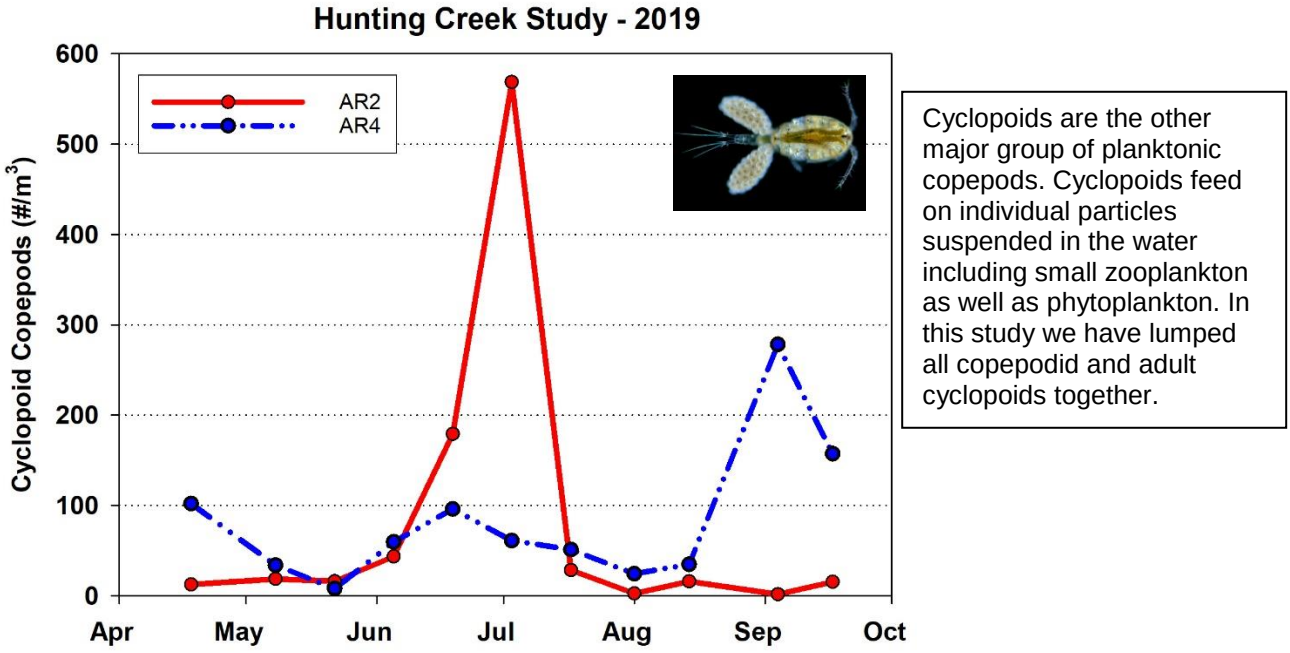

Figure 84. Cyclopoid Copepods by Station (#/m^3).

F. Ichthyoplankton – 2019

We collected 14 samples (7 at Station 2 and 7 at Station 4) during the months April through July and found an average total larval density of 1308 larvae of at least 16 species per 10 m^3 (Table 4). The dominant family was Clupeidae, of which Gizzard Shad (*Dorosoma cepedianum*) had the highest density with an average larval density of 1000 larvae per $10m^3$. *Alosa aestivalis* (Blueback Herring) had the second highest density with an average of 136 larvae per $10m^3$, closely followed by *A. pseudoharengus* (Alewife) with 107 larvae per $10m^3$ on average. Another clupeid present that could positively be identified to the species level is Hickory Shad (*A. mediocris*) at an average of 8.28 larvae per $10m^3$. The taxon Clupeidae, which is comprised of clupeids (*Alosa* or *Dorosoma* sp.) that could not be identified to a lower taxonomic level had an average density of 85 larvae per $10m^3$. A different taxon with relatively high representation is White Perch (*Morone americana*) with an average of 33 larvae per $10m^3$. Quillback (*Carpiodes Cyprinus*) was relatively abundant as well, with an average of 4 larvae per $10m^3$.

Table 4. The average larval density (#/$10m^3$) in Hunting Creek (Station AR2) and the Potomac River (Station AR4) in 2019.

Scientific Name	Common Name	AR2	AR4	Average
Alosa aestivalis	Blueback Herring	153.25	118.47	135.86
Alosa mediocris	Hickory Shad	8.28	3.08	5.68
Alosa pseudoharengus	Alewife	170.94	43.40	107.17
Carpiodes cyprinus	Quillback	7.90	0.24	4.07
Catostomidae	unk. catostomidae species	0.00	0.17	0.08
Clupeidae	unk. clupeid species	148.49	20.64	84.56
Dorosoma cepedianum	Gizzard Shad	711.71	1287.77	999.74
Eggs	eggs	55.07	7.18	31.13
Etheostoma sp.	unk. darter species	0.19	0.00	0.09
Hybognathus regius	Eastern Silvery Minnow	0.19	0.00	0.09
Lepomis gibbosus	Pumpkinseed	0.35	0.00	0.17
Lepomis sp.	unk. sunfish	0.19	0.00	0.09
Menidia beryllina	Inland Silverside	1.05	0.17	0.61
Morone americana	White Perch	32.87	33.44	33.15
Notropis hudsonius	Spottail Shiner	0.00	0.23	0.12
Perca flavescens	Yellow Perch	0.00	0.73	0.37
Unidentified	unidentified	17.37	109.37	63.37
Total		1307.83	1624.88	1466.36

The density of clupeid larvae has a clear seasonal pattern as a result of the spring spawning season of most clupeids that occurs higher upstream. Clupeid larvae in Figure 85 include Blueback Herring, Hickory Shad, Alewife, American Shad and Gizzard Shad. These have similar spawning patterns, so they are lumped into one group for this analysis. Clupeids were absent from the sample until late May, when they appeared in peak abundance of over 800 larvae per 10 m^3, then decreased to over 250 larvae per 10m^3 in early June before disappearing from the sample again after mid-June (Figure 85). Of these clupeids, Alewife and Blueback Herring are the two species that make up river herring, of which we describe the spawning population at the end of this report.

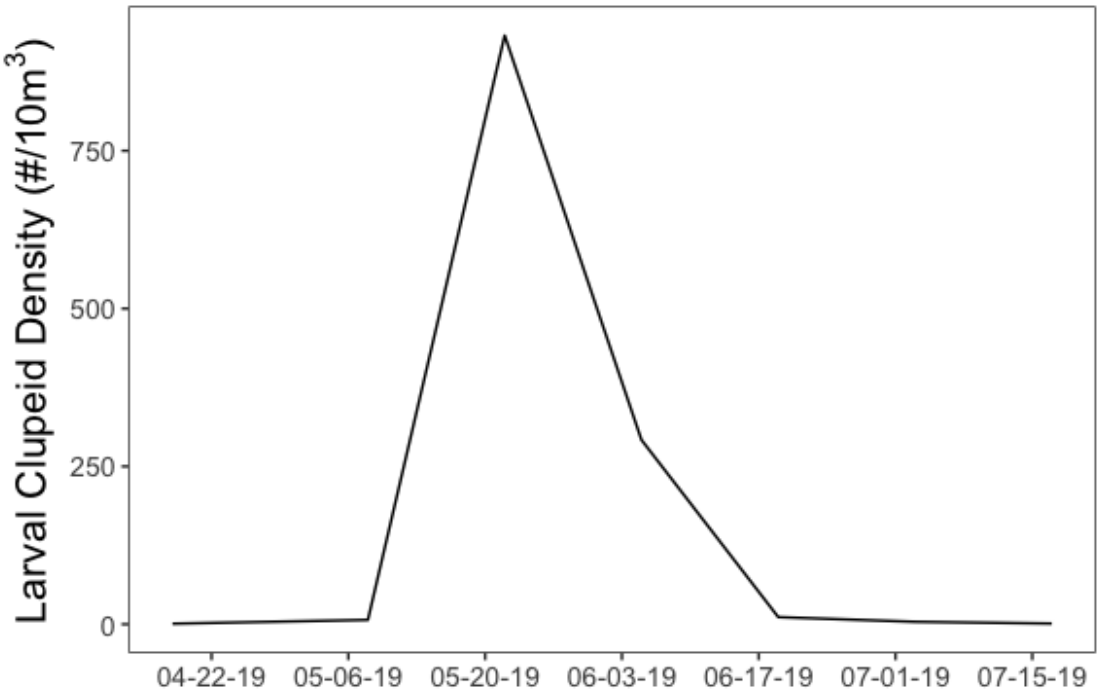

Figure 85. Density of clupeid larvae per 10m^3.

White Perch larvae attained highest density on average at 25 larvae per 10m^3 at the end of may as well (Figure 86), and disappeared from the samples mid-June. The group of larvae that are not positively identified clupeids or *Morone* species are dominated by unidentified larvae (Figure 87). Highest densities of other larvae were found end of May as well. The unidentified larvae were not intact unknown species, but larvae to mangled for proper identification. Because of the high density of clupeid larvae, most unidentified larvae are likely to be clupeids as well.

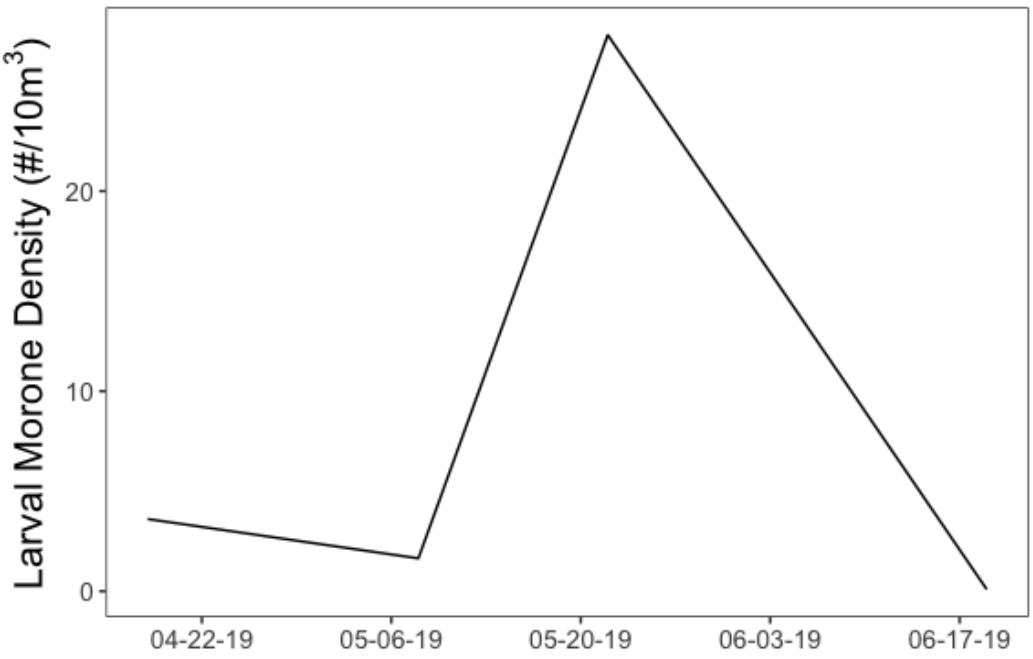

Figure 86. Density of *Morone sp.* (white perch and striped bass) per $10m^3$.

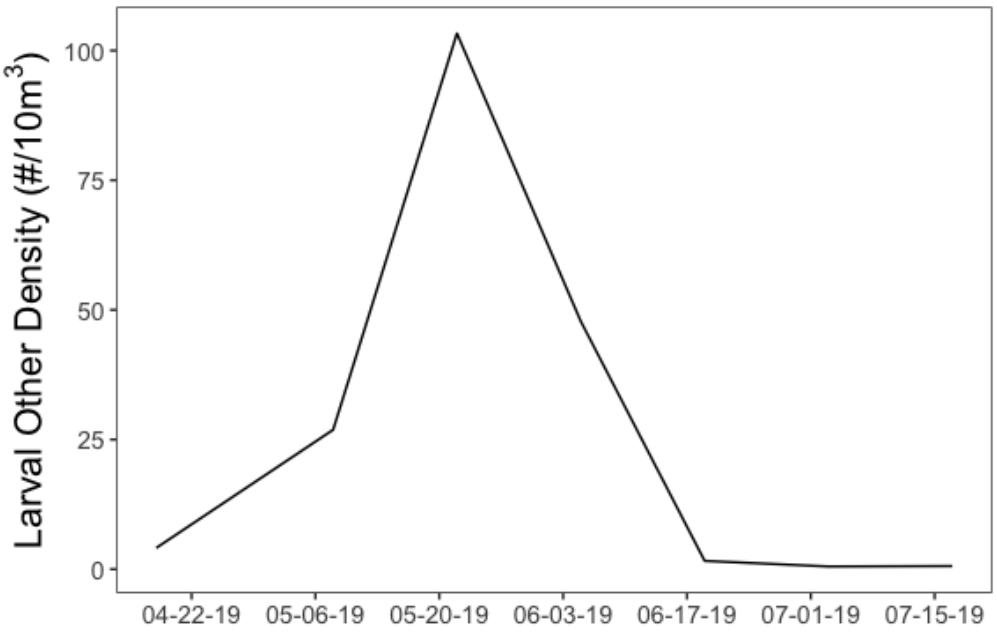

Figure 87. Density of other larvae per $10m^3$.

G. Adult and juvenile fishes – 2019

Trawls

Trawl sampling was conducted between May 3 and September 18 at station 3 and 4. A total of 937 fishes comprising 22 species were collected with trawls (Table 5). This abundance and species diversity is similar to last year. Collections were dominated by White Perch (65.53%). The second most abundant species was Blue Catfish (9.93%). Other relatively abundant species were Spottail Shiner (7.68%), Bay Anchovy (5.87%), species of the Alosa genus (2.67%), Tessellated Darter (2.13%), Alewife (1.60%), and Pumpkinseed (1.28%) (Tables 5 and 6). An interesting find was the collection of native catfishes (Channel Catfish, Brown Bullhead, Yellow Bullhead and White Bullhead), which have seen declining abundances since the invasion of Blue Catfish.

Table 5. Adult and juvenile fish collected by trawling. Hunting Creek - 2019.

Scientific Name	CommonName	Abundance	Percent
Morone americana	White Perch	614	65.53
Ictalurus furcatus	Blue Catfish	93	9.93
Notropis hudsonius	Spottail Shiner	72	7.68
Anchoa mitchilli	Bay Anchovy	55	5.87
Alosa sp.	unk. Alosa species	25	2.67
Etheostoma olmstedi	Tessellated Darter	20	2.13
Alosa pseudoharengus	Alewife	15	1.60
Lepomis gibbosus	Pumpkinseed	12	1.28
Alosa aestivalis	Blueback Herring	5	0.53
Ameiurus natalis	Yellow Bullhead	4	0.43
Perca flavescens	Yellow Perch	4	0.43
Alosa mediocris	Hickory Shad	2	0.21
Alosa sapidissima	American Shad	2	0.21
Ameiurus nebulosus	Brown Bullhead	2	0.21
Cyprinus carpio	Carp	2	0.21
Hybognathus regius	Eastern Silvery Minnow	2	0.21
Ictalurus punctatus	Channel Catfish	2	0.21
Lepomis macrochirus	Bluegill	2	0.21
Ameiurus catus	White Bullhead	1	0.11
Anguilla rostrata	American Eel	1	0.11
Morone saxatilis	Striped Bass	1	0.11
Pomoxis nigromaculatus	Black Crappie	1	0.11
Total		937	100

Table 6. Adult and juvenile fish collected by trawling. Hunting Creek study - 2019.

Scientific Name	Common Name	05/03	05/13	05/29	06/11	06/25	07/09	07/23	08/13	08/28	09/18	Total
Alosa aestivalis	Blueback Herring	0	0	1	4	0	0	0	0	0	0	5
A. mediocris	Hickory Shad	0	0	0	0	0	2	0	0	0	0	2
A.pseudoharengus	Alewife	0	0	1	1	0	12	0	0	1	0	15
A. sapidissima	American Shad	0	0	0	2	0	0	0	0	0	0	2
Alosa sp.	Alosa species	0	0	0	0	0	16	4	0	0	5	25
Ameiurus catus	White Bullhead	0	0	0	0	0	1	0	0	0	0	1
Ameiurus natalis	Yellow Bullhead	0	0	1	0	0	0	0	1	1	1	4
Ameiurus nebulosus	Brown Bullhead	0	0	0	1	0	0	0	0	1	0	2
Anchoa mitchilli	Bay anchovy	0	0	0	0	0	0	0	0	0	55	55
Anguilla rostrata	American Eel	0	0	1	0	0	0	0	0	0	0	1
Cyprinus carpio	Common Carp	0	0	0	0	0	0	2	0	0	0	2
Etheostoma olmstedi	Tessell. Darter	0	0	0	1	0	0	5	13	1	0	20
Hybognathus regius	E. Silvery Minnow	0	0	0	0	0	2	0	0	0	0	2
Ictalurus furcatus	Blue Catfish	3	1	0	3	1	0	1	41	43	0	93
Ictalurus punctatus	Channel Catfish	0	0	0	0	0	0	0	0	2	0	2
Lepomis gibbosus	Pumpkinseed	1	2	0	1	0	1	0	1	4	2	12
L. macrochirus	Bluegill	0	0	0	0	0	1	1	0	0	0	2
Morone americana	White Perch	1	9	1	5	5	53	51	92	362	35	614
Morone saxatilis	Striped Bass	0	0	0	0	0	0	1	0	0	0	1
Notropis hudsonius	Spottail Shiner	0	2	0	1	0	17	20	18	7	7	72
Perca flavescens	Yellow Perch	0	0	0	2	0	1	0	1	0	0	4
Pomoxis nigromaculatus	Black Crappie	0	0	0	0	0	1	0	0	0	0	1
Total		5	14	5	21	6	107	85	167	422	105	937

Trawling collects fish that are located in the open water near the bottom. Due to the shallowness of Hunting Creek, the volume collected is a substantial part of the water column. However, in the river channel, the near bottom habitat through which the trawl moves is only a small portion of the water column. Fishes tend to concentrate near the bottom or along shorelines rather than in the upper portion of the open water.

The highest catch occurred on August 28, which was due to the high abundance of White Perch in that trawl sample (Table 6). In 2019, most catches occurred at station 3, while the difference from the total catch at station 4 was small (Table 7). At both stations, catches of White Perch were mostly responsible for the total catch. The catch at station 4 was similar to last year with 438 individuals, but was less diverse with 6 species (compared to 13 species in 2018). At Station 3, 499 specimens were collected of 20 species as compared to 845 specimens of 16 species in 2018. White Perch was the dominant species as in previous years. Looking at species by dominance (Figure 89A and B) White Perch was the dominant species both at station 3 and 4 in 2019. The species distribution is more even in station 3 than station 4. The biggest differences between catches at station 3 and station 4 are higher catches of Alosas, Bay Achovy, Tesselated Darter and Spottail Shiner at Station 3, and higher catches of Blue catfish at station 4.

Table 7. Adult and juvenile fish collected by trawling. Hunting Creek study - 2019.

Scientific Name	Common Name	AR3	AR4
Alosa aestivalis	Blueback Herring	5	0
Alosa mediocris	Hickory Shad	2	0
Alosa pseudoharengus	Alewife	15	0
Alosa sapidissima	American Shad	2	0
Alosa sp.	unk. Alosa species	25	0
Ameiurus catus	White Bullhead	1	0
Ameiurus natalis	Yellow Bullhead	1	3
Ameiurus nebulosus	Brown Bullhead	2	0
Anchoa mitchilli	Bay anchovy	55	0
Anguilla rostrata	American Eel	1	0
Cyprinus carpio	Common Carp	0	2
Etheostoma olmstedi	Tessellated Darter	20	0
Hybognathus regius	Eastern Silvery Minnow	2	0
Ictalurus furcatus	Blue Catfish	5	88
Ictalurus punctatus	Channel Catfish	0	2
Lepomis gibbosus	Pumpkinseed	12	0
Lepomis macrochirus	Bluegill	2	0
Morone americana	White Perch	273	341
Morone saxatilis	Striped Bass	1	0
Notropis hudsonius	Spottail Shiner	70	2
Perca flavescens	Yellow Perch	4	0
Pomoxis nigromaculatus	Black Crappie	1	0
Total		499	438

White perch (*Morone americana*) is the dominant species in Hunting Creek, and continues to be an important commercial and popular game fish. Adults grow to over 30 cm long. Sexual maturity begins the second year at lengths greater than 9 cm. As juveniles they feed on zooplankton and macrobenthos, but as they get larger consume fish as well.

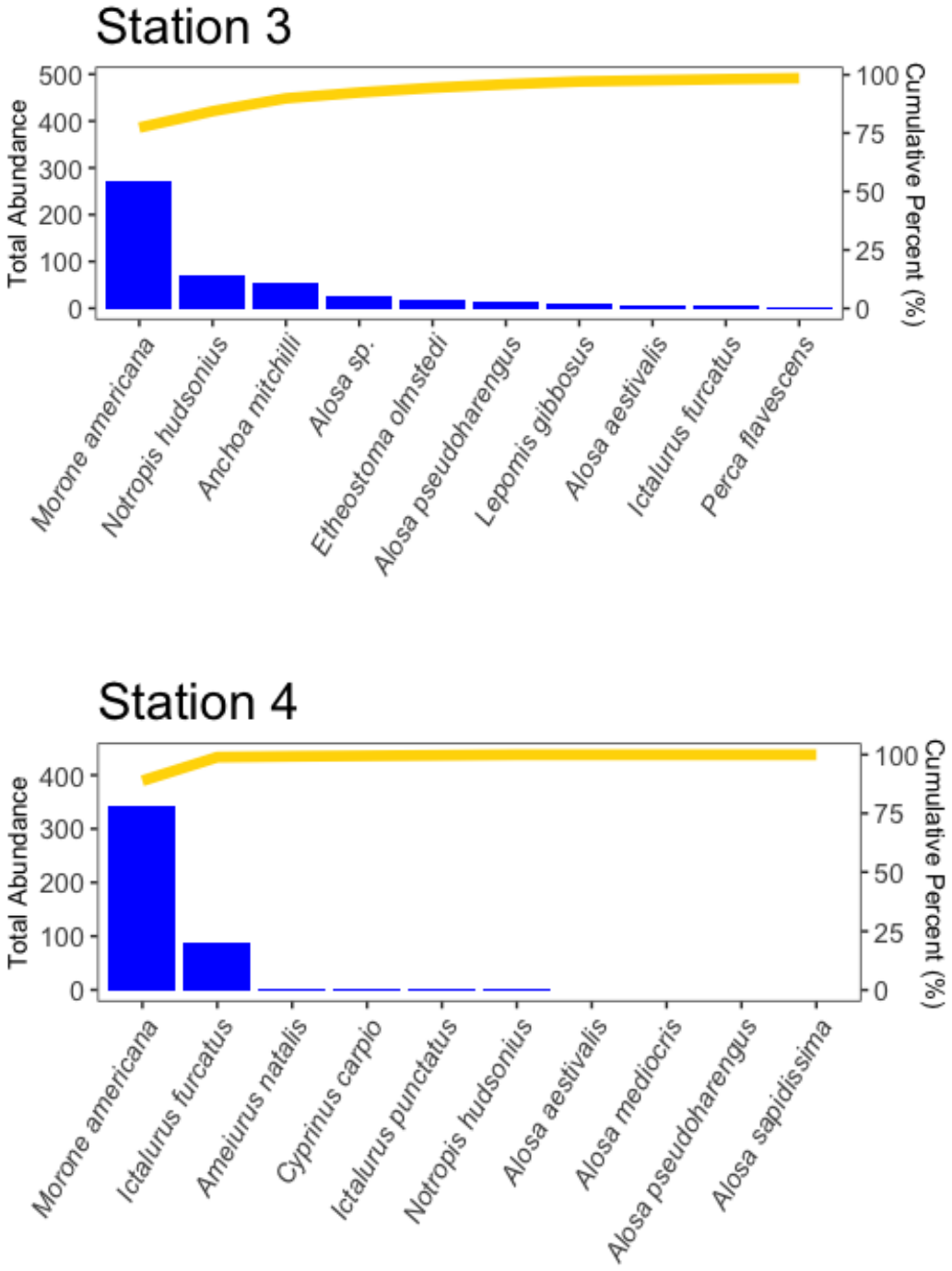

Figure 88A and B. Pareto chart of adult and juvenile fishes collected by trawling. Dominant species by station in total abundance and cumulative percentage of total for Station 3 (top) and Station 4 (bottom).

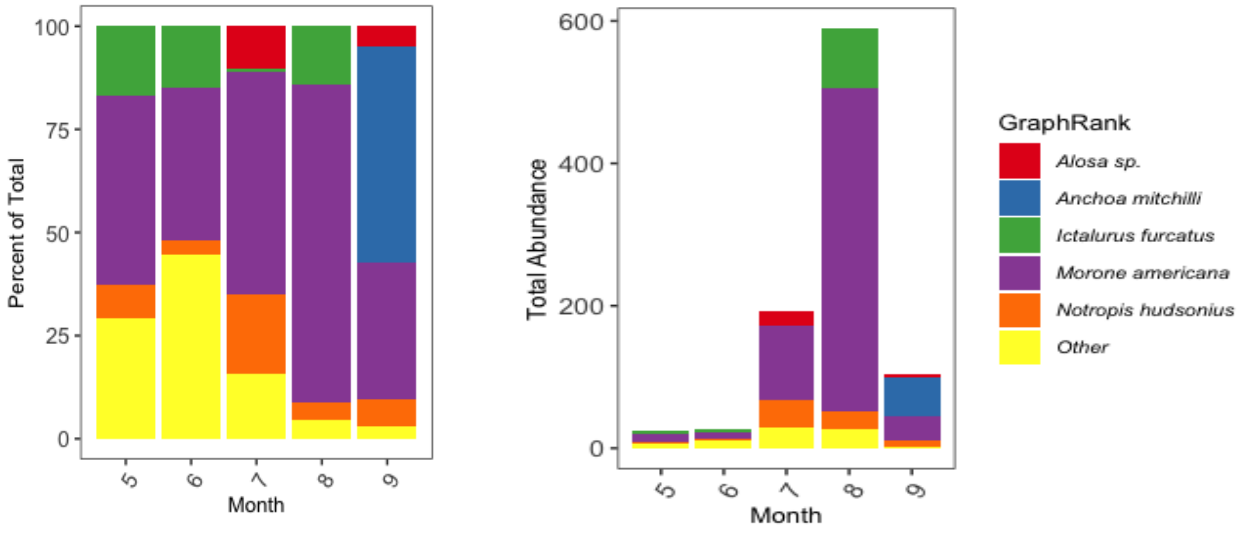

Figure 89 A&B. Adult and juvenile fishes collected by trawling. Dominant species by month in percentage of total (A) and total abundance (B).

Seines

Seine sampling was conducted between May 3 and September 18 at station 5 and 6. The first sampling trip, normally occurring in April, was scheduled for May 3, resulting in 3 sampling trips in May. Further, as planned, two sampling trips per month were performed until (and including) August, and one sampling trip in September. These two seines stations were selected as sites with shallow sloping shorelines that would enable us to tow a beach seine. The net was towed up onto the beach unless high water completely submerged the beach. In those cases, the net was towed into the boat.

A total of 20 seine samples were conducted (10 per station), comprising 2430 fishes of at least 29 species (Table 8). This is more than last year. Unlike previous years, the most dominant species in seine catches was not Banded Killifish (17.41%), likely due to the low coverage of submerged aquatic vegetation in 2019. Instead, higher abundances were found of species of the *Alosa* genus (36.71%) and White Perch (30.41%). Other species with relatively high abundance were Inland Silverside (3.46%), Quillback (2.96%), Gizzard Shad (2.14%), Spottail Shiner (1.52%), Bay Anchovy (1.28%), and Atlantic Menhaden (1.23%). Other species occurred at low abundances (Table 8).

White Perch was present from May to September (throughout the sampling period), and dominant in the June and July collections (Table 9). Banded Killifish was present from May to August, generally in high abundance each sampling date. The high abundance of Alosids is mainly due to the first sampling day on May 3, when 614 specimens were collected, most not further identifiable than the genus level. This event made May the most productive month. The three most abundant taxa (Alosids, White Perch and banded Killifish) were all in highest abundance in station 6 (Table 10). Therefore, the total number of specimens at station 6 was higher than station 5. Evenness distribution of abundance over multiple species was higher at station 6 than station 5, mostly due to the lower relative abundance of Banded Killifish in station 6 (Figure 90 A&B). An interesting find in station 5 was an American Eel, which is listed as endangered on the IUCN red list.

The abundance by month of dominant species shows a clear high catch of Alosids in the first month, which is likely the result of the river herring spawning season that ends in May (Figure 91 A&B). After that, the White Perch dominance becomes apparent, with slowly reducing abundance and dominance over the sampling season. Banded Killifish is still an important representative of the fish assemblage as well, however, the more open water character of Hunting Creek in 2019 favored pelagic species such as White Perch and Alosids over semi-demersal SAV dwellers like banded Killifish. Other species that were abundant but not ubiquitous or dominant in seine collections throughout the sampling season were Inland Silverside and Quilllback (Figures 91 A&B).

Table 8. Adult and juvenile fish collected by seining. Hunting Creek- 2019.

ScientificName	CommonName	Abundance	Percent
Alosa aestivalis	Blueback Herring	27	1.11
Alosa mediocris	Hickory Shad	6	0.25
Alosa pseudoharengus	Alewife	52	2.14
Alosa sapidissima	American Shad	10	0.41
Alosa sp.	unk. Alosa species	797	32.80
Anchoa mitchilli	Bay Anchovy	31	1.28
Anguilla rostrata	American Eel	1	0.04
Brevoortia tyrannus	Atlantic Menhaden	30	1.23
Carpiodes cyprinus	Quillback	72	2.96
Cyprinus carpio	Carp	2	0.08
Dorosoma cepedianum	Gizzard Shad	52	2.14
Etheostoma olmstedi	Tessellated Darter	9	0.37
Fundulus diaphanus	Banded Killifish	423	17.41
Fundulus heteroclitus	Mummichog	14	0.58
Gambusia holbrooki	Mosquitofish	7	0.29
Hybognathus regius	Eastern Silvery Minnow	4	0.16
Lepomis gibbosus	Pumpkinseed	4	0.16
Lepomis macrochirus	Bluegill	1	0.04
Lepomis sp.	unk. sunfish	1	0.04
Menidia beryllina	Inland Silverside	84	3.46
Micropterus dolomieu	Smallmouth Bass	10	0.41
Micropterus salmoides	Largemouth Bass	2	0.08
Morone americana	White Perch	739	30.41
Morone saxatilis	Striped Bass	5	0.21
Moxostoma erythrurum	Golden Redhorse	3	0.12
Notemigonus crysoleucas	Golden Shiner	1	0.04
Notropis hudsonius	Spottail Shiner	37	1.52
Perca flavescens	Yellow Perch	2	0.08
Pomoxis nigromaculatus	Black Crappie	2	0.08
Strongylura marina	Atlantic Needlefish	2	0.08
Total		2430	100

Table 9. Adult and juvenile fish collected by seining. Hunting Creek study - 2019.

Scientific Name	Common Name	05/03	05/13	05/29	06/11	06/25	07/09	07/23	08/13	08/28	09/18	Total
Alosa aestivalis	Blueback Herring	22	0	0	5	0	0	0	0	0	0	27
Alosa mediocris	Hickory Shad	0	0	0	0	0	2	0	3	0	1	6
Alosa pseudoharengus	Alewife	0	29	0	2	0	18	0	0	3	0	52
Alosa sapidissima	American Shad	0	0	0	0	0	10	0	0	0	0	10
Alosa sp.	unk. Alosa species	592	0	0	0	0	15	0	85	68	37	797
Anchoa mitchilli	Bay anchovy	0	0	0	0	0	0	0	1	29	1	31
Anguilla rostrata	American Eel	0	0	0	0	0	0	1	0	0	0	1
Brevoortia tyrannus	Atlantic Menhaden	0	0	0	0	0	0	0	0	0	30	30
Carpiodes cyprinus	Quillback	0	0	0	2	50	19	1	0	0	0	72
Cyprinus carpio	Carp	0	0	1	0	0	1	0	0	0	0	2
Dorosoma cepedianum	Gizzard Shad	0	0	0	0	0	1	0	46	3	2	52
Etheostoma olmstedi	Tessellated Darter	0	1	0	1	1	2	0	3	1	0	9
Fundulus diaphanus	Banded Killifish	7	22	14	16	89	11	233	6	25	0	423
Fundulus heteroclitus	Mummichog	0	0	0	0	0	1	6	1	6	0	14
Gambusia holbrooki	Mosquitofish	0	0	0	0	0	6	0	0	1	0	7

Hybognathus regius	Eastern Silvery Minnow	0	0	0	0	0	3	0	1	0	0	4
Lepomis gibbosus	Pumpkinseed	1	0	0	0	0	1	2	0	0	0	4
Lepomis macrochirus	Bluegill	0	0	0	0	0	1	0	0	0	0	1
Lepomis sp.	unk. sunfish	0	0	0	0	0	1	0	0	0	0	1
Menidia beryllina	Inland Silverside	5	0	0	1	0	0	2	14	29	33	84
Micropterus dolomieu	Smallmouth Bass	1	0	0	1	3	3	2	0	0	0	10
Micropterus salmoides	Largemouth Bass	0	0	0	0	0	1	1	0	0	0	2
Morone americana	White Perch	5	0	1	1	396	47	231	10	42	6	739
Morone saxatilis	Striped Bass	0	0	0	0	1	0	2	2	0	0	5
Moxostoma erythrurum	Golden Redhorse	0	0	0	0	0	3	0	0	0	0	3
Notemigonus crysoleucas	Golden Shiner	1	0	0	0	0	0	0	0	0	0	1
Notropis hudsonius	Spottail Shiner	1	0	0	0	12	3	1	2	15	3	37
Perca flavescens	Yellow Perch	0	0	2	0	0	0	0	0	0	0	2
Pomoxis nigromaculatus	Black Crappie	0	0	0	0	2	0	0	0	0	0	2
Strongylura marina	Atlantic Needlefish	0	0	0	1	0	0	0	1	0	0	2
Total		635	52	18	30	554	149	482	175	222	113	2430

Table 10. Adult and juvenile fish collected by seining. Hunting Creek study – 2019.

ScientificName	CommonName	5	6
Alosa aestivalis	Blueback Herring	22	5
Alosa mediocris	Hickory Shad	1	5
Alosa pseudoharengus	Alewife	44	8
Alosa sapidissima	American Shad	0	10
Alosa sp.	unk. Alosa species	19	778
Anchoa mitchilli	Bay anchovy	8	23
Anguilla rostrata	American Eel	1	0
Brevoortia tyrannus	Atlantic Menhaden	0	30
Carpiodes cyprinus	Quillback	1	71
Cyprinus carpio	Carp	1	1
Dorosoma cepedianum	Gizzard Shad	1	51
Etheostoma olmstedi	Tessellated Darter	5	4
Fundulus diaphanus	Banded Killifish	188	235
Fundulus heteroclitus	Mummichog	13	1
Gambusia holbrooki	Mosquitofish	1	6
Hybognathus regius	Eastern Silvery Minnow	1	3
Lepomis gibbosus	Pumpkinseed	0	4
Lepomis macrochirus	Bluegill	0	1
Lepomis sp.	unk. sunfish	1	0
Menidia beryllina	Inland Silverside	3	81
Micropterus dolomieu	Smallmouth Bass	2	8
Micropterus salmoides	Largemouth Bass	2	0
Morone americana	White Perch	13	726
Morone saxatilis	Striped Bass	0	5
Moxostoma erythrurum	Golden Redhorse	3	0
Notemigonus crysoleucas	Golden Shiner	0	1
Notropis hudsonius	Spottail Shiner	1	36
Perca flavescens	Yellow Perch	0	2
Pomoxis nigromaculatus	Black Crappie	0	2
Strongylura marina	Atlantic Needlefish	1	1
Total		332	2098

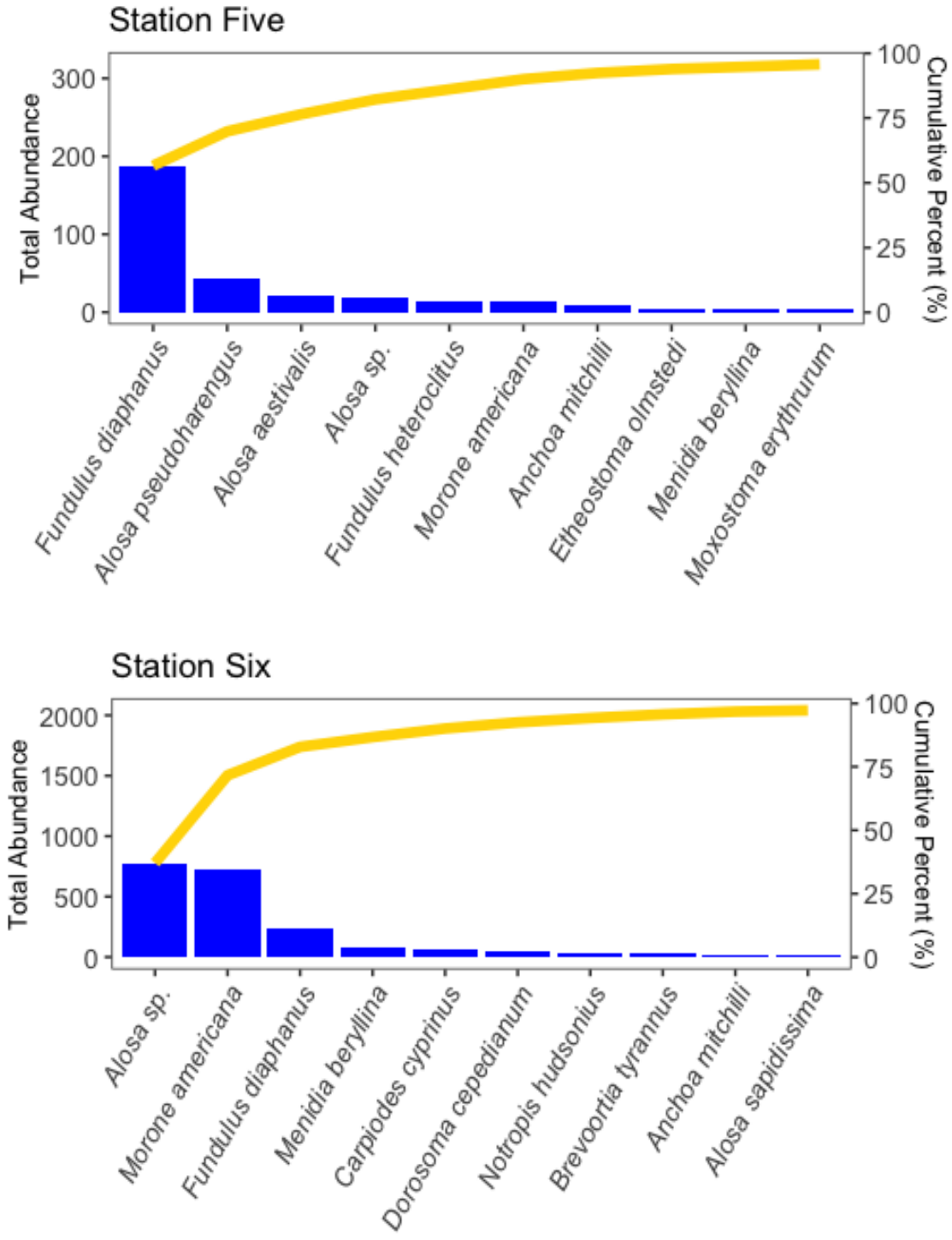

Figure 90A and B. Pareto chart of adult and juvenile fishes collected by seining. Dominant species by station in total abundance and cumulative percentage of total for Station 5 (top) and Station 6 (bottom).

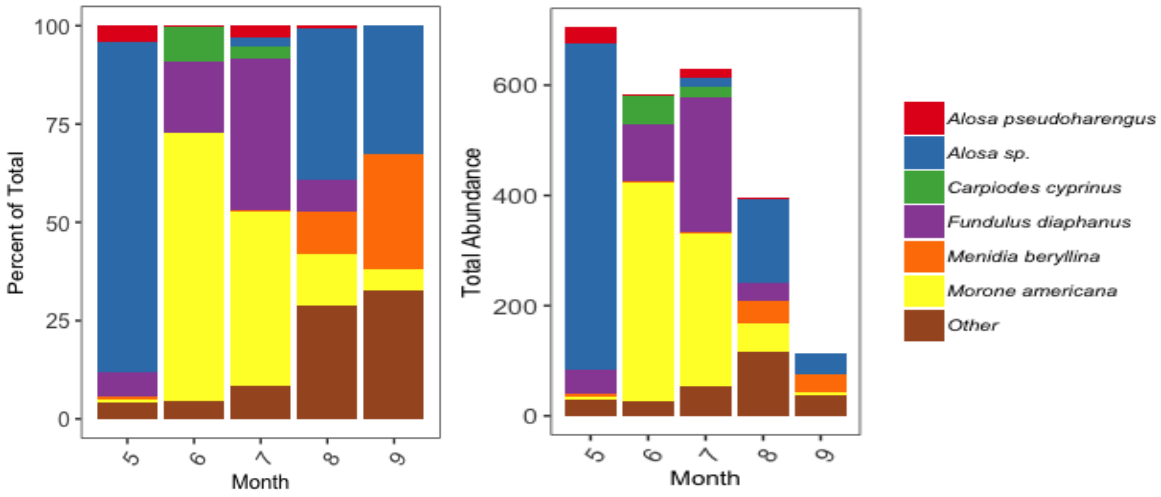

Figure 91A and B. Adult and juvenile fish collected by seining. Dominant species by month in in percentage of total (A) and total abundance (B).

Fyke Nets

Fyke nets were set from May 3 to September 18. Both fyke nets were set near trawl station 3 (Figure 1). We were unable to set the fyke nets on the August 13 sampling trip, resulting in 18 rather than 20 samples. Similar to 2018, the total catch with fyke nets was much less than that with the trawl in 2019. The trade-off between trawl and fyke net catches are likely highly related to the amount of SAV present at the site. The SAV cover was low in 2019, which makes the trawl more effective resulting in a higher catch, and the fyke nest less effective because they are not hidden as well with less dense aquatic plant beds. This highlights the importance of using different gear types to accurately monitor species abundance trends. Fyke nets were very effective in 2017 when the SAV cover was much higher, with high fish abundance reflective of a diversity of species utilizing the SAV habitat. In 2019 the total catch was 35 specimens from 12 species, which is comparable to the collection of 2018.

Unlike previous years, White Perch instead of Banded Killifish was the dominant species collected with fyke nets, representing 31.43% of the total abundance (Table 11). This resembles the trend seen in seine net collections, where White Perch dominated over Banded Killifish as a likely response to the paucity of SAV.

The percent dominance was distributed fairly evenly over the species collected in both fyke nets (Figures 92 A&B). Other species with relatively high abundance were Pumpkinseed (17.14%), and Spottail Shiner (11.43%).

The highest abundance occurred in the month of July (Table 12, Figures 93 A&B). Both fyke nets collected a similarly low number of specimens (Table 13). Fyke Near collected a higher number of species, nine versus seven in Fyke Far.

Table 11. Adult and juvenile fish collected by fyke nets. Hunting Creek study – 2019.

Scientific Name	Common Name	Abundance	Percent
Alosa aestivalis	Blueback Herring	1	2.86
Alosa pseudoharengus	Alewife	2	5.71
Etheostoma olmstedi	Tessellated Darter	1	2.86
Fundulus diaphanus	Banded Killifish	1	2.86
Lepomis gibbosus	Pumpkinseed	6	17.14
Lepomis macrochirus	Bluegill	2	5.71
Lepomis sp.	Unk. Sunfish	3	8.57
Menidia beryllina	Inland Silverside	2	5.71
Micropterus salmoides	Largemouth Bass	1	2.86
Morone americana	White Perch	11	31.43
Notropis hudsonius	Spottail Shiner	4	11.43
Pomoxis nigromaculatus	Black Crappie	1	2.86
Total		35	100.00

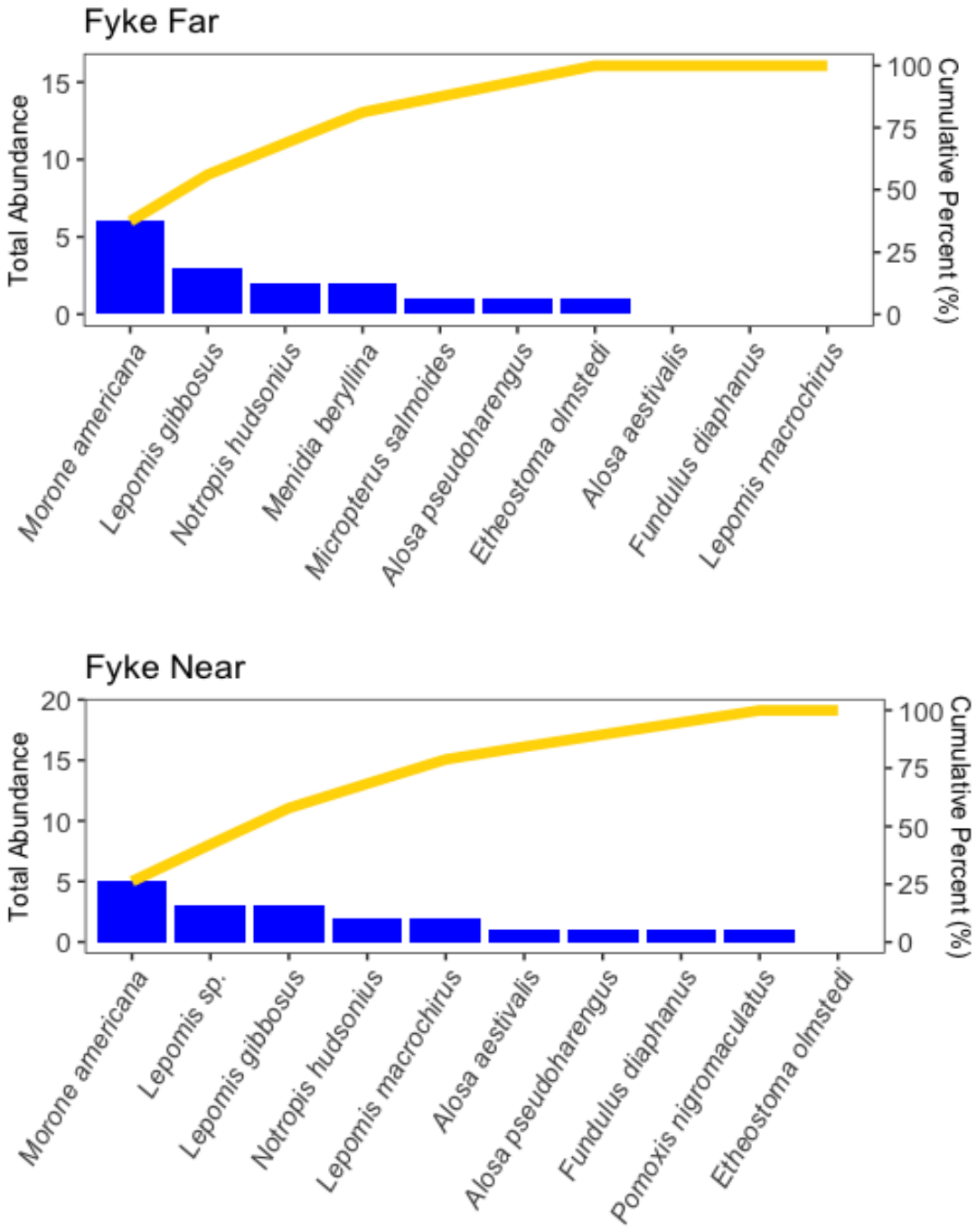

Figure 92A and B. Pareto chart of adult and juvenile fishes collected by fyke nets. Dominant species by station in total abundance and cumulative percentage of total for the Near Fyke (top) and Far Fyke (bottom).

Table 12. Adult and juvenile fish collected by fyke nets. Hunting Creek study - 2019.

Scientific Name	Common Name	05/03	05/13	05/29	06/11	06/25	07/09	07/23	08/28	09/18	Total
Alosa aestivalis	Blueback Herring	1	0	0	0	0	0	0	0	0	1
Alosa pseudoharengus	Alewife	0	1	0	0	1	0	0	0	0	2
Etheostoma olmstedi	Tessellated Darter	0	0	0	0	1	0	0	0	0	1
Fundulus diaphanus	Banded Killifish	0	0	0	0	0	1	0	0	0	1
Lepomis gibbosus	Pumpkinseed	0	0	1	0	3	0	1	0	1	6
Lepomis macrochirus	Bluegill	0	0	1	0	1	0	0	0	0	2
Lepomis sp.	unk. sunfish	0	0	0	0	0	0	3	0	0	3
Menidia beryllina	Inland Silverside	0	0	0	0	1	0	0	0	1	2
Micropterus salmoides	Largemouth Bass	0	0	0	1	0	0	0	0	0	1
Morone americana	White Perch	0	0	0	0	1	9	0	0	1	11
Notropis hudsonius	Spottail Shiner	0	0	0	0	1	0	3	0	0	4
Pomoxis nigromaculatus	Black Crappie	0	0	0	0	0	1	0	0	0	1
Total		1	1	2	1	9	11	7	0	3	35

Table 13. Adult and juvenile fish collected by fyke nets. Hunting Creek study – 2019.

Scientific Name	Common Name	Fyke Far	Fyke Near
Alosa aestivalis	Blueback Herring	0	1
Alosa pseudoharengus	Alewife	1	1
Etheostoma olmstedi	Tessellated Darter	1	0
Fundulus diaphanus	Banded Killifish	0	1
Lepomis gibbosus	Pumpkinseed	3	3
Lepomis macrochirus	Bluegill	0	2
Lepomis sp.	unk. sunfish	0	3
Menidia beryllina	Inland Silverside	2	0
Micropterus salmoides	Largemouth Bass	1	0
Morone americana	White Perch	6	5
Notropis hudsonius	Spottail Shiner	2	2
Pomoxis nigromaculatus	Black Crappie	0	1
NA	NA	16	19

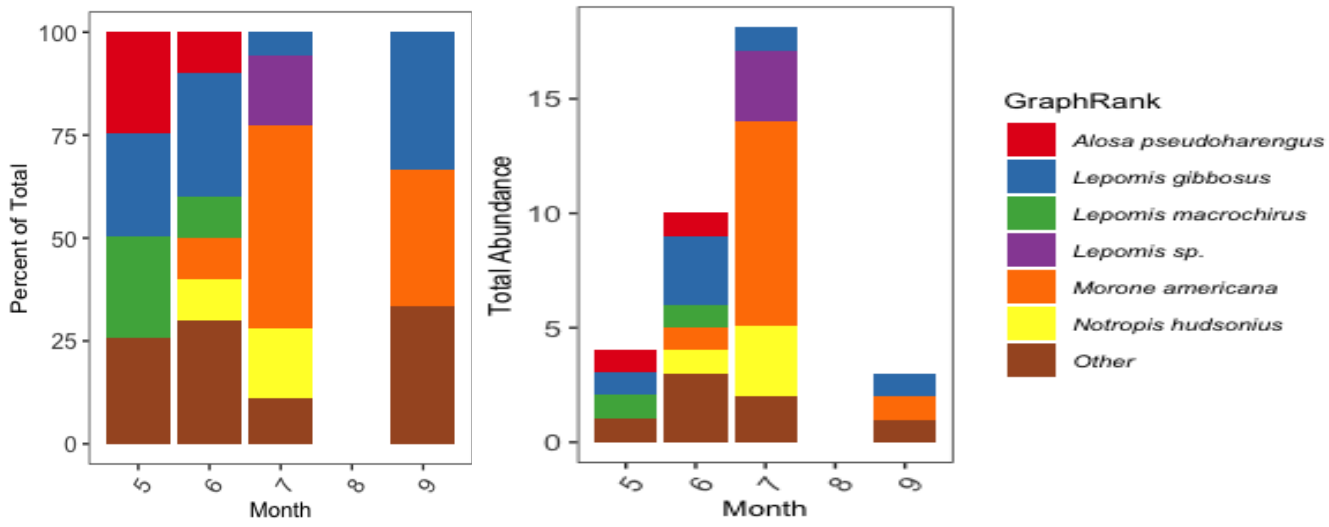

Figure 93 A and B. Adult and juvenile fish collected by fyke nets. Dominant species by month in percentage of total (A) and total abundance (B).

H. Submersed Aquatic Vegetation – 2019

SAV data overflights by VIMS were conducted in 2019 and the aerial imagery is available (Figure 94). This imagery shows very little SAV coverage in 2019 compared with a recent typical year 2016. This is consistent with sampling conducted from the boat during datamapping cruises when only 1 of 49 sites sampled by rake contained SAV (Table 14).

Figure 94. Aerial imagery of Hunting Creek taken in late summer 2019. Extent of beds from 2016 are shown in green outlining. http://web.vims.edu/bio/sav/savwabmap/ downloaded March 3, 2020.

All SAV taxa were greatly reduced in 2018 and virtually absent in 2019. Coontail, a native species, which was dominant in 2017 was greatly reduced in 2018 and absent in 2019. This decline most certainly started with the very turbid water in 2018 which obstructed light penetration. In 2019, conditions were somewhat better, but at key times in the year light penetration dropped following runoff events and this inhibited SAV recovery.

Table 14. Average Density of Submersed Aquatic Vegetation Species in Transects. Average included all sites with water depth less than or equal to 2 m. 2017-1019. Density scale: 0 (absent) – 4 (very abundant).

		Average Density per sample by SAV Species - 2019	
Taxon Scientific Name	Taxon Common Name	July 16	August 19
Ceratophyllum demersum	Coontail	0	0
Heteranthera dubia	Water Stargrass	0	0
Hydrilla verticillata	Hydrilla	0.04	0
Najas guadalupensis	Southern Naiad	0	0
Najas minor	Spiny Naiad	0	0
Various	Filamentous algae	0	0

		Average Density per sample by SAV Species - 2018	
Taxon Scientific Name	Taxon Common Name	July 16	August 28
Ceratophyllum demersum	Coontail	0.20	0.10
Heteranthera dubia	Water Stargrass	0.07	0
Hydrilla verticillata	Hydrilla	0.43	0.27
Najas guadalupensis	Southern Naiad	0.02	0.07
Najas minor	Spiny Naiad	0.07	0
Various	Filamentous algae	0.09	0

		Average Density per sample by SAV Species - 2017	
Taxon Scientific Name	Taxon Common Name	July 12	August 10
Ceratophyllum demersum	Coontail	1.76	1.74
Heteranthera dubia	Water Stargrass	0.19	1.19
Hydrilla verticillata	Hydrilla	0.78	0.32
Najas guadalupensis	Southern Naiad	0.20	0
Najas minor	Spiny Naiad	0.45	0.21
Various	Filamentous algae	0.03	0.43

I. Benthic Macroinvertebrates – 2019

River and Embayment Samples

Taxonomic Groups: Annelid worms (including Oligochaetes and Leeches) were found in high numbers at each site over all dates (Table 15, Figure 94). Overall, they accounted for 80% of all benthic organisms found. Oligochaetes were by far the dominant taxonomic annelid, being found in all samples in substantial number. Leeches were less common and only found at AR2 during August. Insects were the second highest group in abundance across sites and dates, accounting for 9.7% of all individuals and, more importantly, for the greatest number of distinct taxa (six taxa). Chironomids were by far the most numerous and omnipresent insect taxon. Most other insect taxa were present in only a few samples. Crustaceans (including amphipods and isopods) were the third highest group in abundance across sites and dates, accounting for 7.4% of all individuals. Gammarid amphipods (scuds) dominated this group with the isopod *Cyathura polita* being the second most common crustacean (Table 15, Figure 94). The remainder of the taxonomic groups were minor components of the overall abundance and were generally most common at AR4. These included Bivalvia (1.6% of total abundance), Turbellaria (flatworms) (0.7%), and Gastropoda (0.1%). The bivalve group was composed of both the invasive Asian clam, *Corbicula fluminea*, and a native fingernail clam from the Sphaeriidae family. The gastropod (i.e., snails) group was composed of taxa from Pleuroceridae and Viviparidae. The dominant family was Viviparidae, which were the invasive Japanese mystery snails (*Cipangopaludina japonica*), accounting for 82% of all gastropods found. The Hydra (freshwater anemones) were represented by only a few individuals in both AR3 and AR4 samples.

Table 15. Taxa Identified in Hunting Creek Tidal Benthic Samples.

Taxon	Common Name	Average # / ponar		
		AR2	AR3	AR4
Platyhelminthes*	Flatworms	0	0	9.5
Cnidaria-Hydrozoa-Hydra*	Anemone	0	8	2.33
Annelida-Oligochaeta*	Oligochaete worms	233.93	109.53	85.13
Annelida-Hirudinea	Leeches	1	0	0
Bivalva-Corbicula*	Asiatic clams	1	1.17	10.3
Bivalvia- Sphaeriidae	Fingernail clams	0	1	2.5
Gastropoda-Viviparidae*	Mystery snails	1	0	1.6
Gastropoda-Pleuroceridae	Pleurocerid snails	0	0	1
Crustacea-Isopoda-Cyathura*	Isopods	0	0	2.57
Crustacea-Amphipoda-Gammarus*	Amphipods	6.63	6	42.25
Ephemeroptera-Caenidae	Squaregill mayflies	0	0	1
Ephemeroptera-Batidae	Small minnow mayflies	0	0	2
Diptera-Chironomidae*	Midges	28.67	7.87	7.15
Diptera-Chaoboridae	Phantom midges	1	0	0
Diptera-Ceratopogonidae*	Biting midges	6.83	2	6.2
Trichoptera-Pupa	Caddisfly pupa	1.5	0	0
	TOTAL	281.56	135.57	173.53

Taxa identified with an asterisk were found on three or more station-dates and were included in the multivariate analysis. Taxa from Caenidae through Trichoptera-Pupa are in the Insecta.

Spatial trends: The average abundance of organisms per ponar sample was highest at AR2, but this was entirely attributable to the large number of oligochaetes at that station. All three sites were dominated by Annelida, driven by high abundances of Oligochaeta (Figure 94). Sites AR3 and AR4 had a higher diversity of taxa than the Potomac River site, with this effect most obvious at AR4. Due to the high abundance of Annelida across all sites, additional analyses were conducted with non-Annelida taxa. Flatworms were present only at AR4, while gastropods were found at AR2 and AR4 but not AR3. Bivalves were the most abundant at AR4. When examining all non-Annelida taxa, Insects were the dominant group in percent contribution at both AR2 (79%) and AR3 (57%), while Crustaceans dominated at AR4 (48%) (Figure 94). Other taxa varied in their percent contribution by site. For example, Bivalvia and Turbellaria were more abundant at AR4, while Gastropoda contributed little to the average abundances found at AR2 and AR4.

Temporal trends: Members of Annelida, composed of oligochaetes and leeches, were the dominant taxa recorded during all months (Figure 94). There was a seasonal increase in crustaceans driven by Gammarid amphipods, which peaked during June and August most likely due to recruitment and were relatively low during the other months. Bivalve average abundances, dominated by the invasive Asian clam *Corbicula fluminea*, were highest during August at AR4. Average abundances of Turbellaria were also highest during August. The lowest average abundances of insect larvae across all sites occurred during July, with highest abundances in June. Average Gastropod abundances were relatively constant across the sampling period (average of 0-2 individuals/ponar) and were driven by abundances of invasive mystery snails from the Viviparidae. Comparing percent contributions of all non-Annelida taxa across all of the sites, months were dominated by either the Crustacea (June - 63% and August – 42%) or Insecta (May – 44%, July – 44%, September – 69%) (Figure 94). Overall, larger increases in abundances and relative percent contributions over the sampling period for many of the taxa described above are in direct relation to seasonal changes and recruitment.

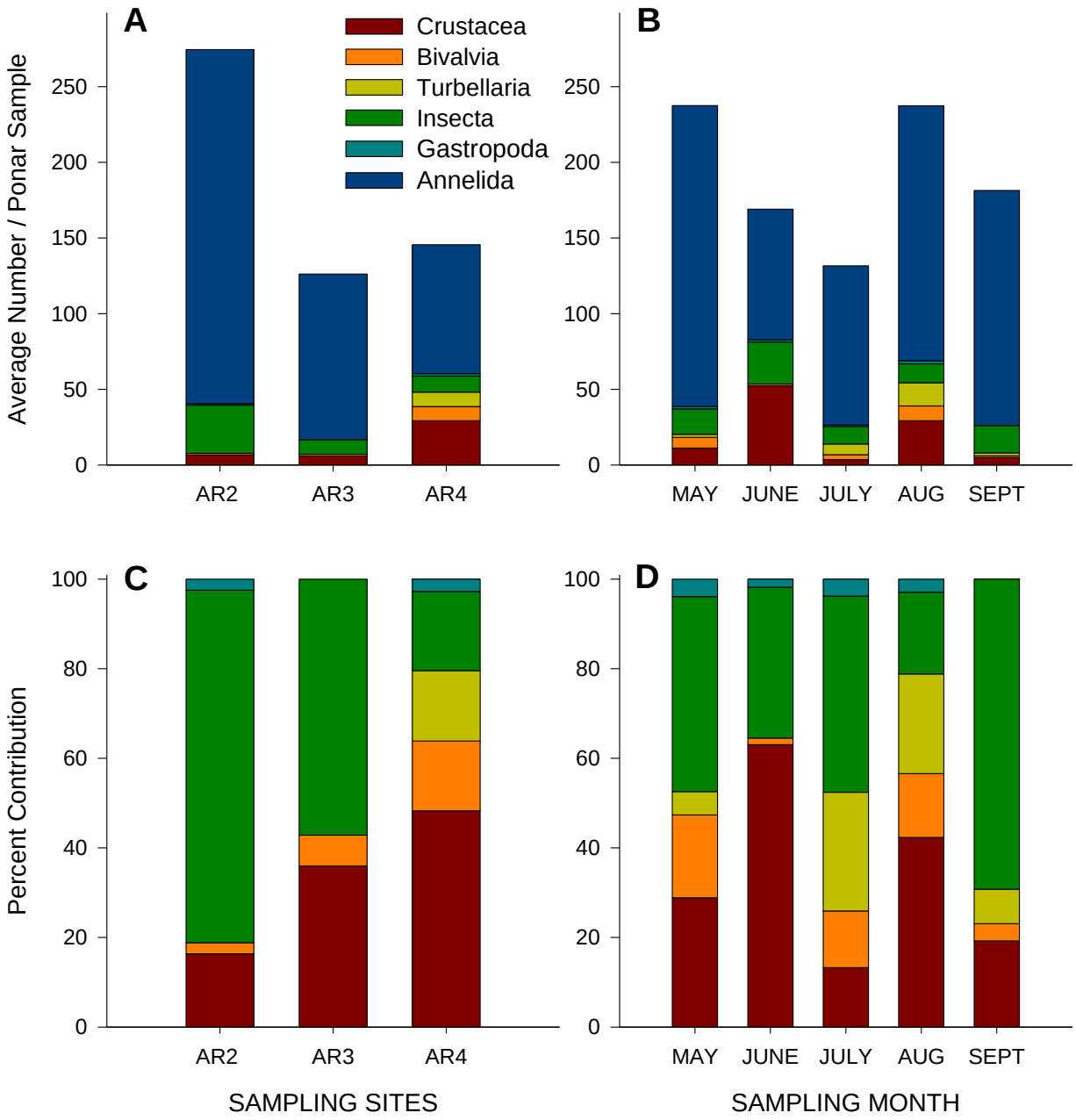

Figure 94. Average number per ponar sample of all benthic macroinvertebrate taxa (A, B) and percent contribution of all non-Annelida benthic macroinvertebrate (C, D) in petite ponar samples collected in 2019 separated by site and month.

Multivariate analyses: Due to the multispecies aspect of benthic communities, it is often useful to use multivariate analyses or ordination to examine relationships among samples. This allows multiple taxa to be considered simultaneously when assessing these relationships. In order to get the most meaningful relationships, the full macroinvertebrate sample/taxa matrix was condensed. Taxa that were present in less than three of the original replicate samples were excluded. Then, the remaining, more consistently found taxa were used in the analysis (indicated by asterisks in Table 15, were averaged over the replicates for each date and station combination). This resulted

in one set of taxa values for each station on each date. This reduced matrix (15 samples x 9 taxa) was then subjected to an ordination using a technique called Non-metric Multidimensional Scaling (nMDS). This allows relationships among samples based on their full complement of taxa to be visualized. If successful, relationships among samples can be shown on a two dimensional plot. The taxa differences responsible for the observed relationships can also be examined. The program PRIMER v.6 was used to conduct the ordinations.
The results of an nMDS ordination using presence-absence data is shown in Figure 95. All of the AR4 samples separate from the AR2 and AR3 samples, as noted by the two circles of data points. The AR4 samples clustered in the right middle of the graph are the samples with the greatest number of taxa (highest taxa richness – 8 or 9). The one AR4 sample at the top of the graph was characterized by low taxa richness similar to that in the AR2 samples. The higher richness at AR4 is probably due to better habitat conditions especially large and more heterogeneous sediment particle size. Also apparent is a seasonal change in community presence/absence in both station clusters. In May and June, samples across all sites cluster closely together, indicating similar communities. By August (green diamonds), the communities start to differentiate more by site, indicated by becoming more spaced out. By September (purple circles), the sites clearly host different communities due to a decrease in taxa richness.

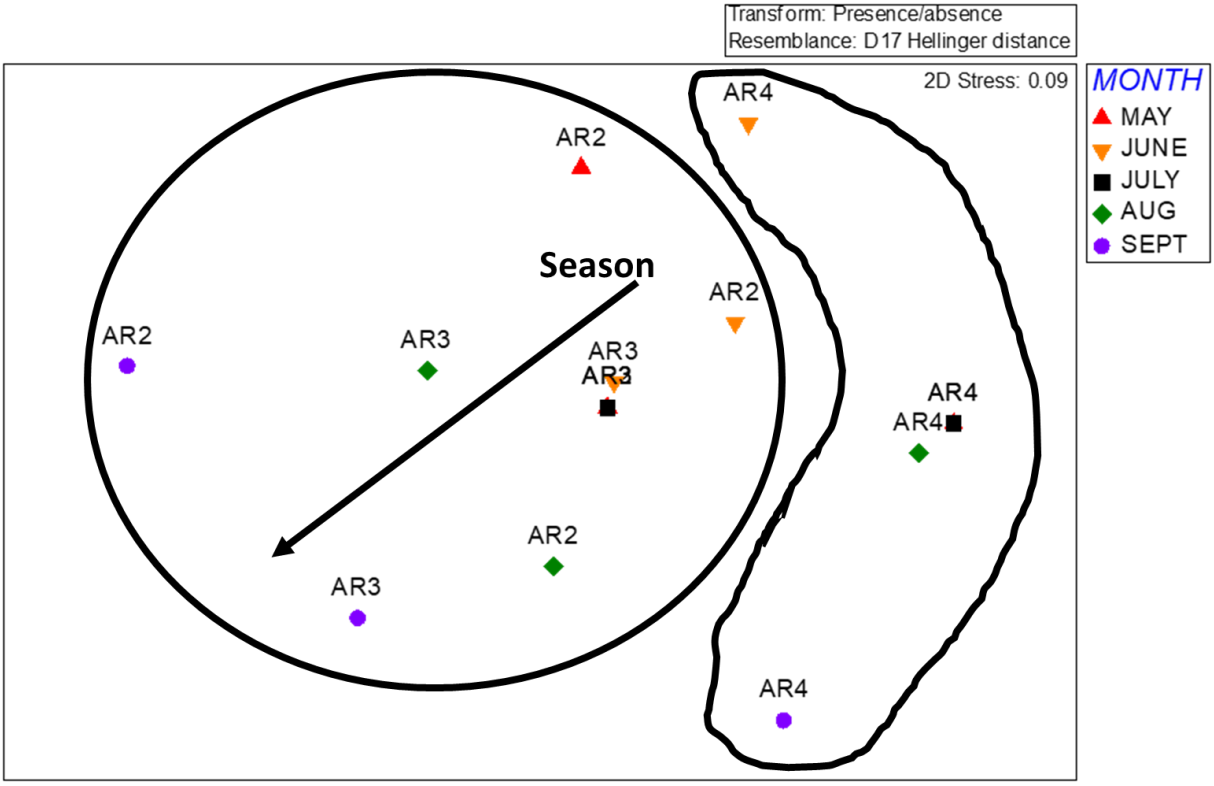

Figure 95. nMDS ordination of benthic samples from tidal stations. The station names are placed above each symbol. Colors represent month. Triplicates were averaged to get a single value for each month-station combination. Data was presence/absence and distance measure was Hellinger.

Summary: Similar to previous years, the macroinvertebrate community was dominated by Annelids (including Oligochaetes, Polychaetes, and Leeches) across sites, with Oligochaetes

contributing most to this group. Outside of the Annelids, Crustaceans (dominated by gammarid amphipods) were the most abundant group at AR4, while AR2 and AR3 (located closer to Hunting Creek proper) was dominated by Insect larvae from the Chironomidae family (midges). AR4 had the highest number of unique taxa (N=5; Platyhelminthes, Gastropoda-Pleuroceridae, Crustacea-Isopoda-*Cyathura polita*, Ephemeroptera-Caenidae, and Ephemeroptera-Batidae). AR2 also had three unique taxa (Annelida-Hirudinea, Diptera-Chaoboridae, and Trichoptera-Pupa), while AR3 shared its taxa list with either of the other two sites. Comparing percent contributions of all non-Annelida taxa across all of the sites, months were dominated by either the Crustacea (June and August) or Insecta (May, July, September) (Figure 95). Ordination analyses of the community indicated a clear separation between communities sampled at the AR4 site and those sampled from AR2 and AR3 across all months. There was also a clear change of the community composition throughout the months, from spring/summer to summer/fall, as it common for aquatic communities experiencing changes in abiotic conditions and recruitment during the summer months.

Tributary Samples

Duplicate kick net samples were taken at eight tributary stations in the Hunting Creek watershed on November 3, 2019. The exact locations of the sampling sites are given in Table 16. Individuals from each sample were identified to lowest taxonomic unit, usually genus, except for Oligochaetes (aquatic worms) and Chironomidae (midges).

Table 16. Location of Tributary Benthos Sampling Stations

Station ID	Stream	Location on Stream
CR	Cameron Run	Just below Metrorail bridge
BR	Backlick Run	At trail bridge just upstream of the confluence with Holmes Run
TR	Turkeycock Run	In Bren Mar Park just above Edsall Road
IR	Indian Run	Just below Bren Mar Drive crossing
HR1	Holmes Run	First riffle upstream of confluence with Backlick Run
HR2	Holmes Run	Holmes Run Park just below pedestrian bridge at Pickett Street
TA	Taylor Run	In Angel Park, underneath the trail bridge
TB	Timber Branch	Just east of Ivy Hill Cemetry at W Timber Branch Parkway

Water quality variables were measured on the date of benthic sampling (Table 17) and were generally supportive of aquatic life. It is important to note that all streams were at base flow conditions during the sampling period; water quality is expected to be more degraded during high flow.

Table 17. Water Quality Results from Tributary Benthos Sampling

Station	Temp (°C)	SpCond (uS/cm)	DO (mg/L)	DO (%)	pH	Turbidity YSI units
Cameron Run	13.1	304.7	10.67	100		1.75
Backlick Run	14.2	211.4	8.92	87		12.56
Turkeycock Run	11.0	297.9	10.29	93.5		0.11
Indian Run	11.0	301.1	10.91	98.9		1.30
Holmes Run 1	12.7	250.7	10.77	100		0.47
Holmes Run 2	12.2	241.5	10.76	100		5.52
Taylor Run	10.3	397.8	10.64	95		15.27
Timber Branch	10.5	414.0	10.54	94.6		0.29

Taxonomic Groups: Across all sites, 24 different taxa were found. The four most abundant taxa observed included two groups of Trichoptera insect larvae (caddisflies of the families Hydropsychidae and Philopotamidae), Turbellaria (i.e., flatworms) and Oligochaeta (Table 18, Figure 96). Of these, only the Oligochaeta and Hydropsychidae were found at all of the sites. The Turbellaria were found at all sites except Backlick Run. All other taxa were significantly less abundant and included Nemerteans (ribbon worms), Hirudinea (leeches), Ephemeroptera (mayflies of the family Baetidae), Crustaceans (Gammarid amphipods), Diptera (families Tipulidae, Simuliidae, Chironomidae, and Dolichopodidae), Coleoptera (family Elmidae), Odonata (families Coenagrionidae and Calopterygidae), Hemiptera (families Hebridae and Veliidae), Gastropods (families Ancylidae, Physidae, and Planorbidae), Hydrachnidia (water mites), Collembola (springtails), and the invasive Asian clam *Corbicula fluminea*. Of the less abundant taxa, none of these were present at all sites.

Spatial trends: Turkeycock Run had, by far the highest abundances of the four dominant taxa (N = 243). Interestingly, dominant taxa differed by site. Hydropsychidae larvae (caddisflies) were the dominant group (N>18) across 62.5% of the sites (i.e., Backlick Run, Cameron Run, Holmes Run 1 and 2, and Turkeycock Run), while Philopotamidae were dominant at Indian Run. Taylor Run was dominated by Turbellaria, while Timber Branch was dominated by Collembola (which was the one site where we found this taxa). Several taxa were only found at Turkeycock Run and included the limpet *Ferrissia rivularis*, snail *Physa acuta*, Elimdae riffle beetles, Calopterygidae damselflies, and Hebridae velvet water bugs. Timber Branch also had some unique taxa, with the snail *Gyraulus parvus* and the Hydrachnidia water mites, only found there.

Table 18. Taxa Identified in Hunting Creek Stream Benthic Samples.

Taxon	Common Name	Average # / kicknet							
		Backlick Run	Cameron Run	Homes Run 1	Holmes Run 2	Indian Run	Taylor Run	Timber Branch	Turkeycock Run
Platyhelminthes	Flatworms	0	1	11	4	7.5	9.5	1	9
Nemertea	Ribbon worms	0	0	5	0	0	0	3.5	0
Annelida-Oligochaeta	Oligochaete worms	1.5	1	3.5	2	10	4.5	3	39.5
Annelida-Hirudinea	Leeches	0	1	0	1	1	0	3	0
Bivalva-Corbicula	Asiatic clams	0	1	3	0	0	0	0	0
Gastropoda-Ancylidae	Limpet	0	0	0	0	0	0	0	1.5
Gastropoda-Physidae	Physid snails	0	0	0	0	0	0	0	2
Gastropoda-Planorbidae	Planorbid snails	0	0	0	0	0	0	8	0
Hydrachnidia	Water mites	0	0	0	0	0	0	1	0
Crustacea-Amphipoda-Gammarus	Amphipods	0	0	2	10	2	0	0	4.5
Collembola	Springtails	0	0	0	0	0	0	11	0
Ephemeroptera-Baetidae	Small minnow mayflies	0	0	0	0	0	1	1	6
Diptera-Tipulidae	Crane fly	3	0	1	0	0	0	2.5	3
Diptera-Chironomidae	Midges	0	0	1	0	2	1	2	7
Diptera-Dolichopodidae	Long-legged flies	0	0	1	0	0	0	0	0
Diptera-Simuliidae	Black fly	0	0	2	0	0	0	0	0
Coleoptera-Elmidae	Riffle beetles	0	0	0	0	0	0	0	1.5
Odonata-Coenagrionidae	Damselflies	0	0	1	0	0	0	0	1
Odonata-Calopterygidae	Broad-winged damselflies	0	0	0	0	0	0	0	1
Hemiptera-Hebridae	Velvet water bugs	0	0	0	0	0	0	0	2
Hemiptera-Veliidae	Small water striders	0	0	0	0	0	1	0	0
Trichoptera-Hydroptilidae	Microcaddisflies	0	0	0	3	1.5	0	0	0
Trichoptera-Hydropsychidae	Hydropsychid caddisflies	5.5	5.5	17.5	30.5	15.5	5.5	9.5	176
Trichoptera-Philopotamidae	Finger-net caddisflies	5	4	6.5	3.5	26.5	0	0	57.5
	TOTAL	15	13.5	54.5	54	66	22.5	45.5	311.5

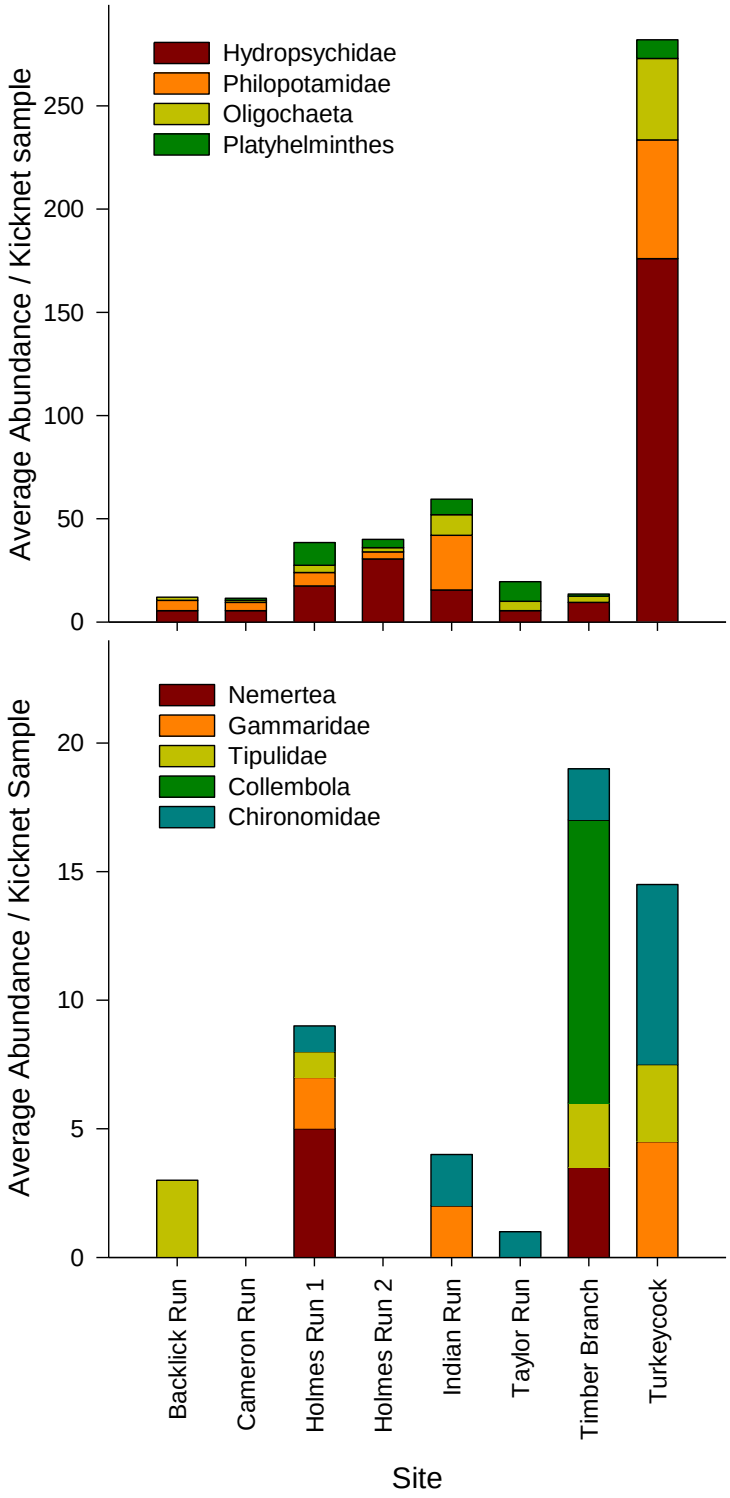

Figure 96 TOP: Average abundance per kicknet sample of the four dominant benthic invertebrate taxa in tributary kick samples. BOTTOM: Average abundance per kicknet sample of five less dominant benthic invertebrate taxa in tributary kick samples. Note the different scales of the y-axes between the two graphs.

Benthic Invertebrate Community Metrics: In general, increasing taxa richness reflects increasing water quality, habitat diversity, or habitat suitability. Taxa richness across all eight sites ranged from 4 to 14 taxa, with lowest richness at Backlick Run and highest richness at Turkeycock Run. "Good" sites were classified as having more than 14 taxa, while "moderate" sites had between 7 and 13; "poor" sites had less than 6 taxa present.

A subset of taxa richness, EPT richness is the number of species from the generally more sensitive Insecta groups Ephemeroptera, Plecoptera, and Trichoptera. In general, if the EPT richness is ≤ 2, then conditions are poor. If between 3 and 5, then conditions are moderate. If ≥ 5, then conditions are good. EPT richness in five sampled locations ≤ 2, indicating poor conditions at the majority of sites. Holmes Run 2, Indian Run and Turkeycock Run had marginally higher EPT richness, at three species, indicative of moderate conditions.

Calculating the percentage of total organisms that are from the Ephemeroptera, Plecoptera, and Trichoptera groups, without including the family Hydropsychidae, provides another metric for stream condition. In this case, if the value is >9.3%, then conditions are good. If the value is between 4.7 and 9.3%, then conditions are moderate. If the value is < 4.7%, then conditions are poor. Both Taylor Run and Timber Branch had values below the threshold of 4.7%. While Holmes Run 2 had moderate percentage values, the rest of the sites all had values >9.3%, indicating good conditions. Of particular note is Indian Run, which had the highest percent of EPT taxa (without Hydropsychidae) at 41.1%.

Examining the Trichopteran family (without Hydropsychidae) closer can provide more detail about the site conditions, as this insect family has a range of tolerance values for abiotic conditions. Here, good conditions are >0.50, moderate are 0.25 – 0.50, and poor are <0.25. All locations scored with good conditions, except Taylor Run and Timber Branch, in which no Trichopterans other than Hydropsychidae were found.

Looking at the Coleopteran (beetle) family can also tell us about the stream conditions. In this case, good conditions are abundance values above 1.5% of the sample, moderate values are 0.75-1.5, and poor conditions are values less than 0.75. Beetles were not found at the majority of sites; only Turkeycock Run had any beetles (three Elmidae larvae).

The Family Biotic Index (FBI) estimates the average tolerance of individuals in a sample toward organic (nutrient) enrichment. Families are assigned a tolerance number from 0 to 10 based on best professional judgement of their sensitivity to organic pollutants; 0 is most sensitive, 10 is most tolerant**.** Low FBI values reflect a higher abundance of sensitive groups, thus a lower level of pollution. Family-level tolerance values from USEPA (Barbour et al. 1999) were used for organisms that could not be identified to the genus level because of size or condition. Taxa with tolerance values ≤3 were considered *intolerant,* whereas those with values ≥7 were considered *tolerant.* Low FBI (≤4.7) values reflect a higher abundance of sensitive groups, indicative of a lower level of pollution; these values were found for the majority of sites. Only one location (Taylor Run) fell into the "good" category (values 4.7 – 5.4), indicating some organic pollution is probable. Only Timber Branch was "poor" (values >5.4), indicating that very substantial pollution was likely (Table 19).

In most cases, as the diversity of a community declines, a few tolerant taxa will dominate the assemblage. Tolerant taxa can replace specialized species, and these communities are indicative of poor stream

quality. Percent dominance is calculated as the total number of individuals in the top three most abundant taxa divided by the total number of individuals. A percent dominance above 79% is considered "poor" quality, a value between 57 and 79 is "moderate", and anything below 57% is "good." This year, the top 3 taxa were two Trichopteran families- Hydropsychidae and Philopotamidae – and Oligochaeta. The majority of sites were dominated by these top three taxa, including Backlick Run, Cameron Run, Indian Run, and Turkeycock Run. Holmes Run 1 and 2 were calculated as moderate, while both Taylor Run and Timber Branch were categorized as good.

The percent of organisms that are clingers, which are those that have fixed retreats or adaptations for attachment to surfaces in flowing water, is another indicator of environmental quality. While this metric would normally also include the percent of organisms are from the Plecoptera group (which are one of the first groups to disappear as human disturbance increases), none of the organisms sampled this year were from that group. Increasing metric values indicate increasing substrate stability. In this case, if the value is >14%, then conditions are good. If the value is between 7 and 14%, then conditions are moderate. If the value is <7%, then conditions are poor. All of the locations had values >14%, indicating good substrate stability.

Shredder taxa are those that tear apart organic material, usually leaves, and dominate low-velocity, high-retention pools. Sites were categorized as "poor" if the percent of shredders was <2, as "moderate" if the percent was between 2 and 4, and as "good" is the percent was higher than 4. While the majority of sites were categorized as "moderate" (Holmes Run 1 and 2, Taylor Run, and Turkeycock Run), Backlick Run, Indian, and Timber Branch all had high percentages of shredders indicating good conditions. Only one location, Cameron Run, had poor percentages of shredders.

Predator taxa are at the top of the food web and depend on a reliable source of other invertebrate prey items. The percentage of taxa that are obligate predators can provide a measure of how trophically complex a site is. Less distributed sites support a greater abundance and diversity of prey items, thus supporting a greater number and diversity of predators. Sites were categorized as "poor" if the percent of predators was <3.2, as "moderate" if the percent was between 3.2 and 6.5, and as "good" is the percent was higher than 6.5. While the majority of sites were categorized as "poor" (Holmes Run 2, Indian Run, Taylor Run, and Turkeycock Run), Backlick Run, Holmes Run 1, and Timber Branch all had high percentages of predators indicating good conditions.

Using these 10 measures of biological health, we can calculate a summary statistic of relative overall health of these streams. In this case, we assign values of high (6), moderate (3), or low (0) health for each metric at each site, sum these values for each site and divide by 60 (i.e., the maximum score achievable). Streams characterized as "good" would achieve summary statistics of 90% or better of the maximum summary statistic. "Moderate" streams would be between 75 and 89%, and "poor" streams would come in at 75% of the summary statistic. Using the criteria for each metric laid out above, all of the streams scored between 30% and 65% of the maximum summary statistic (Table 20). This indicates that all sampled streams are in poor condition based on these metrics.

Table 19. Benthic invertebrate community metrics on the sum total of organisms found from both replicate kicknets. EPT include the Insecta from Ephemeroptera, Plecoptera, and Trichoptera. Color shading indicates relatively good (green), moderate (yellow), or poor (red) conditions for each of the metrics and the summary statistic.

	Abundance	Taxa Richness	EPT Richness	% EPT w/o Hydropsychidae	% Trichoptera w/o Hydropsychidae	% Coleoptera	Family Biotic Index	% Dominance	% Clingers + % Plecoptera	% Shredders	% Predators
Backlick Run	27	4	2	37.0	37.0	0	3.6	88.9	88.9	11.1	11.1
Cameron Run	19	6	2	21.1	21.1	0	4.3	84.2	78.9	0.0	5.3
Holmes Run 1	95	12	2	13.7	13.7	0	4.6	57.9	58.9	2.1	8.4
Holmes Run 2	104	7	3	6.7	9.6	0	4.1	69.2	68.3	2.9	1.0
Indian Run	129	8	3	41.1	43.4	0	4.1	80.6	67.4	5.4	0.8
Taylor Run	42	6	2	2.4	0.0	0	4.9	47.6	28.6	2.4	2.4
Timber Branch	67	11	2	1.5	0.0	0	6.4	37.3	47.8	10.4	28.4
Turkeycock Run	611	14	3	19.8	18.8	0.5	4.1	89.4	78.9	3.3	1.6

Table 20. Index scores of the benthic invertebrate community metrics on the sum total of organisms found from both replicate kicknets. Color shading indicates relatively good (green), moderate (yellow), or poor (red) conditions for each of the metrics and the summary statistic.

	Taxa Richness	EPT Richness	% EPT w/o Hydropsychidae	% Trichoptera w/o Hydropsychidae	% Coleoptera	Family Biotic Index	% Dominance	% Clingers + % Plecoptera	% Shredders	% Predators	**Index Score**
Backlick Run	0	0	6	6	0	6	0	6	6	6	**60%**
Cameron Run	0	0	6	6	0	6	0	6	0	3	**45%**
Holmes Run 1	3	0	6	6	0	6	3	6	3	6	**65%**
Holmes Run 2	0	3	3	6	0	6	3	6	3	0	**50%**
Indian Run	3	3	6	6	0	6	0	6	6	0	**60%**
Taylor Run	0	0	0	0	0	3	6	6	3	0	**30%**
Timber Branch	3	0	0	0	0	0	6	6	6	6	**45%**
Turkeycock Run	3	3	6	6	0	6	0	6	3	0	**55%**

Summary: Twenty-four taxa were identied across all sites in 2019. In general, the top four most abundant taxa observed across all sites stayed the same as in previous years with the exception of a decrease in the Insecta family Chironomidae across all sites. In 2019, Turkeycock Run had the highest abundance of all macroinvertebrates and the four dominant taxa, mostly composed of the Insecta family Hydropsychidae. This site also had the highest occurrence of unique taxa (N=5). Hydropsychidae larvae (caddisflies) were the dominant group at the majority of the sites. Taxa richness across all sites ranged from 4 to 14 taxa,

with lowest richness at Backlick Run and highest richness at Turkeycock Run. Using 10 measures of biological health, we calculated a summary statistic of relative overall health of these streams. Using the criteria for each metric laid out above, all of the streams scored between 30% and 65% of the maximum summary statistic, indicating that all sampled streams are in poor condition.

DISCUSSION

A. 2019 Synopsis

In 2019 temperature was above normal for the entire study period from April through September. There were 41 days with maximum temperature above 32.2ºC (90ºF) in 2019 which is well above the median number over the past decade. Precipitation was closer to normal in 2019 than in the extremely wet year 2018. However, was again well above normal in 2019 especially in July. To better understand relationships between flow events and Hunting Creek ecology, time course graphs were constructed overlaying the sequence of precipitation, stream/river flow, and water quality/plankton sampling dates (Fig. 98a,b). During mid-June, there were some noteworthy flow events related to local precipitation which occurred a few days before the June 19 sampling. And in early July there was a period of substantial rainfall which translated into significant increase in local flow which may have affected the July 17 event. Potomac flows which are impacted by the much larger upstream watershed were elevated in May and July, but did not exhibit a response to the June local precipitation.

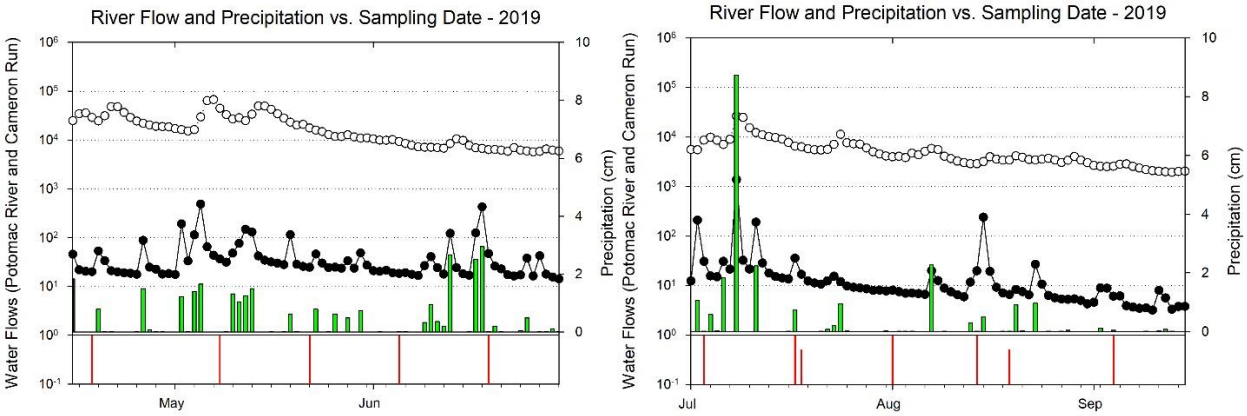

Figures 98a, b. Precipitation (green bars), Cameron Run flows (solid circles), Potomac River flows (open circles) and water quality/plankton sampling events (red lines at bottom).

Water temperature followed a typical seasonal pattern at all stations. A steady increase was observed from April through mid-July to about 30°C followed by a gradual decline through September. Most of the embayment and river stations exhibited a gradual increase in specific conductance over the study period which was interrupted by short declines related to flushing from storms. Both Hunting Creek and mainstem Potomac stations showed a decline in early May whereas the mid-June decline was observed only at the Hunting Creek stations. AR1, at the GW

Parkway bridge, had elevated specific conductance and chloride through most of the year and responded to the mid-June flow, but not the May flows. Dissolved oxygen was generally in the 80-100 percent saturation range indicating that photosynthesis was not robust in the absence of the SAV. There was a marked increase at AR2 in mid-July which corresponded with a peak in phytoplankton chlorophyll values. On the July water quality mapping date elevated DO was also observed in the Hunting Creek embayment. Field and lab pH was generally in the 7-8 range at all stations; in previous years with abundant SAV, pH was often higher. Total alkalinity was generally 70-120 mg/L as $CaCO_3$. Values tended to increase over the study period, but short term declines were seen after runoff events in the same manner as those found for specific conductance.

Secchi disk transparency was generally 0.3-0.7 m. A decline was observed in early May at all stations. After that transparency in the mainstem stations recovered to 0.6-0.8 m for the rest of the study period, but remained low (<0.5 m) at the Hunting Creek embayment stations inhibiting SAV development in 2019. Light attenuation coefficient exhibited a similar pattern with exceptionally poor transparency observed in Hunting Creek in mid-June and early July. Turbidity exhibited a similar pattern.

Ammonia nitrogen showed a general decrease from May through September and all values were quite low (<0.2 mg/L). Nitrate nitrogen also declined seasonally with additional dips in early May and late June related to flushing from the runoff events. Nitrite was very low at all stations and did not show consistent seasonal patterns except for an unexplained spike in August at all stations. Organic nitrogen was mostly in the range 0.2-1.0 mg/L and showed little seasonal pattern. Total phosphorus was generally less than 0.15 mg/L but was elevated on occasion in Hunting Creek. N/P ratio exhibited a general seasonal decline, but remained above 7.2, consistently pointed to P limitation of primary producers. Total suspended solids was typicaly in the 10-30 mg/L range with some higher spikes at the Hunting Creek stations related to runoff events. VSS values hovered around 5 mg/L in the river mainstem with higher values in the Hunting Creek embayment in June and early July.

In the tributaries, water temperature also generally followed air temperature with a steady rise in the spring and summer through late August. Specific conductance was generally 300-600 uS/cm with a gradual decline through July and a slight increase thereafter. Dissolved oxygen was generally near 100 percent saturation. AR11 (Lake Cook) and AR34 (Hooffs Run) were the most variable stations. pH values were consistently 6.5-7.5. Turbidity was generally low (<20 NTU). Total alkalinity was fairly uniform in all of the tributaries and did not vary much seasonally. Total phosphorus and ortho-phosphorus were variable with no clear pattern. Organic nitrogen was typically highest at AR11, AR23, and AR34. Ammonia nitrogen was uniformly low (<0.15 mg/L) at all stream stations except AR11 which was variable. Nitrate nitrogen was consistently elevated at AR33, followed by AR13. Other stations were consistently below 1 mg/L. TSS and was generally less than 20 mg/L except at AR11, AR 23, and AR34 which frequently were higher.

Phytoplankton biomass as indicated by chlorophyll *a* began the year in April and May with typical low springtime values, but increased dramatically during June and July to 20-30 µg/L with highest values in the Hunting Creek embayment. This was followed by a dramatic decline

in early August, probably in response to flushing and poor light conditions in mid- to late July. Recovery was observed in late August and September. Phytoplankton cell density were generally fairly constant and similar at AR2 and AR4 except for a strong peak in early July at AR2 at the time of high chlorophylls. There was a seasonal increase in June and July in phytoplankton biovolume at both stations. At both sites, cyanobacteria consistently dominated phytoplankton density throughout the year. *Anabaena* was dominant during the early July peak at AR2. *Oscillatoria* and an unknown cyanobacterium were dominant in cell density at AR4. Pennate 2 was the consistent diatom cell density dominant in contrast to most previous years when *Melosira* was consistently so. The green alga *Chlamydomonas* and the cryptophyte *Chroomonas* were the most important taxa in the "other" group. Phytoplankton biovolume was dominated by diatoms at both stations with "Other" algae being co-dominant at AR2 and with cryptophytes co-dominant at AR4. Diatom biovolume was a mix of smaller cells like Pennate 2 which was consistently found in all samples and larger taxa like *Surirella* which was found sporadically, but being very large made a big contribution to cell biovolume. The same was true with "other" taxa with *Peridinium* and *Euglena* (large cells) coming in and out of AR2 samples and *Cryptomonas* being consistently most important at AR4.

Rotifers maintained low levels in spring and into early summer, but exhibited a dramatic increase in mid-summer at both AR2 and AR4. Highest levels of over 3000/L were observed at AR2 in mid-August and 2500/L at AR2 in early August. These values were much higher than found in 2018 and among the highest observed to date in the study. *Brachionus* was the strong dominant on every sampling date.

All of the cladocerans displayed short early summer maxima and were generally higher in number at AR2 than at AR4. Many reached a maximum in early July before the flushing events that occurred later in that month. *Bosmina*, *Diaphanosoma*, *Daphnia*, *Sida* and Ceriodaphnia all followed this patter. *Diaphanosoma* and *Daphnia* both exceeded 1000/m^3 at this time. *Leptodora*, the large predaceous cladoceran on the other hand, had a distinct peak earlier, in early June, at both stations. Copepod nauplii peaked in early June and were already declining before the mid-July flows. *Eurytemora* was extremely abundant (>8000/m^3) at AR4 in June. *Diaptomus* and cyclopoid copepods displayed seasonal patterns similar to most of the cladocerans with a distinct maximum in the cove in early July.

B. Correlation Analysis of Hunting Creek Data: 2013-2019

To better understand the ecological relationships in Hunting Creek and the nearby Potomac River, relationships among parameters were assessed using correlation analysis. Due to the uncertain statistical distribution of some parameters, the correlations were conducted using the Spearman rank correlation coefficient rather than the Pearson coefficient. Since all samples were collected by PEREC personnel at the same time, it was possible to pool the data on all field and lab water quality parameters at the level of depth-averages and/or surface samples. Two tables were constructed: PEREC field and lab parameters with each other, ARE lab parameters with each other.

Table 19 shows the correlations among PEREC-collected water quality parameters from the regular sampling. These reflect relationships over all seven years of the study. Indicators of

photosynthesis (DOPPM, DOSAT, Field pH) were highly intercorrelated. Also, measures of particles in the water column and resultant water clarity (turbidity, TSS, Secchi disk depth, and extinction coefficient) were also highly intercorrelated. Indicators of phytoplankton abundance (CHLDI, CHLSF, and AFDWSF) were highly intercorrelated.

Table 21. Spearman correlations among PEREC collected water quality parameters from regular sampling. Depth-integrated samples unless otherwise indicated. AR2, AR3, and AR4 pooled. 2013-2019. April-September. Strongest correlations (r>0.400) are have **bolded** text. Yellow: indicators of photosynthesis. Blue: indicators of water clarity. Green: indicators of phytoplankton abundance.

Spearman Correlation Matrix												
	TEMP	SPC	DOPPM	DOSAT	FIELDPH	SECCHI	EXTCO	CHLDI	CHLSF	DRYWTSF	AFDWSF	YSITURB
TEMPC	1.000											
SPC	0.464	1.000										
DOPPM	**-0.475**	-0.386	1.000									
DOSAT	-0.099	-0.253	**0.882**	1.000								
FIELDPH	0.077	-0.097	**0.544**	**0.633**	1.000							
SECCHI	0.023	0.290	-0.023	-0.064	0.016	1.000						
EXTCOEF	0.086	0.256	-0.076	-0.075	0.102	**0.888**	1.000					
CHLDI	**0.496**	**0.526**	-0.209	-0.003	0.070	-0.077	-0.134	1.000				
CHLSF	**0.491**	**0.515**	-0.251	-0.030	0.035	-0.102	-0.165	**0.962**	1.000			
DRYWTSF	-0.136	-0.216	0.080	0.084	-0.156	**-0.741**	**-0.737**	0.296	0.314	1.000		
AFDWSF	0.038	0.044	0.056	0.160	-0.029	**-0.542**	**-0.581**	**0.556**	**0.566**	**0.824**	1.000	
YSITURB	-0.086	-0.232	0.052	0.036	-0.200	**-0.608**	**-0.706**	0.139	0.141	**0.772**	**0.566**	1.000

TEMP – water temperature (°C), SPC – specific conductance (µS), DOPPM – dissolved oxygen (mg/L), DOSAT – dissolved oxygen (% saturation), FLDPH – field pH,SD - secchi disk depth (m), EXTCO (light attenuation coefficient (m^{-1}), CHLDI – depth-integrated chlorophyll a (µg/L), CHLSF – surface chlorophyll a (µg/L), , DRYWTSF – TSS on surface samples (mg/L), FDWSF – VSS on surface samples (mg/L) YSITUR – Turbidity as measured by YSI sonde *in situ*, n = 81-133.

The correlation coefficients among AR lab parameters are shown in Table 20. Among the most highly correlated variables in this dataset were TSS and VSS (0.931). Total P was positively correlated with TSS and VSS. Most phosphorus is bound to particles so these correlations make sense. TP was negatively correlated with N to P ratio and this makes sense since it is in the denominator of this ratio. And TP was also correlated with nitrogen species. Lab pH was negatively correlated with ammonia nitrogen, but this may just reflect that lab pH is highest in summer when ammonia nitrogen is lowest. Other correlations were not strong.

Table 22. Correlation coefficients between AR lab parameters. AR2, AR3, and AR4 pooled. 2013-2019. April-September. Strongest correlations are **bolded**.

Spearman Correlation Matrix												
	PHLAB	ALK	TP	OP	ON	NO3	NH4	NO2	CLD	TSS	VSS	NTOP
PHLAB	1.000											
ALK	0.275	1.000										
TP	-0.174	-0.080	1.000									
OP	-0.243	-0.315	0.031	1.000								
ON	-0.011	0.094	0.453	-0.207	1.000							
NO3	-0.141	0.047	0.344	0.083	-0.160	1.000						
NH4	**-0.567**	-0.186	0.394	0.268	0.078	0.247	1.000					
NO2	0.003	0.237	0.126	-0.151	0.379	-0.073	0.122	1.000				
CLD	0.041	0.238	-0.108	-0.327	0.086	-0.288	-0.101	0.215	1.000			
TSS	-0.178	0.158	**0.692**	0.005	**0.436**	**0.470**	0.386	0.172	-0.179	1.000		
VSS	-0.136	0.199	**0.686**	0.012	**0.508**	0.347	0.319	0.213	-0.108	**0.890**	1.000	
NTOP	0.009	0.176	**-0.724**	-0.030	-0.341	0.239	-0.151	0.000	-0.009	-0.303	-0.370	1.000

PHLAB – lab pH, ALK – total alkalinity (mg/L as $CaCO_3$), TP – total phosphorus (mg/L), OP – orthophosphorus (mg/L), NO3N – nitrate nitrogen (mg/L), NH4N – ammonia nitrogen (mg/L), NO2N – nitrite nitrogen (mg/L), CLD – chloride (mg/L), TSS – total suspended solids (mg/L), VSS – volatile suspended solids (mg/L), NTOP – nitrogen to phosphorus ratio by mass. n= 128-134

C. Water Quality: Comparison among Years

Since six years of data are now available for the Hunting Creek area, comparisons were made for each parameter among years. And many of the parameters vary seasonally as well as among stations. In order to assess overall patterns in the data among years and stations box plots were constructed. In a box plot, the spread of the middle 50% of the data is shown by a box with a line in the middle which is the median. Whiskers extend out to the limits of the data. In this 2019 data analysis we focused on interannual patterns. And for water quality patterns we focused on the period June through September.

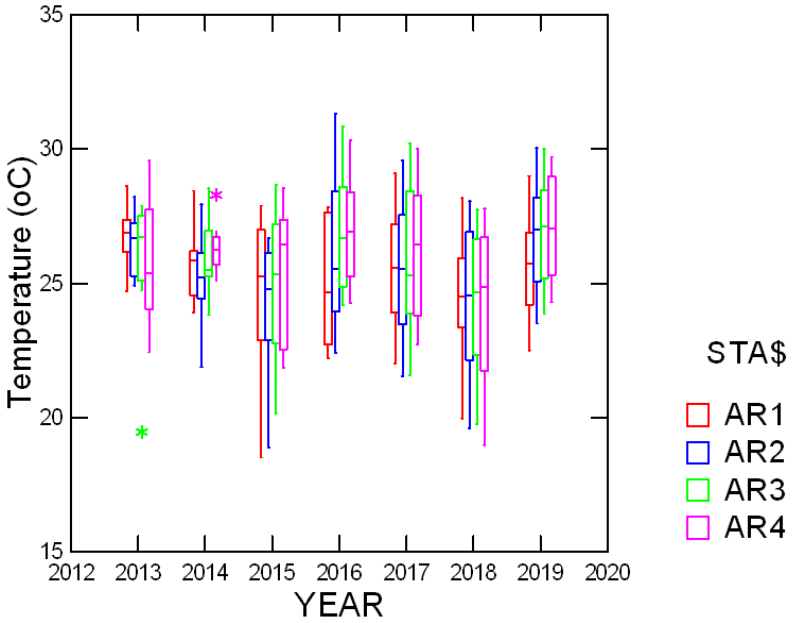

Figure 99. Box plots comparing values of Temperature between years. June through September.

Temperature did not show much difference between the years with the medians in the 24-27ºC range at all sites and years (Figure 99). The 2019 medians were at the higher end of that range and varied very little between stations. Specific conductance showed clear differences among stations in most years with AR 1 consistently higher. This pattern was probably due to input from AR effluent (Figure 100). In 2019, values at all stations increased to levels that were more in line with the first 5 years of the study and well above 2018 levels due to more normal rainfall in 2019.

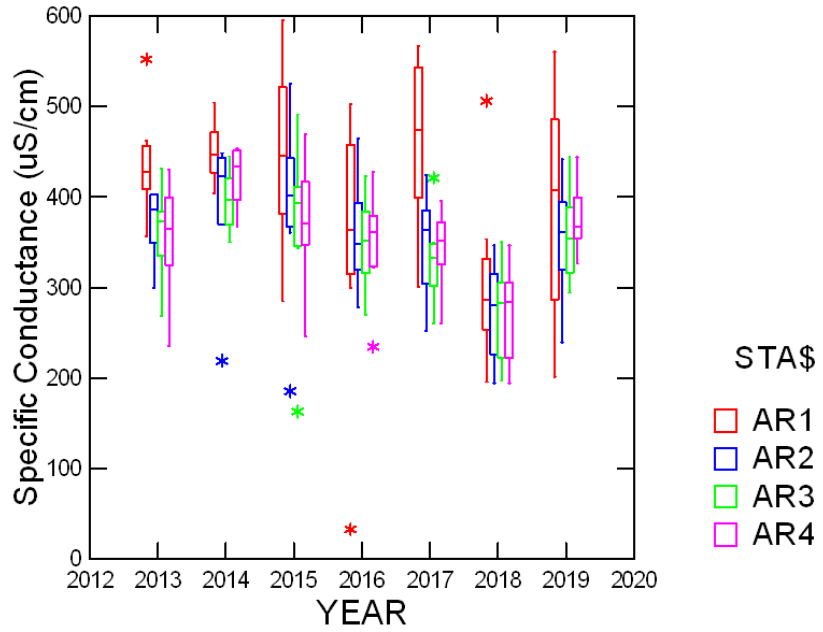

Figure 100. Box plots comparing values of Specific Conductance between years. June through September.

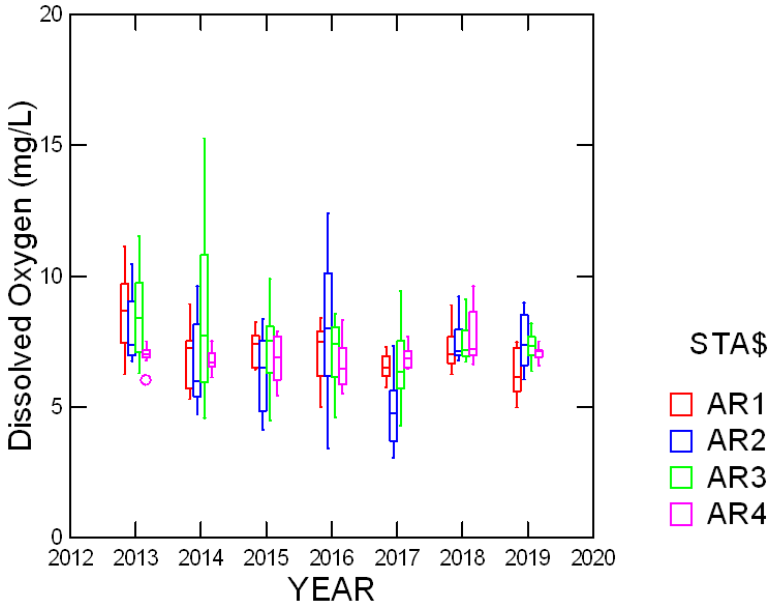

Figure 101. Box plots comparing values of dissolved oxygen as mg/L between years. June through September.

Dissolved oxygen showed little difference among stations in 2019 compared with some more marked differences in previous years (Figure 101). The interquartile range was also quite low at all stations in 2019. A similar pattern was observed in dissolved oxygen (as % saturation) (Figure 102).

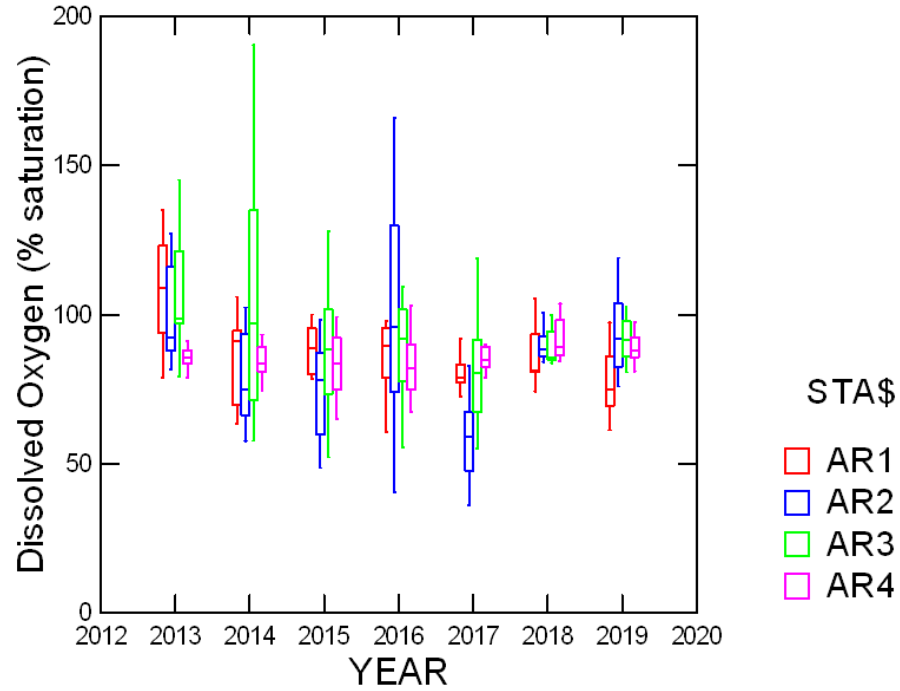

Figure 102. Box plots comparing values of dissolved oxygen as percent saturation between years. June through September.

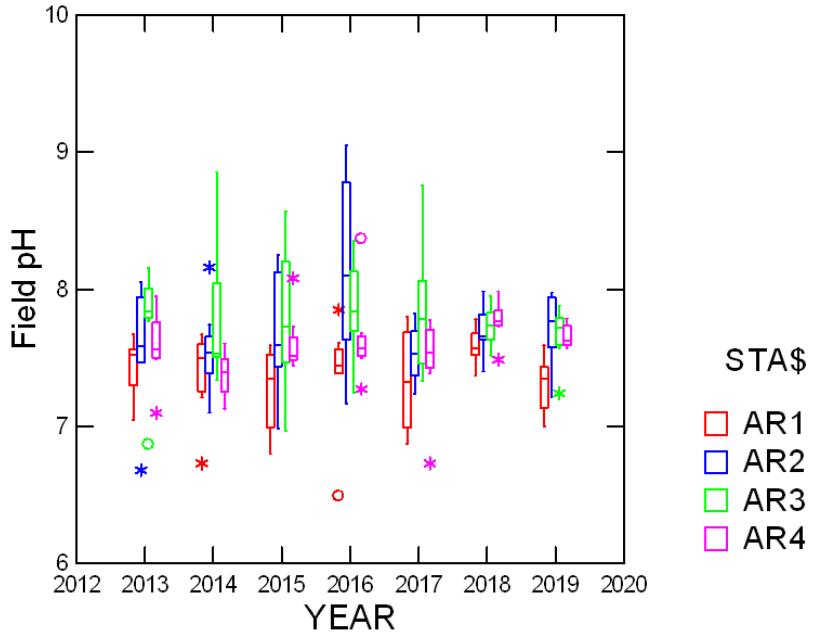

Figure 103. Box plots comparing values of field pH between years. June through September.

Field pH showed a bit wider range in 2019 than in 2018, but less than insome previous years (Figure 103). In some years median values at AR2 and AR3 were much higher than at the other two stations. This was attributed to photosynthesis by SAV which tends to increase pH since the high values were observed in July and August when SAV was most abundant. This explanation works for 2019 too since SAV was again very limited in 2019 and pH variation among stations was minimal.

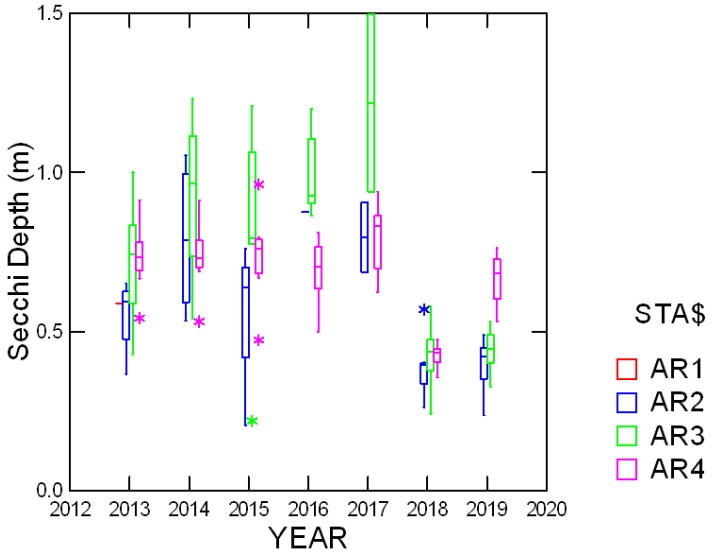

Figure 104. Box plots comparing values of Secchi disk depth between years. June through September.

Secchi disk depth (Figure 104) has generally shown major and consistent differences between stations, attributable to major differences in SAV abundance between the stations. In particular AR3 was often much higher than the other stations. However, the year 2018 was quite different. There was little difference between stations and all stations were greatly reduced in Secchi depth, in other words, the water was much less transparent than normal. 2019 retained this lower transparency at AR2 and AR3, but recovered somewhat at AR4. Light attenuation coefficient is another way of measuring water clarity: less negative values of light attenution coefficient indicate clearer water. Median values in light attenuation coefficient were similar from year to year until 2018 (Figure 105). As with Secchi disk depth, values for light attenuation in 2018 and 2019 showed much reduced water clarity than previous years.

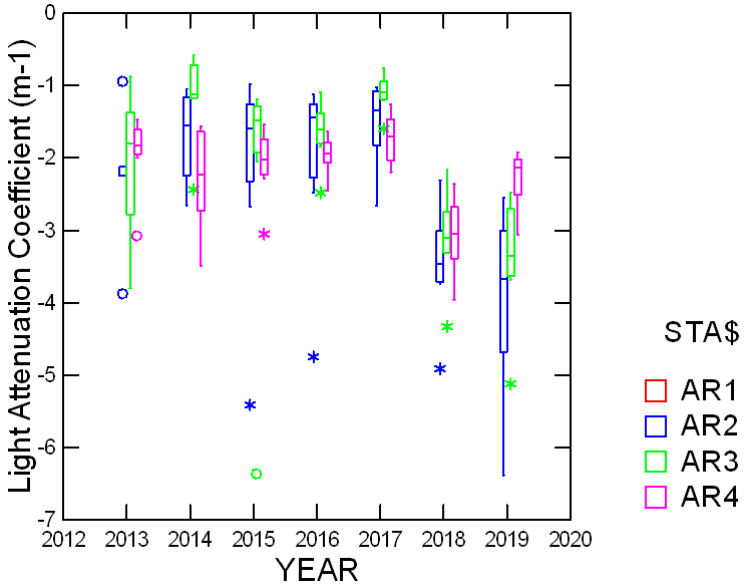

Figure 105. Box plots comparing values of Light Attenuation Coefficient between years. June through September.

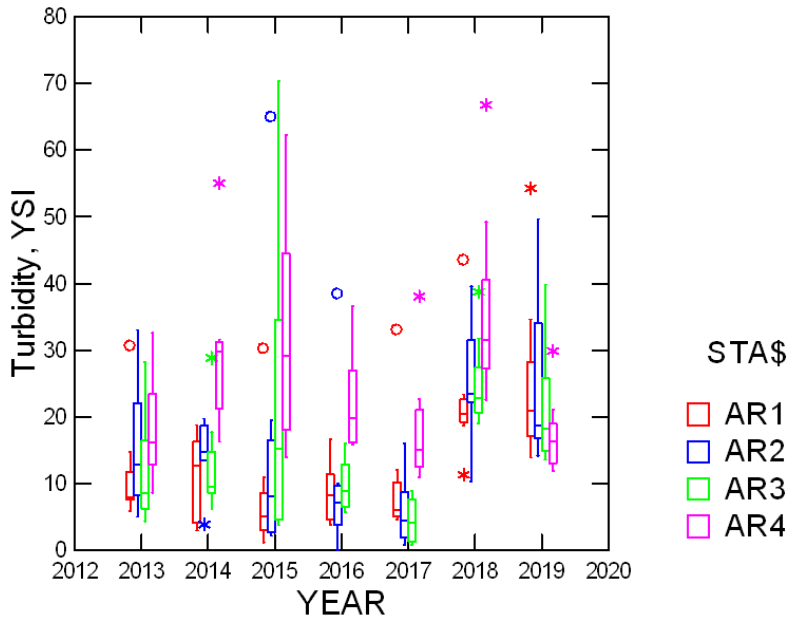

Figure 106. Box plots comparing values of Turbidity between years. June through September.

Turbidity, another measure of water clarity, exhibited much higher values at AR1, AR2, and AR3 in 2018 and 2019 than in previous years (Figure 106). Values at AR4 were not as different as in previous years.

Total phosphorus values were generally higher in 2019 at AR1, AR2, and AR3 than in previous years (Figure 107). In contrast to previous years, AR4 was lower than the other stations, mainly due to their elevated levels.

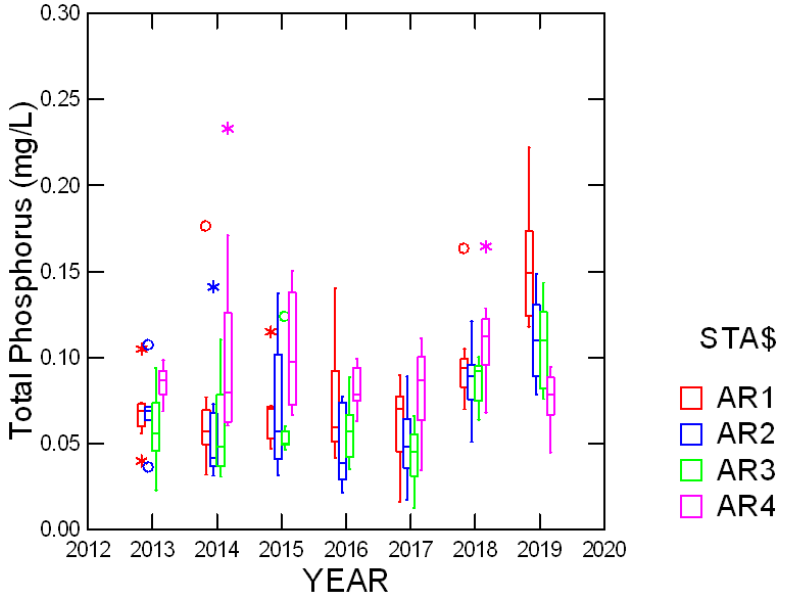

Figure 107. Box plots comparing values of Total Phosphorus between years. June through September.

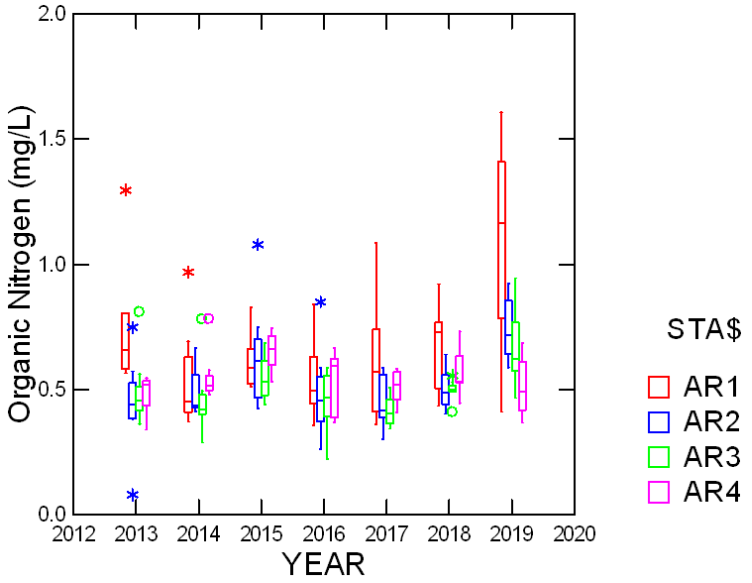

Figure 108. Box plots comparing values of Organic Nitrogen between years. June through September.

Organic nitrogen values in 2019 overlapped extensively with the ranges from previous years (Figure 108). A clear pattern was observed with AR1 highest and greater than normal, while AR4 was little changed compared with previous years. Nitrate nitrogen values in 2019 were consistently lower at all stations than in 2018, returning to the ranges found in previous years (Figure 109).

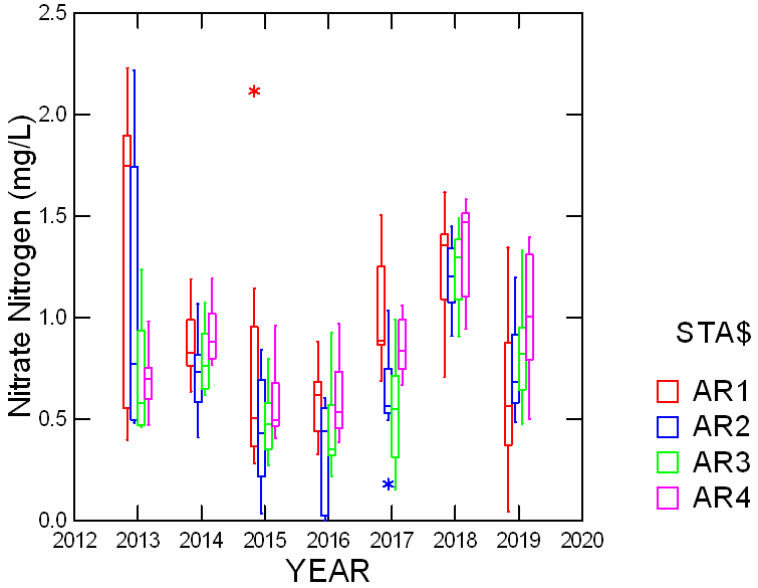

Figure 109. Box plots comparing values of Nitrate Nitrogen between years. June through September.

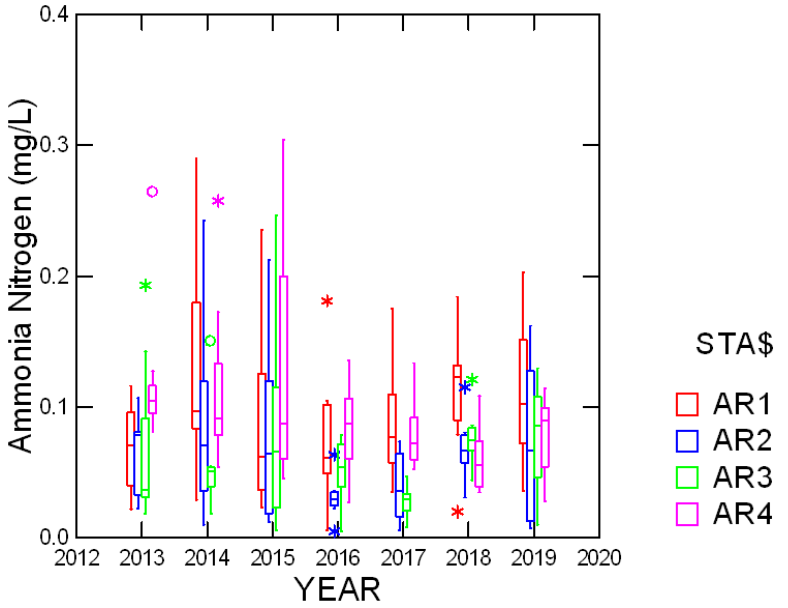

Figure 110. Box plots comparing values of Ammonia Nitrogen between years. June through September.

Ammonia nitrogen values in 2019 were similar to those observed in previous years (Figure 110). 2108 values fell within the range of previous years. There was much overlap in values among stations. Nitrite nitrogen values in 2019 were in the middle of the range for previous years and did not vary much among stations (Figure 111). There was one date on which all stations were much higher.

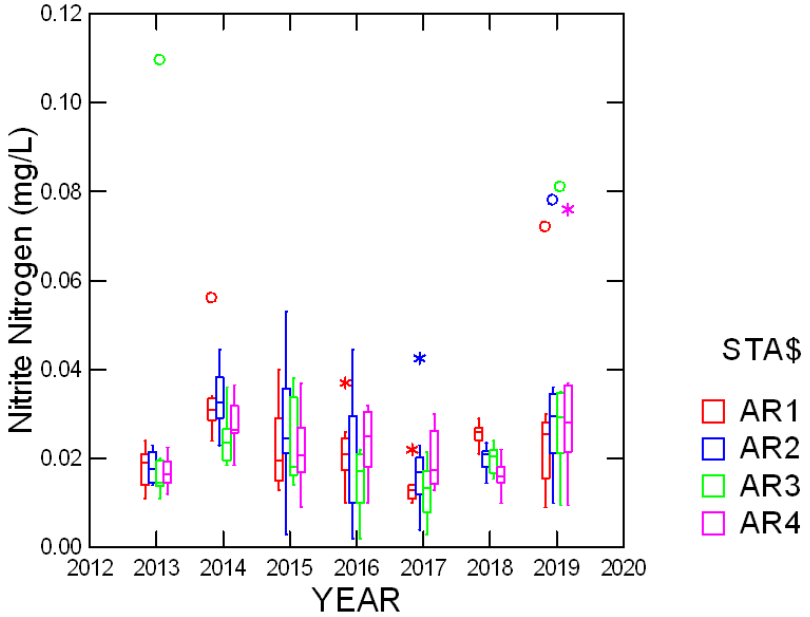

Figure 111. Box plots comparing values of Nitrite Nitrogen between years. June through September.

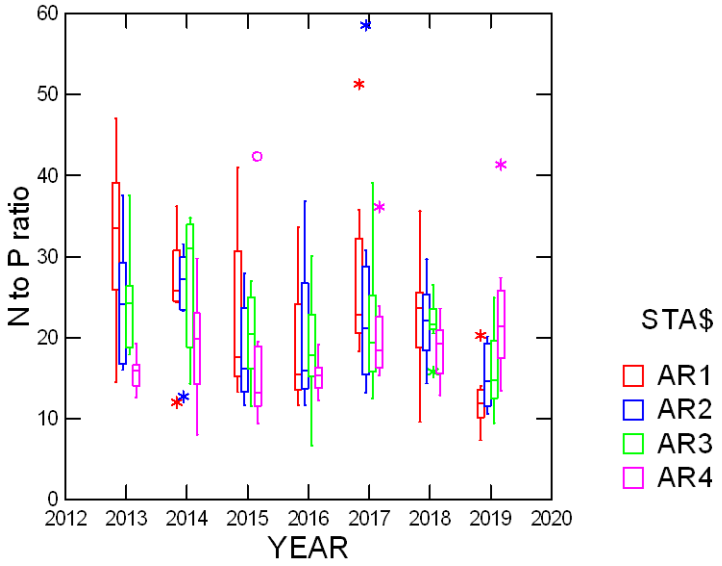

Figure 112. Box plots comparing values of N to P ratio between years. June through September.

N to P ratio for 2019 was in the lower range of values from previous years, but still within the range indicating phosphorus limitation. AR1, AR2, and AR3 were lower than in previous years. There is slight downward trend suggested in data from AR1, AR2, and AR3 while AR4 does not exhibit an obvious change over the years.

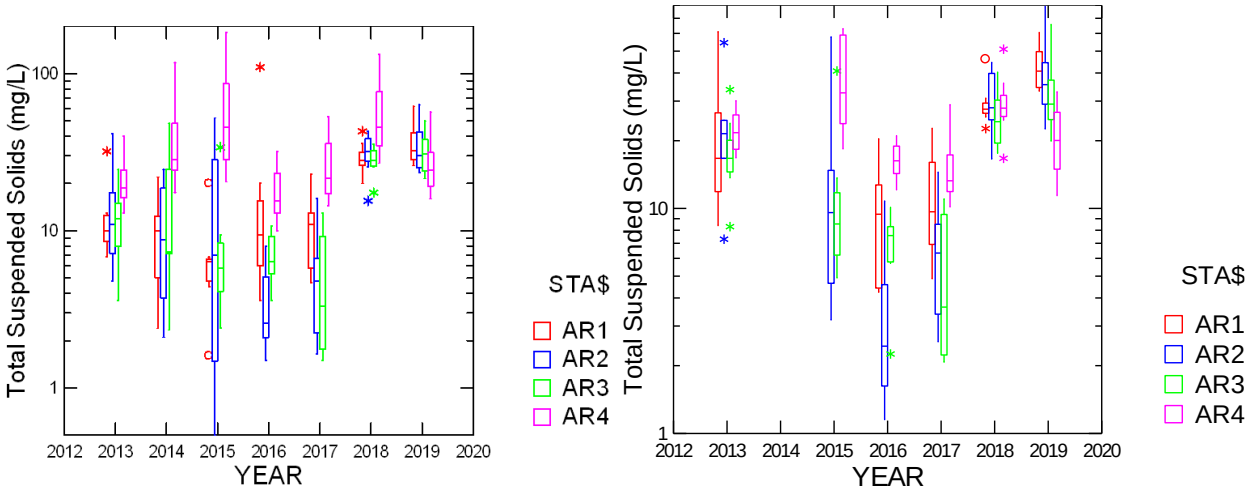

Figure 113. Box plots comparing values of Total Suspended Solids between years. Alex Renew data (a. left) and GMU data (b. right). June through September.

As in 2018 total suspended solids (TSS) for AR1, AR2, and AR3 was higher in 2019 than in previous years (Figure 113a,b). The exception was AR4 where values were lower in 2019 than in 2018 and some other previous years. The patterns were similar in samples analyzed by both Alex Renew and GMU. Volatile suspended solids (VSS) were actually higher in 2019 than 2018 at AR1, AR2, and AR3, but in the middle of the multiyear range at AR4 (Figure 114a,b).

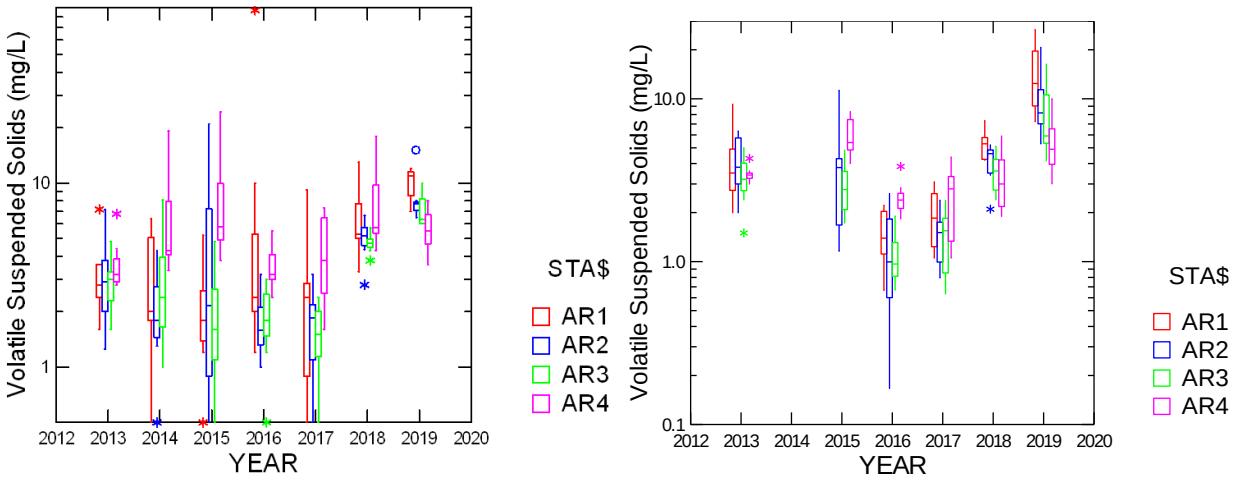

Figure 114. Box plots comparing values of Volatile Suspended Solids between years. Alex Renew Lab data (left) and GMU Lab data (right). June through September.

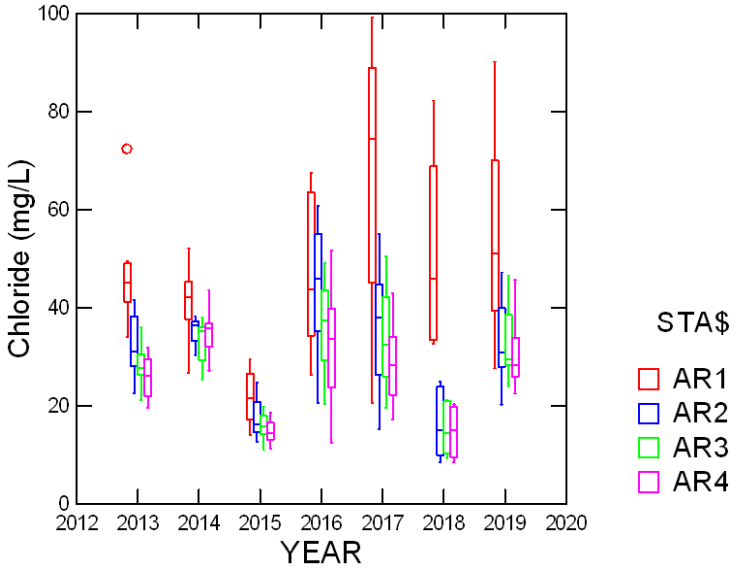

Figure 115. Box plots comparing values of Chloride between years. June through September.

Chloride levels continued to show a clear spatial pattern in 2019 with highest values at AR1 (Figure 115). At the other stations, chloride increased substantially relative to 2018, but was similar to other years. Total alkalinity was higher in 2019 than in previous years at AR2, AR3, and AR4, continuing an upward trend (Figure 116). In contrast to chloride, total alkalinity was generally lower at AR1 than at the other stations.

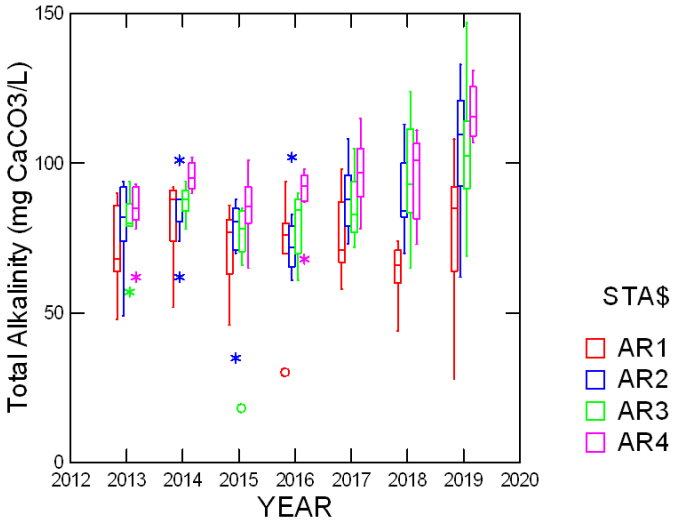

Figure 116. Box plots comparing values of Total Alkalinity between years. June through September.

D. Phytoplankton: Comparison among Years

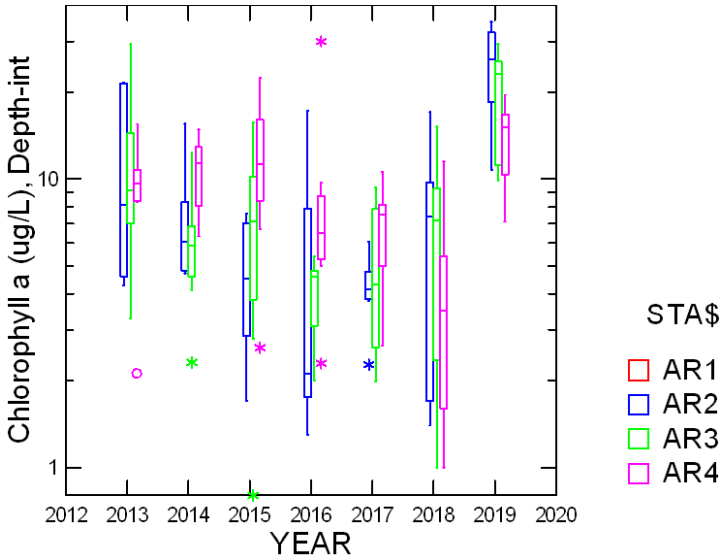

Figure 117. Box plots comparing values of depth-integrated Chlorophyll *a* among years. June through September.

In 2019 chlorophyll *a* levels rebounded strongly from the generally low levels found in 2018 and were actually the highest of all previous years. Also, values at all stations were much less variable than in 2018 (Figure 117, 118). Similar results were observed with surface chlorophyll. Chlorophyll values in the water are a measure of phytoplankton populations which compete with SAV for light and nutrients.

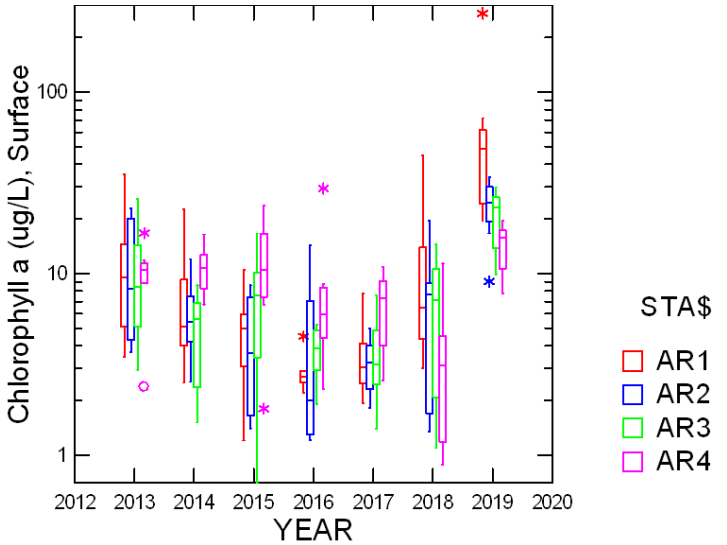

Figure 118. Box plots comparing values of surface Chlorophyll *a* among years. June through September.

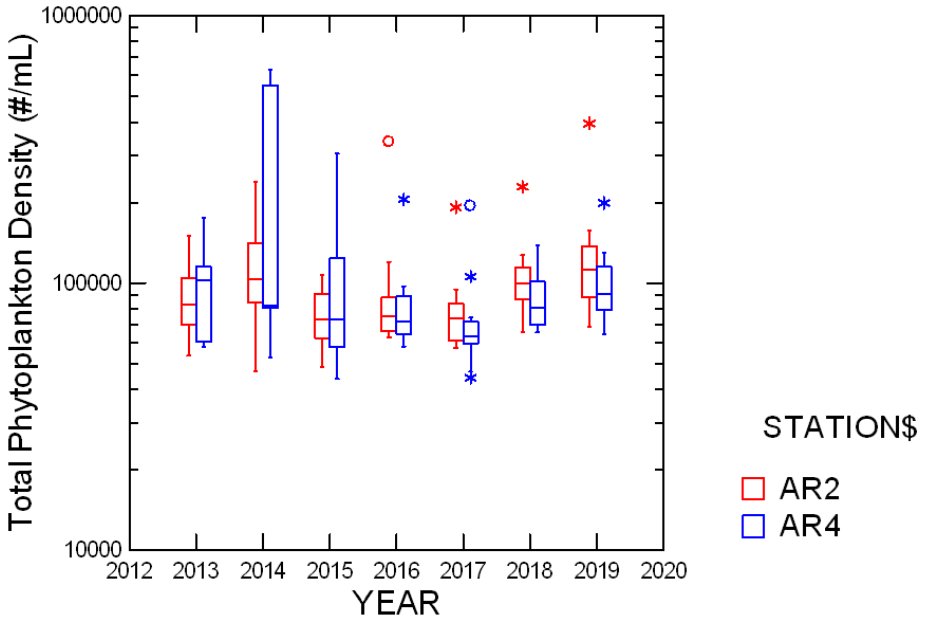

Figure 119. Box plots comparing values of Total Phytoplankton Density.

The median values for total phytoplankton cell density were similar among the six years, although there were more high values in 2015 especially at AR4 (Figure 119). Total phytoplankton cell density in 2019 was in the typical range with values being slightly higher at AR2.. Total cyanobacterial cell density was clearly higher in 2014 at both stations than in the other six years (Figure 120). 2019 values were in the mid-range of previous years. The median value at AR2 was substantially higher at AR2 than AR4 although there was substantial overlap in their range.

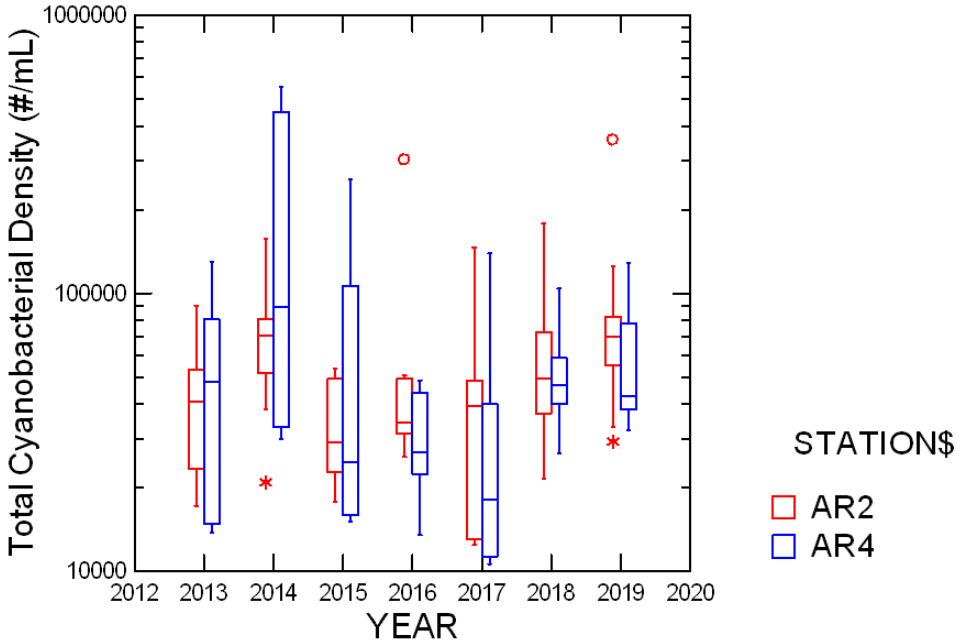

Figure 120. Box plots comparing values of Cyanobacterial Density.

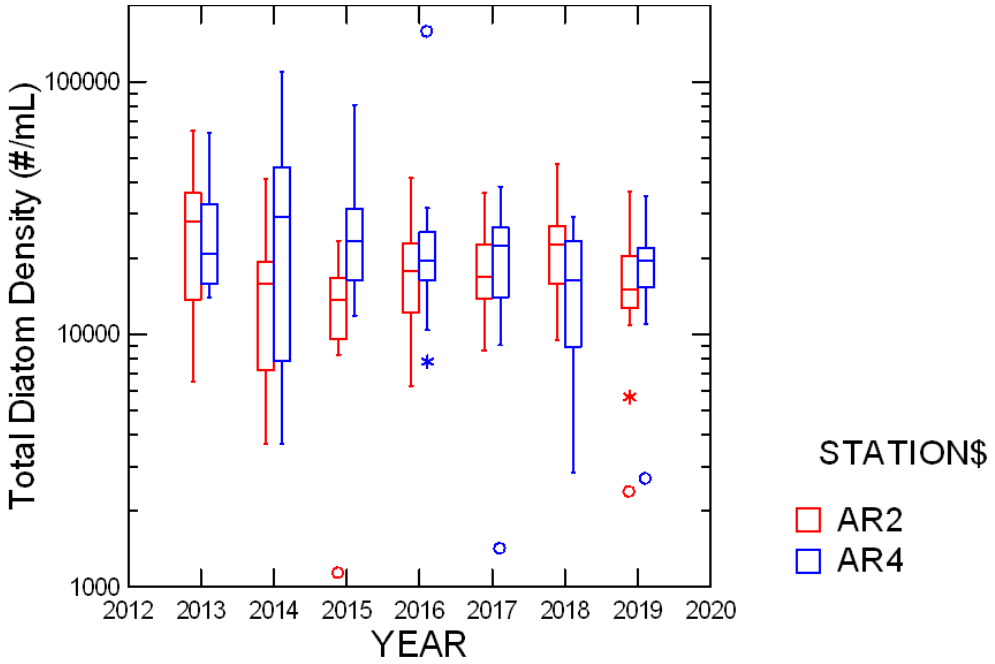

Figure 121. Box plots comparing values of Diatom Density among years.

Median diatom densities in 2019 fell within the range of recent years. Median values at AR4 were slightly greater than those at AR2 (Figure 121). Green algal cell densities were clearly higher in 2019 than in 2018, but did not vary much between stations (Figure 122).

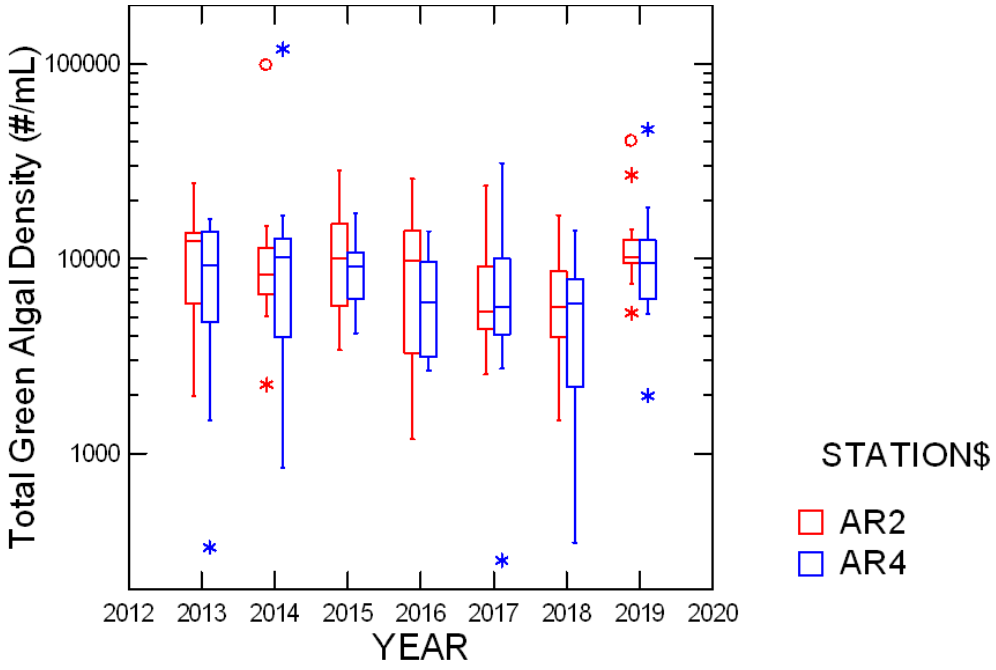

Figure 122. Box plots comparing values of Green Algal Density among years.

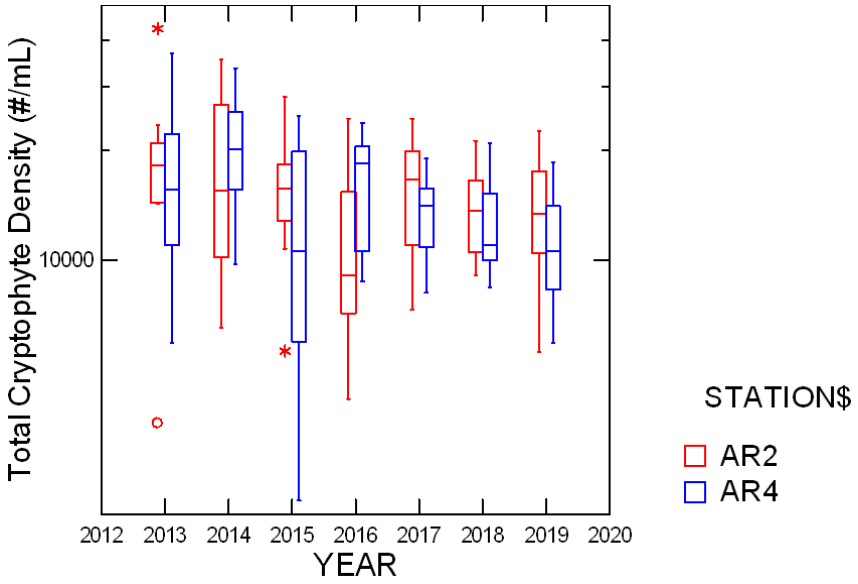

Figure 123. Box plots comparing values of Cryptophyte Density among years.

Median cryptophyte cell densities at AR4 continued a general downward trend observed since 2014 (Figure 123). At AR2 cryptophyte densities were in the middle of the range of previous years and somewhat higher than at AR4.

Other taxa includes those species of phytoplankton in groups not tallied above. These are mainly dinoflagellates, crysophytes and euglenoids whose abundances are somewhat sporadic in the study area. This is reflected in interannual patterns which show a wide range (Figure 124). Since 2016 values have declined consistently at AR4 with 2019 about the same as 2018. At AR2 2019 values were higher than at AR4, but in the midrange of previous years.

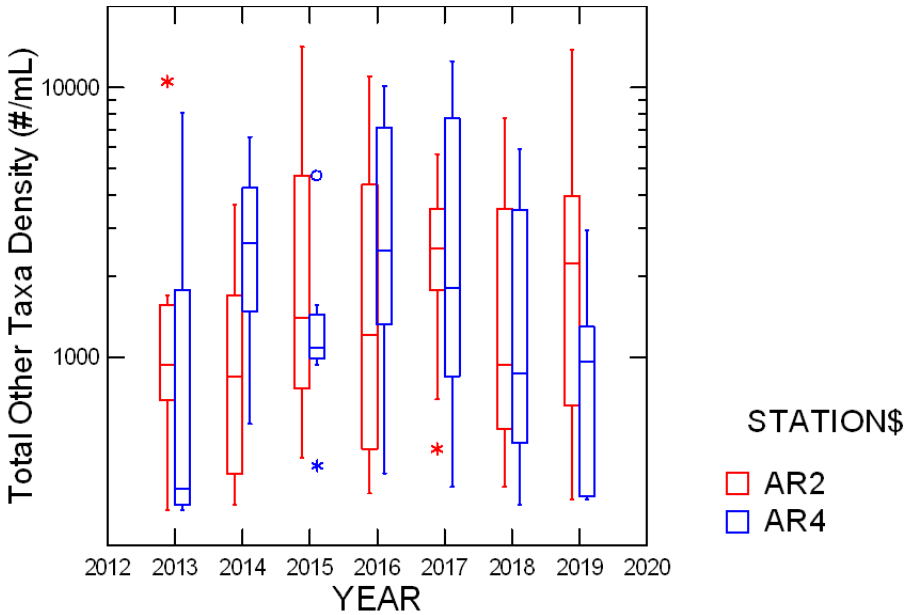

Figure 124. Box plots comparing values of Miscellaneous Taxa Density among years.

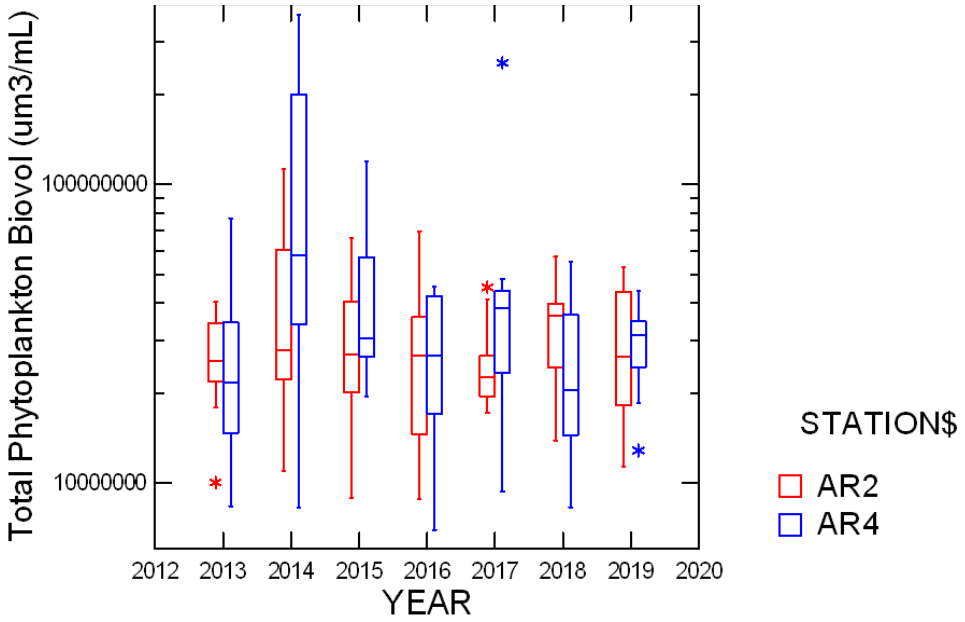

Figure 125. Box plots comparing values of Total Phytoplankton Biovolume among years.

Biovolume takes into account both the number of cells and their relative size. At both stations, median values of total phytoplankton biovolume fell within the range of previous years (Figure 125). Total cyanobacterial biovolume median in 2019 was at the high end of previous annual media. Values at AR4 were lower than in 2018 and in the middle of the range of previous annual media (Figure 126).

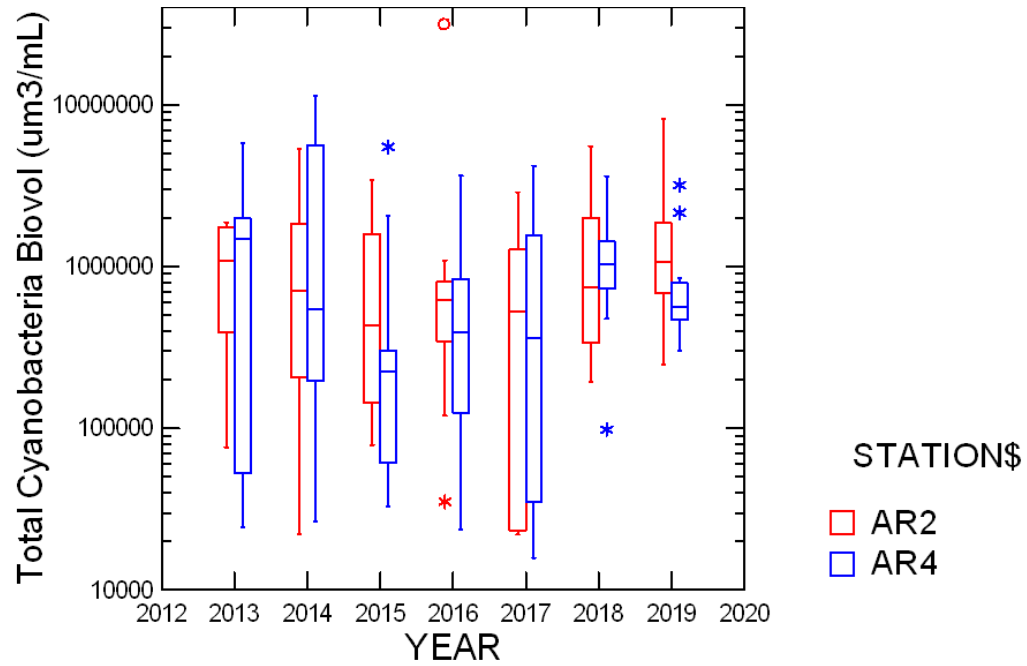

Figure 126. Box plots comparing values of Cyanobacterial Biovolume among years.

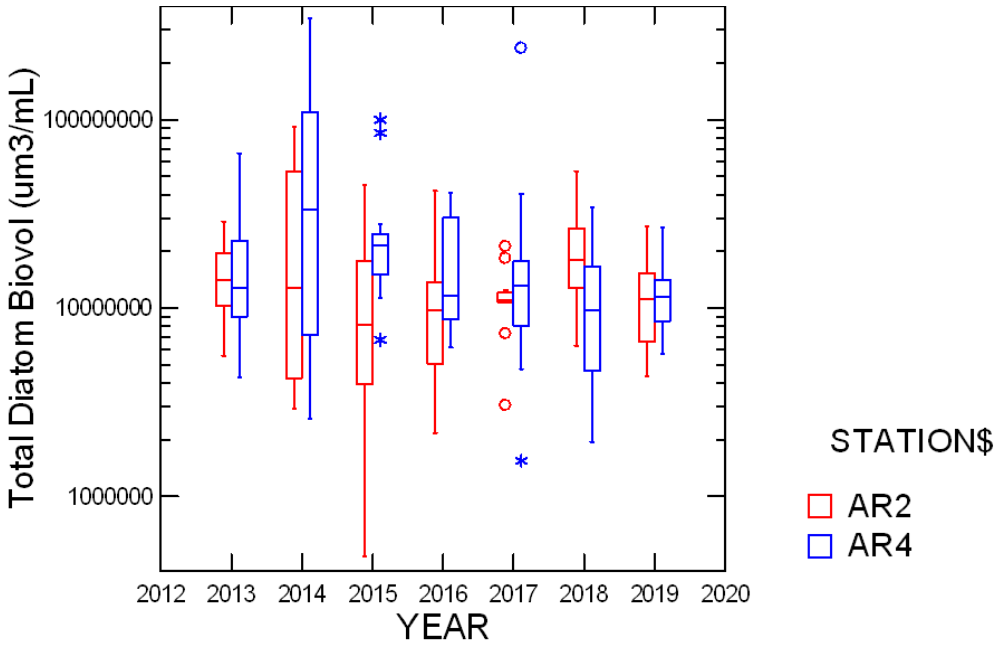

Figure 127. Box plots comparing values of Diatom Biovolume among years.

Median diatom biovolume at both stations was similar at both stations and well within the range of media for previous years (Figure 127). Median values in green algal biovolume at both stations were among the highest observed and were similar at both stations during 2019 (Figure 128).

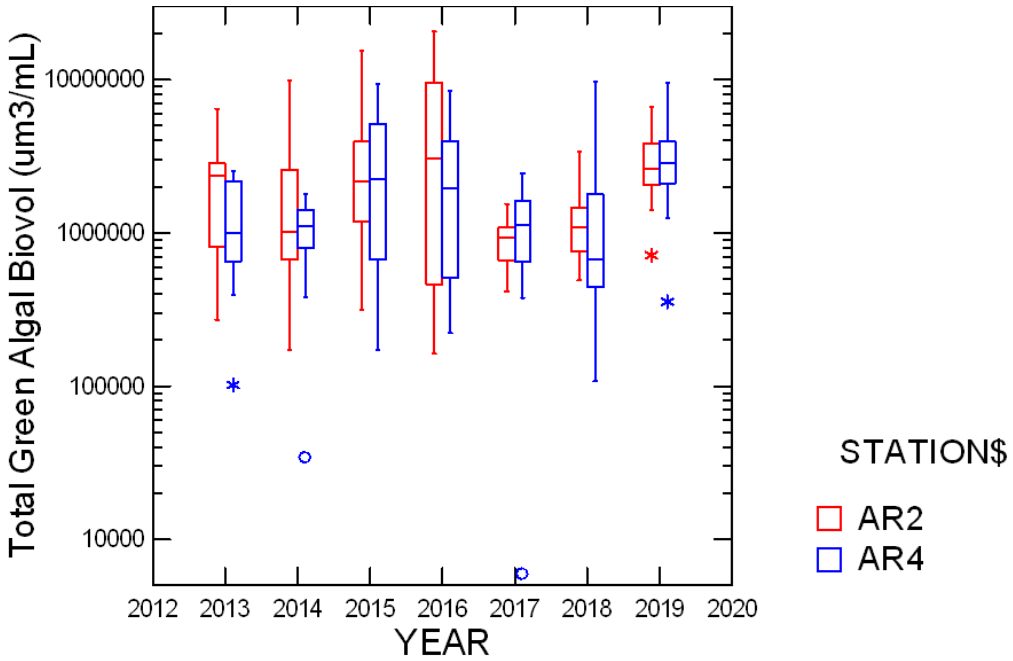

Figure 128. Box plots comparing values of Green Algal Biovolume among years.

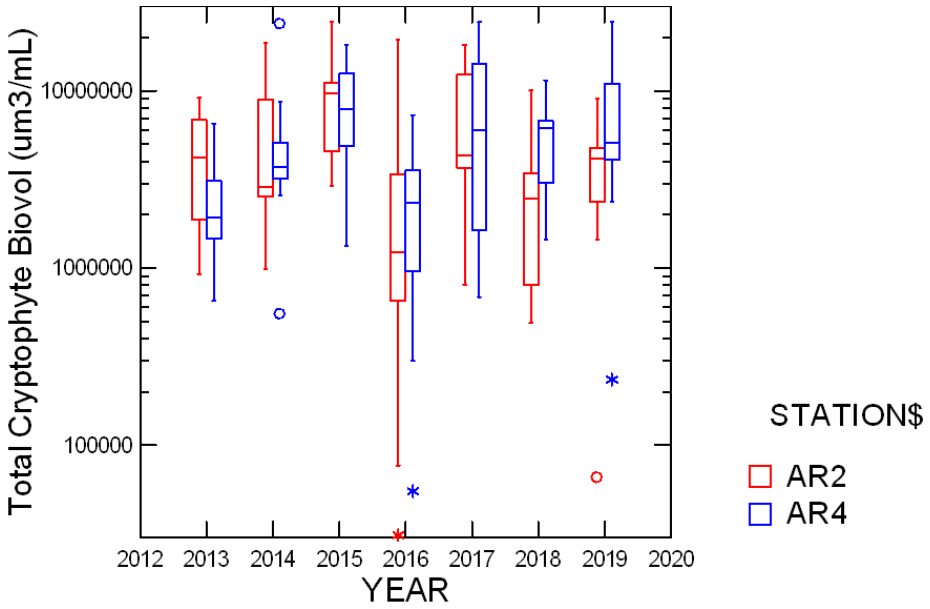

Figure 129. Box plots comparing values of Cryptophyte Biovolume among years.

For the second year in a row, cryptophyte biovolume was distinctly higher at AR4 than at AR2 (Figure 129). Values at both stations were in the range observed in previous years. The patterns in Miscellaneous Taxa Biovolume were a bit sporadic and quite variable in some years (Figure 130). The median values in 2019 fell within the normal range.

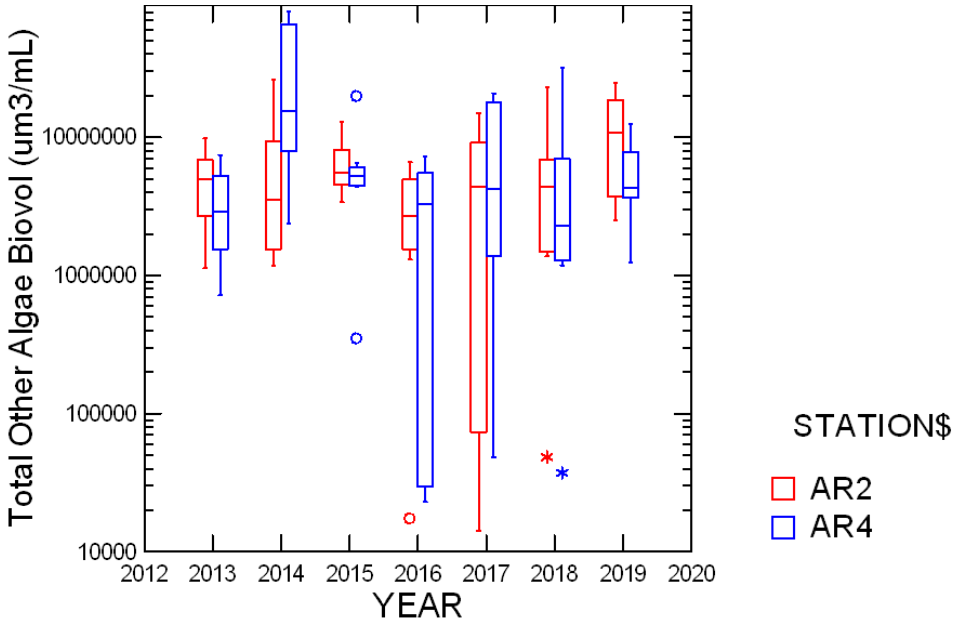

Figure 130. Box plots comparing values of Miscellaneous Biovolume among years.

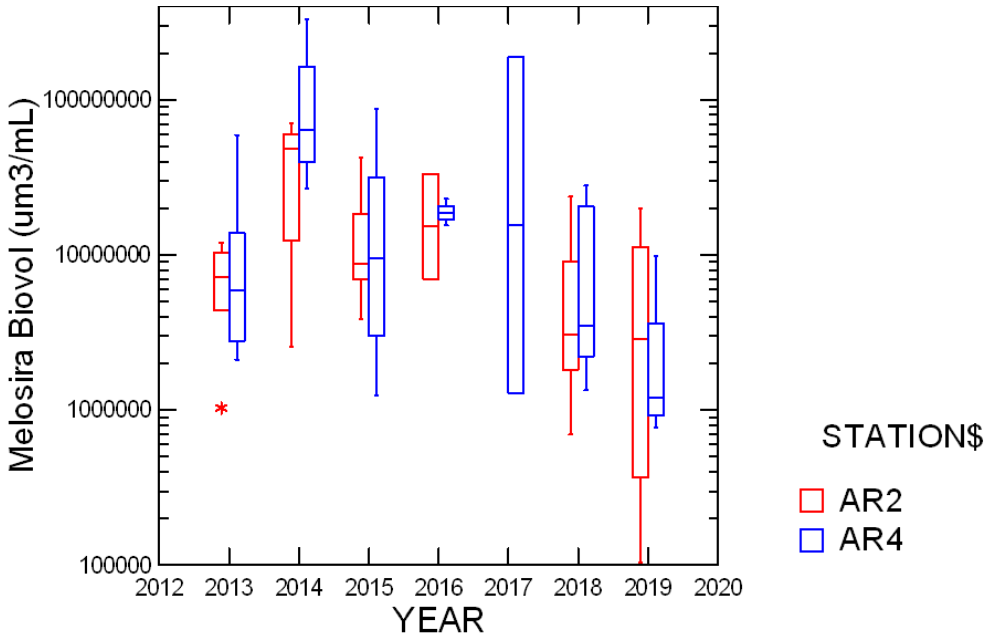

Figure 131. Box plots comparing values of *Melosira* Biovolume among years.

An analysis of interannual and seasonal effects also done for selected individual taxa. Median biovolume values of the filamentous diatom *Melosira* showed a clear peak in 2014 at both stations and has declined steadily since then (Figure 131). Values of *Melosira* in 2019 were about the same as 2018 at AR2 and slightly lower at AR4. Discoid centric biovolume in 2019 was at the lower end of the rangeobserved in recent years and was markedly lower at AR2 than at AR4 (Figure 132).

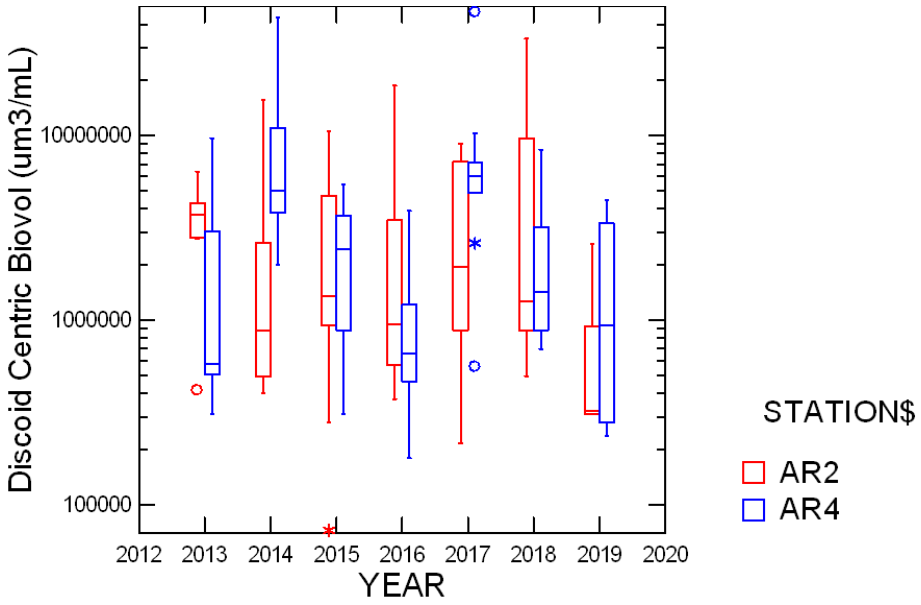

Figure 132. Box plots comparing values of Discoid Centric Diatom Biovolume among years.

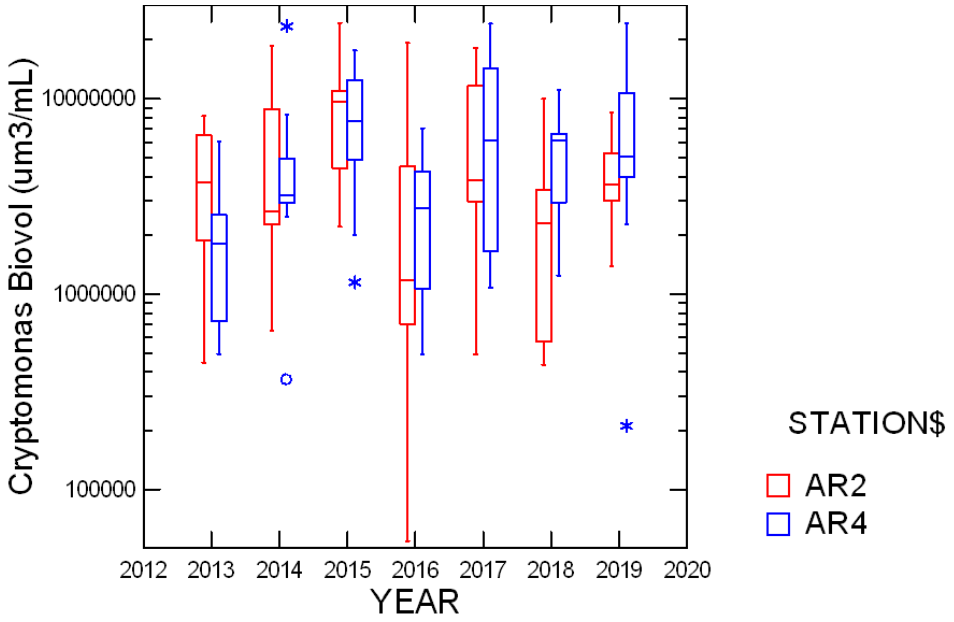

Figure 133. Box plots comparing values of *Cryptomonas* Biovolume among years.

Cryptomonas biovolume increased somewhat in 2019 above 2018 values, but remained within the range of all previous years (Figure 133). Values at AR4 were slightly above those at AR2. *Oscillatoria* is the most consistently abundant cyanobacterium in the study area. In 2019 levels were the lowest of any year observed yet except perhaps 2016 and were distinctly lower than in 2018 (Figure 134).

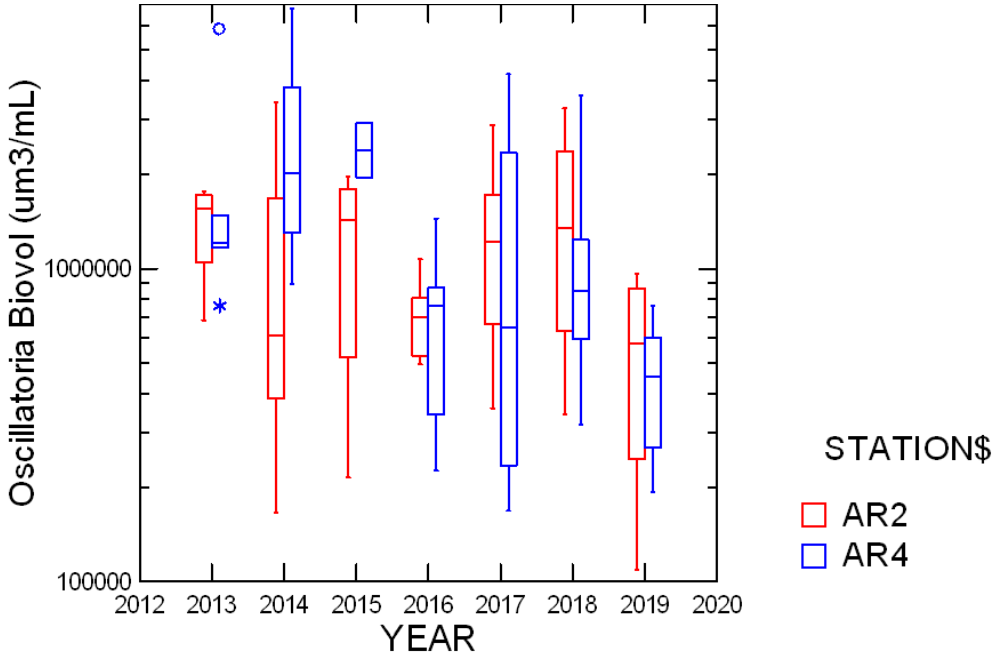

Figure 134. Box plots comparing values of *Oscillatoria* Biovolume among years.

E. Zooplankton: Comparison among Years

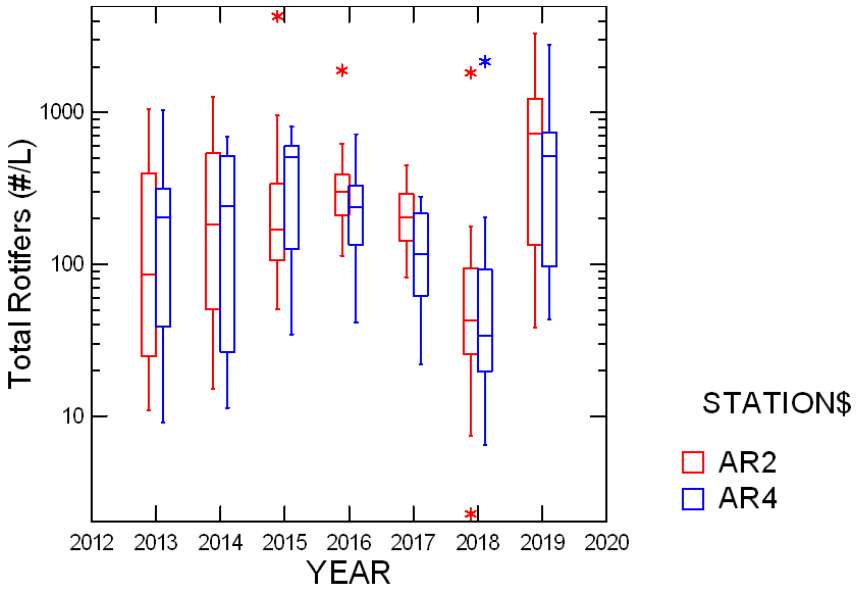

Figure 135. Box plots comparing values of Total Rotifers among years.

Total rotifer densites were very robust in 2019 equalling or exceeding any of the previous study years (Figure 135). Of particular interest was the strong recovery from the record low values of 2018 which were probably a result of the high rainfall and subsequent flushing of organisms observed that year. Episodic flushing occurred in 2019, but may have actually stimulated the rotifers. The common rotifer *Brachionus* (Figure 136) was the dominant tason and displayed a similar trend as total rotifers with 2019 levels very high and 2018 the lowest year to date. *Brachionus* exhibited similar values at both station sin most years.

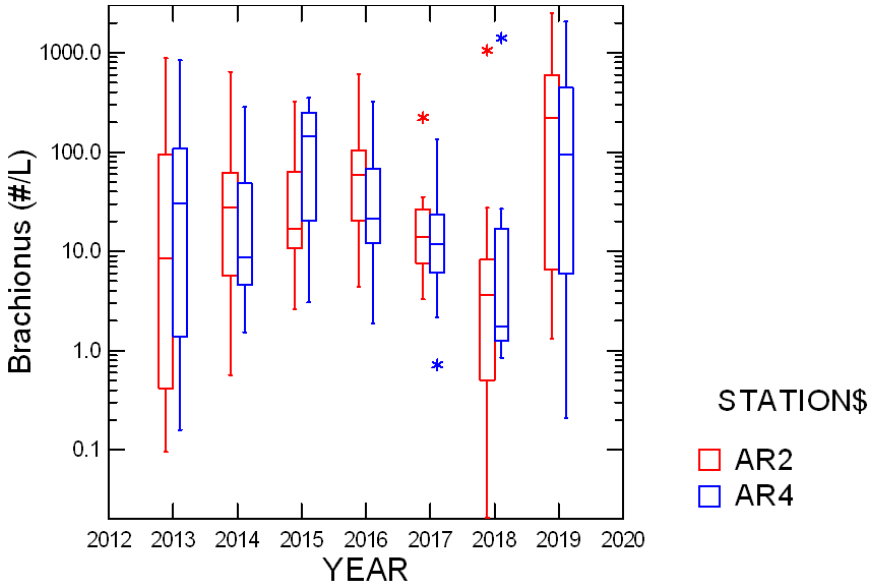

Figure 136. Box plots comparing values of *Brachionus* among years.

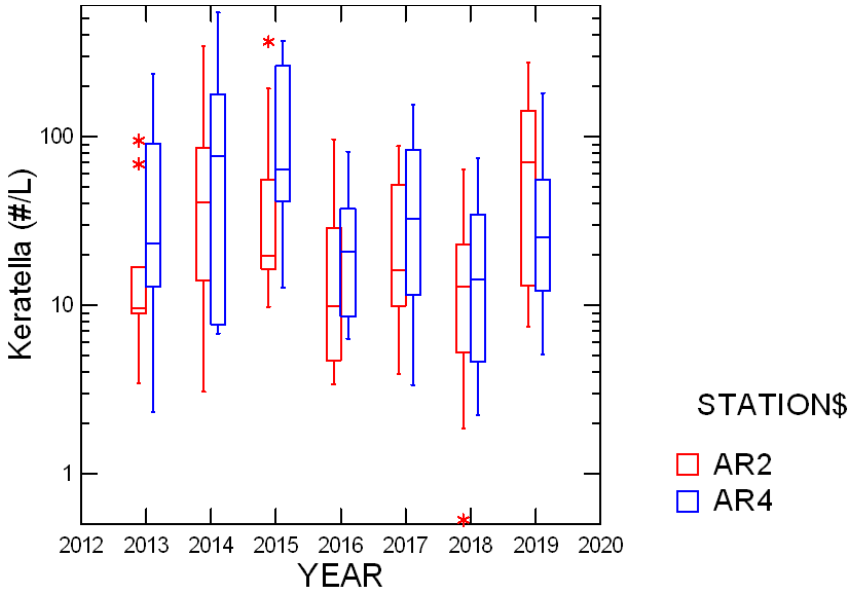

Figure 137. Box plots comparing values of *Keratella* among years.

Another common rotifer *Keratella* exhibited a similar, but less dramatic trend. Values in 2019 were higher in 2019, but 2018 was not as low relative to other years. Median in 2019 was the highest of any year at AR2, but at AR4 was mid-range relative to previous years (Figure 137). *Polyarthra*, consistently observed, but less common than *Brachionus* or *Keratella*, displayed a pattern similar to that observed for total rotifers and *Brachionus* (Figure 138). It was present at similar levels at both AR2 and AR4.

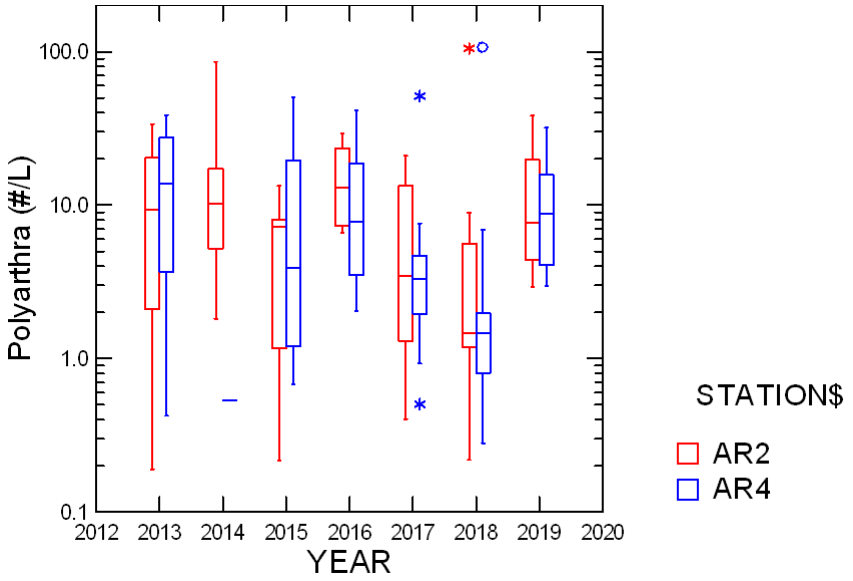

Figure 138. Box plots comparing values of *Polyarthra* among years.

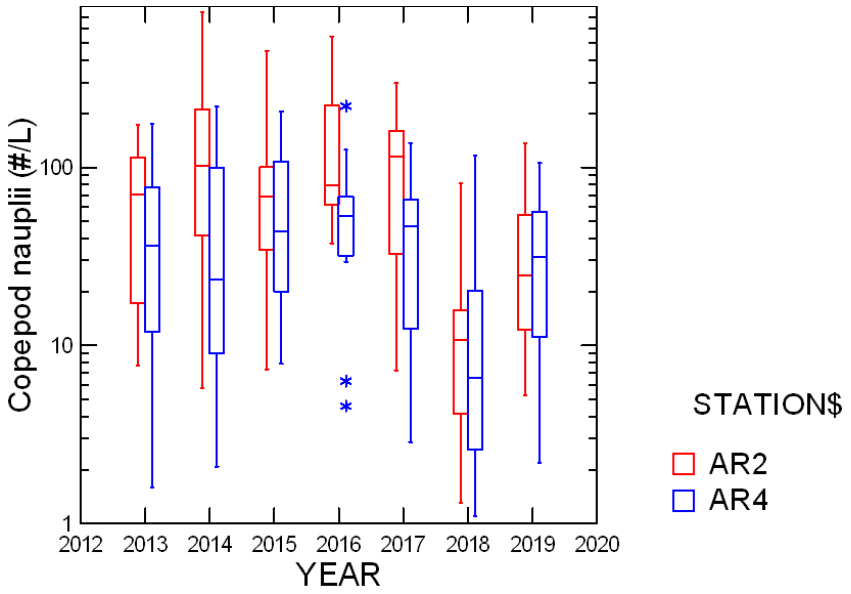

Figure 139. Box plots comparing values of Copepod Nauplii among years.

Nauplii are the juvenile stages of copepods. As such it is hard to identify them to species since they do not have mature characteristics so they have been lumped for all copepod taxa. Nauplii showed a clear recovery in 2019 after the low values of 2018, but were still at the low end of levels from earlier years of the study (Figure 139). Values were similar at the two stations. *Bosmina* is a small cladoceran enumerated in the 44 µm samples, but related to *Daphnia* and *Diaphanosoma* collected in the 202 µm nets. As with copepod nauplii, *Bosmina* recovered markedly after the sharp decline in 2018 (Figure 140). There was not a consistent difference in *Bosmina* levels between the two stations.

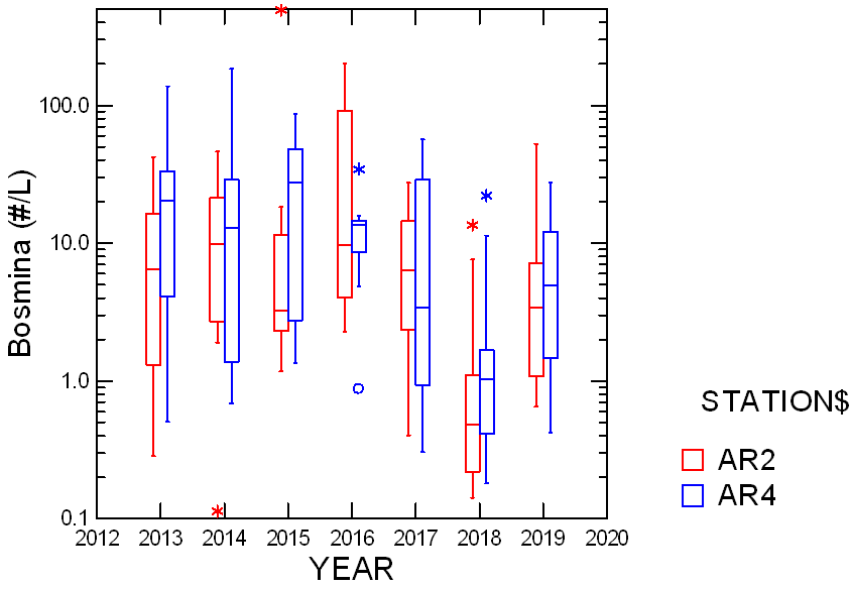

Figure 140. Box plots comparing values of *Bosmina* among years.

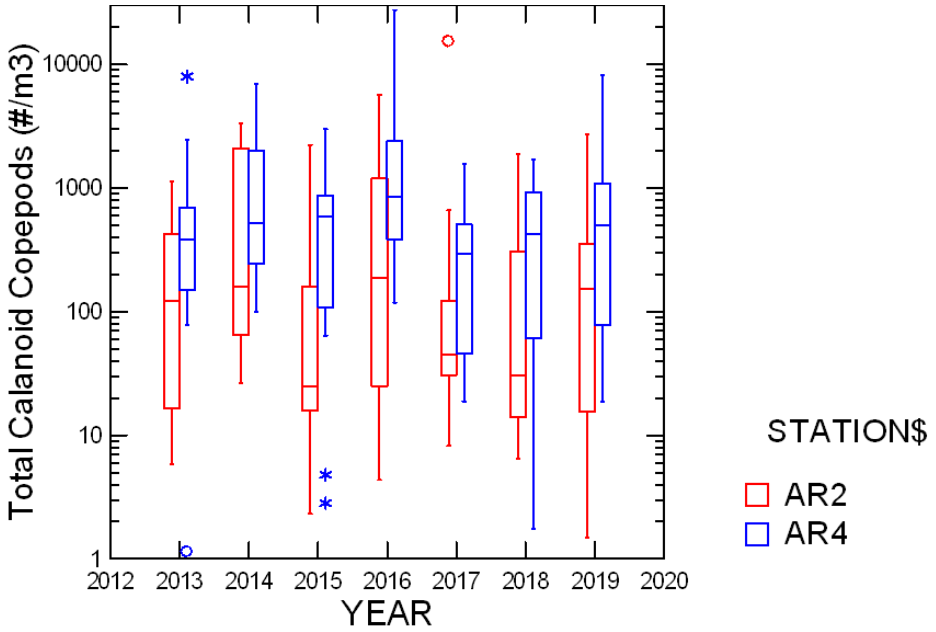

Figure 141. Box plots comparing values of Total Calanoid Copepods among years.

Median calanoid copepod densities were similar over all years at AR4 and consistently greater there than at AR2 (Figure 141). Median AR2 values in 2019 recovered from the low values of 2017 and 2018, *Eurytemora* is the most common calanoid copepod. Its interannual pattern was quite similar to that observed for total calanoids (Figure 142) with AR4 clearly higher than AR2. *Eurytemora* did not exhibit much response to the very different flow regimes of 2018 and 2019.

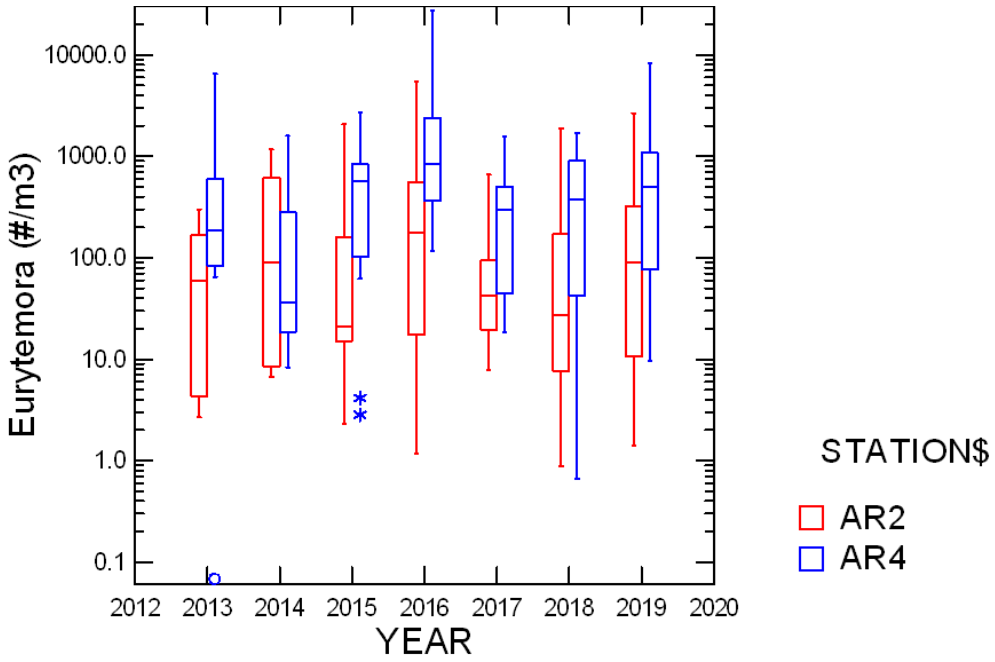

Figure 142. Box plots comparing values of *Eurytemora* among years.

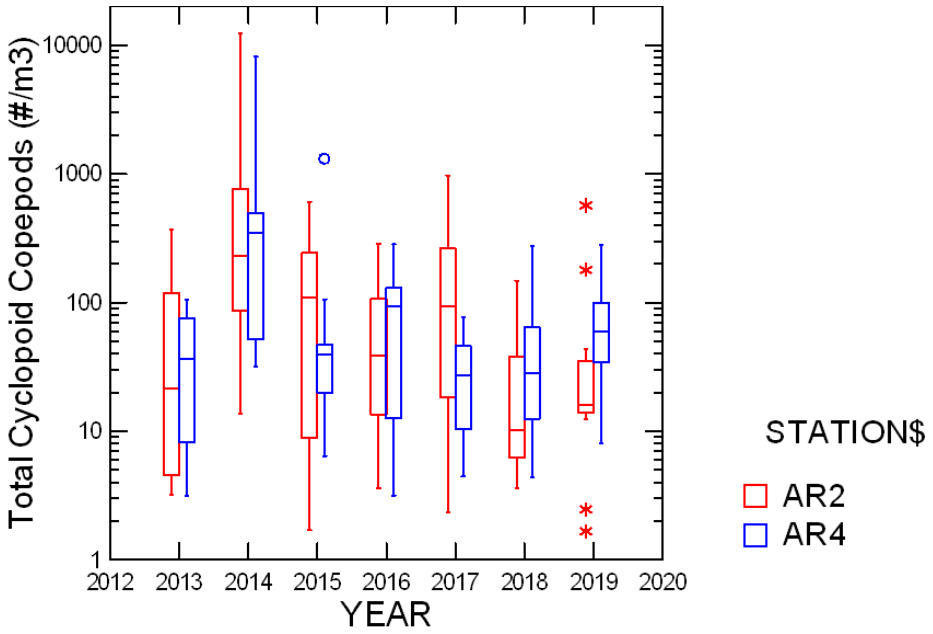

Figure 143. Box plots comparing values of Cyclopoid Copepods among years.

Cyclopoid copepods were present at similar levels in 2019 as in most previous years (Figure 143). There was a slight increase in 2019 over 2018. *Mesocyclops* is one of the more common cyclopoid copepods. Median values of *Mesocyclops* at AR2 continued to be at the low end of the range of previous years, while AR4 levels showed little change (Figure 144).

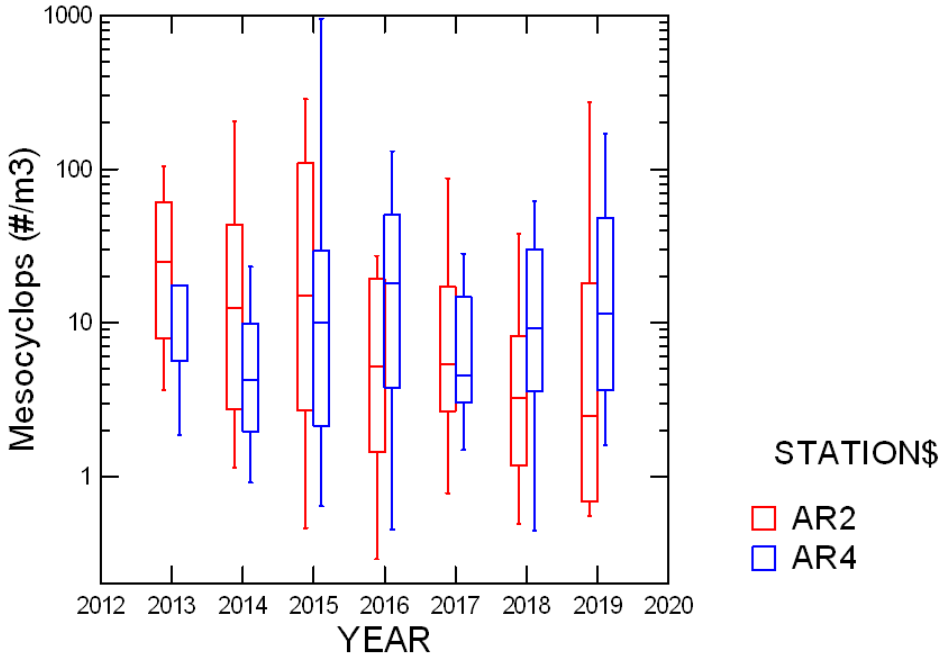

Figure 144. Box plots comparing values of *Mesocyclops* among years.

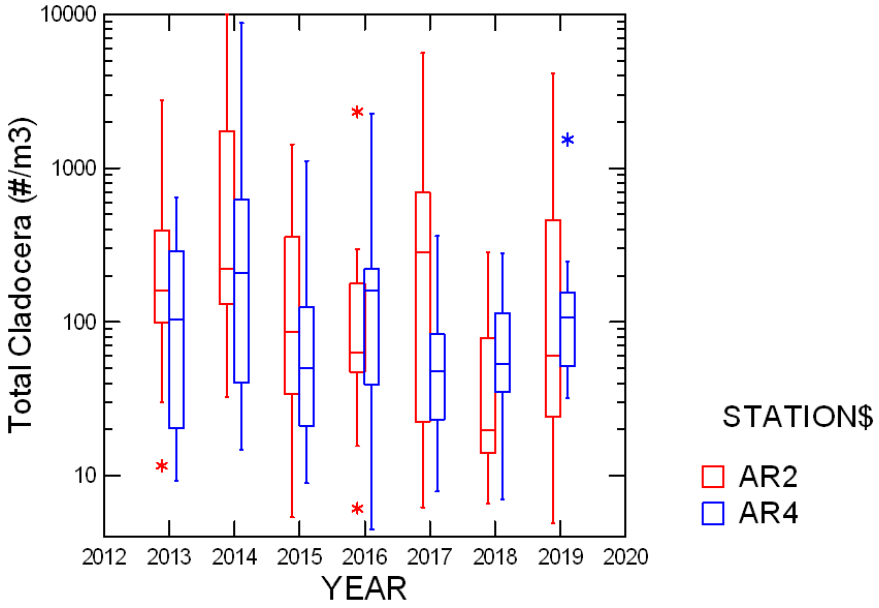

Figure 145. Box plots comparing values of Total Cladocerans among years.

Total cladoceran values (excluding *Bosmina*) at AR2 recovered somewhat in 2019 after the low levels in 2018 (Figure 145). Values at AR4 remained within the range of previous years. *Daphnia* was found at clearly higher levels in 2014 than in the other years of the study (Figure 146). Values observed in 2019 continued an upward trend after a low in 2017. *Daphnia* did not exhibit the clear decline in 2018 and recovery in 2019 pattern observed for some other zooplankton.

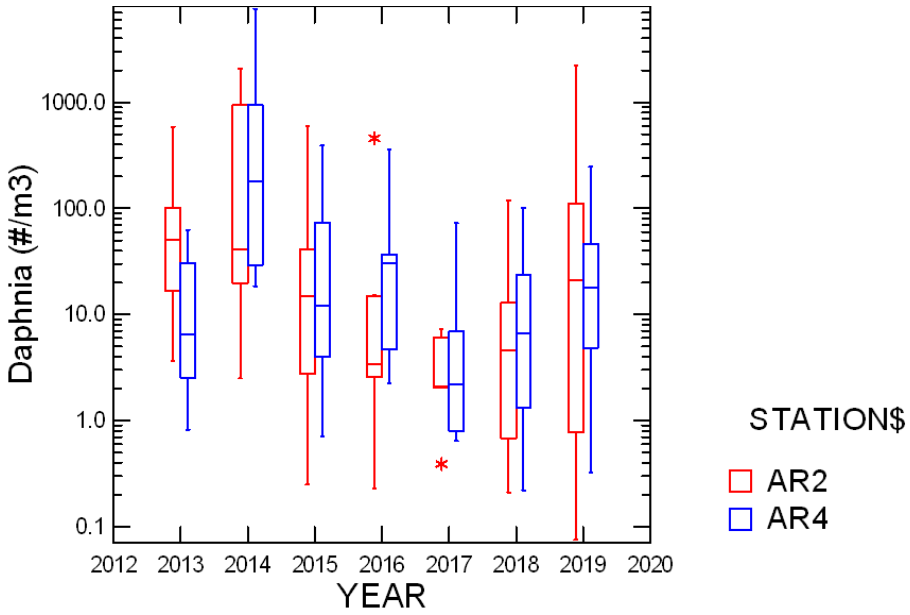

Figure 146. Box plots comparing values of *Daphnia* among years.

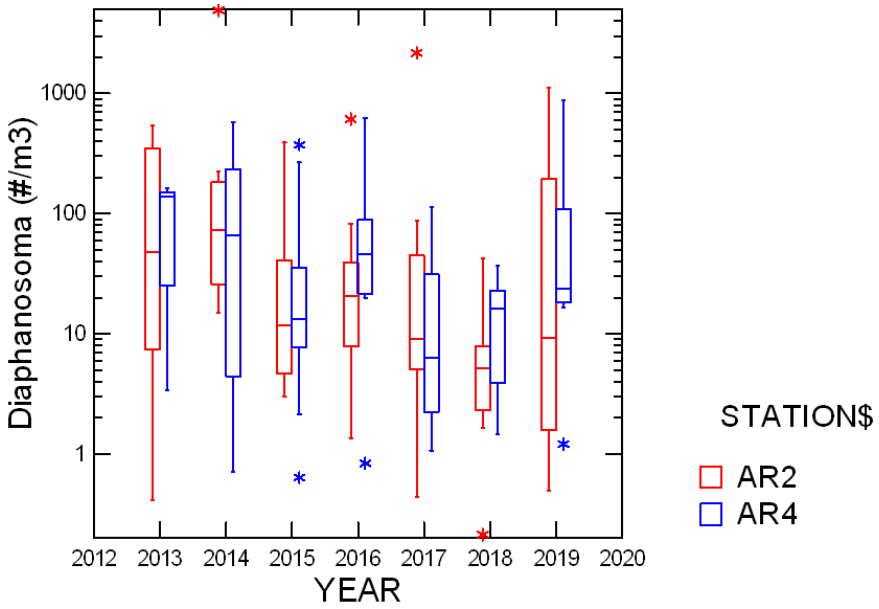

Figure 147. Box plots comparing values of *Diaphanosoma* among years.

Diaphanosoma is a very abundant cladoceran in Gunston Cove, but has proven to be less abundant in the Hunting Creek area, although still important. *Diaphanosoma* levels at AR2 were at record lows in 2018, and showed some recovery in 2019 (Figure 147). Levels at AR4 were also higher in 2019. *Sida* was generally less abundant than *Diaphanosoma*, but has maintained its levels over time. It was also reduced in 2018 did not recover much in 2019 (Figure 148).

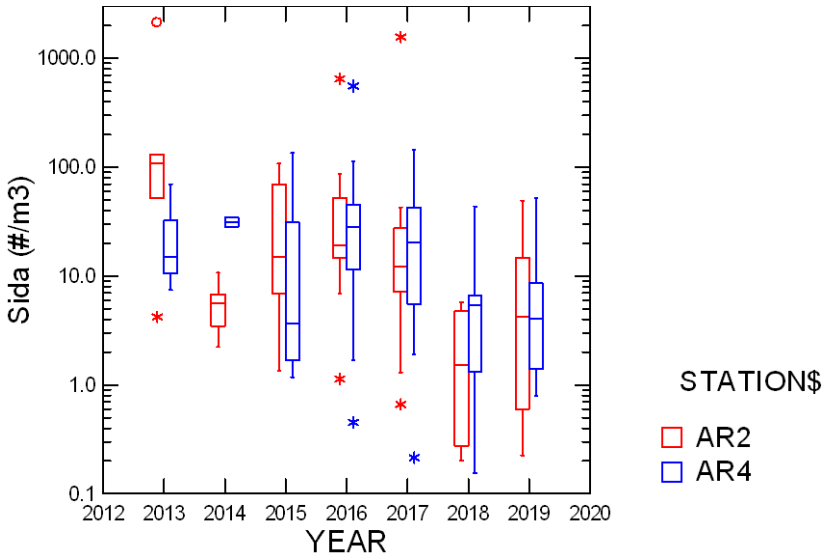

Figure 148. Box plots comparing values of *Sida* among years.

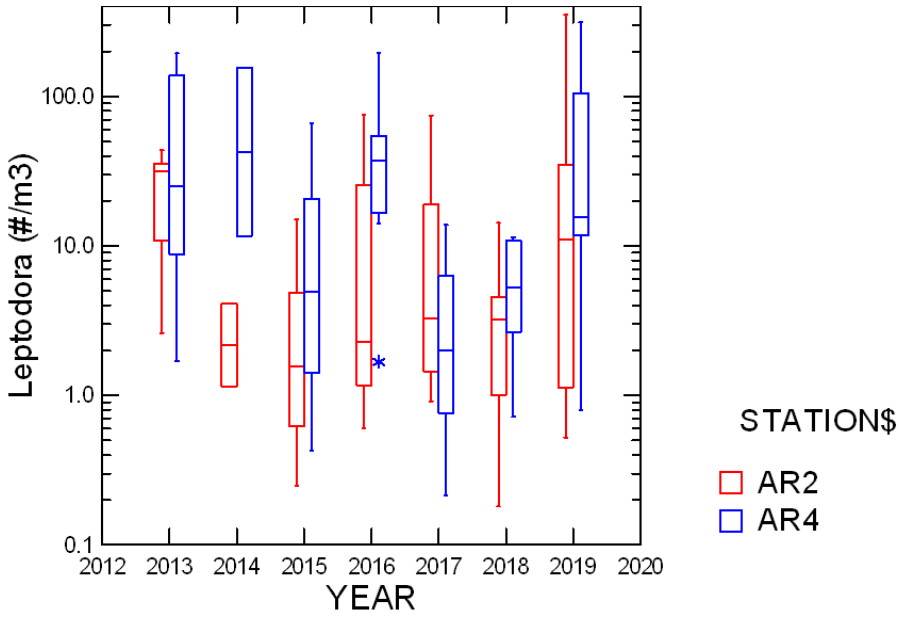

Figure 149. Box plots comparing values of *Leptodora* among years.

Leptodora is a large predacious cladoceran which occurs consistently in the study area (Figure 149). Values in 2019 were among the highest observed to date at both stations and were distinctly higher than in 2017 and 2018. *Leptodora* was generally higher at AR4 as has been usual. Total macrozooplankton, those collected in the 202 µm net, showed a clear interannual pattern with greatest numbers at both stations in 2014 (Figure 150). 2018 values were much reduced at AR2, but similar to recent years at AR4. Both stations showed a slight increase in 2019 over 2018.

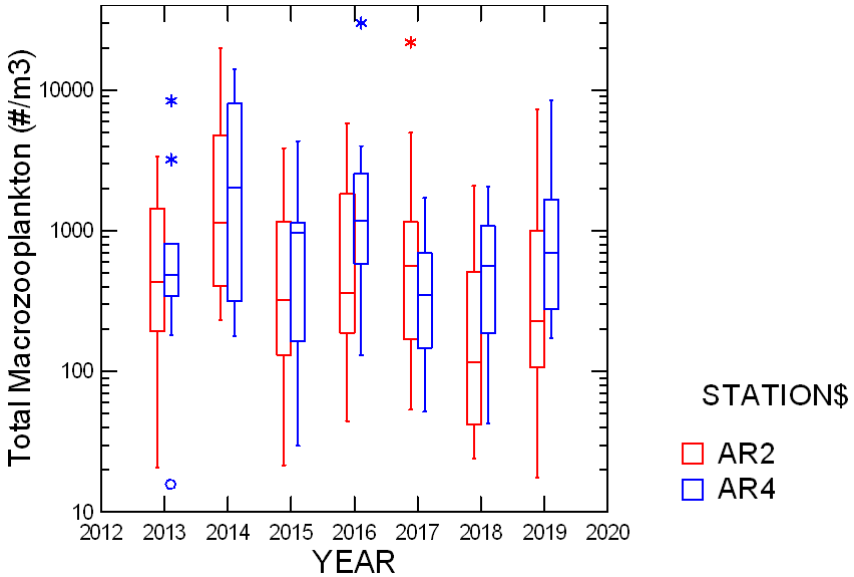

Figure 150. Box plots comparing values of Total Macrozooplankton among years.

F. Ichthyoplankton: Comparison among Years

2019 marks the seventh year of our fish collections in Hunting Creek. Both trends and inter-annual variability become apparent when comparing the years of data. In the larval data a high dominance of different species in the herring or shad family (clupeids) are consistently present, and in high densities (Table 14). These include anadromous species of concern such as Blueback Herring and Alewife, for which we also monitor the spawning populations as part of this study.

Table 23. Density of larvae collected all years.

Scientific Name	Common Name	2013	2014	2015	2016	2017	2018	2019
Alosa aestivalis	Blueback Herring	61.69	200.35	382.05	91.54	205.29	56.54	271.72
Alosa mediocris	Hickory Shad	4.80	4.13	12.11	9.63	4.28	1.58	11.36
Alosa pseudoharengus	Alewife	139.80	57.71	265.97	78.52	81.75	38.85	214.34
Alosa sapidissima	American Shad	0.12	1.32	0.61	1.97	2.80	0.15	0.00
Alosa sp.	unk. Alosa species	0.00	18.49	0.00	0.00	0.00	0.00	0.00
Carassius auratus	Goldfish	56.78	0.89	0.00	0.30	7.02	0.00	0.00
Carpiodes cyprinus	Quillback	0.00	0.00	0.00	0.78	0.00	0.92	8.14
Catostomidae	unk. catostomidae species	0.00	0.00	0.00	0.00	0.00	0.00	0.17
Centrarchidae	unk. centrarchidae species	0.00	0.00	0.00	0.13	0.00	0.00	0.00
Clupeidae	unk. clupeid species	422.94	781.67	444.54	175.51	193.31	129.35	169.13
Cyprinidae	unk. cyprinidae species	1.14	0.00	0.59	0.00	0.00	0.00	0.00
Cyprinus carpio	Carp	0.00	0.00	0.00	0.00	2.98	0.00	0.00
Dorosoma cepedianum	Gizzard Shad	438.39	381.85	592.25	221.54	293.50	83.18	1999.48
Eggs	eggs	0.16	3.09	2.69	17.80	25.66	11.17	62.25
Enneacanthus gloriosus	Bluespotted Sunfish	0.00	0.24	0.00	0.00	0.00	0.00	0.00
Etheostoma olmstedi	Tessellated Darter	0.00	0.00	0.00	0.13	0.00	0.00	0.00
Etheostoma sp.	unk. darter species	0.00	0.00	0.00	0.00	0.00	0.00	0.19
Fundulus diaphanus	Banded Killifish	0.00	0.00	0.00	0.00	0.50	0.00	0.00
Hybognathus regius	Eastern Silvery Minnow	0.00	0.00	0.00	0.00	0.50	0.00	0.19
Lepisosteus osseus	Longnose Gar	0.00	0.00	0.00	0.00	0.25	0.00	0.00
Lepomis cyanellus	Green Sunfish	0.00	0.00	0.00	0.41	0.50	0.00	0.00
Lepomis gibbosus	Pumpkinseed	0.00	0.00	0.00	1.62	0.99	0.39	0.35
Lepomis macrochirus	Bluegill	0.00	0.00	0.00	0.00	0.50	0.00	0.00
Lepomis sp.	unk. sunfish	0.60	2.83	0.49	0.00	8.23	0.00	0.19
Menidia beryllina	Inland Silverside	2.48	3.32	1.98	20.36	60.78	0.66	1.21
Micropterus dolomieu	Smallmouth Bass	0.00	0.00	0.00	0.00	0.25	0.00	0.00
Morone americana	White Perch	0.00	5.90	15.93	8.60	17.54	15.48	66.30
Morone saxatilis	Striped Bass	0.00	4.02	0.00	1.10	7.71	0.00	0.00
Morone sp.	unk. perch/bass species	39.06	43.46	4.32	14.11	3.71	0.00	0.00
Notemigonus crysoleucas	Golden Shiner	0.00	0.84	0.00	0.00	0.00	0.00	0.00
Notropis hudsonius	Spottail Shiner	0.00	0.00	0.00	0.39	2.48	4.94	0.23
Perca flavescens	Yellow Perch	38.22	1.41	0.00	0.65	0.50	0.74	0.73
Strongylura marina	Atlantic Needlefish	0.00	0.12	0.00	0.00	0.13	0.00	0.00
Unidentified		11.45	84.35	27.42	34.65	84.23	6.43	126.74
Total		1217.66	1595.98	1750.95	679.72	1005.39	350.38	2932.72

The density of river herring larvae seems to be increasing over time, which is a good sign and likely due to the moratorium on river herring in plavce in Virginia since 2012. Overall, larval density was much higher in 2019 than in previous years, mostly due to a record high density of Gizzard Shad, another clupeid.

G. Adult and Juvenile Fish: Comparison among Years

The total number of adult and juvenile fishes collected in 2019 was average, with both higher and lower abundances collected in previous years (Table 15). The SAV beds that have been increasing in cover since the start of the study are a likely contributor to the lower catches in 2016 and 2017 compared to 2013-2015; conversely the lower density of SAV in 2018 and 2019 may have contributed to the increase in catch in 2018 and 2019. It is important to note that the SAV growth obstructs our ability to effectively collect trawl and seine samples, therefore lower numbers with denser SAV beds likely do not represent reduced abundances; rather it reflects our reduced ability to collect representative samples. There are clear benefits to the presence of SAV, it for example provides fish habitat and helps improve water clarity. The high amount of organic matter that SAV represents is still indicative of a eutrophic system, but a system with higher functionality than a phytoplankton dominated system. There was less SAV cover in the system in 2019 than there was in previous years, which allowed for effective trawl collections all season long.

To address the problem of our reduced ability to tow nets when SAV growth is high, we have added fyke nets to our sampling gear since 2016. The extensive SAV growth makes it highly suitable gear for the location, and total catch with fyke nets actually exceeded that of the trawls in both 2016 and 2017. The fyke nets are likely the most efficient gear to sample thick SAV beds, and we recommend continued use of this gear in our surveys. In 2019, catches with the seine and trawl increased as compared to the three previous years, while the collections with the fyke nets decreased. Low SAV cover reduces the effectiveness of the fyke nets, likely because they are not well-hidden between the plants like they are in years with dense SAV beds. By having both trawls and fyke nets collecting samples at the same location, we can better evaluate true abundance changes trough time instead of erroneously assuming that SAV growth reduces fish abundance.

The two most dominant species throughout the sampling period, White Perch and Banded Killifish, seem to have opposite trends through the years, with Banded Killifish abundances declining and White perch abundances increasing. The opposite trend is seen in the longer survey record of Gunston Cove (Jones and De Mutsert 2018), which seems mostly due to SAV resurgence since 2005. The decline in SAV cover in Hunting Creek in recent years could be a reason for the decreasing Banded Killifish abundances and increasing White Perch abundances. Other consistently present species are Spottail Shiner, Inland Silverside, Mummichog, Tessellated Darter and various species of sunfish and Herring and Shad. A species that has been increasing in abundance over the period of record is Blue Catfish, which is an invasive species.

In 2019, 35 different species were collected, which is similar to previous years, and a sign of a healthy diversity. The Simpson's Index of Diversity (calculated as $1-(\mathbf{\Sigma}\ (n_i/N)^2)$) was

calculated for all years based on adult and juvenile abundances (Figure 151). Note that in the 2016 report the Simpson's index (D) was reported, in which communities with higher diversity or evenness approach zero. In the reports since 2016 we calculated the Simpson's Index of Diversity, which is 1-D. In this index the communities with higher diversity have higher values (approaching 1) which is more intuitive to interpret. While evenness was reduced each year of sampling before 2017, 2017 and 2018 showed high Simpson's Index of Diversity values, with 2019 slithly lower but still very close to that (Figure 66). Overall, the fish species found in Hunting Creek are characteristic of Potomac River tributaries.

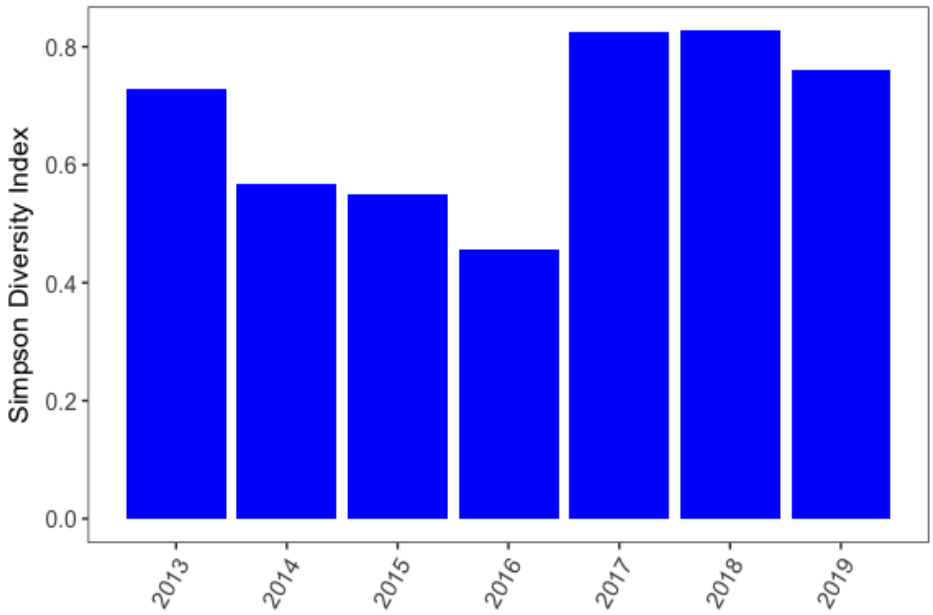

Figure 151. Simpson Diversity Index of fish species collected in Hunting Creek all years.

Table 24. Abundances of species (adults and juveniles) collected all years.

Scientific Name	Common Name	2013	2014	2015	2016	2016 with Fyke	2017	2017 with Fyke	2018	2018 with Fyke	2019	2019 with Fyke
Alosa aestivalis	Blueback Herring	16	8	12	29	29	0	0	0	0	32	33
A. mediocris	Hickory Shad	0	0	0	0	0	0	0	0	0	8	8
A. pseudoharengus	Alewife	6	23	28	12	12	0	0	14	14	67	69
A. sapidissima	American Shad	208	32	163	19	19	2	2	2	2	12	12
Alosa sp.	unk. Alosa species	299	8	55	11	12	3	3	433	433	822	822
Ameiurus catus	White Bullhead	0	0	0	1	2	0	0	8	8	1	1
Ameiurus natalis	Yellow Bullhead	0	0	0	0	0	0	0	0	0	4	4
Ameiurus nebulosus	Brown Bullhead	3	2	3	3	3	2	5	13	13	2	2
Anchoa mitchilli	Bay anchovy	69	70	7	0	0	0	0	0	0	86	86
Anguilla rostrata	American Eel	1	3	2	0	0	0	0	0	1	2	2
Brevoortia tyrannus	Atlantic Menhaden	0	0	0	0	0	0	0	0	0	30	30
Carassius auratus	Goldfish	20	39	2	0	9	18	107	1	1	0	0
Carpiodes cyprinus	Quillback	9	19	2	0	0	0	0	0	0	72	72
Cyprinella spiloptera	Spotfin shiner	0	0	1	0	0	0	0	0	0	0	0
Cyprinus carpio	Carp	0	3	1	7	14	3	3	2	2	4	4
Dorosoma cepedianum	Gizzard Shad	5	1	3	0	0	0	0	50	50	52	52
Enneacanthus gloriosus	Bluespotted Sunfish	0	0	0	0	0	27	47	0	0	0	0
Erimyzon oblongus	Creek Chubsucker	0	0	0	0	0	0	0	1	1	0	0
Etheostoma olmstedi	Tessellated Darter	292	49	39	3	8	33	35	212	221	29	30
Fundulus diaphanus	Banded Killifish	1798	2382	2723	1387	1547	692	769	777	777	423	424
F. heteroclitus	Mummichog	53	152	174	16	16	62	62	20	20	14	14
Gambusia holbrooki	Mosquitofish	11	69	19	0	0	1	1	0	0	7	7
Hybognathus regius	Eastern Silvery Minnow	0	6	31	2	4	40	40	13	14	6	6
Ictalurus furcatus	Blue Catfish	12	4	4	1	1	6	6	57	57	93	93
Ictalurus punctatus	Channel Catfish	0	0	2	0	0	0	0	2	2	2	2
Lepisosteus osseus	Longnose Gar	0	0	3	1	1	1	1	0	0	0	0
Lepomis auritus	Redbreast Sunfish	0	0	1	2	2	0	0	0	0	0	0
Lepomis cyanellus	Green Sunfish	0	0	2	0	0	4	7	0	0	0	0

Lepomis gibbosus	Pumpkinseed	6	17	11	11	22	39	180	91	100	16	22
L. macrochirus	Bluegill	12	52	21	8	20	28	188	75	81	3	5
L. megalotis	Longear Sunfish	0	0	0	0	0	1	1	0	0	0	0
L. microlophus	Redear Sunfish	6	11	5	2	8	0	0	0	0	0	0
Lepomis sp.	unk. sunfish	5	12	5	27	85	50	169	0	2	1	4
Menidia beryllina	Inland Silverside	15	6	73	209	210	114	124	107	120	84	86
Micropogonias undulatus	Atlantic Croaker	1	0	0	0	0	0	0	0	0	0	0
Micropterus dolomieu	Smallmouth Bass	5	5	9	6	6	62	70	20	20	10	10
M. punctulatus	Spotted Bass	1	0	0	0	0	0	0	0	0	0	0
M. salmoides	Largemouth Bass	3	7	0	5	5	2	2	4	4	2	3
Micropterus sp.	unk. bass species	1	0	0	0	0	0	0	0	0	0	0
Morone americana	White Perch	574	107	693	19	57	393	439	667	675	1353	1364
Morone saxatilis	Striped Bass	2	0	2	1	5	5	8	2	2	6	6
Morone sp.	unk. perch/bass species	0	1	0	0	0	0	0	0	0	0	0
Moxostoma erythrurum	Golden Redhorse	0	0	0	0	0	0	0	0	0	3	3
M. macrolepidotum	Shorthead Redhorse	0	0	0	0	0	0	0	1	1	0	0
Notemigonus crysoleucas	Golden Shiner	2	3	13	2	2	2	2	5	5	1	1
Notropis hudsonius	Spottail Shiner	338	666	87	13	17	11	13	124	125	109	113
Perca flavescens	Yellow Perch	22	16	7	7	7	1	2	36	37	6	6
Pomoxis nigromaculatus	Black Crappie	0	0	4	0	1	0	0	3	3	3	4
Sander vitreus	Walleye	0	0	0	0	0	0	0	1	1	0	0
Strongylura marina	Atlantic Needlefish	2	4	3	0	0	9	9	1	1	2	2
Unidentified		2	0	0	0	0	0	0	0	0	0	0
Total		3798	3777	4210	1804	2125	1611	2294	2742	2794	3367	3402

H. Submersed Aquatic Vegetation: Comparison among Years

According to annual reports of the Virginia Institute of Marine Science (VIMS) SAV Monitoring Program (http://web.vims.edu/bio/sav/maps.html), virtually the entire surface area of the Hunting Creek embayment was covered with submersed aquatic vegetation during the first five years of this study (2013-2017). In 2018 there was a severe decline in SAV coverage. Furthermore, due to the frequent rainfall events and resulting poor water clarity, VIMS was unable to conduct the aircraft remote sensing so we were not able to make direct comparisons of 2018 coverage with 2016 and 2017. In 2019 VIMS was able to obtain aerial imagery which is shown in the Results section of this report. While this has not been completely analyzed, the aerial imagery appears to show no SAV growing in Hunting Creek. In 2016 and 2017 mapping of species was done via boat in association with the water quality mapping surveys and the results have been reported in the results section of these reports. In 2017 the native SAV species *Ceratophyllum demersum* was substantially more abundant than the exotic species *Hydrilla verticillata* in contrast to 2016 when they had a similar abundance. The boat transects studies in 2018 and 2019 confirmed the severe dieback.

I. Benthic Macroinvertebrates: Comparison among Years

River and Embayment Samples

Comparison among Years: As we expected, the macroinvertebrate community from the embayment of Hunting Creek has been dominated by Oligochaete worms across all sites and years (Figure 152). However, if Annelids are removed and we examine the other dominant taxon groups, we see a few different trends in dominant taxa between the three Hunting Creek sites across years (Figure 153). In general, AR2 is dominated by the insect larvae of Chironomids (midges), AR3 is dominated by Gastropods (mostly composed of the invasive Japanese mystery snails), and AR4 is dominated by Gammarid amphipods. AR2 is the site closest to the outflow from Hunting Creek, and across years, this site is mostly dominated by Chironomids (2013, 2014, 2018, and 2019), but some years Gammarid amphipods (2016, 2017) and Gastropods (2015) dominate (Figure 153). The AR4 site is within the mainstem of the Potomac River and has been consistently dominated by Gammarid amphipods over the past six years (2014-2019). Only in 2013 were the samples dominated by Chironomid insect larvae (Figure 153). The AR4 site also has the highest relative abundances of Bivalvia (mostly driven by the invasive Asian clam *Corbicula fluminea*) and Isopoda (Crustacean). AR4 receives higher water flow and movement, which many species of Bivalvia require, and may help explain why there are higher abundances of Bivalvia located closer to the Potomac River. The site with the most fluctuations in percent contributions of macroinvertebrate taxa was AR3, which is located in the middle of the embayment. In any given year, dominant macroinvertebrate groups change from Gastropods (2013, 2015, and 2016) to Gammarid amphipods (2014, 2017, and 2018) or Chironomid insect larvae (2019). AR3 is also the only site where Gastropods dominate the community composition frequently. This site is probably influenced by both the Potomac River, through the daily movement of the tidal freshwater water body, and by the outfall of Hunting Creek, which moves nutrients and sediments from terrestrial sources. Only in a few years do AR2 and AR3 share the same dominant taxa; in 2015, they were both dominated by Gastropods (mostly composed of the invasive Japanese mystery snails), in 2017 by Gammarid amphipods, and in 2019 by Chironomid

insect larvae. In comparison, AR4 seems to show different patterns of dominance than either of the other two sites further in the embayment. The relative importance of both of these waterbodies in determining benthic macroinvertebrate community structure probably varies annually due to climatic events such as high flows.

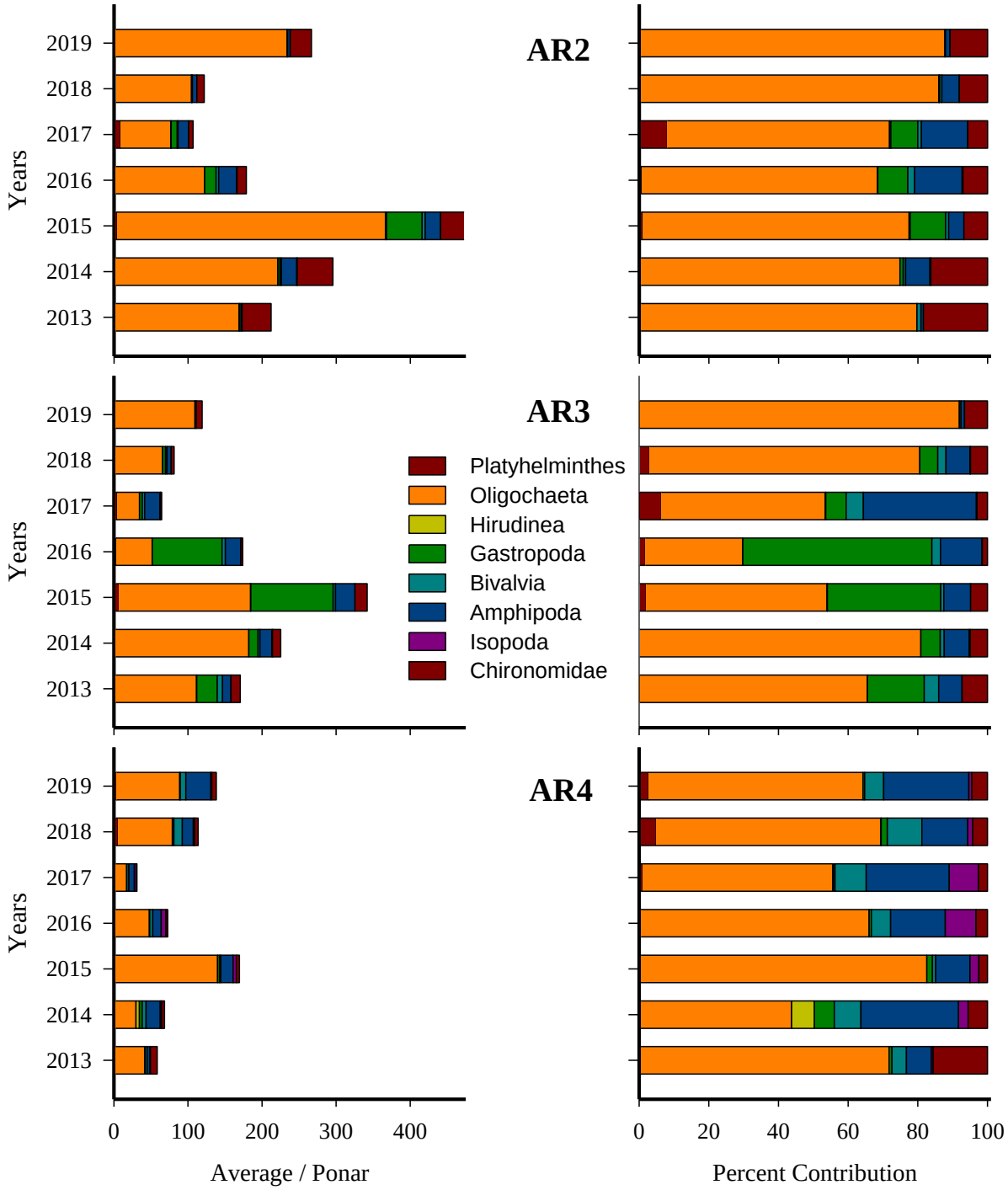

Figure 152. Average number per ponar sample (Left) and percent contribution (Right) of the eight dominant benthic invertebrate taxa in Hunting Creek embayment samples collected

between 2013 and 2019 separated by site and year. Note the dominance of the Oligochaeta (worms).

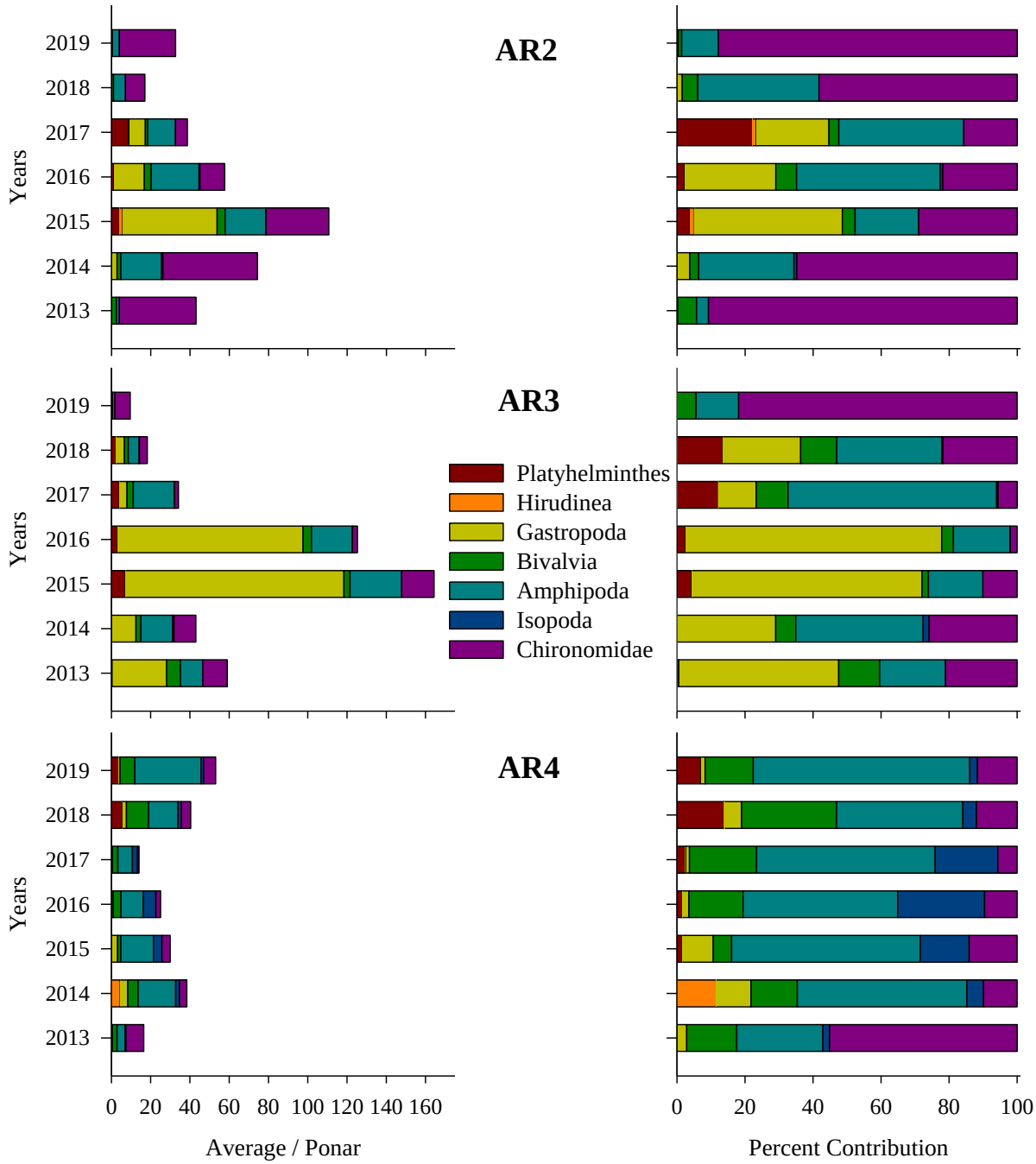

Figure 153. Without Oligochaeta, average number per ponar sample (Left) and percent contribution (Right) of the dominant benthic invertebrate taxa in Hunting Creek embayment samples collected between 2013 and 2019 separated by site and year.

Tributary Samples

Comparison among Years: We have been collecting benthic macroinvertebrate samples from the original six streams emptying into Hunting Creek since 2016 (Figure 154). Taylor Run and Timber Branch are excluded from the analyses here, as they were first sampled only in 2018. Looking across all sites and years, the taxon that dominates is the Insecta family Hydropsychidae. It is the dominant group 42% of the time across all years and sites. All sites sampled in 2019, except Indian Run and Turkeycock Run, were dominated by the Hydropsychidae (highest was 65% at Cameron Run, lowest 25% at Indian Run). Members within this family are netspinning caddisflies, which live in debris and under stones and spin concave silken nets that face upstream to capture floating or swimming prey. All of these sites have stones and gravel as habitat. The next most dominant group across all sites and years are members of the Insecta family Chironomidae (21% across all years and sites), known as midges. Chironomid larvae are filter-feeders and often live in tubes in the mud. None of the sites were dominated by Chironomdae in 2019, although Indian Run was dominated by Hydropsychidae during both 2016 (49%) and 2018 (94%). Other macroinvertebrate groups can dominate a site during particular years. For example, Oligochaetes (worms) were the most frequently encountered group at Cameron Run during 2017 and at Holmes Run-1 and Turkeycock Run in 2018. Turbellarians (flatworms) have only been the most dominant group at Holmes Run-1 during 2016 and at Turkeycock Run in 2019. Members of the Insecta family Philopotamidae and Baetidae are rarely the dominant group at a site; although Philopotamidae were the most frequently encountered group at Indian Run in 2019 (accounting for 43% of organisms counted). In general, across all years, Backlick Run and Cameron Run are dominated by Chironomidae. Holmes Run-2, Indian Run, and Turkeycock Run are dominated by Hydropsychidae, and Holmes Run-1 is dominated by Turbellarians. All of these sites are probably influenced by differences in the types and amounts of nutrients and sediments moving from terrestrial sources, the flow of water, and anthropogenic impacts to the system. The relative importance of a variety of abiotic factors on determining benthic macroinvertebrate community structure probably varies annually, and even monthly, due to climatic events. Therefore, site-level trends may become more apparent with continued annual sampling.

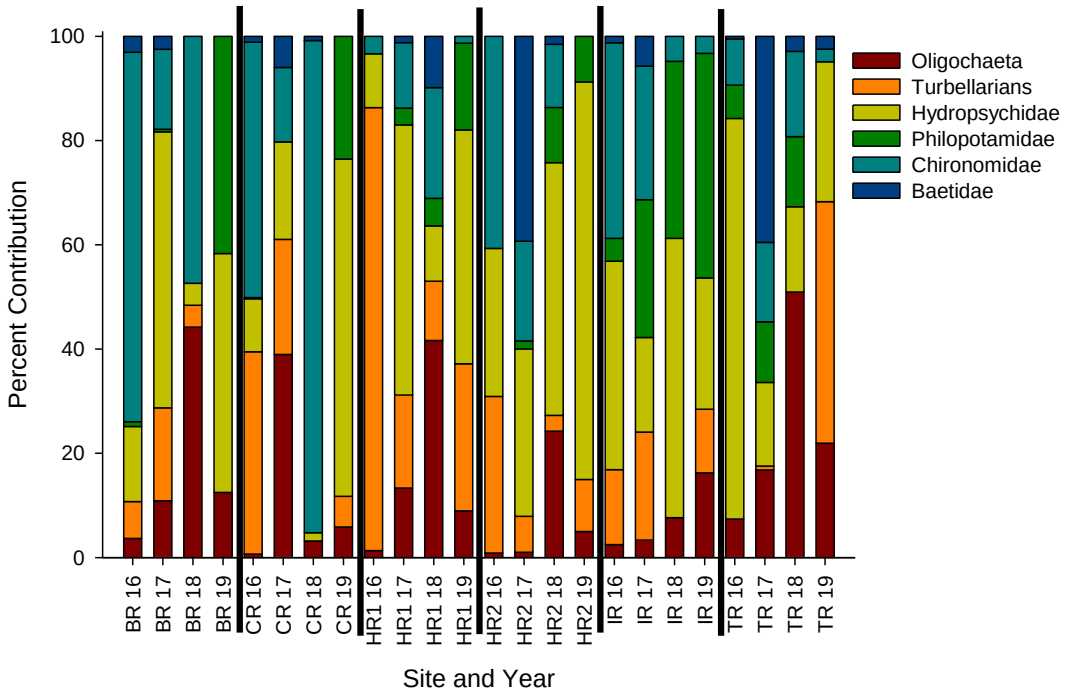

Figure 154. Percent contribution of of the six dominant benthic invertebrate taxa in tributary kick samples collected between 2016 and 2019 separated by site and year. Sites have been separated with black lines for ease of interpretation. Abbreviations for sites are noted in Table 16.

LITERATURE CITED

Bigelow, H.B. and W.C.Schroeder. 1953. Fishes of the Gulf of Maine. Fishery bulletin No. 74, Vol. 53. U.S. Government Printing Office. Washinton, D.C. 577 pp.

Carter, V., P.T. Gammon, and N.C. Bartow. 1983. Submersed Aquatic Plants of the Tidal Potomac River. Geological Survey Bulletin 1543. U.S. Geological Survey. 63 pp.

Chesapeake Bay Program. 2006 Ambient water quality criteria for dissolved oxygen, water clarity, and chlorophyll *a* for the Chesapeake Bay and its tidal tributaries. 2006 Addendum. Downloaded from Bay Program website 10/13/2006.

Cummings, H.S., W.C. Purdy, and H.P. Ritter. 1916. Investigations of the pollution and sanitary conditions of the Potomac watershed. Treasury Department, U.S. Public Health Service Hygienic Laboratory Bulletin 104. 231 pp.

Dahlberg, M.D. 1975. Guide to coastal fishes of Georgia and nearby states. University of Georgia Press. Athens, GA 187 pp.

Douglass, R.R. 1999. A Field Guide to Atlantic Coast Fishes: North America (Peterson Field Guides). Houghton Mifflin Harcourt, Boston. 368 pp.

Eddy, S. and J.C. Underhill. 1978. How to know the freshwater fishes. 3rd Ed. W.C. Brown Co. Dubuque, IA. 215 pp.

Froese, R. and D. Pauly (Eds.). 2012. Fish Base. World Wide Web electronic publication. www.fishbase.org, version (04/2012).

Hildebrand and Schroeder. 1928. Fishes of the Chesapeake Bay. U.S. Bureau of Fisheries

Bulletin 53, Part 1. Reprinted 1972. T.F.H. Publishing, Inc. Neptune, NJ. 388 pp.
Hogue, J.J, Jr., R.Wallus, and L.K. Kay. 1976. Preliminary guide to the identification of larval fishes in the Tennessee River. Technical Note B19. Tennessee Valley Authority. Knoxville, TN.
Islam, S. 2001. Seasonal dynamics of micro-, nanno-, and picoplankton in the tidal freshwater Potomac River in and around Gunston Cove. Ph.Dissertation. George Mason University. 127 pp.
Jenkins, R.E. and N.M. Burkhead. 1994. The freshwater fishes of Virginia. American Fisheries Society. Washington, DC. 1080 pp.
Jones, P.W., F.D. Martin, and J.D. Hardy, Jr. 1978. Development of fishes of the Mid-Atlantic bight. Volumes I-VI. Fish and Wildlife Service, U.S. Department of the Interior. FWS/OBS-78/12.
Kraus, R.T. and R.C. Jones. 2011. Fish abundances in shoreline habitats and submerged aquatic vegetation in a tidal freshwater embayment of the Potomac River. Environmental Monitoring and Assessment. Online: DOI 10.1007/s10661-011-2192-6.
Kelso, D.W., R.C. Jones, and P.L. deFur. 1985. An ecological study of Gunston Cove - 1984-85. 206 pp.
Lippson, A.J. and R.L. Moran. 1974. Manual for identification of early development stages of fishes of the Potomac River estuary. Power Plant Siting Program, Maryland Department of Natural Resources. PPSP-MP-13.
Loos, J.J., W.S. Woolcott, and N.R. Foster. 1972. An ecologist's guide to the minnows of the freshwater drainage systems of the Chesapeake Bay area. Association of Southeastern Biologists Bulletin 19: 126-138.
Lund, J.W.G., C. Kipling, and E.C. LeCren. 1958. The inverted microscope method of estimation algal numbers and the statistical basis of estimations by counting. Hydrobiologia 11: 143-170.
Mansueti, A.J. and J.D. Hardy, Jr. 1967. Development of fishes of the Chesapeake Bay region: an atlas of egg, larvae and juvenile stages: Part 1. Natural Resources Institute. University of Maryland. 202 pp.
Merritt, R.W. and K.W. Cummins. 1984. An introduction to the aquatic insects of North America. 2nd edition. Kendall/Hunt Publishing Co., Dubuque, IA. 722 pp.
Pennack, R.W. 1978. Fresh-water invertebrates of the United States. 2nd ed. Wiley-Interscience. New York, NY.
Schloesser, R.W., M.C. Fabrizio, R.J. Latour, G.C. Garman, G.C., B. Greenlee, M. Groves and J. Gartland. 2011. Ecological role of blue catfish in Chesapeake Bay communities and implications for management. American Fisheries Society Symposium 77:369-382.
Scott, W.B. and E.J. Crossman. 1973. Freshwater fishes of Canada. Bulletin 184. Fisheries Research Board of Canada. Ottawa, Canada. 966 pp.
Standard Methods for the Examination of Water and Wastewater. 1980. American Public Health Association, American Waterworks Association, Water Pollution Control Federation. 15th ed. 1134 pp.
Thorp, J.H. and A.P. Covich, eds. 1991. Ecology and classification of North American Freshwater Invertebrates. Academic Press. San Diego, CA. 911 pp.
Wetzel, R.G. 1983. Limnology. 2nd ed. Saunders. 767 pp.
Wetzel, R.G. and G.E. Likens. 1991. Limnological analyses. 2nd ed. Springer-Verlag. 391 pp.

Anadromous Fish Survey of Cameron Run – 2019

Final Report
By

Kim de Mutsert
Assistant Professor, Department of Environmental Science and Policy
Associate Director, Potomac Environmental Research and Education Center
George Mason University

Introduction

The anadromous fishes in the herring family (Clupeidae) live as adults in the coastal ocean, but return to freshwater creeks and rivers to spawn. In the mid-Atlantic region, four species are present: American Shad (*Alosa sapidissima*), Blueback Herring (*Alosa aestivalis*), Alewife (*Alosa pseudoharengus*), and Hickory Shad (*Alosa mediocris*). Two other herring family species are semi-anadromous and spawn in Potomac River tributaries. These are Gizzard Shad (*Dorosoma cepedianum*) and Threadfin Shad (*Dorosoma petenense*). Both are very similar morphologically and ecologically, but only *D. cepedianum* is found as far upriver on the Potomac River watershed as Hunting Creek/Cameron Run. Previous reports describe the history of herring populations in the Potomac River watershed (Jones et al. 2014).

The focus of the Cameron Run fish survey is river herring, the collective name of Blueback Herring and Alewife. River herring populations have declined drastically over their range, spurring conservation efforts since 1970, which have been intensified since 2005 with implementation of moratoria. Identifying all areas used as spawning habitat by Alewife and/or Blueback Herring is an important component of their conservation. Since 1988, George Mason University researchers have focused a monitoring program on the spawning of these species in other tributaries such as Pohick Creek, Accotink Creek, and, less regularly, Dogue Creek. With this study Cameron Run was added in 2013, which has not been monitored for presence of river herring or other anadromous species by either George Mason or other fisheries biologists before the start of this study (Jim Cummins, pers. comm.). Our 2013 survey provided the first confirmation of Cameron Run as River Herring spawning habitat (Alan Weaver, VDGIF, pers. comm.). Use of Cameron Run by river herring upstream from where the effluent of Alexandria Renew Enterprises enters Cameron Run signifies that the effluent does not deter river herring from using Cameron Run as spawning habitat. In 2014 we moved the collection site approximately 500 m downstream (still above the Alexandria Renew Enterprises effluent), which increased our catches, and allows us to estimate the size of the spawning population. The new location proved successful and will remain the collection site for any subsequent surveys.

Methods

We conducted weekly sampling trips from March 29 to May 31 in 2019. During each trip (when conditions allowed it) a hoop net was set with wings blocking the complete creek (referred to as block net) to collect adults swimming upstream, and ichthyoplankton nets were set to collect larvae floating downstream. Cross-section and flow were measured to calculate discharge, and physical parameters were measured using a handheld YSI. In some occasions, the conditions were not right to complete one or more procedures, Table 1 provides the information on which procedures were completed each sampling day in 2019. The sampling location was chosen to be upstream from the Alex Renew effluent, and downstream of the first dam in Cameron Run (Figure 1).

Figure 1. Sampling location Cameron Run.

Table 1. Procedures completed each sampling date. Note that the number of flow meter rotations rather than the minutes are used to calculate sampling volume of the plankton nets.

Date	Block Net	Plankton Nets	Flow Profile
3/29/19	24 hrs	10 mins	Yes
4/5/19	No net set	10 mins	Yes
4/12/19	24 hrs	24 mins	Yes
4/19/19	24 hrs	15 mins	Yes
4/26/19	24 hrs	20 mins	Yes
5/3/19	24 hrs	10 mins	Yes
5/10/19	24 hrs	20 mins	Yes
5/17/19	24 hrs	10 mins	Yes
5/23/19	24 hrs	25 mins	Yes
5/31/19	24 hrs	10 mins	Yes

Ichthyoplankton was collected by setting two conical plankton net with a mouth diameter of 0.25 m and a square mesh size of 0.333 mm in the stream current for 20 minutes. A mechanical flow meter designed for low velocity measurements was suspended in the net opening and provided estimates of water volume filtered by the net. The number of rotations of the flow meter attached to the net opening was multiplied by 5760 and then divided by 999999 to gain volume filtered (m3) based on the correction equations provided by the General Oceanics flow meter user manual (https://www.forestry-suppliers.com/Documents/588_msds.pdf). Larval density (#/m^3) per species was calculated using the following formula:

Larval density (#/m^3) = number of larvae in one sample (#) /volume filtered (m^3).

We collected 2 ichthyoplankton samples per trip, and these were spaced out evenly along the stream cross-section. Coincident with plankton samples, we calculated stream discharge rate from measurements of stream cross-section area and current velocity using the following equation:

Depth (m) x Width (m) x Velocity (m/s) = Discharge (m^3/s)

Velocity was measured using a handheld digital flow meter that measures flow in cm/s, which had to be converted to m/s to calculate discharge. Both depth and current velocity were measured at 12 to 20 locations along the cross-section. At each sampling trip other physical parameters of the creek were recorded as well (water temperature, dissolved oxygen, pH, and specific conductivity).

The ichthyoplankton samples were preserved in 70% ethanol and transported to the GMU laboratory for identification and enumeration of fish larvae. Identification of larvae was accomplished with multiple taxonomic resources: primarily Lippson & Moran (1974), Jones et al. (1978), and Walsh et al. (2005). River herring (both species) have semi-demersal eggs (tend to sink to the bottom) that are frequently adhesive. As this situation presents a significant bias, we are not treating egg abundance in the samples as a reliable estimate of egg abundance, and this is not used in population productivity estimates. We estimate total larval production (P) during the period of sampling by multiplying the larval density (m^{-3}) with total discharge (m^3) during the spawning period, which we assume is represented with our sampling period.

The block net was deployed once each week in the morning and retrieved the following morning (see Figure 2). Fish in the block net were identified, enumerated, and measured.

Since the net was set 24 hours per week during the spawning season, and the spawning season is estimated to last 10 weeks, we approximated total abundance of spawning river herring during the time of collection by extrapolating the mean catch per hour per species during the time the creeks were blocked over the total collection period as follows:

Average catch/24 hours * 1680 hours = total abundance of spawners

Our total collection period is assumed to be a good approximation of the total time of the spawning run of Alewife.

In response to problems with animals tearing holes in our nets in previous sampling experiences, we used a fence device in front of the mouth of the net that significantly reduces this problem. The device effectively excluded wildlife such as otters and turtles, while it has slots that allowed up-running fish to be captured.

Figure 2. Block net (hoop net with deer fencing attached to block the creek) deployed in Cameron Run. The hedging is angled downstream in order to funnel up-migrating herring into the opening of the net.

Results and Discussion

During the sampling period, we caught forty adult Alewife, ten adult Blueback Herring, three unknown Alosas (likely river herring), and a few non river herring species (Table 2). The abundance of river herring collected in 2019 was similar to last year, which signifies the consistent use of Cameron Run as spawning ground. The net is set in such a way that fishes need to swim upstream into Cameron Run to be caught in the net, which is a behavior associated with spawning. We collected adult Blueback Herring specimens this year again, of which we had only collected one in 2014 so far. Through the years after 2014, we did continuously positively identify Blueback Herring among the larvae collected, so we know the site is used as spawning grounds for Blueback Herring. Since the spawning populations is small and sampling variability high (for larval density, a small portion of the water column is sampled for 20 minutes per week), sampling over multiple years provides us with increasingly better estimates of the spawning population of Alewife and Blueback Herring in Cameron Run. The collection of adult Blueback Herring this year allows us to make an estimate of the size of the spawning population of Blueback Herring in addition to Alewife.

Table 2. Species collected in Cameron Run with the block net during weekly sampling from March 29-May 31, 2019. River herring are indicated by bold font.

Date	ScientificName	CommonName	Count
2019-04-12	***Alosa pseudoharengus***	**Alewife**	**17**
2019-04-19	***Alosa aestivalis***	**Blueback Herring**	**10**
2019-04-19	***Alosa pseudoharengus***	**Alewife**	**23**
2019-04-19	*Alosa sp.*	unk. Alosa species	3
2019-04-19	*Dorosoma cepedianum*	Gizzard Shad	1
2019-05-03	*Cyprinus carpio*	Carp	1
2019-05-03	*Lepomis auritus*	Redbreast Sunfish	1
2019-05-03	*Salmo trutta*	Brown Trout	1
2019-05-31	*Ameiurus natalis*	Yellow Bullhead	1
2019-05-31	*Lepomis macrochirus*	Bluegill	1
2019-05-31	*Notropis procne*	Swallowtail Shiner	1

We did not collect as many larvae in 2019 as we did in 2018, but the high ichthyoplankton density in 2018 was unprecedented. In the 2019 ichthyoplankton samples we could positively identify 211 Alewife larvae, and 10 Blueback Herring larvae (Table 3). The unidentified larvae (17) and especially the unidentified clupeids (31) could potentially include more Alewife and/or Blueback Herring larvae. We found 3 Gizzard Shad (*Dorosoma cepedianum*) larvae, which is a clupeid as well, which is much less than previous years. Gizzard Shad is usually the dominant clupeid. A few larvae of other species were present in the samples as well, including Goldfish (*Carassius auratus*), Eastern Silvery minnow (*Hybognathus regius*), Spottail Shiner (*Notropis hudsonius*), Comely Shiner (*Notropis amoenus*), Golden Shiner (*Notemigonus crysoleucas*), Common Carp (*Cyprinus carpio*), Inland Silverside (*Menidia beryllina*), and White Perch (*Morone americana*; Table 3).

Table 3. Larvae collected in Cameron Run. Herring larvae (river herring and other clupeids) are in bold. Fish larvae too damaged for identification to species level were identified at the highest level possible.

Date	ScientificName	Count	Volume	AvgDensity
2019-03-29	Eggs	21	26.492	0.841
2019-03-29	Unidentified	1	26.492	0.048
2019-04-05	***Alosa aestivalis***	**3**	**35.022**	**0.084**
2019-04-05	***Alosa pseudoharengus***	**143**	**35.022**	**4.224**
2019-04-05	***Clupeidae***	**26**	**35.022**	**0.701**
2019-04-05	Eggs	105	35.022	3.320
2019-04-05	Unidentified	7	35.022	0.263
2019-04-12	***Alosa pseudoharengus***	**7**	**0.107**	*****
2019-04-12	Eggs	7	0.107	*

2019-04-12	Unidentified	1	0.107	*
2019-04-18	***Alosa aestivalis***	**5**	**18.043**	**0.260**
2019-04-18	***Alosa pseudoharengus***	**18**	**18.043**	**1.002**
2019-04-18	*Carassius auratus*	1	18.043	0.059
2019-04-18	***Clupeidae***	**2**	**18.043**	**0.111**
2019-04-18	*Cyprinidae*	1	18.043	0.059
2019-04-18	***Dorosoma cepedianum***	**2**	**18.043**	**0.104**
2019-04-18	Eggs	113	18.043	6.184
2019-04-18	*Hybognathus regius*	2	18.043	0.104
2019-04-18	*Morone americana*	1	18.043	0.052
2019-04-18	Unidentified	6	18.043	0.341
2019-04-25	***Alosa pseudoharengus***	**4**	**0.088**	*****
2019-04-25	*Cyprinus carpio*	1	0.088	*
2019-04-25	Eggs	9	0.088	*
2019-05-02	***Alosa aestivalis***	**1**	**12.373**	**0.041**
2019-05-02	***Alosa pseudoharengus***	**6**	**12.373**	**NA**
2019-05-02	***Clupeidae***	**1**	**12.373**	**0.041**
2019-05-02	Eggs	8	12.373	**
2019-05-02	*Menidia beryllina*	2	12.373	0.081
2019-05-02	*Notropis amoenus*	2	12.373	**
2019-05-02	*Notropis hudsonius*	6	12.373	**
2019-05-02	Unidentified	2	12.373	**
2019-05-10	***Alosa pseudoharengus***	**1**	**0.113**	*****
2019-05-10	***Clupeidae***	**1**	**0.113**	*****
2019-05-10	***Dorosoma cepedianum***	**1**	**0.113**	*****
2019-05-10	Eggs	2	0.113	*
2019-05-17	***Alosa aestivalis***	**1**	**4.620**	******
2019-05-17	***Alosa pseudoharengus***	**31**	**4.620**	******
2019-05-17	***Clupeidae***	**1**	**4.620**	**0.112**
2019-05-17	Eggs	9	4.620	**
2019-05-23	*Cyprinus carpio*	1	0.088	*
2019-05-30	***Alosa pseudoharengus***	**1**	**22.816**	**0.064**
2019-05-30	*Carassius auratus*	1	22.816	0.033
2019-05-30	*Cyprinidae*	1	22.816	0.033
2019-05-30	Eggs	49	22.816	2.182
2019-05-30	*Notemigonus crysoleucas*	1	22.816	0.033

*The flow velocity in Cameron Run was too low at this date for the flow meter to function properly; therefore, volume sampled is likely an underestimate, and larval density not calculated. **The flow velocity in one plankton net was abnormally low, and this taxa of larvae was only found in that net.

We measured creek discharge and other physical parameters at the same location and times where ichthyoplankton samples were taken, which was about 100 m downstream from the block net (Table 4). Mean creek discharge was higher than last year but in the same range as previous years. Mean discharge in 2019 was 0.638 $m^3 s^{-1}$, ranging from 0.05 $m^3 s^{-1}$ to 3.43 $m^3 s^{-1}$. There was one date when discharge could not be calculated because the flow was so low that the flow meter did not function properly. Water temperature was above 10 °C on all sampling day, which is the minimum temperature at which river herring spawning is observed. The first sampling date where we found Alewife (larvae) was April 5, when the average temperature had been just above 10 for about a week. Dissolved oxygen (DO), and pH were in the benign range for occurrence of river herring throughout the sampling period (Table 4).

Table 4. Physical parameters measured at Cameron Run during each sampling week.

Date	Discharge $m^3 s^{-1}$	WaterTemp °C	Spcond $\mu S\ s^{-1}$	DO mg L^{-1}	pH
2019-03-29	0.91	10.7	0.22	14.92	7.89
2019-04-05	0.84	10.8	0.47	14.65	8.25
2019-04-12	0.05	15.2	0.46	15.03	8.80
2019-04-19	3.43	18.2	0.48	11.71	7.67
2019-04-26	0.05	17.8	0.47	12.10	7.73
2019-05-03	0.23	23.1	0.45	10.13	7.85
2019-05-10	NA	20.5	0.41	9.86	8.04
2019-05-17	0.28	17.6	0.39	10.68	7.79
2019-05-23	0.29	20.2	0.42	10.62	7.78
2019-05-31	0.29	28.4	0.43	8.73	8.34

NA = flow too low to calculate discharge

During the sampling period of 10 weeks, the total discharge was estimated to be on the order of 3.9 million cubic meters (Table 5). This is higher than last year but comparable to previous years. Given the observed mean densities of larvae, the total production of river herring larvae was estimated at approximately 2.2 million for Cameron Run (Table 5). Note that the estimate is based on a small sample (0.0002 % of the total discharge). With 40 adult Alewife and 10 adult Blueback Herring collected, and extrapolating over period of the spawning run as explained in the methods, this could mean that the river herring spawning population in 2019 was the size of 389 individuals (similar to last year).

Table 5. Estimation of river herring (alewife and blueback herring) larval production and spawner abundance from Cameron Run during spring 2019.

Parameter	Cameron Run
Mean discharge (m^3 s^{-1})	0.638
Total discharge (m^3)	3,858,275.833
Total plankton nets volume sampled (m^3)	119.760
Mean Alosa larvae density (m^{-3})	0.567
Total river herring production (# larvae)	2,189,069.395
Total adult river herring (#)	388.889

Conclusions

After finding that Cameron Run is used as river herring spawning habitat with just one adult river herring and seven larvae in 2013, we were able to confirm this finding by collecting more river herring adults and larvae from 2014-2019 (Figure 3). By moving our sampling site approximately 500 m downstream in 2014 we have found a better sampling location. Even further downstream Cameron Run becomes too deep and wide for our sampling strategy.

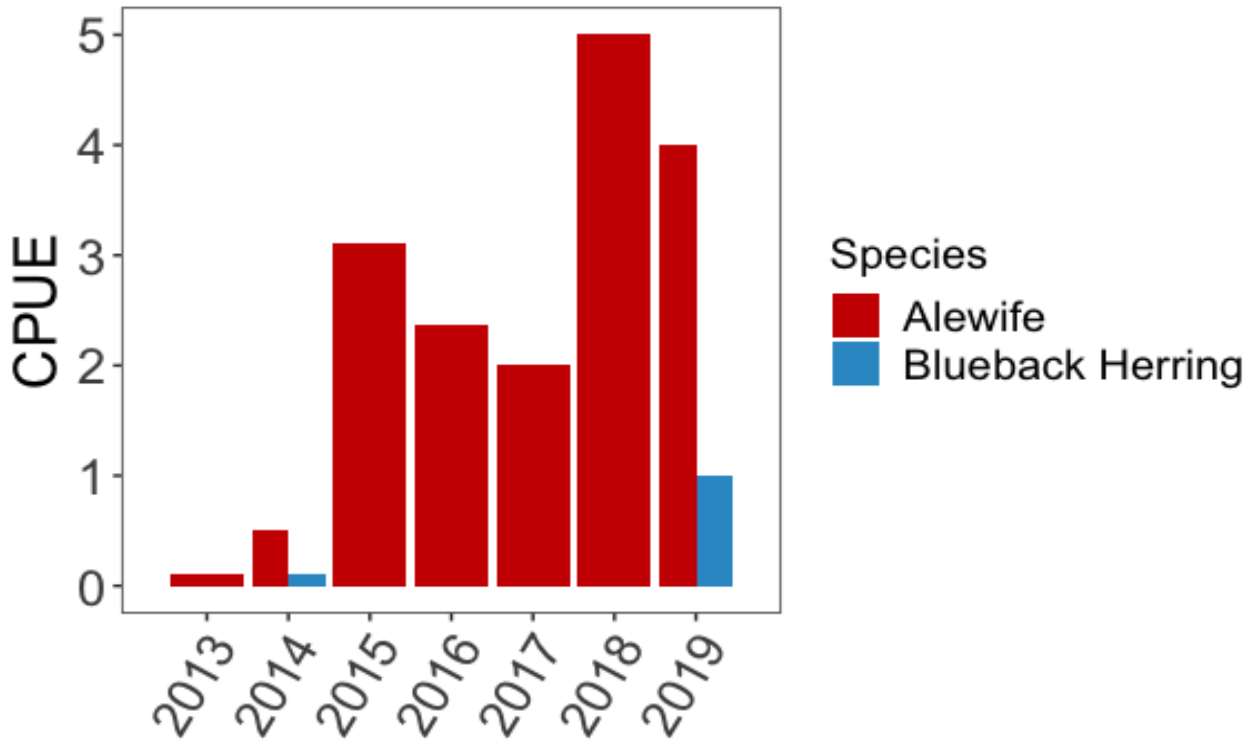

Figure 3. Catch per Unit Effort of Alewife and Blueback Herring (number of individuals per block net) collected with the block net in each year.

The finding of river herring adults and larvae in an area above the outflow of the Alexandria Renew Enterprises wastewater reclamation facility signifies that the water of Cameron Run is clean enough to use as spawning habitat for these species of concern. These finding will not affect AlexRenew, but will affect the terms of construction permits in and around Cameron Run (i.e. some construction activities may be restricted by the Virginia Department of Game and Inland Fisheries (VDGIF) during the annual spawning period (mid-March to mid-May) of river herring (Alan Weaver, VDGIF, pers. comm.).

Although the current evidence suggests that the importance of Cameron Run may be marginal to Alewife and Blueback Herring populations, it is important to recognize that marginal habitats may sustain fish populations during periods of declining abundance and low recruitment (Kraus and Secor 2005). Due to the moratorium on river herring set in place bay-wide in 2012, annual estimation of spawner abundance should be a continued priority for annual monitoring of this and other Potomac River tributaries. The peak in abundance in 2015 was 3 years after the 2012 moratorium, which is about the time it takes for Alewife to grown to adulthood and return to their spawning grounds. This peak has been seen in other tributaries to the Potomac River as well (Jones and De Mutsert 2016) and could signify the effect of the release from the fishery. This effect was not seen throughout Virginia however (Alan Weaver, VDGIF, pers. comm.), and was not maintained to the same level in the subsequent years (2016 and 2017). Anadromous fishes typically exhibit strong year-class fluctuations, and we expected a high return of river herring in 2018 if the offspring of the successful 2015 year-class was able to return. We indeed saw even higher numbers return in 2018, which is a sign that the high abundance in 2015 may have given a lasting boost to the population. It is a good sign that the same level of return spawners was registered in 2019, and that adult Blueback Herring were among the river herring collected this year. Additional years of data collection (at least through 2 generation lengths ~ a decade) will allows us to see if this cycle continues into the future and helps with the slow built-up of river herring populations.

Literature cited

General Oceanics. ND. General Oceanics digital flowmeter mechanical and electronic operators manual. https://www.forestry-suppliers.com/Documents/588_msds.pdf.

Jones, P. W., F. D. Martin, and J. D. Hardy, Jr. 1978. Development of fishes of the Mid-Atlantic Bight: an atlas of egg, larval, and juvenile stages, volume 1. Acipenseridae through Ictaluridae. U.S. Fish and Wildlife Service, FWS/OBS-78/12.

Jones, R. C., De Mutsert, K., and G. D. Foster. 2014. An Ecological Study of Hunting Creek-2013. Final report to Alexandria Renew Enterprises, Alexandria, VA. 123 p.

Jones, R. C. and De Mutsert, K. 2016. An Ecological Study of Gunston Cove-2015. Final report. Potomac Environmental research and education Center, Fairfax, VA.

Kraus, R. T. and D. H. Secor. 2005. Application of the nursery-role hypothesis to an estuarine fish. Marine Ecology Progress Series 290:301-305.

Lippson, A. J., and R. L. Moran. 1974. Manual for the identification of early developmental stages of fishes of the Potomac River estuary. Maryland Department of Natural Resources, Baltimore.

Walsh H.J., L.R Settle, and D.S. Peters. 2005. Early life history of blueback herring and alewife in the lower Roanoke River, North Carolina. Transactions of the American Fisheries Society 134:910-926.

ESCHERICHIA COLI ABUNDANCES IN HUNTING CREEK/CAMERON RUN AND ADJACENT POTOMAC RIVER - 2019

Final Report
By

Benoit Van Aken
Associate Professor, Department of Chemistry & Biochemistry
George Mason University

Introduction

During 2019, in connection with examination of ecological and chemical parameters, a study of *Escherichia coli* in waters in the areas of Hunting Creek/Cameron Run and adjacent waters of the Potomac River was continued with samples being collected at 15 sites. Eleven sites sampled in the prior years (2016 – 2018) included AR1, AR2, AR3, AR4, AR10, AR11, AR12, AR13, AR21, AR23, and AR30. Note that AR11 and AR22 were not accessible in 2018 and AR22 was not accessible in 2019 due to existence of large-scale construction projects including renovations at Lake Cook (AR11, 2018) and earthwork along the stream bank of Huntington Park (AR22, 2018 and 2019). In addition to these 11 sites, four new sites were sampled in 2019 including two off-shore sites: AR31 (Potomac Mainstem upstream of Outfall 001) and AR32 (Potomac Mainstem downstream of Outfall 001), and two shore sites: AR33 (Hooffs Run at Linden St) and AR34 (Hooffs Run at Alex Renew).

This work provides current microbiological water quality information in these aquatic ecosystems adjacent to and receiving water from the wastewater reclamation facility operated by Alexandria Renew Enterprises (Alex Renew). The research continues to determine if these waters are impaired under the Clean Water Act in terms of their uses as designated by the Commonwealth of Virginia.

The text of the Virginia Water Quality Standards (9 VAC 25-260-10) is as follows:

"All state waters, including wetlands, are designated for the following uses: recreational uses, e.g., swimming and boating; the propagation and growth of a balanced, indigenous population of aquatic life, including game fish, which might reasonably be expected to inhabit them; wildlife; and the production of edible and marketable natural resources, e.g., fish and shellfish." (VSWCB 2011)

Section 9VAC25-260-170 of the Virginia Water Quality Standards (amended as of January 2011) specifies the bacteriological criteria for *E. coli* that apply to primary contact recreational use surface waters:

1. "*E.coli* bacteria shall not exceed a monthly geometric mean of **126 CFU/100 mL** in freshwater […]."

2. "Geometric means shall be calculated using all data collected during any calendar month with a minimum of four weekly samples."

3. "If there are insufficient data to calculate monthly geometric means in freshwater, no more than 10% of the total samples in the assessment period shall exceed **235 *E.coli* CFU/100 mL** […]."

5. "For beach advisories or closures, a single sample maximum of **235 *E.coli* CFU/100 mL** in freshwater […] shall apply." (VSWCB 2011b)

Of all of the conditions in rivers and streams which can lead to a listing of 'impaired water', the one criterion that, more than any other, results in such a listing is coliform bacteria or *E. coli* abundances (USEPA 2014). Both Hunting Creek and Cameron Run were listed as impaired under the Clean Water Act for exceedances of Virginia's water quality criterion for *E. coli* bacteria (VADEQ, 2012), although the earlier impairment listing of Hunting Creek was based on the then applicable fecal coliform criterion (VADEQ 2010). The fecal coliform criterion was subsequently changed to *E. coli* based on the understanding that this subset of fecal coliforms is more specifically associated with fecal material from humans and other warm-blooded animals. The U.S. EPA (USEPA 2012) recommended and the Commonwealth of Virginia accepted *E. coli* as the better indicator of health risk related to recreational water contact. That is the current microbiological water quality criterion.

Due to this impairment, total maximum daily load (TMDL) allocations for *E. coli* were developed for both of these watersheds in late 2010 (VADEQ 2010). The City of Alexandria is working toward achieving the bacteriological criteria for these waters through a variety of programs including a storm water program, minimizing combined storm water sewer system overflows and eventually eliminating those discharges, reductions in pet waste sources, and discovery of illegal discharges. Because the sources of *E. coli* to water systems are many and varied, including wildlife sources which are generally not controlled unless at a nuisance level, continued monitoring of *E. coli* in these waterways is an important aspect of maintaining and improving water quality. The results reported here add to the understanding of the microbiological quality of these systems.

Methods

Sampling Regime

Samples were collected on 11 dates from 18 April 2019 to 17 September 2019 (**Table EC1**). Water samples were collected at 15 stations on each sampling day. Station identifiers and locations are shown in **Table EC2** (the map of EC sample station is provided in Appendix A, **Figure A1**). Samples were collected in clean, steam sterilized (autoclaved), 1-liter, wide-mouth polypropylene bottles. Nine of the stations were approached from the shore: AR1, AR11, AR12, AR13, AR21, AR23, AR30, AR33, and AR34, and 6 stations: AR2, AR3, AR4, AR10, AR31, and AR32, were sampled from a

small, outboard-powered research vessel. Among the shore stations, stations AR11, AR21, and AR30 were sampled from the shore without wading into the stream. At these stations, samples were simply collected as grab samples using the 1-liter bottle. Sampling was operated in the most active flow zone that could be reached from the shore. At station AR1, samples were collected remotely using a sterilized, 1- or 4-liter round, polypropylene wide-mouth bottle fitted with a harness and nylon line. The sample bottle was deployed from atop the George Washington Parkway Bridge over Hunting Creek on the downstream side approximately at mid-span. At stations AR23 and AR34, samples were also collected remotely using a sterilized, 1- or 4-liter round, polypropylene wide-mouth bottle fitted with a harness and nylon line. The sample bottle was deployed from the shore and thrown to about 5-10 yards into the water. Collection of three shore-approached samples required wading in the streams. At station AR12, we waded into the water downstream of the collection site to approximately midstream, waited for the current to carry away any disturbed sediment and then collected the sample by submerging the 1-liter bottle upstream of the sample collector. At station AR 13, the bottom of the stream at the approach site is paved with concrete. At this site, we waded to approximately midstream and to the edge of the concrete paved segment. After waiting for any disturbed sediment to be washed away, the sampled was collected by submerging the sterile 1-liter bottle in the stream. At station AR 33, the bottom of the stream is entirely paved with concrete. At this site, we waded (or simply walked when the water flow was low) to approximately midstream. After waiting for any disturbed sediment to be washed away, the sampled was collected again by submerging the sterile 1-liter bottle in the stream. Boat-approached sites, AR 2, AR3, AR4, AR10, AR 31, and AR32, were sampled by submerging the collection bottles over the side of the research vessel as the vessel coasted on final approach to the station. In all cases, the bottles were rinsed twice with sample water and then the final sample was collected. Immediately after collection, samples were placed in dark, insulated containers packed with ice. Samples were returned to the George Mason University at the Potomac Science Center, where they were processed within about 5 hours of collection.

Table EC1. Sampling Dates

Date	Date Code for Figures
18-Apr-19	20190418
8-May-19	20190508
22-May-19	20190522
5-Jun-19	20190605
19-Jun-19	20190619
3-Jul-19	20190703
17-Jul-19	20190717
1-Aug-19	20190801
14-Aug-19	20190814
3-Sep-19	20190903
17-Sep-19	20190918

Table EC2. Station identifiers, locations and access type

Station ID	Access Type	Location Description
AR 1	Shore	Hunting Cr just above GW Parkway Bridge
AR 2	Boat	Northern portion of Hunting Cr.
AR 3	Boat	Southern portion of Hunting Cr.
AR 4	Boat	Potomac River Channel off Hunting Cr.
AR 10	Boat	Potomac River North of Wilson Bridge
AR 11	Shore	Outlet of Lake Cook
AR 12	Shore	Last Riffle of Cameron Run near Beltway crossing
AR 13	Shore	Hoff's Run upstream of Alex renew outfall
AR 21	Shore	South side of Cameron Run downstream from Lake Cook drain
AR 22	Shore	South side of Cameron Run at north end of Fenwick Dr. – NOT SAMPLED in 2018
AR 23	Shore	South side of Cameron Run across from AlexRenew outfall
AR 30	Shore	Cameron Run upstream near metro rail bridge
AR 31	Boat	Potomac Mainstem upstream of Outfall 001
AR 32	Boat	Potomac Mainstem downstream of Outfall 001
AR 33	Shore	Hooffs Run at Linden St
AR 34	Shore	Hooffs Run at Alex Renew

Analytical Method

Determination of the abundance of *E. coli* was performed following the EPA Method 1603 (*Escherichia coli* in Water by Membrane Filtration Using Modified Membrane-Thermotolerant *Escherichia coli* Agar–Modified mTEC). This is an EPA-approved method for determining abundance of *E. coli* in fresh water. It is a one-step modification of the EPA Method 1103.1. It is based on *E. coli* production of β-D-glucuronidase and the consequent metabolism of 5-bromo-6-chloro-3-indolyl-β-D-glucuronide in the medium to glucuronic acid and a red- or magenta-colored product (USEPA 2009).

For this work, mTEC medium (Fisher) was prepared in our laboratory at George Mason University (Potomac Science Center) shortly before each sampling trip. The medium was prepared as per package directions, and ~5 mL of the molten medium was placed aseptically into sterile, 50-mm Petri dishes with tight fitting lids. Prepared medium was stored at 4°C in the dark until use. Phosphate buffered saline (PBS) was prepared as per Method 1603 and autoclave sterilized. PBS was added to smaller samples (1.0 mL and 10 mL) to make volumes up to at least 20 mL before filtration. This aids in distributing bacteria uniformly across the membrane surface. The PBS was also used for blank controls.

Upon return to the laboratory, samples were processed immediately. Sterile, gridded, 0.45 µm membrane filters were aseptically positioned, grid side up, on the base of a

sterile, polycarbonate filter holder, and the filter tower was placed in position on a vacuum flask over the filter and base. Samples were shaken vigorously to assure complete mixing and appropriate volumes (1.0 mL, 10.0 mL, and 100.0 mL) of sample were added to each of three replicate filter systems. Before adding the two smaller volume aliquots to the filter funnels, sufficient PBS was added to make the final volume approximately 20 mL. Samples were then filtered with vacuum (approximately 10 in. Hg). Each filter was then removed from the filter holder base aseptically with sterile, blunt-tipped forceps and placed onto the surface of the mTEC agar without trapping any air bubbles beneath the filter. After replacing the Petri dish tops the plates were incubated in a 35°C incubator for 2 ± 0.5 hours. They were then removed, placed in tightly closed double, zipper-locked plastic bags and submerged in a water bath at 44.5°C ± 0.2°C for 22 ± 2 hours. Blank controls consisting of 100 mL of PBS were checked each time samples were processed. Generally, no *E. coli* were detected in these blank controls, although occasionally controls had one or two presumptive *E. coli* colonies. The data were not corrected for this low background as it was generally far less than 1 percent of the abundances on countable plates.

After the water bath incubation, samples were retrieved and observed immediately for typical red or magenta *E. coli* colonies. All Petri dishes (3 volumes x 3 replicates = 9 Petri dishes per sample) were observed. Although only dilutions yielding colony counts between 20 and 80 needed to be enumerated, we generally recorded colonies for each countable dilution. Often, however, when *E. coli* were too abundant, the higher volume samples were not countable due to overgrowth. Calculation of final *E. coli* abundances followed the procedures described in Appendix B of the EPA Method 1603 (USEPA 2009). Since there were triplicate analyses of each dilution, the colony count per Petri dish was separately converted to *E. coli* abundance per 100 mL and then the triplicates were averaged. If no dilution gave individual counts between 20 and 80, the nearest count was selected and used for the final calculation as described in appendix B of the EPA Method 1603.

Results & Discussion

In 2019, typical *E. coli* colonies were observed in some dilution(s) in every sample tested, with the exception of one sample (AR10 collected on August 1, where no colonies were observed; *E. coli* number was reported as 'less than 1 count/100 mL'). There is a point estimate of *E. coli* per 100 mL for each sample. *E. coli* abundances grouped by station are shown in **Figure EC1** and *E. coli* abundances grouped by sampling date are shown in **Figure EC3** (tabular data is in Appendix A, **Table A1** and **A2**).

Since there was no situation in which 4 weekly samples were collected in a calendar month, the 235 per 100 mL (more than 10%) criterion is applicable in determining impairment.

Data Grouped by Station

In 2019, thermotolerant *E. coli* abundances grouped by station exceed the 235 per 100 mL 'impaired water' criterion *at all stations* at some point during the sampling period, as they did in 2015, 2016, 2017, and 2018 (**Figure EC1**). This is in contrast to observations made in a prior monitoring campaigns, 2014, when, at 4 of the 8 stations sampled (AR3, AR4, AR10, and AR11), *E. coli* abundances never exceeded 235 per 100 mL. In addition, the majority of the stations (8 over 15) sampled throughout the spring and summer 2019 showed exceedance of 235 per 100 mL the majority of the time: 100% of the time for AR13 and AR33, 90% of the time for AR34, 75% of the time for AR21, and 65% of the time for AR1, AR12, AR23, and AR30. On the other hand, 7 stations exceeded that value more sporadically: 35% of the time for AR2, 30% of the time for AR3 and AR11, 20% of the time for AR32, and less than 10% of the time for AR4, AR10, and AR31. In summary, in 2019, exceedance of 235 CFUs per 100 mL was observed more than 10% of the time at 12 over 15 stations. The three stations with observed exceedance less than 10% of the time are all off-shore, in the Potomac River at a distance form Hunting Creek discharge point.

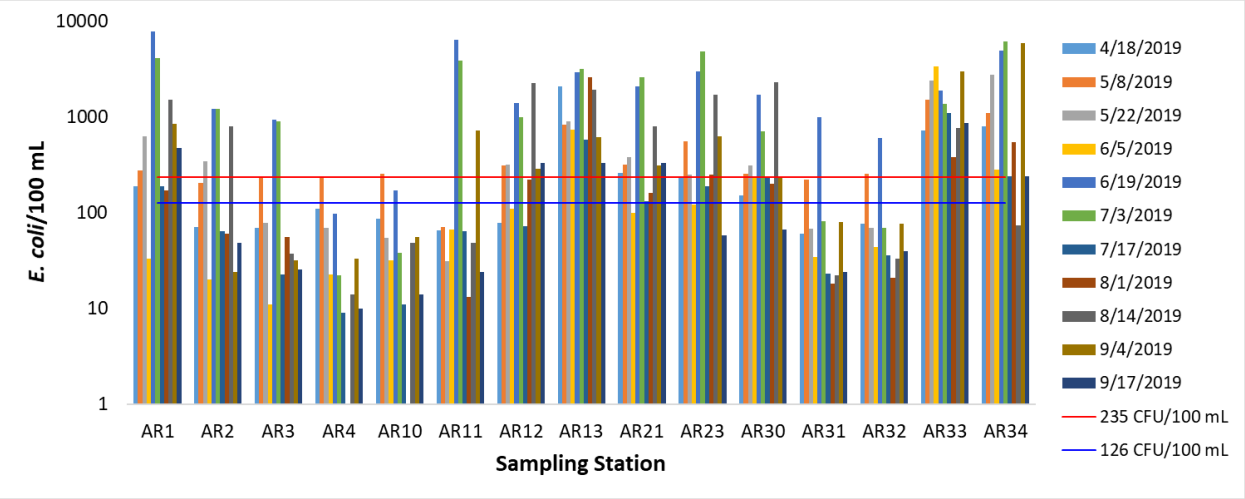

Figure EC1. *E. coli* abundance per 100 mL in Cameron Run, Hunting Creek, and the adjacent Potomac River grouped by stations from April to September 2019. The blue horizontal line represents the *E. coli* criterion for the geometric monthly mean allowable abundance (126 per 100 mL), and the red line represents the criterion for allowable abundance in the absence of four monthly samples (235 per 100 mL).

E. coli abundance at station AR13, Hooffs Run, which exceeded 235 per 100 mL on all 11 dates from April through September in 2015, 2016, and 2017, and on 10 dates in 2018, showed also exceedance on all the dates sampled in 2019. *E. coli* abundance at station AR13 averaged 1,515 ± 1,045 counts per 100 mL and had a maximum of 2,933 counts per 100 mL on June 19, 2019. Stations AR33 and AR34, on Hooffs Run which were not sampled in the prior years, also showed high frequency of exceedance and high counts, with an average of 1,572 ± 971 and 2,094 ± 2,428 counts, respectively.

Figure EC2 shows the box plots of *E. coli* numbers per 100 mL as arrayed by site. The pattern of statistical metrics is very similar to the one obtained in 2018 (with the

exception of AR11 and AR31 to AR34, which were not monitored in 2018), showing the consistency of our analyses. AR1 is Hunting Creek at the GW Parkway Bridge. AR2 to AR10 are off-shore stations in the Potomac River (**Figure A1**). AR2 and AR3 are in the Hunting Creek embayment. AR4 is in the Potomac River channel just east of the Hunting Creek embayment. AR10 is a Potomac River site upstream of the Wilson Bridge. AR11, AR21, and AR23 are in tidal Cameron Run. AR12 and AR30 are in the flowing part of Cameron Run. AR13 is in Hooffs Run, a tributary of Cameron Run. The new stations are AR31 and AR32, which are off-shore sites intended to bracket the CSO outfall of Alexandria in the Orinoco Bay, and AR 33 and 34 which are in upstream and downstream station AR13 in Hooffs Run. **Figure EC2** reveals the large variability of the numbers recorded at each station, with extremes spanning several orders of magnitude. The highest *E. coli* numbers on average were observed in AR13, AR33, and AR34 in Hooffs Run, which flows into Hunting Creek nearby the AlexRenew effluent outfall. This observation suggests that the main contributor of *E. coli* in Hunting Creek is Hooffs Run (**Photo EC1**), and not the Alex Renew effluent. The lowest numbers were the off-shore stations in the Potomac River, AR2, AR3, AR4, AR10, AR31, and AR32. We observed a steady decrease of the numbers from AR1 to AR4, suggesting that Hunting Creek is a significant source of *E. coli* to the Potomac River, even though not necessarily from the Alex Renew effluent. The highest off-shore *E. coli* numbers were at station AR10, AR31, and AR32, which are in the Potomac River channel, upstream of Hunting Creek discharge, which suggests upstream sources of contamination, possibly including the CSO outfall of Alexandria. AR1 and AR23, which are both potentially impacted by Hooffs Run/Cameron Run and the Alex Renew outfall showed the second highest numbers. However, interestingly AR21, which was above tidal influence, had rather high numbers as well, perhaps due to runoff from the Lake Cook area. The farthest upstream station, AR30, was also higher than the embayment-river stations.

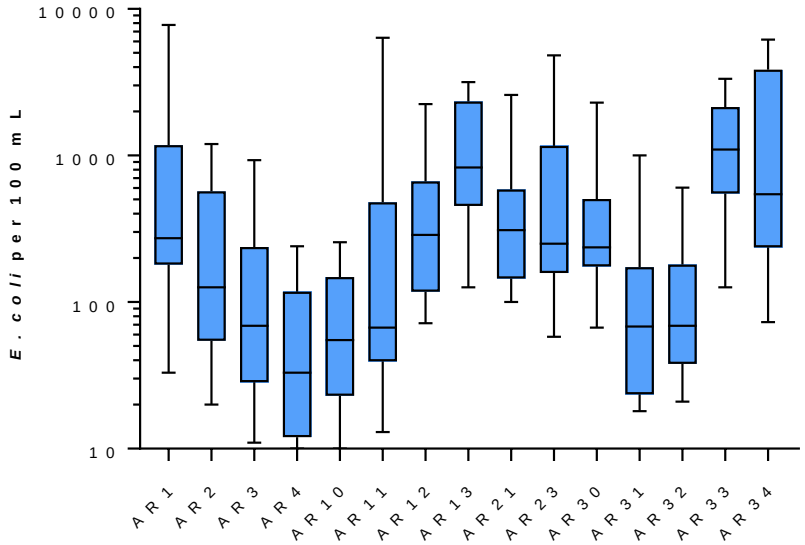

Figure EC2. Box plots of *E. coli* abundance per 100 mL for each site in Cameron Run, Hunting Creek, and the adjacent Potomac River over the sampling period. The bars show the minimum and maximum counts, the boxes show the 25 and 75-percentile, and the median.

Photo EC1. Hooffs Run at station AR33, at the level of Linden Street, upstream AR13.

Data Grouped by Date

E. coli abundance grouped by dates showed that environmental and/or climatic conditions may have played an important role on some sampling dates, resulting in large *E. coli* numbers and exceedance of the 235 CFUs per 100 mL (**Figure EC3** and **EC4**). The highest average *E. coli* numbers and higher exceedance of 235 CFUs per 100 mL were observed on June 19 and July 3, which were also the days when the highest discharge of Cameron Creek (40.4 and 29.6 cf/sec) and 3-day precipitation (5.5 and 1.1 cm) and 7-day (8.2 and 1.2 cm) precipitation were recorded in the area (discharge data are from USGS, https://waterdata.usgs.gov/va/nwis/current/?type=flow and precipitation data are from National Airport). A good correlation was observed between Cameron Run discharge and 3-day precipitation and average *E. coli* abundance over all stations (Pearson's correlation coefficient, r = 0.64 and 0.81, respectively). However, it is noteworthy that, on a date-by-date basis, the relationship between *E. coli* numbers and rainfall/discharge data is not very consistent: for instance, the second highest Cameron Run discharge value (36.1 cf/sec) was recorded on May 8, when the average *E. coli* numbers were relatively low (442 CFUs per 100 mL).

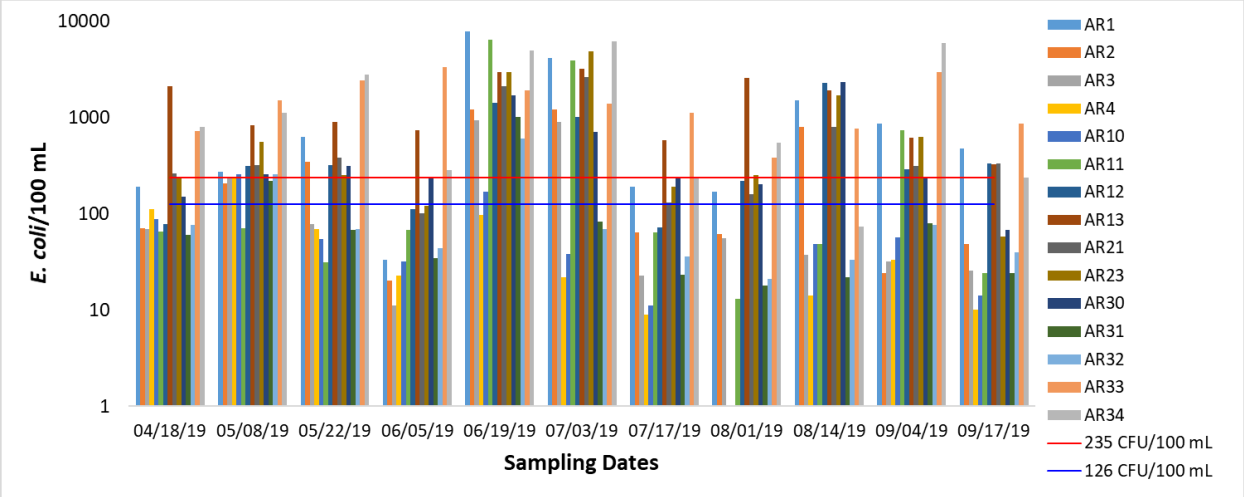

Figure EC3. *E. coli* abundance per 100 mL in Cameron Run, Hunting Creek, and the adjacent Potomac River grouped by sampling dates for all stations. The blue horizontal line represents the *E. coli* criterion for the geometric monthly mean allowable abundance (126 per 100 mL), and the red line represents the criterion for allowable abundance in the absence of four monthly samples (235 per 100 mL).

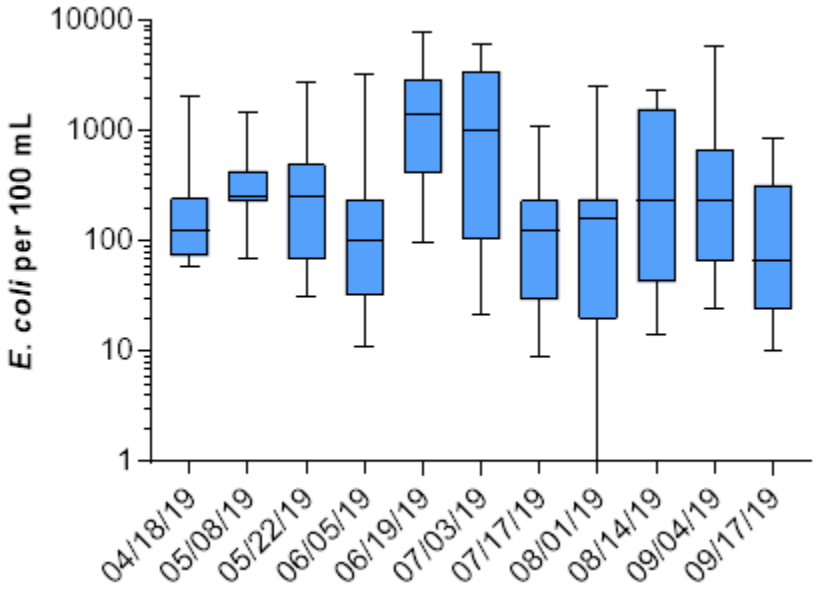

Figure EC4. Box plots of *E. coli* abundance per 100 mL for each site in Cameron Run, Hunting Creek, and the adjacent Potomac River over the sampling period. The bars show the minimum and maximum values, the boxes show the 25 and 75-percentile, and the median.

Temporal Trends

Although the number of stations and sampling events have increased since 2014 (8 sites and 6 sampling times in 2014, 8 sites and 11 sampling times in 2015, 12 sites and 11 sampling times in 2016 and 2017, 10 sites and 11 sampling times in 2018, and 15 sites and 11 sampling times in 2019), we present here a timeline of changes in the percentage of samples that exceeded the 235 per 100 mL standard (**Figure EC5**). Even though over the period 2014 – 2017, this trend globally suggested increasing

exceedances of the 235 CFUs per 100 mL standard (as mentioned in the 2018 Final Report), examination of the *E. coli* abundances per 100 mL over the period 2017 – 2019 does not indicate any worsening of the conditions, on the contrary (**Figure EC6**).

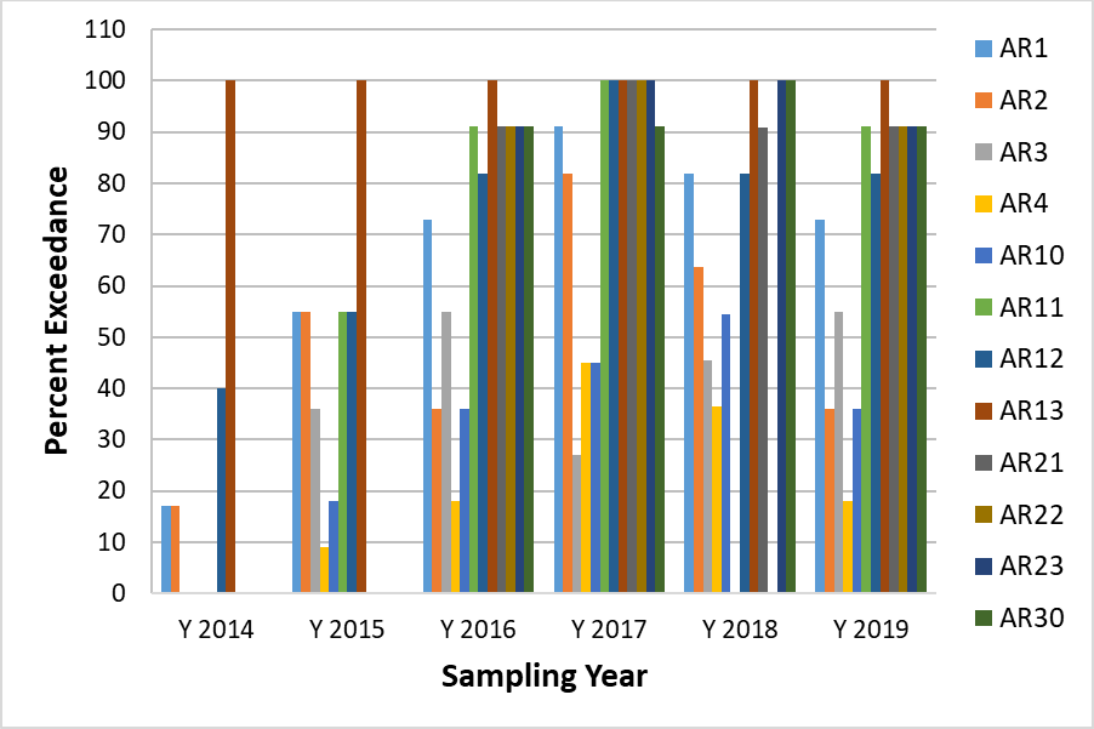

Figure EC5: Percentage of sample events when *E. coli* abundances exceeded 235 per 100 mL in year 2014, 2015, 2016, 2017, 2018, and 2019. Samples were collected 6 times during 2014, whereas in each of the subsequent years, samples were collected 11 times.

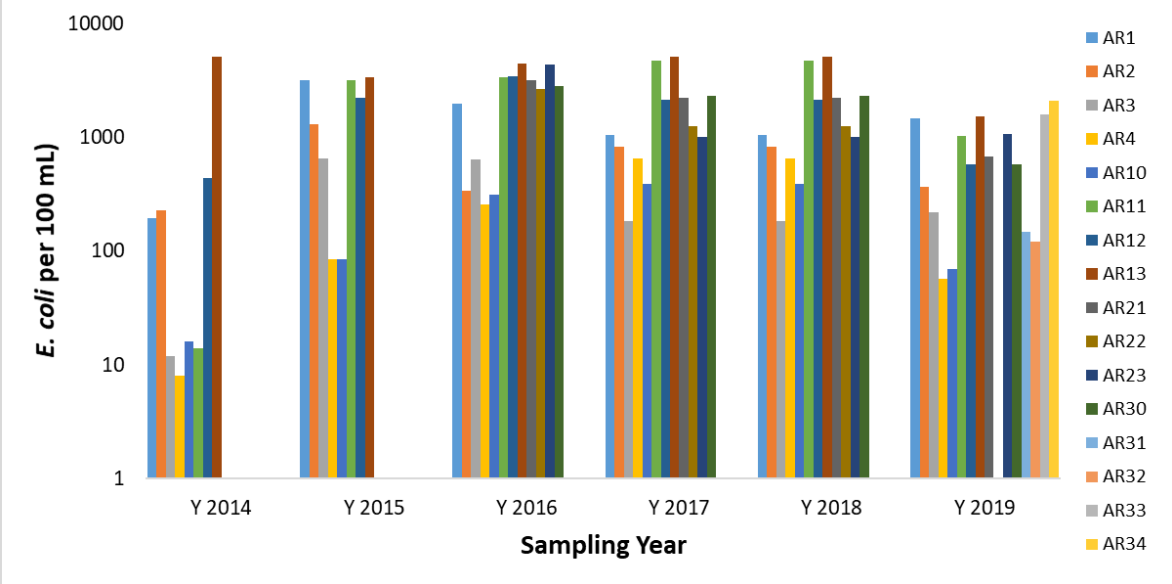

Figure EC6: *E. coli* abundances per 100 mL in year 2014, 2015, 2016, 2017, 2018, and 2019. Samples were collected 6 times during 2014, whereas in each of the subsequent years, samples were collected 11 times.

CONCLUSIONS:

The data continue to support a conclusion that the entire area sampled, including the mainstem of the Potomac River (AR4), is impaired for the bacteriological water quality criterion (*E. coli*) content under Section 9VAC25-260-170 of the Virginia Water Quality Standards that applies to primary contact recreational use surface waters. Although our data showed an increase of the *E. coli* abundance and percent exceedance of the 235 criterion from 2014 to 2016, these numbers seemed to have peaked in 2016 – 2017 and even showed a slight decrease in 2018 and 2019.

Sampling of two additional sites in Hooffs Run seems to indicate that Hooffs Run is a significant contributor of the Hunting Creek contamination by *E. coli*.

It is noteworthy that the large geographical and temporal variability that we observed during the sampling events prevents to draw clear conclusion on the trend of water quality impairment.

Finally, the highest counts in 2019 were observed in June and July (as in 2017), although the highest counts in 2018 were observed in April and September, revealing no clear seasonal trend in the data. High counts seem to reflect rainfall data instead of a seasonal trend.

Acknowledgements:

We thank the following students who helped with sample collection and analysis: Fanella Zamcho, Steven Chan, Alison Gomeiz, Aaron Newborn, Nga Thanh (Skye) Nguyen, Rana Rora, and Nicholas Mill.

Literature Cited

U.S. Environmental Protection Agency (USEPA). 2009. Method 1603: *Escherichia coli* (*E. coli*) in Water by Membrane Filtration Using Modified membrane-Thermotolerant *Escherichia coli* Agar (Modified mTEC). Available at: < http://water.epa.gov/scitech/methods/cwa/bioindicators/> search Method 1603, December 2009.

U.S. Environmental Protection Agency (USEPA). 2012. Water: Monitoring & Assessment: 5.11 Fecal Bacteria. Available at: http://water.epa.gov/type/rsl/monitoring/vms511.cfm

U.S. Environmental Protection Agency (USEPA). 2014. National Water Quality Assessment Report, water Quality Assessment and Total Maximum Daily Loads Information. Available at:
<http://ofmpub.epa.gov/waters10/attains_index.control>

Virginia Department of Environmental Quality (VADEQ). 2010. Bacteria TMDLs for the

Hunting Creek, Cameron Run, and Holmes Run Watersheds. Available at: <deq.state.va.us>

Virginia Department of Environmental Quality (VADEQ). 2012. 2012 Impaired Waters: Category 4 & 5 by Basin and Stream Name, Potomac and Shenandoah River Basins, Cause Group Code: A13R-03-BAC - Cameron Run/Hunting Creek. Available at: <http://www.deq.virginia.gov/Programs/Water/WaterQualityInformationTMDLs/WaterQualityAssessments.aspx>

Virginia. *State Water Control Board* (VSWCB). 2011. 9 VAC 25-260-10 Designation of uses. Virginia Water Quality Standards. Available at: <http://lis.virginia.gov/cgi-bin/legp604.exe?000+reg+9VAC25-260-10>

Virginia. *State Water Control Board* (VSWCB). 2011b. 9 VAC 25-260-170 Bacteria; other recreational waters. Virginia Water Quality Standards. Available at: <http://lis.virginia.gov/cgi-bin/legp604.exe?000+reg+9VAC25-260-170>

Appendix A

Figure A1. Map of sampling sites

Table A1. 2019 *E. coli* abundances per 100 mL for all station, all sampling dates

Date	Station	CFUs/100 mL	Date	Station	CFUs/100 mL	Date	Station	CFUs/100 mL
4/18/2019	AR1	190	6/19/2019	AR1	7800	8/14/2019	AR1	1500
	AR2	71		AR2	1200		AR2	800
	AR3	69		AR3	930		AR3	37
	AR4	110		AR4	97		AR4	14
	AR10	87		AR10	170		AR10	48
	AR11	65		AR11	6367		AR11	48
	AR12	78		AR12	1400		AR12	2250
	AR13	2100		AR13	2933		AR13	1917
	AR21	260		AR21	2100		AR21	800
	AR23	230		AR23	2967		AR23	1700
	AR30	150		AR30	1700		AR30	2300
	AR31	60		AR31	1000		AR31	22
	AR32	76		AR32	603		AR32	33
	AR33	720		AR33	1900		AR33	760
	AR34	790		AR34	4933		AR34	73
	Control	0		Control	0		Control	3
5/8/2019	AR1	273	7/3/2019	AR1	4100		AR1	850
	AR2	205		AR2	1200		AR2	24
	AR3	240		AR3	900		AR3	32
	AR4	240		AR4	22		AR4	33
	AR10	257		AR10	38		AR10	56
	AR11	71		AR11	3867		AR11	727
	AR12	313		AR12	1000		AR12	287
	AR13	830		AR13	3167		AR13	610
	AR21	317		AR21	2600		AR21	310
	AR23	553		AR23	4833		AR23	627
	AR30	255		AR30	700		AR30	237
	AR31	220		AR31	82		AR31	79
	AR32	253		AR32	69		AR32	76
	AR33	1500		AR33	1370		AR33	2967
	AR34	1100		AR34	6167		AR34	5900
	Control	0		Control	0		Control	1
5/22/2019	AR1	620	7/17/2019	AR1	190		AR1	470
	AR2	343		AR2	64		AR2	48
	AR3	78		AR3	23		AR3	25
	AR4	69		AR4	9		AR4	10
	AR10	55		AR10	11		AR10	14
	AR11	31		AR11	64		AR11	24
	AR12	315		AR12	72		AR12	330
	AR13	900		AR13	580		AR13	327
	AR21	377		AR21	130		AR21	333
	AR23	250		AR23	190		AR23	58
	AR30	310		AR30	235		AR30	67
	AR31	68		AR31	23		AR31	24
	AR32	69		AR32	36		AR32	40
	AR33	2400		AR33	1100		AR33	860
	AR34	2767		AR34	240		AR34	237
	Control	0		Control	6		Control	0
6/5/2019	AR1	33	8/1/2019	AR1	170			
	AR2	20		AR2	61			
	AR3	11		AR3	55			
	AR4	23		AR4	1			
	AR10	32		AR10	0			
	AR11	67		AR11	13			
	AR12	110		AR12	220			
	AR13	735		AR13	2567			
	AR21	100		AR21	160			
	AR23	120		AR23	250			
	AR30	240		AR30	200			
	AR31	34		AR31	18			
	AR32	44		AR32	21			
	AR33	3333		AR33	380			
	AR34	280		AR34	545			
	Control	0		Control	0			

Table A2. Mean of *E. coli* abundances per 100 mL for 2019, seasonal means and standard deviations and percent exceedances of the 126 and 235 CFUs/100 mL criteria

Station	Seasonal Mean	Seasonal St. Dev.	Percent Exceedance 126 CFUs/100 mL	Percent Exceedance 235 CFUs/100 mL
AR1	1472	2399	91	64
AR2	367	471	45	36
AR3	218	350	27	27
AR4	57	71	9	9
AR10	70	77	18	9
AR11	1031	2106	27	27
AR12	580	692	73	64
AR13	1515	1045	100	100
AR21	681	853	91	73
AR23	1071	1529	82	64
AR30	581	731	91	64
AR31	148	288	18	9
AR32	120	172	18	18
AR33	1572	971	100	100
AR34	2094	2428	91	91